frontiers
RESEARCH TOPICS

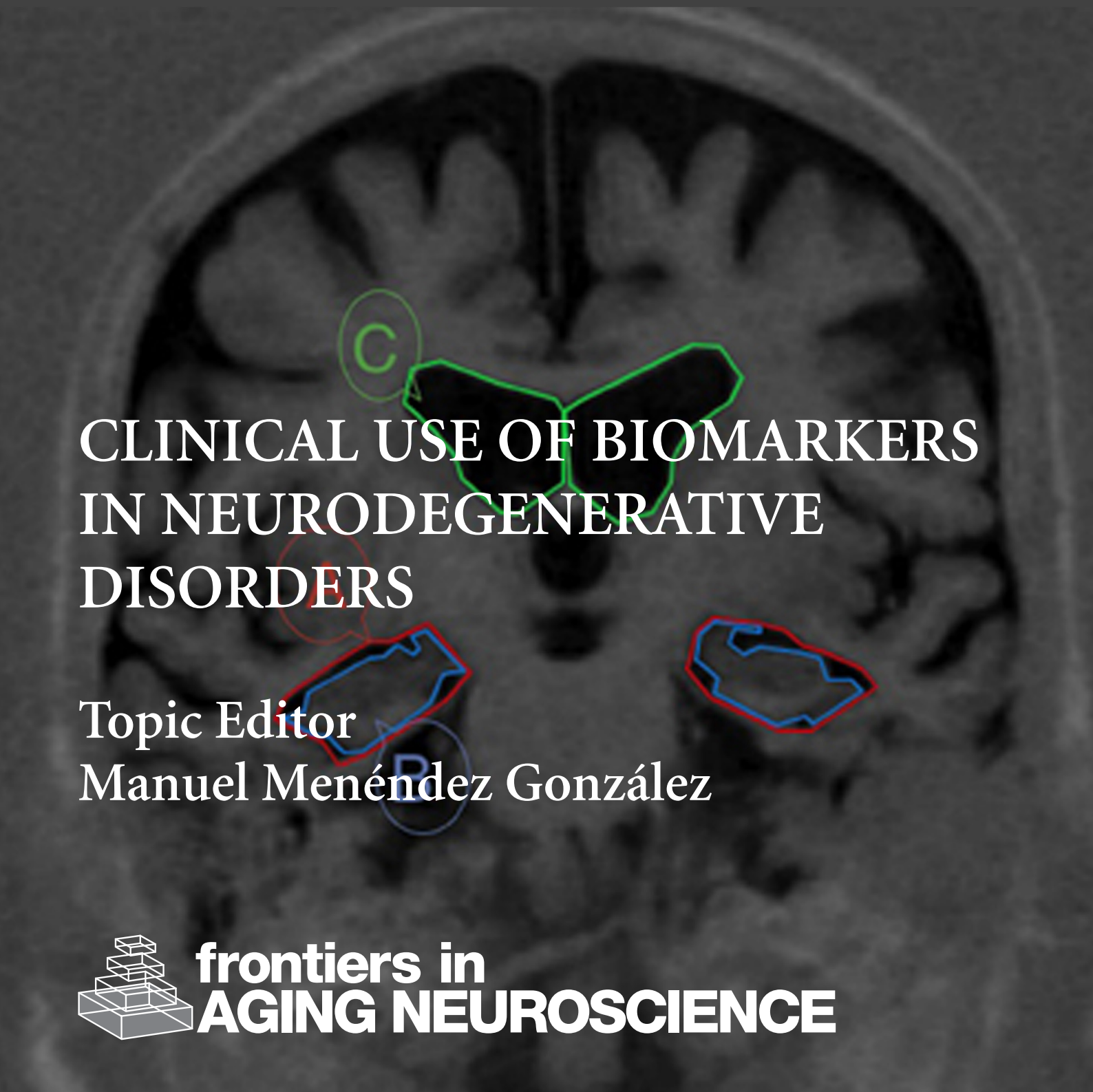

CLINICAL USE OF BIOMARKERS IN NEURODEGENERATIVE DISORDERS

Topic Editor
Manuel Menéndez González

frontiers in
AGING NEUROSCIENCE

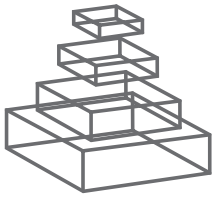

frontiers

ISSN 1664-8714
ISBN 978-2-88919-400-1
DOI 10.3389/978-2-88919-400-1

ABOUT FRONTIERS

Frontiers is more than just an open-access publisher of scholarly articles: it is a pioneering approach to the world of academia, radically improving the way scholarly research is managed. The grand vision of Frontiers is a world where all people have an equal opportunity to seek, share and generate knowledge. Frontiers provides immediate and permanent online open access to all its publications, but this alone is not enough to realize our grand goals.

FRONTIERS JOURNAL SERIES

The Frontiers Journal Series is a multi-tier and interdisciplinary set of open-access, online journals, promising a paradigm shift from the current review, selection and dissemination processes in academic publishing.
All Frontiers journals are driven by researchers for researchers; therefore, they constitute a service to the scholarly community. At the same time, the Frontiers Journal Series operates on a revolutionary invention, the tiered publishing system, initially addressing specific communities of scholars, and gradually climbing up to broader public understanding, thus serving the interests of the lay society, too.

DEDICATION TO QUALITY

Each Frontiers article is a landmark of the highest quality, thanks to genuinely collaborative interactions between authors and review editors, who include some of the world's best academicians. Research must be certified by peers before entering a stream of knowledge that may eventually reach the public - and shape society; therefore, Frontiers only applies the most rigorous and unbiased reviews.
Frontiers revolutionizes research publishing by freely delivering the most outstanding research, evaluated with no bias from both the academic and social point of view.
By applying the most advanced information technologies, Frontiers is catapulting scholarly publishing into a new generation.

WHAT ARE FRONTIERS RESEARCH TOPICS?

Frontiers Research Topics are very popular trademarks of the Frontiers Journals Series: they are collections of at least ten articles, all centered on a particular subject. With their unique mix of varied contributions from Original Research to Review Articles, Frontiers Research Topics unify the most influential researchers, the latest key findings and historical advances in a hot research area!
Find out more on how to host your own Frontiers Research Topic or contribute to one as an author by contacting the Frontiers Editorial Office: researchtopics@frontiersin.org

CLINICAL USE OF BIOMARKERS IN NEURODEGENERATIVE DISORDERS

Topic Editor:
Manuel Menéndez-González, Hospital Álvarez-Buylla, Spain; Universidad de Oviedo, Spain; Instituto de Neurociencias, Spain

The prevalence of neurodegenerative disorders is increasing dramatically and one of the major challenges today is the need of early and accurate diagnosis, the other is the need of more effective therapies -in turn the development of such therapies also requires early and accurate diagnosis-. The main hope for an earlier and more accurate diagnosis comes from the use of biomarkers.

Much research is being done trying to solve the many interrogates related to the role of biomarkers in clinical practice, including the early diagnosis, differential diagnosis and follow-up of neurodegenerative disorders. This is a field where translational research is intense enough to make this topic interesting for basic researchers and clinicians. Indeed, the amount and quality of articles received in response to the call for contributions was very good.

This eBook contains a good amount of high quality articles devoted to diverse techniques across several neurodegenerative disorders from different perspectives, including original reports, reviews, methods reports and opinion letters on biochemical biomarkers in biological fluids, neuroimaging techniques and multidimensional approaches linking clinical findings with biomarkers. The disorders covered are also diverse: Alzheimer's disease, Frontotemporal Dementia, Dementia with Lewy Bodies, Huntington's disease, Parkinson's disease among others.

As we can learn from articles in this Research Topic, biomarkers are allowing us to expand the knowledge on the biological and anatomical basis of neurodegenerative diseases and to implement diagnostic techniques in clinical practice and clinical trials.

Table of Contents

frontiers in
AGING NEUROSCIENCE

EDITORIAL
published: 21 October 2014
doi: 10.3389/fnagi.2014.00281

Biomarkers in neurodegenerative disorders: translating research into clinical practice

Manuel Menéndez-González [1,2,3]*

[1] Neurology Unit, Hospital Álvarez-Buylla, Oviedo, Spain
[2] Departamento de Morfología y Biología Celular, Universidad de Oviedo, Oviedo, Spain
[3] Instituto de Neurociencias, Universidad de Oviedo, Oviedo, Spain
*Correspondence: manuelmenendezgonzalez@gmail.com

Edited and reviewed by:
Rodrigo Orlando Kuljiš, Zdrav Mozak Limitada, Chile

Keywords: biomarker, MTAi, neurodegenerative disease, Neurodegenerative Diseases, Parkinson's Disease, Huntington's Disease, Frontotemporal dementia (FTD), CSF biomarkers

When I was invited by Frontiers to serve as Guest Editor of a Research Topic I had no doubts about the topic to address: the clinical use of biomarkers for neurodegenerative disorders. The prevalence of ND is increasing dramatically and one of the major challenges today is the need of early and accurate diagnosis, the other is the need of more effective therapies -in turn the development of such therapies also requires early and accurate diagnosis-. The main hope for an earlier and more accurate diagnosis comes from the use of biomarkers. Much research is being done trying to solve the many interrogates related to the role of biomarkers in the early diagnosis, differential diagnosis, and follow-up of neurodegenerative disorders. This is a filed where translational research is intense enough to make this topic interesting for basic researchers and clinicians. Indeed, the response to the call for contributions was very good. I had the opportunity to receive and edit a good amount of high quality articles devoted to diverse techniques across several ND from different perspectives.

Several articles are devoted to laboratory, biochemical biomarkers in neurodegenerative dementias. Researchers from Japan assessed the association of plasmatic annexin A5 with Alzheimer's disease and with Dementia with Lewy Bodies, and they found annexin A5 is indeed a good markers of both conditions (Sohma et al., 2013). Regarding the usefulness of CSF biomarkers in the differential diagnosis of FTLD vs. AD, an interesting review by D Irwin, J Trojanowski, and M Grossman highlight that CSF measurements of Aβ1-42, t-tau, and p-tau differ significantly in FTLD from the abnormal levels seen in AD, and in a subset of both FTLD-tau and FTLD-TDP there are extremely low levels of t-tau of unclear etiology (Irwin et al., 2013). In other review, J Moreth, C Mavoungou, and K Schindowski discuss the role of CSF Aβ in ongoing clinical trials for AD as well as the latest regulatory strategies (Moreth et al., 2013). Researchers for the Alzheimer's Disease Neuroimaging Initiative (ADNI) evaluated the association of APOE with amyloid deposition, cerebrospinal fluid levels (CSF) of Aβ, tau, and p-tau, brain atrophy, cognition, and cognitive complaints in patients with early-Mild Cognitive Impairment (E-MCI) and cognitively healthy older adults (HC) and found that cortical amyloid deposition and CSF levels of Aβ were significantly associated with APOE ε4 status but not E-MCI diagnosis, with ε4 positive participants showing more amyloid deposition and lower levels of CSF Aβ than ε4 negative participants (Risacher et al., 2013). These findings have practical repercussion, since clinicians, and researchers should consider APOE genotyping when evaluating biomarkers in early stages of the disease.

A number of articles addressed neuroimaging techniques. Researchers from Karolinska Institute and King's College London explored how the progression of atrophy in dementia may be predicted on the basis of the anatomical connectivity of the first atrophic region and found that the subcallosal medial prefrontal cortex is atrophied (in different extent depending on the brain hemisphere assessed) in FTD, SD, PNFA an AD (Lindberg et al., 2012). These results should also be taken into account when using neuroimaging biomarkers in the differential diagnosis of neurodegenerative dementias. There are two neuroimaging methods reports. One proposes the use of viscous fluid registration in voxel based morphometry studies to enhance sensitivity and localizing power in the software package SPM (Pereira et al., 2013) and the other describes the Medial Temporal Atrophy index (MTAi), a simple planimetric method for measuring the relative extent of atrophy of the Medial Temporal Lobe (MTA) in relation to the global brain atrophy (Menéndez-González et al., 2014a). Following with simple methods for assessing MTA in the clinical setting, researchers from Florida describe the utility of age-specific cut-offs for visual rating of medial temporal atrophy in classifying Alzheimer's disease, MCI, and cognitively normal elderly subjects (Duara et al., 2013).

Some other studies followed a multidimensional approach. In a multicentric study researchers performed a longitudinal and multidimensional assessment of individuals with the gene expansion for Huntington disease (HD) but not yet diagnosed who were evaluated annually. They identified three clusters that represented primarily cognitively impaired, behaviorally impaired, and cognitively preserved phenotypes. Thus, this multidimensional method results in an earlier diagnosis with less motor and cognitive impairment than a motor diagnosis. These findings have implications for designing preventive trials and providing clinical care in prodromal HD (Biglan et al., 2013). Again researchers for the ADNI, show how the short-term (1 year) prognosis of progression from amnesic MCI to dementia relates strongly to baseline markers of neurodegeneration, with the AD signature MRI biomarker of cortical thickness performing the best among MRI and CSF

markers studied here. However, longer-term (3 year) prognosis in these individuals was better predicted by a marker indicative of brain amyloid. Prediction of time-to-event in a survival model was predicted by the combination of these biomarkers. These results provide further support for emerging models of the temporal relationship of pathophysiologic events in AD and demonstrate the utility of these biomarkers at the prodromal stage of the illness (Dickerson and Wolk, 2013). Gómez-Ramírez and Wu review the network-based approach in biomarker discovery as a source of key insights to fully understand the network degeneration hypothesis (the disease starts in specific network areas and progressively spreads to connected areas of the initial loci-networks, a concept also addressed in the article by Lindberg et cols.) and introduce a new framework for the quantitative study of biomarkers that can help shorten the transition between academic research and clinical diagnosis in AD (Gómez-Ramírez and Wu, 2014).

We also have two original reports on Parkinson's disease (PD) and parkinsonisms. One is on the use of DaTSPECT in the diagnosis of patients with hard-to-classify tremor who have a normal DaT-SPECT. Researchers from Spain and Mexico make a clinical follow up study and provide a list of the final diagnosis behind these cases (Menéndez-González et al., 2014b) at the time of discussing the role of DaTSPECT in the diagnosis of patients with tremor. In the other report, a group of researchers leaded by Prof Parnetti, assesses the differential role of CSF alpha-synuclein species, tau, and Aβ42 in PD and conclude that the combination of CSF o/t-α-syn and Aβ42/tau ratios improve the diagnostic accuracy of PD and that PD patients showing low CSF Aβ42 levels at baseline are more prone to develop cognitive decline (Parnetti et al., 2014).

Finally, I also had the opportunity of publishing a couple of opinion articles: one on the many questions arising about the use of biomarkers for diagnosing neurodegenerative diseases routinely (Menéndez-González, 2014a) and other discussing the safety issues related to lumbar punctures performed for CSF analysis for the diagnosis of AD in daily clinical practice (Menéndez-González, 2014b).

Research on biomarkers on neurodegenerative disorders is a hot topic where much work has to be done yet. As we can learn from this Research Topic, biomarkers are allowing us to expand the knowledge on the biological and anatomical basis of neurodegenerative diseases and to implement diagnostic techniques in clinical practice and clinical trials.

REFERENCES

Biglan, K. M., Zhang, Y., Long, J. D., Geschwind, M., Kang, G. A., Killoran, A., et al. (2013). Refining the diagnosis of Huntington disease: the PREDICT-HD study. *Front. Aging Neurosci.* 5:12. doi: 10.3389/fnagi.2013.00012

Dickerson, B. C., and Wolk, D. A. (2013). Biomarker-based prediction of progression in MCI: comparison of AD signature and hippocampal volume with spinal fluid amyloid-β and tau. *Front. Aging Neurosci.* 5:55. doi: 10.3389/fnagi.2013.00055

Duara, R., Loewenstein, D. A., Shen, Q., Barker, W., Varon, D., Greig, M. T., et al. (2013). The utility of age-specific cut-offs for visual rating of medial temporal atrophy in classifying Alzheimer's disease, MCI and cognitively normal elderly subjects. *Front. Aging Neurosci.* 5:47. doi: 10.3389/fnagi.2013.00047

Gómez-Ramírez, J., and Wu, J. (2014). Network-based biomarkers in Alzheimer's disease: review and future directions. *Front. Aging Neurosci.* 6:12. doi: 10.3389/fnagi.2014.00012

Irwin, D. J., Trojanowski, J. Q., and Grossman, M. (2013). Cerebrospinal fluid biomarkers for differentiation of frontotemporal lobar degeneration from Alzheimer's disease. *Front. Aging Neurosci.* 5:6. doi: 10.3389/fnagi.2013.00006

Lindberg, O., Westman, E., Karlsson, S., Östberg, P., Svensson, L. A., Simmons, A., et al. (2012). Is the subcallosal medial prefrontal cortex a common site of atrophy in Alzheimer's disease and frontotemporal lobar degeneration? *Front. Aging Neurosci.* 4:32. doi: 10.3389/fnagi.2012.00032

Menéndez-González, M. (2014a). The many questions on the use of biomarkers for neurodegenerative diseases in clinical practice. *Front. Aging Neurosci.* 6:45. doi: 10.3389/fnagi.2014.00045

Menéndez-González, M. (2014b). Routine lumbar puncture for the early diagnosis of Alzheimer's disease. Is it safe? *Front. Aging Neurosci.* 6:65. doi: 10.3389/fnagi.2014.00065

Menéndez-González, M., López-Muñiz, A., Vega, J. A., Salas-Pacheco, J. M., and Arias-Carrión, O. (2014a). MTA index: a simple 2D-method for assessing atrophy of the medial temporal lobe using clinically available neuroimaging. *Front. Aging Neurosci.* 6:23. doi: 10.3389/fnagi.2014.00023

Menéndez-González, M., Tavares, F., Zeidan, N., Salas-Pacheco, J. M., and Arias-Carrión, O. (2014b). Diagnoses behind patients with hard-to-classify tremor and normal DaT-SPECT: a clinical follow up study. *Front. Aging Neurosci.* 6:56. doi: 10.3389/fnagi.2014.00056

Moreth, J., Mavoungou, C., and Schindowski, K. (2013). Is abeta a sufficient biomarker for monitoring anti-abeta clinical studies? A critical review. *Front. Aging Neurosci.* 5:25. doi: 10.3389/fnagi.2013.00025

Parnetti, L., Farotti, L., Eusebi, P., Chiasserini, D., De Carlo, C., Giannandrea, D., et al. (2014). Differential role of CSF alpha-synuclein species, tau, and Aβ42 in Parkinson's disease. *Front. Aging Neurosci.* 6:53. doi: 10.3389/fnagi.2014.00053

Pereira, J. M. S., Acosta-Cabronero, J., Pengas, G., Xiong, L., Nestor, P. J., and Williams, G. B. (2013). VBM with viscous fluid registration of gray matter segments in SPM. *Front. Aging Neurosci.* 5:30. doi: 10.3389/fnagi.2013.00030

Risacher, S. L., Kim, S., Shen, L., Nho, K., Foroud, T., Green, R. C., et al. (2013). The role of apolipoprotein E (APOE) genotype in early mild cognitive impairment (E-MCI). *Front. Aging Neurosci.* 5:11. doi: 10.3389/fnagi.2013.00011

Sohma, H., Imai, S.-I., Takei, N., Honda, H., Matsumoto, K., Utsumi, K., et al. (2013). Evaluation of annexin A5 as a biomarker for Alzheimer's disease and dementia with lewy bodies. *Front. Aging Neurosci.* 5:15. doi: 10.3389/fnagi.2013.00015

Conflict of Interest Statement: The author declares that the research was conducted in the absence of any commercial or financial relationships that could be construed as a potential conflict of interest.

Received: 13 August 2014; accepted: 25 September 2014; published online: 21 October 2014.

*Citation: Menéndez-González M (2014) Biomarkers in neurodegenerative disorders: translating research into clinical practice. Front. Aging Neurosci. **6**:281. doi: 10.3389/fnagi.2014.00281*

This article was submitted to the journal Frontiers in Aging Neuroscience.

frontiers in
AGING NEUROSCIENCE

ORIGINAL RESEARCH ARTICLE
published: 05 April 2013
doi: 10.3389/fnagi.2013.00015

Evaluation of annexin A5 as a biomarker for Alzheimer's disease and dementia with lewy bodies

Hitoshi Sohma[1,2]*, Shin-ichi Imai[2], Norio Takei[2], Hirohito Honda[3], Kyoichi Matsumoto[4], Kumiko Utsumi[5], Kayo Matsuki[2], Eri Hashimoto[6], Toshikazu Saito[6] and Yasuo Kokai[2]

[1] *Department of Educational Development, Center for Medical Education, Sapporo Medical University, Sapporo, Japan*
[2] *Department of Biomedical Engineering, School of Medicine, Sapporo Medical University, Sapporo, Japan*
[3] *Mikuri Immunology Laboratory, Inc., Osaka, Japan*
[4] *Sanyo Chemical Industries, Ltd., Kyoto, Japan*
[5] *Department of Neuropsychiatry, Sunagawa City Medical Center, Sunagawa, Japan*
[6] *Department of Neuropsychiatry, School of Medicine, Sapporo Medical University, Sapporo, Japan*

Edited by:
Manuel Menéndez-González, Hospital Álvarez-Buylla, Spain

Reviewed by:
Daniel Ortuño-Sahagun, Centro Universitario de Ciencias Biológicas y Agropecuarias, Mexico
Junming Wang, University of Mississippi Medical Center, USA

****Correspondence:***
Hitoshi Sohma, Department of Educational Development, Center for Medical Education, Sapporo Medical University, South-1, West-17, Chuo-ku, Sapporo 060-8556, Japan.
e-mail: sohma@sapmed.ac.jp

Background: Alzheimer's disease (AD) differs from other forms of dementia in its relation to amyloid beta peptide ($A\beta_{42}$). Using a cell culture model we previously identified annexin A5, a Ca^{2+}, and phospholipid binding protein, as an AD biomarker. Plasma level of annexin A5 was significantly higher in AD patients compared to that in a control group. On the other hand, AD has been identified to share a number of clinical and pathological features with Dementia with Lewy bodies (DLB). The present study was done to examine whether or not plasma annexin A5 is a specific marker for AD, when being compared with the levels of DLB patients. As Apolipoprotein E (ApoE) gene subtype ε4 (ApoE-ε4) has been noticed as the probable genetic factor for AD, we also examined and compared ApoE genotype in both AD and DLB.

Methods: Blood samples were obtained from 150 patients with AD (aged 77.6 ± 6.5 years), 50 patients of DLB (79.4 ± 5.0) and 279 community-dwelling healthy elderly individuals of comparable age and sex (75.6 ± 8.1). All AD patients met NINCDS-ADRDA criteria and all DLB patients were diagnosed as probable DLB according to the latest consensus diagnostic criteria. Quantification was done using the Chemiluminescent Enzyme Immunoassay (CLEIA) Technique (SphereLight assay) using the monoclonal antibodies against annexin A5. DNA genotyping of ApoE was performed by distinguishing unique combinations of Hha1 fragments of PCR-amplified genomic DNA products.

Results: The plasma level of annexin A5 was significantly higher in AD patients than in the healthy individuals (control) ($P < 0.0001$). The plasma annexin A5 level was also significantly higher in DLB patients than in the control group ($P < 0.0001$). From the ROC curves with plasma annexin A5 concentrations, the mean areas under the curve were 0.863 and 0.838 for the AD/control and DLB/control, respectively. The rate of ApoE4 carrier status and the frequency of the ε4 allele were significantly higher in AD or DLB than in control and there was no significant difference between AD and DLB.

Conclusions: These results suggest that both annexin A5 and ApoE4 are common markers for AD and DLB.

Keywords: plasma biomarker, Alzheimer's disease, dementia with lewy bodies, annexin A5, Ca^{2+}-stress, ROC curve, ApoE

INTRODUCTION

The augmented number of dementia patients is remarkable in the aging of society in advanced countries. Alzheimer's disease (AD) accounts for more than half of all dementia, and Dementia with Lewy bodies (DLB) are the second most common, accounting for approximately 15% of cases at autopsy (McKeith et al., 2004), both of which are common forms of neurodegenerative dementia. DLB shares clinical and pathological features with other dementia subtypes such as AD, vascular dementia and Parkinson's disease (PD), which makes it difficult to distinguish in clinical practice. Also, the lack of valid and reliable methods for assessing the core clinical symptoms of both AD and DLB makes its identification even more difficult. The diagnosis of AD is reliant on the use of National Institute of Neurological and Communicative Disorders and Stroke-AD and related Disorders Association (NINCDS-ADRDA) criteria. The NINCDS-ADRDA criteria have high sensitivity (0.93), but low specificity (0.23) in the diagnosis of AD among a group of patients with cortical dementias [AD and frontotemporal dementia (FTD)] (Varma et al., 1999). On the other hand, consensus

criteria for DLB were developed in 1996 to assist with the antemortem diagnosis (McKeith et al., 2005). Although the criteria have high specificity (79–100%), the sensitivity is low (20–60%), so that the diagnosis can be missed in many cases during life (Litvan et al., 2003). The revised clinical consensus criteria were published in 2005, which gives greater diagnostic weight to clinical features suggestive of DLB (McKeith et al., 2005). In light of the limited sensitivity of current methods of clinical diagnosis, it is important to establish additional markers that can improve diagnostic accuracy in combination with clinical assessment.

Amyloid β peptide (Aβ), which is a proteolytic product of amyloid precursor protein (APP), accumulates in the brains of AD patients. Its toxicity is thought to cause neural cell death (Mattson, 2004). Amyloid-dependent neurotoxicity is known to perturb Ca^{2+} homeostasis in neuronal cells (LaFerla, 2002). Possibly, Aβ impairs membrane Ca^{2+} pumps and enhances Ca^{2+} influx through voltage-dependent channels and ionotropic glutamate receptors. Focusing on this mechanism, we identified the Ca^{2+}-related protein as a potential biomarker for AD using primary neurons as a cell culture model (Yamaguchi et al., 2010). It was shown that the level of annexin A5 was augmented in both the brain and blood plasma in an AD-model mouse (Tg2576 transgenic mouse), overexpressing mutant human APP (Yamaguchi et al., 2010). In addition, the plasma level of annexin A5 was significantly increased in AD patients compared to that in a control group (p-value of less than 0.0001 in the logistic regression analysis), suggesting that annexin A5 is a favorable marker for AD (Yamaguchi et al., 2010). As annexin A5 binds both Ca^{2+} and lipids, it might have a role to protect against Ca^{2+}-induced damage. A defensive role against apoptosis by annexin A5 is also reported, in that annexin A5 plays a role in interacting with and reducing the toxicity of the amyloidogenic proteins, islet amyloid polypeptides and α-synuclein inclusion (Bedrood et al., 2009).

Apolipoprotein E (ApoE), which is a major component of lipoproteins, is comprised of 299 amino acid residues and plays a role in the metabolism and redistribution of cholesterol. ApoE mediates the uptake of lipoprotein particles in the brain via the low-density lipoprotein (LDL), receptor related protein (LRP), and the very low-density family lipoprotein receptor (VLDL) (Mahley, 1988; Paolo and Kim, 2011). The three major isoforms of ApoE, referred to as ApoE2, E3, and E4, are products of three alleles (ε2, ε3, ε4) at a single gene locus (Mahley, 1988). Three homozygous phenotypes (Apo-E2/2, E3/3, and E4/4) and three heterozygous phenotypes (Apo-E2/3, E3/4, and E2/4) arise from the expression of any two of the three alleles. The ε4 allele of the ApoE gene was identified as the strongest genetic risk factor for AD (Bertram and Tanzi, 2008). Neuropathological studies demonstrated that the frequency of the ApoE gene subtype ε4 (ApoE ε4) allele in DLB is similar to AD and that ApoE4 has also been implicated in the development of DLB (Singletona et al., 2002). We reported that ApoE4 genotypes were similar in AD and DLB, giving further evidence that the ε4 allele is a risk factor for both disorders in Japanese subjects (Kobayashi et al., 2011).

The present study was done to examine whether or not plasma annexin A5 is a specific marker for AD, in comparison with the levels of DLB patients. For that purpose, we analyzed plasma level of DLB patients and compared with those of AD patients and age-matched community dwelling healthy persons as a control. We further discuss taking ApoE4 frequencies into consideration.

MATERIALS AND METHODS

HUMAN BLOOD PLASMA

The Sapporo Medical University Ethics Committee approved human plasma studies on dementia biomarker study in 2007. Informed written consent was obtained from all subjects. All healthy volunteers and patients provided written permission. For patients with impaired cognition we obtained written permission from their family in accordance with the Declaration of Helsinki. Blood samples were obtained from 150 patients with AD (aged 77.6 ± 6.5 years), 50 patients of DLB (aged 79.4 ± 5.0 years), and 279 community-dwelling elderly individuals (healthy volunteers) of comparable age and sex (75.6 ± 8.1 years). All AD patients met NINCDS-ADRDA criteria (McKhann et al., 1984) and DLB patients were diagnosed as probable DLB according to the latest consensus diagnostic criteria (McKeith et al., 2005). The patient's clinical symptoms were evaluated using the revised Hasegawa Dementia scale (HDS-R) (Hasegawa, 1983), Mini-Mental State Examination (MMSE), and clinical dementia rating (CDR). The diagnosis of AD was also confirmed in all patients either by brain magnetic resonance imaging or single photon emission computed tomography. Blood was drawn with Venoject II vacuum tubes containing EDTA-Na (final 4.5 mM) (Terumo, Tokyo, Japan) and the plasma fraction was isolated by centrifugation at 2500 g for 15 min. This was repeated once to avoid possible cell debris in blood. Blood was centrifuged within 6 h after sampling. Plasma fractions were stored at −80°C until use.

QUANTIFICATION OF PLASMA LEVEL OF ANNEXIN A5 USING SANDWICH CLEIA (SPHERELIGHT ASSAY)

Plasma annexin A5 was quantified using the Chemiluminescent Enzyme Immunoassay (CLEIA) Technique (SphereLight assay) as described (Yamaguchi et al., 2010). Briefly, annexin A5 present in the specimen was trapped by a monoclonal antibody (mAb) against annexin A5 (clone No. 23), conjugated to a glass bead and a horseradish peroxidase (HRP)-labeled mAb against annexin A5 (clone No. 49). Unbound materials were removed by washing. The chemiluminescent reagent consists of a luminol solution that includes a phenol-derivative as an enhancer, to which a hydrogen peroxide solution was added. The HRP in the bound conjugate catalyzes the oxidation of the luminol derivative, producing light. The light signals were read by the Olympus SphereLight180 fully automated system (Olympus Optical Co., Ltd., Tokyo, Japan). The amount of HRP conjugate bound was directly proportional to the annexin A5 concentration. The required time and volume of the specimens were 20 min and 40 μl, respectively, for the SphereLight assay. The detection limit proved to be 0.16 ng/ml for annexin A5 and this system was useful to quantify plasma annexin A5 within the range of 0.16–20.0 ng/ml. Reproducible data were obtained by intra-assay and inter-assay (data not shown). Because annexin A5 is present in blood cells (Masuda et al., 2004), if a prolonged period of time has passed (longer than 12 h) after collecting blood until centrifuging, the plasma annexin A5 level

increases (data not shown) due to physical damage such as temperature change, osmotic pressure change and so on. To avoid inducible leakage of annexin A5 from blood cells, all the plasma was separated by centrifugation within 6 h of sampling. The detection limit proved to be 0.16 ng/ml of annexin A5 as previously described (Yamaguchi et al., 2010). We also performed a plasma dilution test and reproducibility studies of intra-assay and inter-assay, which confirmed the assay method is reliable (Yamaguchi et al., 2010).

APOLIPOPROTEIN E (ApoE) GENOTYPING

DNA genotyping of ApoE was performed according to the protocol described by Hixson and Vernier (1990). Briefly, using a QIAamp DNA Blood Mini Kit (QIAGEN, Tokyo, Japan), genomic DNA was extracted from the buffy coat after centrifugation of the blood sample according to the manufacturer's instructions. The leukocyte DNA was amplified by PCR using the oligonucleotide primers, Primer 1 (59-TAAGCTTGGCACGGCTGTCCAAGGA-39), and Primer 2 (59-ACAGAATTCGCCCCGGCCTGGTACAC-39) set on common sequence parts of ApoE isoforms. The PCR products were digested with HhaI (New England Biolabs, Japan, Inc., Tokyo, Japan) and the resulting digestion fragments were separated by electrophoresis on polyacrylamide gels (SuperSepTMDNA 15% gel (Wako, Tokyo, Japan)). Each genotype of ApoE was distinguished by unique combinations of Hha1 fragment sizes in all homozygotic and heterozygotic combinations (Hixson and Vernier, 1990). After determining the ApoE genotypes, we investigated the ApoE4 carrier status and the frequency of the ε4 allele in the 279 controls, 150 AD, and 50 DLB cases.

STATISTICAL ANALYSIS

The mean response of each experimental group was compared with its simultaneous control by the unpaired Student's *t*-test. Analysis of variance was used to compare the mean responses of the experimental and control groups. A significant difference was set at $p < 0.05$. Logistic regression modeling was employed to construct receiver operator curves (ROC) by using JMP 9.0.0 (SAS Institute Inc., Cary, NC) to examine the plasma annexin A5 levels in diagnoses of AD and DLB. ROC curve comparisons were based on the area under the curve (AUC), SE, and the associated 95% confidence interval (CI). We subsequently calculated sensitivity of the various models using the predicted probability of each subject by logistic regression modeling with specificity of at least eighty percent. Fisher's exact tests were used to assess the frequencies of the ε4 allele between groups using JMP 9.0.0 (SAS Institute, Cary, NC, USA).

RESULTS

Plasma level of annexin A5 was analyzed using CLEIA Technique (SphereLight assay) as described in Materials and Methods. In this study, we measured 150 samples of AD (age 77.6 ± 6.5), 50 samples of DLB (age 79.4 ± 5.0), and 279 age-matched community dwelling healthy persons (age 75.6 ± 8.1) as a control. When average concentrations of plasma annexin A5 are compared among AD, DLB, and control groups, the values of AD (3.33 ± 1.60) and DLB (3.02 ± 1.08) were significantly higher than healthy control subjects (1.95 ± 0.68) (**Figure 1**). The probability of both AD and DLB can be predicted by a logistic regression model with the plasma level of annexin A5. The ROC analyses revealed good separation of patients with either AD or DLB from healthy control subjects (**Figure 2**). The areas under the curve were 86.3% ($P < 0.0001$) and 83.8% ($P < 0.0001$) for AD and DLB, respectively. That is statistically significant, suggesting that annexin A5 is also a potential biomarker for both AD and DLB. On the other hand, no significant difference was observed between AD and DLB ($p = 0.36$).

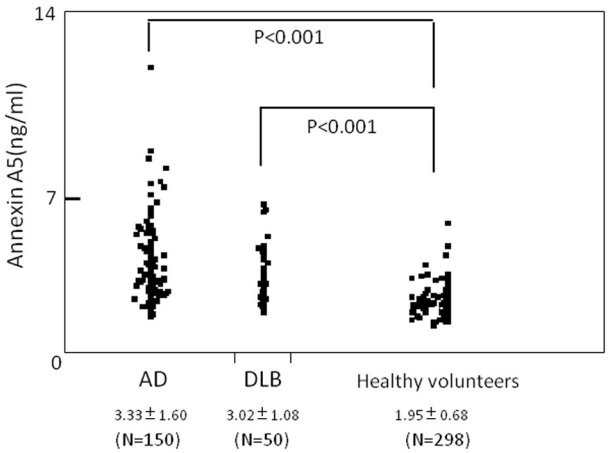

FIGURE 1 | Comparison of plasma levels of annexin A5 in AD, DLB patients, and healthy volunteers (control). For quantitative analysis, we established a chemiluminescent enzyme immunoassay system with monoclonal antibodies against human annexin A5 and measured human plasma annexin A5. Dot blot is shown. Each point represents the plasma annexin A5 concentration of individual. AD, Alzheimer's disease; DLB, dementia with Lewy bodies.

Several risk factors for AD have been suggested such as medical history, life style, environment and genes. Of these, ApoE-ε4 has been noticed as one of the genetic factors. We next identified ApoE gene typing by analyzing the restriction enzyme products of the PCR-amplified ApoE gene as shown in Materials and Methods (**Table 1**, **Figure 3**). In the control group, 51 out of 279 subjects were ApoE4 carriers (18.3%). Three subjects were homozygous for the ε4 allele (1.1%) and 48 subjects were heterozygous for the e4 allele (17.2%). The total frequency of the ε4 allele was 9.7%. In the AD group, 63 out of 150 subjects were ApoE4 carriers (42.0%). Nine subjects were homozygous for the ε4 allele (6.0%) and 54 subjects were heterozygous for the ε4 allele (36.0%). The total frequency of the ε4 allele was 24.0%. In the DLB group, 21 out of 50 subjects were ApoE4 carriers (42.0%). Three subjects were homozygous for the ε4 allele (6.0%) and 18 subjects were heterozygous for the ε4 allele (36.0%). The total frequency of the ε4 allele was 24.0%. ApoE4 frequencies were compared among AD, DLB, and control groups (Fisher's exact test). ApoE4 carrier status was significantly different between AD and control groups ($p < 0.0001$), and between DLB and control ($p = 0.0004$). Allele frequencies of ApoE ε4 were significantly higher in AD ($p < 0.0001$) and DLB ($p < 0.0001$) than in the control

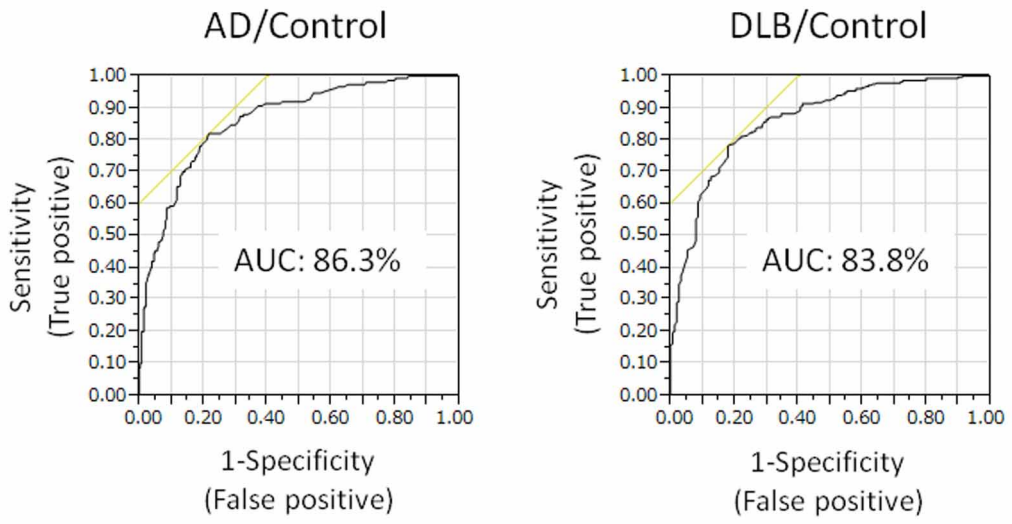

FIGURE 2 | Receiver operating characteristic (ROC) curves showing prediction of either AD or DLB by plasma annexin A5. The probability of either AD or DLB can be predicted by a logistic regression model with the plasma level of annexin A5. The areas under the curve are 86.3 and 83.8% for AD and DLB, respectively. AD, Alzheimer's disease; DLB, dementia with Lewy bodies.

Table 1 | Distribution of ApoE4 carrier status and the frequency of ApoE ε4 allele in the population of AD, DLB, and control groups.

	ApoE4 carrier*		ApoE ε4 allele**	
	Positive	**Negative**	**Positive**	**Negative**
C	51 (18.3%)	228 (81.7%)	57 (10.2%)	501 (89.8%)
AD	63 (42.0%)	87 (58.0%)	72 (24.0%)	228 (76%)
DLB	21 (42.0%)	29 (58.0%)	27 (24.0%)	73 (76.0%)

Numbers in parentheses represent the frequencies of ApoE4 carrier or ApoE ε4 allele. C, control group; AD, Alzheimer's disease group; DLB, dementia with Lewy bodies group.

**Significantly different between AD and control groups ($p < 0.0001$), and between DLB and control ($p = 0.0004$).*

***Significantly higher in AD ($p < 0.0001$) and DLB ($p < 0.0001$) than in the control group. No significant differences in rates of ApoE4 carrier status and the frequencies of the ε4 allele between AD and DLB.*

group. However, there were no significant differences in rates of ApoE4 carrier status ($p = 0.57$) and the frequencies of the ε4 allele ($p = 0.32$) between AD and DLB. These results also indicate the similarity of AD and DLB.

DISCUSSION

SIMILARITY OF AD AND DLB

The toxicity of Aβ is thought to cause neural cell death, which is involved in the pathogenesis AD (Mattson, 2004). Decreased degradation or dyscatabolism of Aβ, presumably related to aging, results in both the accumulation of amyloid beta peptide ($A\beta_{42}$) in the brain and the decreased concentration of $A\beta_{42}$ in CSF. Thus, lowered concentration of CSF $A\beta_{42}$ has been noted as a barometer for AD (Andreasen et al., 2001). AD is the most common neurodegenerative dementia and DLB is the second most common. DLB shares clinical and pathological features with AD, which makes it difficult to distinguish in clinical practice. The CSF levels of $A\beta_{42}$ are similar between AD and DLB (Gomez-Tortosa et al., 2003; Mollenhauer et al., 2005a). Amyloid-dependent neurotoxicity is known to perturb Ca^{2+} homeostasis in neuronal cells (LaFerla, 2002). Possibly, Aβ impairs membrane Ca^{2+} pumps and enhances Ca^{2+} influx through voltage-dependent channels and ionotropic glutamate receptors. Focusing on proteins concerning Ca^{2+} signaling, we identified annexin A5 which is augmented in $A\beta_{42}$ dependent manner and showed it as a potential biomarker for AD (Yamaguchi et al., 2010). Moreover, the plasma level of annexin A5 was shown to be elevated in AD (Yamaguchi et al., 2010). In the present study, plasma level of annexin A5 was shown to be elevated not only in AD but also in DLB.

Genetic factors are increasingly recognized as major risk factors for dementia. Evidence from numerous studies has identified the ApoE gene on chromosome 19 as a major risk factor for AD. ApoE, which is a major component of lipoproteins, is comprised of 299 amino acid residues and plays a role in the metabolism and redistribution of cholesterol (Hatters et al., 2006). Three major common isoforms, designated ApoE2, ApoE3, and ApoE4. ApoE colocalizes with extracellular amyloid deposits, resulting in isoform-specific clearance of Aβ. However, ApoE isoforms differently interact with Aβ isoform specific effects on Aβ-clearance. In ApoE4, domain interaction occurs as a result of a putative salt bridge, leading to tight structural formation. This interaction does not occur to the same extent in ApoE2 and ApoE3 (Dong et al., 1994; Dong and Weisgraber, 1996). ApoE ε4 is associated with an increased risk for AD with an earlier age of disease onset (Kim et al., 2009). On the other hand, findings regarding ApoE polymorphisms in DLB have so far been inconclusive. It was

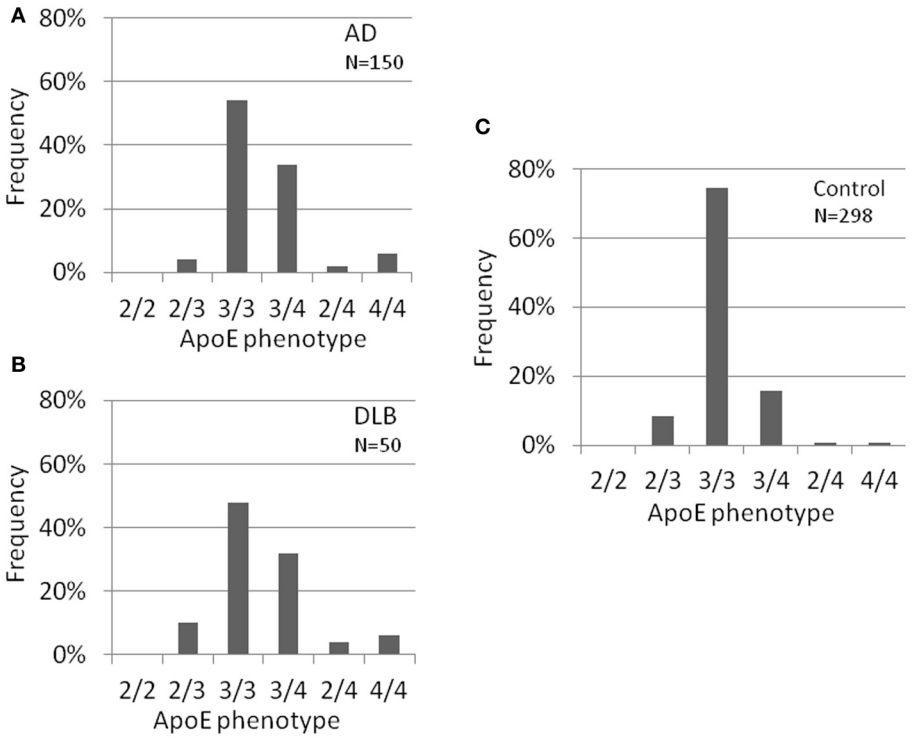

FIGURE 3 | ApoE carrier statuses of AD (A), DLB (B), and healthy volunteers (control) (C). ApoE carrier statuses are significantly different between AD and control, and between DLB and control. However, no significant differences were observed between AD and DLB. ApoE typing was done using pcr and restriction enzyme digestion using genomic DNA. AD, Alzheimer's disease; DLB, dementia with Lewy bodies.

reported that ApoE4 carrier frequency was the highest in AD among AD, DLB, and control groups, and it was higher in DLB than in control groups (Carrillo Garcia et al., 2008). Other findings have shown that ApoE4 carrier and allelic frequencies were comparable for those with AD and DLB [(Kobayashi et al., 2011) and **Table 1**].

Our results for annexin A5 and ApoE4 also revealed similar characteristics for both AD and DLB patients.

DIFFERENCE BETWEEN AD AND DLB

It is apparent that DLB differs from AD in the disease progression and cure response experienced by patients. Accordingly, early differentiation between the two forms of dementia is important for effective and safe management (Aarsland et al., 2008; Sinha et al., 2011). CSF levels of tau protein have been shown to be significantly lower in DLB than in AD, which may help to differentiate between the two diseases (Mollenhauer et al., 2005a,b). On the other hand, another study also suggests that the concentration of phosphorylated tau in CSF, which is highly correlated with total tau levels, may provide a higher specificity to differentiate AD and DLB (Vanderstichele et al., 2006). α-Synuclein is the major constituent of Lewy bodies found in neurons in DLB. As a consequence of increased accumulation of α-synuclein intraneuronally in DLB, several studies have attempted its quantification in CSF. α-Synuclein has been shown to induce disruption of cellular inorganic ion homeostasis such as Ca^{2+}, leading to cell death (Lowe et al., 2004; Danzer et al., 2007; Ying et al., 2011). Whereas some groups show a decrease in the total concentration of CSF α-synuclein in DLB in comparison to other dementias (Mollenhauer et al., 2008; Kasuga et al., 2010), other groups do not find the significant difference for DLB (Spies et al., 1998; Noguchi-Shinohara et al., 2009). Thus, future study on the discrimination of these diseases is expected.

ABOUT BIOMARKERS

One of the main focuses of public health is prevention of disease. Different stages in the disease process can be targeted for preventative action, including prior to development of the disease, during the asymptomatic stage, and following clinical diagnosis. Therefore, three stages of prevention can be recognized (Wright et al., 2009; Weber et al., 2012).

From the CSF proteins identification, and MRI and PET imaging studies, the alteration of both CSF biomarkers ($A\beta_{42}$ and Tau) takes place prior to the appearance of brain structural change or dementia symptoms (Jack et al., 2010). Our *in vitro* data demonstrated that annexin A5 is elevated following the stimulation by $A\beta_{42}$ (Yamaguchi et al., 2010). Thus, onset of the annexin A5 elevation in dementia occurs at the similar time to the deposition of $A\beta_{42}$. Annexin A5 might be expected to be useful in the secondary and tertiary stages. It is conceivable that the appropriate stage for utilizing each biomarker candidate is dependent upon the properties of the biomarker. Therefore, to determine when each biomarker candidate should be utilized it will be necessary

to examine the significance of any biological changes that appear at various stages.

Discrimination between neurodegenerative and non-neurodegenerative dementia is another expectation for biomarkers. Shared clinical symptoms between AD and depression in elderly have been reported (Starkstein et al., 2005), which might lead to confusion in medical intervention. Our preliminary data suggest that plasma annexin A5 levels of the six patients with depression was comparable with controls (data not shown), which might implicate annexin A5 as a biomarker for discriminating between neurodegenerative and non-neurodegenerative diseases.

Biomarkers should be reliable, reproducible, non-invasive, simple to perform, and inexpensive. To achieve this role both protein-based and genetic biomarkers have been particularly investigated. Especially plasma biomarker is beneficial by being less invasive in comparison with CSF biomarker. Gene typing is also less invasive since it is available with leukocytes from a blood sample and genetic biomarkers are of great use. ApoE4 ε4 is widely recognized as a potential biomarker for the risk of AD. As we demonstrated in this paper, ApoE ε4 is also a risk factor for DLB, indicating that ApoE ε4 is unable to discriminate between AD and DLB. No applicable genetic marker for such purpose has been reported. Detailed molecular mechanism of the onset of both AD and DLB may be needed to explore genetic factors.

ACKNOWLEDGMENTS

We thank Mr. Kenneth E. Hartman for critical reading of the manuscript. This study was supported by grants from the Ministry of Health, Labor, and Welfare of Japan and from the Ministry of Education, Culture, Sports, Science, and Technology of Japan (grant number 24591686).

REFERENCES

Aarsland, D., Kurz, M., Beyer, M., Bronnick, K., Nore, S. P., and Ballard, C. (2008). Early discriminatory diagnosis of dementia with Lewy bodies. *Dement. Geriatr. Cogn. Disord.* 25, 195–205.

Andreasen, N., Minthon, L., Davidsson, P., Vanmechelen, E., Vanderstichele, H., Winblad, B., et al. (2001). Elevation of CSF-tau and CSF-Aβ42 as diagnostic markers for Alzheimer disease in clinical practice. *Arch. Neurol.* 58, 373–379.

Bedrood, S. S., Jayasinghe, D., Sieburth, M., Chen, S., Erbel, P. C., Butler, R., et al. (2009). Annexin A5 direcly interacts with amyloidogenic proteins and reduces their toxicity. *Biochemistry* 48, 10568–10576.

Bertram, L., and Tanzi, R. E. (2008). Thirty years of Alzheimer's disease genetics: the implications of systematic meta-analysis. *Nat. Rev. Neurosci.* 9, 768–778.

Carrillo Garcia, F., Gil Neciga, E., Alberca, R., Garcia-Solis, D., Millan, J., Rodriguez Uranga, J. J., et al. (2008). Apolipoprotein ε4 in dementia with Lewy bodies. *Neurologia* 23, 152–156.

Danzer, K. M., Haasen, D., Karow, A. R., Moussaud, S., Habeck, M., Giese, A., et al. (2007). Different species of alpha-synuclein oligomers induce calcium influx and seeding. *J. Neurosci.* 27, 9220–9232.

Dong, L.-M., and Weisgraber, K. H. (1996). Human apolipoprotein E4 domain interaction. Arginine 61 and glutamic acid 255 interact to direct the preference for very low density lipoproteins. *J. Biol. Chem.* 271, 19053–19057.

Dong, L.-M., Wilson, C., Wardell, M. R., Simmons, T., Mahley, R. W., Weisgraber, K. H., et al. (1994). Human apolipoprotein E. Role of arginine 61 in mediating the pipoprotein preferences of the E3 and E4 isoforms. *J. Biol. Chem.* 269, 22358–22365.

Gomez-Tortosa, E., Gonzalo, I., Fanjul, S., Sainz, M. J., Cantarero, S., Cemillan, C., et al. (2003). Cerebrospinal fluid markers in dementia with Lewy bodies compared with Alzheimer disease. *Arch. Neurol.* 60, 1218–1222.

Hasegawa, K. (1983). "The clinical assessment of dementia in the aged: a dementia screening scale for grading the cognitive state of patients for clinician," in *Aging in the Eighties and Beyond*, ed M. E. A. Bergener (New York, NY: Springer), 207–218.

Hatters, D. M., Peters-Libeu, C. A., and Weisgraber, K. H. (2006). Apolipoprotein E structure: insights into function. *Trends Biochem. Sci.* 31, 445–454.

Hixson, J. E., and Vernier, D. T. (1990). Restriction isotyping of human apolipoprotein E by gene amplification and cleavage with HhaI. *J. Lipid Res.* 31, 545–548.

Jack, C. R. Jr., Knopman, D. S., Jagust, W. J., Shaw, L. M., Aisen, P. S., Weiner, M. W., et al. (2010). Hypothetical model of dynamic biomarkers of the Alzheimer's pathological cascade. *Lancet Neurol.* 9, 119–128.

Kasuga, K., Tokutake, T., Ishikawa, A., Uchiyama, T., Tokuda, T., Onodera, O., et al. (2010). Differential levels of α-synuclein, β-amyloid42 and tau in CSF between patients with dementia with Lewy bodies and Alzheimer's disease. *J. Neurol. Neurosurg. Psychiatry* 81, 608–610.

Kim, J., Basak, J. M., and Holtzman, D. M. (2009). The role of apolipoprotein E in Alzheimer's disease. *Neuron* 63, 287–303.

Kobayashi, S., Tateno, M., Park, T. W., Utsumi, K., Sohma, H., Ito, Y. M., et al. (2011). Apolipoprotein E4 frequencies in a Japanese population with Alzheimer's disease and dementia with Lewy bodies. *PLoS ONE* 6:e18569. doi: 10.1371/journal.pone.0018569

LaFerla, F. M. (2002). Calcium dyshomeostasis and intracellular signalling in Alzheimer's disease. *Nat. Rev. Neurosci.* 3, 862–872.

Litvan, I., Bhatia, K. P., Burn, D. J., Goetz, C. G., Lang, A. E., McKeith, I., et al. (2003). SIC task force appraisal of clinical diagnostic criteria for Parkinsonian disorders. *Mov. Disord.* 18, 467–486.

Lowe, R., Pountney, D. L., Jensen, P. H., Gai, W. P., and Voelcker, N. (2004). Calcium (II) selectively induces α-synuclein annular oligomers via interaction with the C-terminal domain. *Protein Sci.* 13, 3245–3252.

Mahley, R. W. (1988). Apolipoprotein E: cholesterol transport protein with expanding role in cell biology. *Science* 240, 622–629.

Masuda, J., Takayama, E., Satoh, A., Ida, M., Shinohara, T., Kojima-Aikawa, K., et al. (2004). Levels of annexin IV and V in the plasma of pregnant and postpartum women. *Thromb. Haemost.* 91, 1129–1136.

Mattson, M. P. (2004). Pathways towards and away from Alzheimer's disease. *Nature* 430, 631–639.

McKeith, I., Mintzer, J., Aarsland, D., Burn, D., Chiu, H., Cohen-Mansfield, J., et al. (2004). Dementia with Lewy bodies. *Lancet Neurol.* 3, 19–28.

McKeith, I. G., Dickson, D. W., Lowe, J., Emre, M., O'Brien, J. T., Feldman, H., et al. (2005). Diagnosis and management of dementia with Lewy bodies: third report of the DLB Consortium. *Neurology* 65, 1863–1872.

McKhann, G., Drachman, D., Folstein, M., Katzman, R., Price, D., and Stadlan, E. M. (1984). Clinical diagnosis of Alzheimer's disease: report of the NINCDS-ADRDA work group under the auspices of department of health and human services task force on Alzheimer's disease. *Neurology* 34, 939–944.

Mollenhauer, B., Bibl, M., Trenkwalder, C., Stiens, G., Cepek, L., Steinacker, P., et al. (2005a). Follow-up investigation in cerebrospinal fluid of patients with dementia with Lewy bodies and Alzheimer's disease. *J. Neural Transm.* 112, 933–948.

Mollenhauer, B., Cepek, L., Bibl, M., Wiltfang, J., Schulz-Schaeffer, W. F., Ciesielczyk, B., et al. (2005b). Tau protein, Aβ42 and S-100B protein in cerebrospinal fluid of patients with dementia with Lewy bodies. *Dement. Geriatr. Cogn. Disord.* 19, 164–170.

Mollenhauer, B., Cullen, V., Kahn, I., Krastins, B., Outeiro, T. F., Pepivani, I., et al. (2008). Direct quantification of CSF alpha-synuclein by ELISA and first cross-sectional study in patients with neurodegeneration. *Exp. Neurol.* 213, 315–325.

Noguchi-Shinohara, M., Tokuda, T., Yoshita, M., Kasai, T., Ono, K., Nakagawa, M., et al. (2009). CSF alpha synuclein levels in dementia with Lewy bodies and Alzheimer's disease. *Brain Res.* 1251, 1–6.

Paolo, G. D., and Kim, T.-W. (2011). Linking lipids to Alzheimer's disease: cholesterol and beyond. *Nat. Rev. Neurosci.* 12, 284–296.

Singletona, A. B., Whartona, A., O'Briena, K. K., Walker, M. P., McKeith, I. G., Ballard, C. G., et al. (2002). Clinical and neuropathological correlates of apolipoprotein E genotype in Dementia with Lewy Bodies. *Dement. Geriatr. Cogn. Disord.* 167–175.

Sinha, N., Firbank, M., and O'Brien, J. T. (2011). Biomarkers in dementia with Lewy bodies: a review. *Int. J. Geriatr. Psychiatry* 27, 443–453.

Spies, C. D., Kissner, M., Neumann, T., Blum, S., Voigt, C., Funk, T., et al. (1998). Elevated carbohydrate-deficient transferrin predicts prolonged intensive care unit stay in traumatized men. *Alcohol Alcohol.* 33, 661–669.

Starkstein, S. E., Jorge, R., Mizrahi, R., and Robinson, R. G. (2005). The construct of minor and major depression in Alzheimer's disease. *Am. J. Psychiatry* 162, 2086–2093.

Vanderstichele, H., De Vreese, K., Blennow, K., Andreasen, N., Sindic, C., Ivanoiu, A., et al. (2006). Analytical performance and clinical utility of the INNOTEST PHOSPHO-TAU181P assay for discrimination between Alzheimer's disease and dementia with Lewy bodies. *Clin. Chem. Lab. Med.* 44, 1472–1480.

Varma, A. R., Snowden, J. S., Lloyd, J. J., Talbot, P. R., Mann, D. M. A., and Neary, D. (1999). Evaluation of the NINCDS-ADRDA criteria in the differentiation of Alzheimer's disease and frontotemporal dementia. *J. Neurol. Neurosurg. Psychiatry* 66, 184–188.

Weber, G. F., Warren, J., Sohma, H., Chen, T., Halim, A., and Chakravarty, G. (2012). Biomarkers—a pot of gold or a can of worms? Meeting report from the 2nd World Congress on Biomarkers and Clinical Research, 2011, Baltimore, USA. *Cancer Biol. Ther.* 13, 831–835.

Wright, C. F., Hall, A., Matthews, F. E., and Brayne, C. (2009). Biomarkers, dementia, and public health. *Ann. N.Y. Acad. Sci.* 1180, 11–19.

Yamaguchi, M., Kokai, Y., Imai, S., Utsumi, K., Matsumoto, K., Honda, H., et al. (2010). Investigation of annexin A5 as a biomarker for Alzheimer's disease using neuronal cell culture and mouse model. *J. Neurosci. Res.* 88, 2682–2692.

Ying, Z., Lin, F., Gu, W., Su, Y., Arshad, A., Quuing, H., et al. (2011). α-Synuclein increases U251 cells vulnerability to hydrogen peroxide by disrupting calcium homeostasis. *J. Neural Transm.* 118, 1165–1172.

Conflict of Interest Statement: The authors declare that the research was conducted in the absence of any commercial or financial relationships that could be construed as a potential conflict of interest.

Received: 23 December 2012; accepted: 19 March 2013; published online: 05 April 2013.

*Citation: Sohma H, Imai S-i, Takei N, Honda H, Matsumoto K, Utsumi K, Matsuki K, Hashimoto E, Saito T and Kokai Y (2013) Evaluation of annexin A5 as a biomarker for Alzheimer's disease and dementia with lewy bodies. Front. Aging Neurosci. **5**:15. doi: 10.3389/fnagi.2013.00015*

frontiers in
AGING NEUROSCIENCE

REVIEW ARTICLE
published: 21 February 2013
doi: 10.3389/fnagi.2013.00006

Cerebrospinal fluid biomarkers for differentiation of frontotemporal lobar degeneration from Alzheimer's disease

David J. Irwin*[1,2]*, John Q. Trojanowski*[1] *and Murray Grossman*[2]*

[1] *Department of Pathology and Laboratory Medicine, Center for Neurodegenerative Disease Research, Alzheimer's Disease Core Center, Institute on Aging, University of Pennsylvania, Philadelphia, PA, USA*

[2] *Department of Neurology, Center for Frontotemporal Dementia, Perelman School of Medicine, University of Pennsylvania, Philadelphia, PA, USA*

Edited by:
Manuel Menéndez-González, Hospital Álvarez-Buylla, Spain

Reviewed by:
Junming Wang, University of Mississippi Medical Center, USA
Angela de Iuliis, University of Padova, Italy

****Correspondence:***
Murray Grossman, Department of Neurology, University of Pennsylvania School of Medicine, Hospital of the University of Pennsylvania, 3400 Spruce Street, Philadelphia, PA 19104, USA.
e-mail: mgrossma@mail.med.upenn.edu

Accurate ante mortem diagnosis in frontotemporal lobar degeneration (FTLD) is crucial to the development and implementation of etiology-based therapies. Several neurodegenerative disease-associated proteins, including the major protein constituents of inclusions in Alzheimer's disease (AD) associated with amyloid-beta ($A\beta_{1-42}$) plaque and tau neurofibrillary tangle pathology, can be measured in cerebrospinal fluid (CSF) for diagnostic applications. Comparative studies using autopsy-confirmed samples suggest that CSF total-tau (t-tau) and $A\beta_{1-42}$ levels can accurately distinguish FTLD from AD, with a high t-tau to $A\beta_{1-42}$ ratio diagnostic of AD; however, there is also an urgent need for FTLD-specific biomarkers. These analytes will require validation in large autopsy-confirmed cohorts and face challenges of standardization of within- and between-laboratory sources of error. In addition, CSF biomarkers with prognostic utility and longitudinal study of CSF biomarker levels over the course of disease are also needed. Current goals in the field include identification of analytes that are easily and reliably measured and can be used alone or in a multi-modal approach to provide an accurate prediction of underlying neuropathology for use in clinical trials of disease modifying treatments in FTLD. To achieve these goals it will be of the utmost importance to view neurodegenerative disease, including FTLD, as a clinicopathological entity, rather than exclusively a clinical syndrome.

Keywords: cerebrospinal fluid, biomarker, tau, $A\beta_{1-42}$, frontotemporal dementia, primary progressive aphasia, Alzheimer's disease

INTRODUCTION

Most neurodegenerative diseases are characterized by specific abnormally-modified protein aggregates, with resulting neuronal cell loss and gliosis. The gold standard for diagnosis is microscopic examination at autopsy; however, there is considerable variability of clinical manifestations associated with underlying neuropathological diagnoses, as clinical symptoms most often reflect the regional burden of pathology within the central nervous system (CNS) rather than the specific underlying proteinopathy. This is especially true in the heterogeneous family of frontotemporal lobar degeneration (FTLD) clinical syndromes.

Two main pathologic FTLD subtypes exist (**Figures 1A**, **2**): cases with inclusions formed from the microtubule-binding protein tau (FTLD-tau) and those with TAR DNA binding protein-43 (TDP-43) pathology (FTLD-TDP) (Mackenzie et al., 2010). FTLD-tau includes the following tauopathies (**Figures 2A–D**): Pick's disease (PiD), corticobasal degeneration (CBD), progressive supranuclear palsy (PSP), FTD and parkinsonism linked to chromosome 17 (pathogenic *MAPT* mutations; FTDP-17), and unclassifiable tauopathies (Mackenzie et al., 2010). FTLD-TDP (**Figures 2E–G**) can be subdivided into four subtypes (A–D) based on the morphology and distribution of lesions (Mackenzie et al., 2011) and can also be associated with TDP-43 inclusions in the anterior horn of the spinal cord and gliosis of the corticospinal tracts, suggesting a continuum of FTLD with amyotrophic lateral sclerosis (ALS; FTLD-ALS) (Geser et al., 2008, 2009). A smaller number of FTLD cases are associated with inclusions of another DNA-binding protein, fused-in-sarcoma protein (*FUS;* FTLD-FUS), or other rare, less-defined pathologies (FTLD-UPS, FTLD-ni) (Mackenzie et al., 2010). The major

Abbreviations: FTLD, frontotemporal lobar degeneration; AD, Alzheimer's disease; Aβ, amyloid-beta; CSF, cerebrospinal fluid; CNS, central nervous system; FTLD-tau, FTLD with tau pathology; TDP-43, TAR DNA binding protein-43; FTLD-TDP, FTLD with TDP pathology; PiD, Pick's disease; CBD, corticobasal degeneration; PSP, progressive supranuclear palsy; pathogenic *MAPT* mutations-FTDP-17, FTD and parkinsonism linked to chromosome 17; ALS, amyotrophic lateral sclerosis; FUS, fused-in-sarcoma protein; FTLD-FUS, FTLD with FUS pathology; FTLD-UPS, FTLD with tau- and TDP-43-negative ubiquitinated inclusions; FTLD-ni, FTLD in the absence of significant neuropathological inclusions; *GRN*, progranulin gene; *MAPT*, tau gene; *C9orf72*, C9orf72 gene; *VCP*, valosin-containing protein gene; *TARDBP*, TDP-43 gene; FTLD-ALS, clinical FTLD with ALS; *CHMP2B*, charged mutlivesciular body protein 2B gene; bvFTD, behavioral-variant frontotemporal dementia; PPA, primary progressive aphasia; lvPPA, logopenic-variant PPA; svPPA, semantic-variant PPA; naPPA, non-fluent aggramatic variant PPA; CBS, corticobasal syndrome; $A\beta_{1-42}$, β-amyloid; MCI, mild cognitive impairment; t-tau, total-tau; p-tau, phosphorylated-tau; $p\text{-}tau_{181}$, phosphorylated tau at serine 181; $p\text{-}tau_{231}$, phosphorylated tau at threonine 231; ELISA, enzyme-linked immunosorbent assay; xMAP, luminex flow immunoassay; MRI, magnetic resonance imaging; DIAN, dominantly-inherited AD network; MTBD, microtubule-binding domain; DTI, diffusion-tensor imaging; GM, gray matter; GWAS, genome-wide association studies.

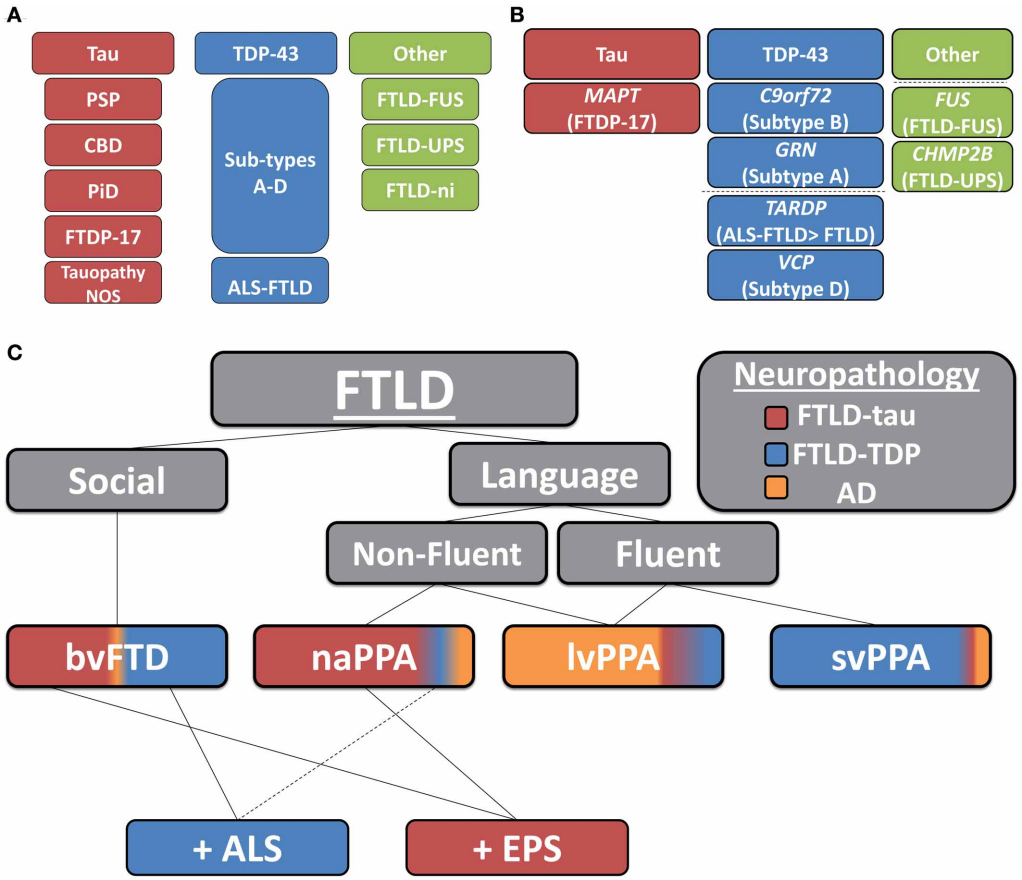

FIGURE 1 | Clinicopathological and genetic associations in FTLD. **(A)** Neuropathological classification of FTLD-tau and FTLD-TDP subtypes (PSP, progressive supranuclear palsy; CBD, corticobasal degeneration; PiD, Pick's disease; FTDP17, frontotemporal dementia with Parkinsonism linked to chromosome 17; Tauopathy NOS, unclassifiable tauopathy; Subtypes A–D, morphological subtypes of FTLD-TDP; ALS-FTLD, amyotrophic lateral sclerosis with FTLD-TDP; FTLD-FUS, FTLD with fused in sarcoma protein inclusions; FTLD-UPS, FTLD with tau- and TDP-43-negative ubiquitinated inclusions; FTLD-ni, FTLD in the absence of significant neuropathological inclusions), **(B)** pathogenic mutation associations with underlying neuropathology (dashed-line separates less common molecular etiologies of FTLD; *MAPT*, tau resulting in FTDP-17; *C90rf72*, pathogenic hexanucleotide expansion resulting in FTLD and/or ALS associated with FTLD-TDP B; *GRN*, progranulin resulting in FTLD-TDP type A; *TARDP*, TDP-43 resulting in ALS ± FTLD and less commonly FTLD; *VCP*, valosin-containing protein resulting in inclusion body myopathy with Paget's disease of bone and frontotemporal dementia with FTLD-TDP subtype D; *FUS*, fused-in sarcoma protein resulting in FTLD-FUS; and *CHMP2B*, charged mutlivesciular body protein 2B resulting in FTLD-UPS), **(C)** clinicopathological correlations of FTLD (colored regions of clinical syndromes represent relative percentages of neuropathological subtypes found in autopsy studies; AD, Alzheimer's disease; bvFTD, behavioral variant of FTLD; PPA, primary progressive aphasia; svPPA, semantic variant PPA; naPPA, nonfluent agrammatic variant PPA; lvPPA, logopenic variant PPA; +ALS, co-morbid amyotrophic lateral sclerosis; +EPS, co-morbid extra-pyramidal Parkinsonian symptoms: i.e., features of akinetic-rigid syndromes of PSP or corticobasal syndrome).

genetic etiologies resulting in FTLD are exclusively associated with specific underlying neuropathologies (**Figure 1B**), despite heterogeneous expression of FTLD clinical syndromes, and include pathogenic mutations in the gene for progranulin (*GRN*) (Baker et al., 2006; Cruts et al., 2006), tau (*MAPT*) (Hutton et al., 1998), and C9orf72 (*C9orf72)* (Dejesus-Hernandez et al., 2011; Renton et al., 2011). Less common genetic etiologies of FTLD include: valosin-containing protein (*VCP*) resulting in inclusion body myopathy with Paget's disease of bone and frontotemporal dementia with FTLD-TDP subtype D neuropathology, *TARDBP* coding for TDP-43 protein and causing ALS or ALS-FTLD (rarely FTLD-TDP alone), *CHMP2B* coding for charged mutlivesciular body protein 2B and resulting in FTLD-UPS, and mutations in *FUS* causing FTLD-FUS (**Figure 1B**) (Mackenzie et al., 2010).

Clinically, FTLD can be broadly divided into two main subtypes, those with predominant behavioral and social comportment disorder (behavioral-variant frontotemporal dementia, bvFTD) (Rascovsky et al., 2011) and those with primary language disturbances (primary progressive aphasia, PPA) (Mesulam, 1982, 2001). Among PPA patients, three subgroups have been recently divided (Gorno-Tempini et al., 2011) into the logopenic (lvPPA) (Gorno-Tempini et al., 2004, 2008), semantic (svPPA) (Hodges and Patterson, 2007), and non-fluent aggramatic variant (naPPA) (Turner et al., 1996). Clinicopathological correlations of these syndromes are complex (Josephs, 2008; Grossman, 2010). For example, large studies of autopsy-confirmed FTLD (behavioral and aphasic variants) find roughly equal numbers of FTLD-tau and FTLD-TDP (Hodges et al., 2004; Kertesz et al.,

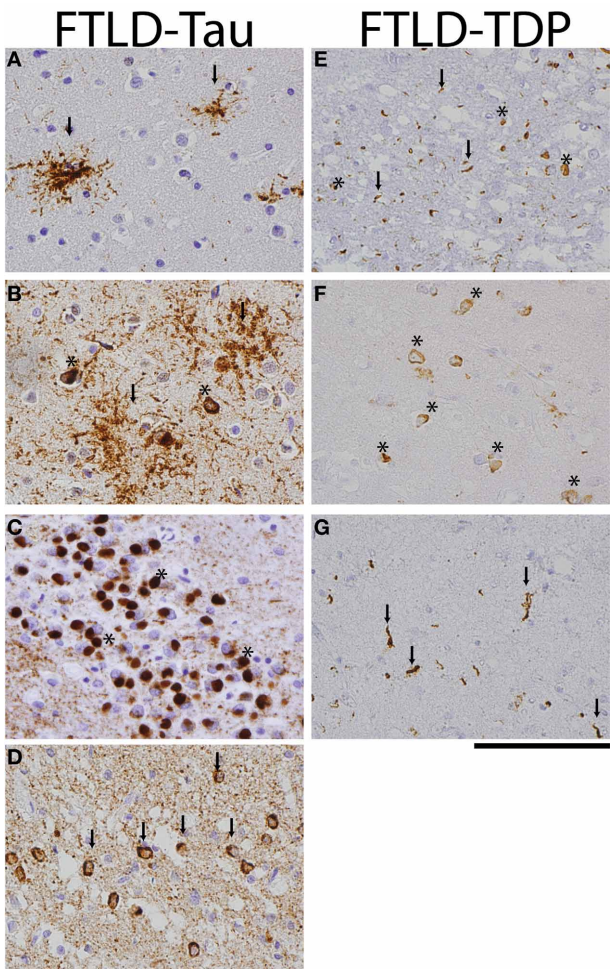

FIGURE 2 | FTLD-Tau and FTLD-TDP histology. Photomicrographs of FTLD-tau **(A–D)** and FTLD-TDP **(E–G)** visualized with immunohistochemistry (PHF-1 and pTDP 409/410 for tau and TDP, respectively). **(A)** PSP frontal cortex with tau-positive tufted astrocytes (arrows), **(B)** CBD temporal cortex with diffuse astrocytic plaques (arrows) and neuronal tangles (asterisks), **(C)** Pick's disease with round tau-positive Pick bodies (asterisks) in the dentate nucleus of the hippocampus, **(D)** FTDP-17 case with p.P301L pathogenic mutation with tau-positive neuronal tangles (arrows) and diffuse neuropil threads in temporal cortex, **(E)** FTLD-TDP subtype A with cytoplasmic neuronal inclusions (asterisks) and short dystrophic neurites (arrows) in superficial layers of frontal cortex, **(F)** FTLD-TDP subtype B with prominent cytoplasmic inclusions (asterisks) in deep temporal cortical layer, and **(G)** long dystrophic neurites (arrows) in superficial layers of mid-frontal cortex of a patient with FTLD-TDP subtype C. Scale bar = 100 μm.

2005; Knopman et al., 2005; Shi et al., 2005; Forman et al., 2006). Furthermore, a primary neuropathological diagnosis of Alzheimer's disease (AD) has been found in up to 30% of autopsy-confirmed clinically defined FTLD cohorts (Kertesz et al., 2005; Knopman et al., 2005; Forman et al., 2006; Knibb et al., 2006). Examination of focal presentations of AD found it to be the primary diagnosis in 7% of bvFTD, 44% of naPPA, 10% of svPPA, and 50% of the extrapyramidal and cognitive disorder, corticobasal syndrome (CBS) patients (Alladi et al., 2007). Others have also found a substantial proportion of AD in PPA cases (Forman et al., 2006; Knibb et al., 2006) especially in lvPPA (Grossman et al., 2008; Mesulam et al., 2008; Grossman, 2010) and also CBS (Lee et al., 2011). Thus, differentiation of AD and FTLD spectrum disorders poses a serious diagnostic challenge for clinicians.

Within the FTLD neuropathological spectrum, examination of the specific clinical subtypes finds varying degrees of association with FTLD-tau and FTLD-TDP (**Figure 1C**). FTLD-tau has been overrepresented in some naPPA cohorts (Hodges et al., 2004; Josephs et al., 2006a,b; Knibb et al., 2006; Snowden et al., 2007; Mesulam et al., 2008; Grossman et al., 2012), especially when associated with apraxia of speech (Josephs et al., 2006a; Snowden et al., 2007) and svPPA has been predominantly associated with TDP-43 pathology (Hodges et al., 2004; Josephs et al., 2006a; Snowden et al., 2007; Grossman et al., 2008); while bvFTD contains similar proportions of FTLD-tau and FTLD-TDP (Forman et al., 2006; Josephs et al., 2006b; Snowden et al., 2007). Extrapyramidal symptoms may predict a tauopathy (Forman et al., 2006; Josephs et al., 2006b) while co-morbid ALS is almost certainly due to TDP-43 aggregation (Shi et al., 2005; Forman et al., 2006; Josephs et al., 2006b). Clinicopathological associations from these large autopsy studies are summarized in **Figure 1C**.

A major challenge in the development and implementation of disease-modifying therapy in FTLD is the accurate identification of the neuropathological diagnosis during life, including differentiation from AD, so that patients may be triaged to the appropriate protein-targeted therapy (i.e., tau or TDP-43 targeted agents).

Biofluid biomarkers have the potential to optimize diagnostic accuracy and detect disease earlier in the course of an illness and possibly pre-symptomatically, such as prior to structural changes of neurodegeneration seen on neuroimaging (Hu et al., 2010a; Jack et al., 2010), making further exploration in this area promising for the development of disease modifying treatments. In addition, some clinical measures of disease progression in FTLD, including functional scales, may be limited by floor- and ceiling-effects (Knopman et al., 2008), so biofluid biomarkers are potentially attractive surrogate end points for use in clinical trials (Boxer et al., 2012b). The cerebrospinal fluid (CSF) is relatively easy to obtain and contains a direct connection to the pathological milieu in central nervous system, making it a desirable biofluid for study. In this review we will discuss the current state of CSF biomarker research in FTLD in terms of differentiation from AD and future directions and challenges for the field in development of FTLD-specific biomarkers.

ALZHEIMER'S DISEASE RELATED CSF BIOMARKERS: $A\beta_{1-42}$ AND tau

STUDIES IN ALZHEIMER'S DISEASE

As a first step in biofluid-based biomarker assessment of neurodegenerative disease, it is valuable to distinguish broadly between AD and FTLD. CSF values of the major constituents of AD pathology, tau and β-amyloid, ($A\beta_{1-42}$) have been widely studied using immune-based analytical platforms in AD and amnestic mild cognitive impairment (MCI) patients, with lower $A\beta_{1-42}$ values and higher levels of total- and phosphorylated-tau (t-tau, p-tau) compared with controls across multiple large studies (Shaw et al.,

2009, 2011; De Meyer et al., 2010; Trojanowski et al., 2010; Weiner et al., 2010). Furthermore, our group has shown prognostic utility of these markers by accurately predicting MCI conversion to AD (Shaw et al., 2009; De Meyer et al., 2010).

The majority of atypical clinical presentations of AD in early-onset patients consisting of predominantly visuo-spatial difficulties (i.e., consistent with poster cortical atrophy) or asymmetric apraxia/rigidity (i.e., consistent with CBS) may have a similar CSF biomarker profile to that of typical amnestic-AD (De Souza et al., 2011; Seguin et al., 2011), with a further elevated t-tau level in one study (Koric et al., 2010). Elevated CSF t-tau and low $A\beta_{1-42}$ levels have also been described in some PPA patients (i.e., lvPPA) (Bibl et al., 2011; De Souza et al., 2011) most likely due to underlying AD neuropathology in these individuals; however, to our knowledge no autopsy-confirmed studies of atypical clinical AD presentations have been performed.

The exact relationship between AD neuropathologic change (i.e., tau neurofibrillary pathology and $A\beta_{1-42}$ extracellular plaques) and observed measurement of these analytes in CSF is unclear; however, the total tau level is thought to reflect underlying neurodegeneration and neuron loss, as elevations are also seen in other CNS insults (Otto et al., 1997; Hesse et al., 2000; Jin et al., 2006; Ost et al., 2006; Krut et al., 2013). Lower $A\beta_{1-42}$ CSF levels may be the result of sequestration of soluble interstitial brain $A\beta_{1-42}$ into extracellular plaques as there is an inverse correlation of CSF $A\beta_{1-42}$ levels and the degree of cortical plaque pathology (Tapiola et al., 2009; Patel et al., 2012; Seppala et al., 2012) and *in vivo* neuroimaging evidence of amyloidosis (Fagan et al., 2006). Phosphorylated epitopes of tau (p-tau) can be measured in CSF as well; while most phospho-epitopes of tau are also found in healthy non-diseased brains and are not AD-specific, pathological tau species overall are highly phosphorylated in AD (Matsuo et al., 1994) and this altered state reflects the elevated levels of p-tau seen in AD. The most commonly studied p-tau epitopes are serine 181 ($p\text{-}tau_{181}$) (Vanmechelen et al., 2000), and threonine 231 ($p\text{-}tau_{231}$) (Buerger et al., 2002a,b).

STUDIES IN FRONTOTEMPORAL LOBAR DEGENERATION

FTLD is not characterized pathologically by cerebral $A\beta_{1-42}$ amyloidosis, and only FTLD-tau is characterized by significant tau inclusions. From this perspective, measures of CSF t-tau and $A\beta_{1-42}$ may have helpful diagnostic utility in excluding AD neuropathology. Indeed, in clinically-defined cohorts AD cases have higher levels of t-tau, $p\text{-}tau_{181}$ and lower levels of $A\beta_{1-42}$ compared to FTLD and controls in group-wise comparisons (Blennow et al., 1995; Arai et al., 1997; Green et al., 1999; Sjogren et al., 2000a, 2001; Vanmechelen et al., 2000; Riemenschneider et al., 2002; Clark et al., 2003; Pijnenburg et al., 2004, 2007; Schoonenboom et al., 2004, 2012; Engelborghs et al., 2006; Bibl et al., 2007, 2011; Kapaki et al., 2008; Verwey et al., 2010; De Souza et al., 2011; Gabelle et al., 2011; Van Harten et al., 2011).

A major challenge in FTLD CSF biomarker studies is the heterogeneity of the condition (**Figure 1**), making autopsy-confirmation of diagnostic classification a crucial issue. As mentioned previously, up to 30% of clinically-defined FTLD cohorts may have underlying AD neuropathologic change as the etiology of their symptoms (Kertesz et al., 2005; Knopman et al., 2005; Forman et al., 2006; Knibb et al., 2006) and contamination with these atypical AD cases could influence results significantly. Indeed, examination of diagnostic accuracy of CSF t-tau and $A\beta_{1-42}$ in a large autopsy-confirmed dementia cohort found that use of the clinical diagnosis, rather than neuropathological diagnosis as the gold standard for biomarker performance resulted in a 10–20% underestimation of biomarker accuracy (Toledo et al., 2012). Furthermore, since 1995 there has been over a 10-fold increase in the number of FTLD manuscripts published (NLM/NIH, 2012) and due to this exponential increase in research in the field and our expanding knowledge of FTLD, clinical criteria (Gorno-Tempini et al., 2011; Rascovsky et al., 2011) have evolved resulting in refinement of our clinical definitions. Indeed, the emergence of the new clinical variant of PPA, lvPPA (Gorno-Tempini et al., 2008, 2011), which is most often associated with AD neuropathology (Mesulam et al., 2008; Rabinovici et al., 2008; Grossman, 2010) (**Figure 1C**), and therefore suggested to be excluded from FTLD clinical trials (Knopman et al., 2008), could influence group-wise CSF tau and $A\beta_{1-42}$ results. Thus, the makeup of clinical cohorts used in earlier studies may not be entirely translatable to newer studies, limiting the meaningful interpretation of the literature of clinically-derived cohorts.

As such, study of autopsy/genetic-confirmed cases has been a focus for our center. In an early study of autopsy-confirmed cases by our group, AD was differentiated from a mixed dementia cohort (including 13 FTLD cases) with reasonable sensitivity (72%) and specificity (69%) using CSF t-tau levels (Clark et al., 2003). Focused analysis of FTLD (with autopsy confirmation in 9 cases) in a later study found lower levels of t-tau and higher levels of $A\beta_{1-42}$ than AD, and roughly 30% of FTLD cases had significantly decreased t-tau from controls (Grossman et al., 2005). In a follow-up large autopsy/genetically confirmed FTLD series ($n = 30$) t-tau levels were significantly lower in FTLD than AD, while similar to controls on group-wise comparison; individual-case analysis revealed that a considerable subset of FTLD patients had markedly low t-tau values (Bian et al., 2008). Interestingly, FTLD cases with substantially lower t-tau levels included both FTLD-tau and FTLD-TDP (Bian et al., 2008), although a non-significant trend was found for lower t-tau in FTLD-tau (Hu et al., 2011). Furthermore, FTLD was differentiated from AD with high accuracy using the t-tau/$A\beta_{1-42}$ ratio; that is, FTLD cases had a lower ratio (lower t-tau and higher $A\beta_{1-42}$) (Bian et al., 2008).

Measurement of these analytes in the CSF in most studies utilizes one of two immune-based platforms: enzyme-linked immunosorbent assay (ELISA; Innotest, Innogenetics), and a multiplex assay based on flow-cytometry of antibody-coated fluorescent beads (INNO-BIA AlzBio3 xMAP; Luminex, Innogenetics). Absolute values obtained from these platforms differ because the coefficient of variance (%CV) with the xMAP Luminex platform is much narrower than with ELISA, but they are highly correlated (Olsson et al., 2005; Lewczuk et al., 2009; Fagan et al., 2011; Wang et al., 2012) and have similar levels of diagnostic accuracy for AD (Fagan et al., 2011; Wang et al., 2012) and differentiating AD from FTLD (Toledo et al., 2012). Thus, values from one platform can be effectively transformed into equivalent units of the other using a conversion

factor (Fagan et al., 2011; Wang et al., 2012). Indeed, we were able to transform values obtained from ELISA to equivalent xMAP units using linear regression to create a larger autopsy/genetic-confirmed FTLD dataset and help confirm our pervious observations of the diagnostic utility of the t-tau/Aβ_{1-42} ratio to differentiate FTLD from AD (Irwin et al., 2012b). Maximizing available data is crucial for these extremely valuable and well-annotated research samples. In summary, in multiple large-scale autopsy-confirmed studies we have demonstrated the diagnostic utility of CSF t-tau, p-tau, and Aβ_{1-42} in differentiation of AD and FTLD (Bian et al., 2008; Irwin et al., 2012b; Toledo et al., 2012).

Few other CSF studies have used autopsy-confirmed cohorts of FTLD patients (**Table 1**). One study included 10 autopsy-confirmed FTLD patients and found similar results of lower t-tau and p-tau$_{181}$ levels in FTLD compared with AD, with high diagnostic accuracy of p-tau$_{181}$ (Koopman et al., 2009). Another study including 12 confirmed FTLD patients described "slightly elevated tau levels" in several patients compared to an age-dependent reference range and low compared to the majority of AD cases (Brunnstrom et al., 2010). Neuropathological subgroups of FTLD (FTLD-TDP, $n = 5$ and FTLD-tau, $n = 7$) had similar mean values, with 4/12 patients below the reference limit by >70 pg/ml (Brunnstrom et al., 2010). Thus, this study also found a subset of individual FTLD patients with lower than normal t-tau levels. The diagnostic utility of t-tau/Aβ_{1-42} in differentiating FTLD was not systematically explored in this small group of AD cases ($n = 8$). Finally, to our knowledge the only additional studies utilizing autopsy-confirmed FTLD cohorts included a small number of FTLD cases (<10) in a non-AD category, with no direct comparison of FTLD and AD (Engelborghs et al., 2008; Tapiola et al., 2009; Schoonenboom et al., 2012). Thus, further study is required in large prospective, autopsy-confirmed samples to confirm our observations.

The higher Aβ_{1-42} in FTLD compared to AD most likely reflects the absence of significant cerebral amyloidosis while the biological basis for observed low CSF t-tau in some FTLD patients is uncertain. One possibility is related to cortical tau depletion (Zhukareva et al., 2001, 2003; Grossman et al., 2005) through sequestration into the neuronal and glial inclusions in the absence of significant extracellular tau pathology (FTLD-tau) Dickson, 2004, such as extracellular "ghost tangles" as seen in AD (Schmidt et al., 1988), or altered post-translational stability of tau in FTLD-TDP (Zhukareva et al., 2001, 2003); furthermore, CSF t-tau does appear related to underlying FTLD pathophysiology as t-tau levels

Table 1 | Comparative studies of CSF biomarkers in autopsy/genetic-confirmed FTLD and AD cohorts.

Study	Patients	Aβ_{1-42}	t-tau	p-tau$_{181}$	Diagnostic accuracy (AD vs. FTLD)
Clark et al., 2003	(10) FTLD(74) AD*73 (4) CN	AD < FTLD, CN	CN < FTLD < AD	NA	No statistical analysis of FTLD diagnostic accuracy performed
Grossman et al., 2005	73 (11) FTLD(17) AD13 CN	AD < FTLD, CN	CN, FTLD < AD	CN, FTLD < AD	t-tau AUC = 0.86, sens = 74%, spec = 82.4%
Bian et al., 2008	(30) FTLD(19) AD13 CN	AD < FTLD, CN	CN, FTLD < AD	NA	t-tau/Aβ_{1-42} AUC = 0.93, sens = 78.9%, spec = 96.6%
Engelborghs et al., 2008	(2) FTLD(73) AD*100 CN	NA	NA	NA	No statistical analysis of FTLD diagnostic accuracy performed
Koopman et al., 2009	(10) FTLD(95) AD	AD < FTLD	FTLD < AD	FTLD < AD	p-tau$_{181}$ AUC = 0.85, sens = 91%, spec = 80%
Tapiola et al., 2009	(9) FTLD(83) AD	NA	NA	NA	No statistical analysis of FTLD diagnostic accuracy performed
Brunnstrom et al., 2010	(12) FTLD(8) AD*	NA	NA	NA	No statistical analysis of FTLD diagnostic accuracy performed
Irwin et al., 2012b	(20) FTLD(41) AD*	NA	NA	NA	t-tau/Aβ_{1-42} AUC = 0.99, sens = 90–100%, spec = 90–96%
Toledo et al., 2012	(71) AD(29) FTLD66 CN	AD < FTLD < CN	CN, FTLD < AD	CN, FTLD < AD	t-tau/Aβ_{1-42} (ELISA) AUC = 0.96, sens = 90, spec = 82% p-tau$_{181}$/Aβ_{1-42} (xMAP) AUC = 0.98, sens = 100%, spec = 88%

Other diagnostic groups that may be present in some studies are omitted and only direct comparisons of FTLD group to AD or CN are reported. "<" or ">" denotes significant difference between groups and "," denotes non-significant difference between groups, () denotes autopsy/genetic confirmed cohort.
*CN, non-demented controls; *, AD group contains cases with co-morbid Lewy Body or Vascular Disease; NA, Not assessed; AUC, Area under the curve for receiver operating curve analysis; ELISA, enzyme-linked immunosorbent assay; xMAP, luminex multiplex assay.*

in FTLD patients correlated to areas of frontal and temporal cortical atrophy on magnetic resonance imaging (MRI) (Grossman et al., 2005; McMillan et al., 2013). Further study of CSF protein dynamics in animal models of disease may help clarify these seemingly discordant associations of low tau levels with underlying neuropathology in FTLD-tau and FTLD-TDP.

Despite the clear distinction of t-tau and $A\beta_{1-42}$ levels between AD and FTLD, there is more variability in the literature for the relationship of these markers in FTLD compared with non-demented controls (**Table 1**). There are several reasons for these discrepancies; first, even in most autopsy-based studies, autopsy data on controls is lacking (**Table 1**) and a significant proportion of non-demented elderly can have underlying AD neuropathology (Davis et al., 1999), and thus influence CSF analyte measures. Next, even with pathologic confirmation, patient classification in FTLD is challenging, as another potential confounding issue is the presence of mixed pathologies in dementia patients. Indeed, our group has shown in a large autopsy-confirmed sample that mixed pathology is present in roughly 30% of cases, and that FTLD patients with significant AD neuropathologic change can influence the CSF t-tau and $A\beta_{1-42}$ levels, causing higher t-tau and lower $A\beta_{1-42}$ in cases with mixed FTLD and AD pathology compared to "pure" FTLD (Toledo et al., 2012). Additionally, a recent largely clinically-defined cohort study found an AD CSF biomarker profile in 30% of FTLD (Schoonenboom et al., 2012) which may be due, in part, to mixed pathology or inclusion of atypical AD cases mimicking the FTLD clinical syndrome (Toledo et al., 2012). Thus, the use of autopsy-confirmed samples is essential for in-depth study and validation of the diagnostic accuracy of potential biomarkers in FTLD.

Finally, variability in measurement between studies is another potential issue as significant variation between centers in absolute values measured in "spiked" pooled CSF control samples with known concentrations of analyte has been described (Shaw et al., 2011). These discrepancies are most likely due to sources of variation in CSF collection, handling and storage (pre-analytical), equipment, reagents and methods of analysis (analytical), and data management and interpretation (post-analytical) (Mattsson et al., 2011). For these reasons, large scale studies of measurement precision of these analytes and coordinated multi-center quality control programs with standard operating procedures to minimize these sources of variation have been conducted (Mattsson et al., 2011; Shaw et al., 2011).

Despite these issues, we have demonstrated (Bian et al., 2008; Irwin et al., 2012b; Toledo et al., 2012) that these AD-specific analytes (t-tau to $A\beta_{1-42}$ ratio) may perform within the range of sensitivity and specificity (>80%) for use in clinical trials (Trojanowski and Growdon, 1998) to differentiate FTLD from AD; however, these analytes are not as effective for differentiation of FTLD from normal controls (Bian and Grossman, 2007; Toledo et al., 2012). Although patients may present with decompensated psychiatric issues or other non-progressive non-degenerative etiologies resembling FTLD (phenocopy syndrome) (Kipps et al., 2010), these patients may be identified with serial clinical exams and neuroimaging (Kipps et al., 2010). The more urgent need is for FTLD-specific biomarkers and those that can differentiate between the two major neuropathologic subtypes (FTLD-tau and FTLD-TDP) (Hu et al., 2011).

FUTURE DIRECTIONS

FURTHER STUDY OF CSF tau AND $A\beta_{1-42}$

Previous work in large cross-sectional studies in AD suggests a temporal progression of dynamic biomarker change in AD (Jack et al., 2010, 2012), as $A\beta_{1-42}$ amyloidosis, and resultant lower CSF $A\beta_{1-42}$, is thought to occur decades before clinical symptoms emerge in AD, while increased CSF t-tau is thought to be a later event in disease progression and correlates more closely with cognitive decline. It is likely that t-tau, p-tau and potential novel CSF biomarkers could display similar changes throughout the course of disease in FTLD and could correlate with clinical symptoms. Few studies have examined the change in CSF biomarkers over time or their relation to clinical symptoms. One study included a follow up CSF analysis in one FTLD-tau patient, with similar t-tau and $A\beta_{1-42}$, roughly 18 months between CSF collections (Brunnstrom et al., 2010). Interestingly, a recent study of bvFTD patients found a significant correlation with $A\beta_{1-42}$ levels and cognitive performance, even after removal of patients with CSF profile suggestive of AD neuropathology (Koedam et al., 2012). These results could suggest an influence of co-morbid AD neuropathology; however autopsy information in these cases was lacking. Other studies in clinical series without autopsy confirmation found no association of these markers and clinical measures or disease severity (Riemenschneider et al., 2002; Engelborghs et al., 2006; De Souza et al., 2011). Further study of clinical correlates of CSF biomarkers and longitudinal profiles of CSF analyte change throughout the course of disease will be helpful.

Similar to the dominantly-inherited AD network (DIAN) initiative to study patients with known pathogenic mutations to cause AD (Bateman et al., 2012), study of prodromal FTLD patients with pathogenic mutations may provide additional insights into the temporal sequence of biomarkers in FTLD (Boxer et al., 2012a). Furthermore, CSF analyte levels in symptomatic patients with genetic forms of FTLD have not been explored in detail and could potentially differ from sporadic cases. Indeed, we found a more rapid rate of progression in cognitive measures corresponding to more severe neurodegeneration in *C9orf72*-associated FTLD (Irwin et al., 2013) and others have described unique neuroimaging patterns of atrophy across different genetic forms of FTLD (Whitwell et al., 2012). This evidence of biologic differences in genetic and sporadic FTLD suggest alterations in CSF biomarker profiles are also a possibility, although one study found similar levels of CSF tau and $A\beta_{1-42}$ in genetically-confirmed FTDP-17 ($n = 9$) compared to sporadic FTLD ($n = 17$) (Rosso et al., 2003).

DEVELOPMENT OF FTLD-SPECIFIC BIOMARKERS

In the context of disease-modifying therapies targeting a specific histopathologic abnormality, an important goal is to distinguish between FTLD due to TDP-43 and FTLD due to tau. Exploratory analyses for novel biomarkers that have diagnostic utility in FTLD are ongoing and include several basic approaches.

First, measurement of biologically relevant molecules is the most straightforward approach, as tau and $A\beta_{1-42}$ have been successful biomarker candidates in AD. Using this rationale, the two most obvious candidates for FTLD-specific biomarkers are TDP-43 progranulin. Indeed, TDP-43 has been detected in human CSF (Steinacker et al., 2008; Kasai et al., 2009) and serum (Foulds et al., 2008), suggesting elevated levels may occur in some patients with TDP-43 proteinopathies, but initial studies show limited diagnostic accuracy. Low serum progranulin may identify FTLD patients with a pathogenic *GRN* mutation resulting in progranulin haploinsufficiency (Ghidoni et al., 2008), which could be useful in monitoring potential progranulin-replacing therapies in development for FTLD (Boxer et al., 2012b).

Other biologically relevant potential biomarkers for FTLD include specific isoforms or neoepitopes of tau. Tau undergoes multiple post-translational modifications thought to contribute to tangle formation. Indeed, we found acetylation of tau at a specific residue in the microtubule-binding domain (MTBD) to be exclusively found in tauopathies, providing promise for this epitope as a useful marker of AD and FTLD-tau (Cohen et al., 2011; Irwin et al., 2012a). Translating these immunohistochemical observations to clinical assays may prove difficult, as levels of tau in CSF are near the lower limits of biologic detection (Hampel et al., 2010) limiting the further identification of a specific subset of tau in the form of a neoepitope; although one group has found promising evidence for diagnostic utility of specific C-truncated isoforms of tau in PSP through immunoprecipitation and western blotting techniques (Borroni et al., 2008, 2009) and others have developed assays to measure 3- and 4R tau in CSF (Luk et al., 2012). Alternatively-truncated forms of $A\beta_{1-42}$ may also have diagnostic importance in FTLD (Pijnenburg et al., 2007; Bibl et al., 2011, 2012; Gabelle et al., 2011) and cytoskeletal proteins, such as neurofilament have also been explored (Sjogren et al., 2000b; De Jong et al., 2007). These potential biomarkers warrant further study and validation.

Another, possible approach is to screen a large number of potential analytes without an a priori biologic rationale in a proteomic analysis of CSF in FTLD. Indeed, using an immune-based multiplex approach our group found promising CSF biomarker candidates to differentiate FTLD-TDP and FTLD-tau with high sensitivity and specificity, but these candidate analytes need further study to confirm their utility as FTLD biomarkers (Hu et al., 2010b). Finally, other non-immune based methods, such as mass-spectrometry are also being explored to identify novel biofluid biomarkers in FTLD (Mattsson et al., 2008).

Potential FTLD-specific biofluid biomarkers will be faced with the same challenges of testing reliability and sources of variation (i.e., analytical, pre-/post-analytical) currently experienced by CSF t-tau and $A\beta_{1-42}$ measurements. As such, coordinated and cooperative efforts between multiple centers will undoubtedly be necessary to help validate potential FTLD-specific CSF biomarkers prior to clinical use.

Most likely, a multimodal assessment incorporating potential novel biofluid biomarker values with clinical, neuroimaging and genetic markers may be the most effective approach to accurately identify FTLD subtypes. Neuropsychological testing can help differentiate AD from FTLD (Rascovsky et al., 2008; Libon et al., 2011) as routine cognitive measures may not be sensitive enough to detect the behavioral and language deficits in FTLD. Indeed, our group has explored quantitative approaches to language (Ash et al., 2006, 2009; Gunawardena et al., 2010) and social cognition (Massimo et al., 2009, 2013; Grossman et al., 2010; Eslinger et al., 2012; McMillan et al., 2012b) to examine brain-behavior relationships and improve diagnostic accuracy in FTLD. Neuroimaging is another potential method with diagnostic utility alone, or as an adjunct to clinical and biofluid biomarkers in FTLD; we have found combining neuropsychological testing and MRI can improve diagnostic accuracy in PPA (Hu et al., 2010c); and others find combination of CSF tau isoform levels and midbrain atrophy improve identification of PSP (Borroni et al., 2010). Multiple modalities of MRI methods, including diffusion-tensor imaging (DTI) of white matter may help identify FTLD patients in dementia cohorts. We have demonstrated increased diagnostic sensitivity to differentiate AD from FTLD cases using a combination of gray matter (GM) density and DTI measures (McMillan et al., 2012a). In addition, we have also discovered promising diagnostic utility for differentiating FTLD-tau and FTLD-TDP using DTI (unpublished data). Cortical atrophy and CSF biomarker levels appear to be highly correlated as we have recently demonstrated that GM density could predict CSF t-tau and $A\beta_{1-42}$ levels, and these predicted values could accurately distinguish AD and FTLD (McMillan et al., 2013). These results indicate that MRI could potentially serve as a surrogate for CSF, which would have significant utility for patients where lumbar puncture would be difficult or for clinical trial endpoints where repeated lumbar puncture may be needed. Finally, recent genome-wide association studies (GWAS) have found risk alleles associated with FTLD-TDP (Van Deerlin et al., 2010) and FTLD-tau (Hoglinger et al., 2011). Further knowledge of clinical, neuroimaging, and biofluid correlates of these risk alleles in FTLD could provide further useful diagnostic and prognostic information. Thus, comparative studies of clinical, genetic, biofluid, and neuroimaging biomarkers in longitudinally followed, well-annotated, autopsy-confirmed subjects will be a powerful method for improving our understanding of the pathophysiology of FTLD and further directing diagnostic and treatment efforts.

SUMMARY

CSF measurements of $A\beta_{1-42}$, t-tau, and p-tau in FTLD differ significantly from the abnormal levels seen in AD, and in a subset of both FTLD-tau and FTLD-TDP there are extremely low levels of t-tau of unclear etiology. These properties allow for accurate distinction of FTLD from AD in autopsy-confirmed cohorts, while FTLD-specific markers are still lacking.

As we move toward therapies that impact the progression of the disease and target the underlying pathophysiology in FTLD and other neurodegenerative disorders it will be essential for clinicians to view these disorders as clinicopathological entities with the underlying neuropathological substrate in mind. Indeed, new clinical criteria for AD incorporate this ideology with the designation of "pre-symptomatic AD" (Sperling et al., 2011). In the

study of the complex clinicopathological spectrum of FTLD disorders, where heterogeneity is the rule, useful markers to develop homogenous clinical, genetic, and neuropathologic subgroups will be crucial to further our goals toward meaningful treatments that could potential slow disease progression and limit patient disability.

ACKNOWLEDGMENTS

We thank the patients studied here and their families who made the research reviewed here possible. Funding for this study was provided by the National Institutes of Health grants P30 AG10124, AG17586, and T32-AG000255 as well as the Wyncote Foundation.

REFERENCES

Alladi, S., Xuereb, J., Bak, T., Nestor, P., Knibb, J., Patterson, K., et al. (2007). Focal cortical presentations of Alzheimer's disease. *Brain* 130, 2636–2645.

Arai, H., Morikawa, Y., Higuchi, M., Matsui, T., Clark, C. M., Miura, M., et al. (1997). Cerebrospinal fluid tau levels in neurodegenerative diseases with distinct tau-related pathology. *Biochem. Biophys. Res. Commun.* 236, 262–264.

Ash, S., Moore, P., Antani, S., McCawley, G., Work, M., and Grossman, M. (2006). Trying to tell a tale: discourse impairments in progressive aphasia and frontotemporal dementia. *Neurology* 66, 1405–1413.

Ash, S., Moore, P., Vesely, L., Gunawardena, D., McMillan, C., Anderson, C., et al. (2009). Non-Fluent Speech in Frontotemporal Lobar Degeneration. *J. Neurolinguistics* 22, 370–383.

Baker, M., Mackenzie, I. R., Pickering-Brown, S. M., Gass, J., Rademakers, R., Lindholm, C., et al. (2006). Mutations in progranulin cause tau-negative frontotemporal dementia linked to chromosome 17. *Nature* 442, 916–919.

Bateman, R. J., Xiong, C., Benzinger, T. L., Fagan, A. M., Goate, A., Fox, N. C., et al. (2012). Clinical and biomarker changes in dominantly inherited Alzheimer's disease. *N. Engl. J. Med.* 367, 795–804.

Bian, H., and Grossman, M. (2007). Frontotemporal lobar degeneration: recent progress in antemortem diagnosis. *Acta Neuropathol.* 114, 23–29.

Bian, H., Van Swieten, J. C., Leight, S., Massimo, L., Wood, E., Forman, M., et al. (2008). CSF biomarkers in frontotemporal lobar degeneration with known pathology. *Neurology* 70, 1827–1835.

Bibl, M., Gallus, M., Welge, V., Esselmann, H., Wolf, S., Ruther, E., et al. (2012). Cerebrospinal fluid amyloid-beta 2-42 is decreased in Alzheimer's, but not in frontotemporal dementia. *J. Neural Transm.* 119, 805–813.

Bibl, M., Mollenhauer, B., Lewczuk, P., Esselmann, H., Wolf, S., Otto, M., et al. (2011). Cerebrospinal fluid tau, p-tau 181 and amyloid-beta38/40/42 in frontotemporal dementias and primary progressive aphasias. *Dement. Geriatr. Cogn. Disord.* 31, 37–44.

Bibl, M., Mollenhauer, B., Wolf, S., Esselmann, H., Lewczuk, P., Kornhuber, J., et al. (2007). Reduced CSF carboxyterminally truncated Abeta peptides in frontotemporal lobe degenerations. *J. Neural Transm.* 114, 621–628.

Blennow, K., Wallin, A., Agren, H., Spenger, C., Siegfried, J., and Vanmechelen, E. (1995). Tau protein in cerebrospinal fluid: a biochemical marker for axonal degeneration in Alzheimer disease? *Mol. Chem. Neuropathol.* 26, 231–245.

Borroni, B., Gardoni, F., Parnetti, L., Magno, L., Malinverno, M., Saggese, E., et al. (2009). Pattern of Tau forms in CSF is altered in progressive supranuclear palsy. *Neurobiol. Aging* 30, 34–40.

Borroni, B., Malinverno, M., Gardoni, F., Alberici, A., Parnetti, L., Premi, E., et al. (2008). Tau forms in CSF as a reliable biomarker for progressive supranuclear palsy. *Neurology* 71, 1796–1803.

Borroni, B., Malinverno, M., Gardoni, F., Grassi, M., Parnetti, L., Agosti, C., et al. (2010). A combination of CSF tau ratio and midsaggital midbrain-to-pons atrophy for the early diagnosis of progressive supranuclear palsy. *J. Alzheimers Dis.* 22, 195–203.

Boxer, A. L., Gold, M., Huey, E., Gao, F. B., Burton, E. A., Chow, T., et al. (2012a). Frontotemporal degeneration, the next therapeutic frontier: Molecules and animal models for frontotemporal degeneration drug development. *Alzheimers Dement.* doi: 10.1016/j.jalz.2012.03.002. [Epub ahead of print].

Boxer, A. L., Gold, M., Huey, E., Hu, W. T., Rosen, H., Kramer, J., et al. (2012b). The advantages of frontotemporal degeneration drug development (part 2 of frontotemporal degeneration: the next therapeutic frontier). *Alzheimers Dement.* doi: 10.1016/j.jalz.2012.03.003. [Epub ahead of print].

Brunnstrom, H., Rawshani, N., Zetterberg, H., Blennow, K., Minthon, L., Passant, U., et al. (2010). Cerebrospinal fluid biomarker results in relation to neuropathological dementia diagnoses. *Alzheimers Dement.* 6, 104–109.

Buerger, K., Teipel, S. J., Zinkowski, R., Blennow, K., Arai, H., Engel, R., et al. (2002a). CSF tau protein phosphorylated at threonine 231 correlates with cognitive decline in MCI subjects. *Neurology* 59, 627–629.

Buerger, K., Zinkowski, R., Teipel, S. J., Tapiola, T., Arai, H., Blennow, K., et al. (2002b). Differential diagnosis of Alzheimer disease with cerebrospinal fluid levels of tau protein phosphorylated at threonine 231. *Arch. Neurol.* 59, 1267–1272.

Clark, C. M., Xie, S., Chittams, J., Ewbank, D., Peskind, E., Galasko, D., et al. (2003). Cerebrospinal fluid tau and beta-amyloid: how well do these biomarkers reflect autopsy-confirmed dementia diagnoses? *Arch. Neurol.* 60, 1696–1702.

Cohen, T. J., Guo, J. L., Hurtado, D. E., Kwong, L. K., Mills, I. P., Trojanowski, J. Q., et al. (2011). The acetylation of tau inhibits its function and promotes pathological tau aggregation. *Nat. Commun.* 2:252. doi: 10.1038/ncomms1255

Cruts, M., Gijselinck, I., Van Der Zee, J., Engelborghs, S., Wils, H., Pirici, D., et al. (2006). Null mutations in progranulin cause ubiquitin-positive frontotemporal dementia linked to chromosome 17q21. *Nature* 442, 920–924.

Davis, D. G., Schmitt, F. A., Wekstein, D. R., and Markesbery, W. R. (1999). Alzheimer neuropathologic alterations in aged cognitively normal subjects. *J. Neuropathol. Exp. Neurol.* 58, 376–388.

De Jong, D., Jansen, R. W., Pijnenburg, Y. A., Van Geel, W. J., Borm, G. F., Kremer, H. P., et al. (2007). CSF neurofilament proteins in the differential diagnosis of dementia. *J. Neurol. Neurosurg. Psychiatry* 78, 936–938.

De Meyer, G., Shapiro, F., Vanderstichele, H., Vanmechelen, E., Engelborghs, S., De Deyn, P. P., et al. (2010). Diagnosis-independent Alzheimer disease biomarker signature in cognitively normal elderly people. *Arch. Neurol.* 67, 949–956.

De Souza, L. C., Lamari, F., Belliard, S., Jardel, C., Houillier, C., De Paz, R., et al. (2011). Cerebrospinal fluid biomarkers in the differential diagnosis of Alzheimer's disease from other cortical dementias. *J. Neurol. Neurosurg. Psychiatry* 82, 240–246.

Dejesus-Hernandez, M., Mackenzie, I. R., Boeve, B. F., Boxer, A. L., Baker, M., Rutherford, N. J., et al. (2011). Expanded GGGGCC hexanucleotide repeat in noncoding region of C9ORF72 causes chromosome 9p-linked FTD and ALS. *Neuron* 72, 245–256.

Dickson, D. (2004). "Sporadic tauopaties: Pick's disease, corticobasal degeneration, progressive supranuclear palsy and argyrophilic grain disease," in *The Neuropathology of Dementia 2nd Edn*, eds M. Esiri, V. M-Y. Lee, and J. Q. Trojanowski (New York, NY: Cambridge University Press), 227–256.

Engelborghs, S., De Vreese, K., Van De Casteele, T., Vanderstichele, H., Van Everbroeck, B., Cras, P., et al. (2008). Diagnostic performance of a CSF-biomarker panel in autopsy-confirmed dementia. *Neurobiol. Aging* 29, 1143–1159.

Engelborghs, S., Maertens, K., Vloeberghs, E., Aerts, T., Somers, N., Marien, P., et al. (2006). Neuropsychological and behavioural correlates of CSF biomarkers in dementia. *Neurochem. Int.* 48, 286–295.

Eslinger, P. J., Moore, P., Antani, S., Anderson, C., and Grossman, M. (2012). Apathy in frontotemporal dementia: behavioral and neuroimaging correlates. *Behav. Neurol.* 25, 127–136.

Fagan, A. M., Mintun, M. A., Mach, R. H., Lee, S. Y., Dence, C. S., Shah, A. R., et al. (2006). Inverse relation between *in vivo* amyloid imaging load and cerebrospinal fluid Abeta42 in humans. *Ann. Neurol.* 59, 512–519.

Fagan, A. M., Shaw, L. M., Xiong, C., Vanderstichele, H., Mintun, M. A., Trojanowski, J. Q., et al. (2011). Comparison of analytical platforms for cerebrospinal fluid measures of {beta}-amyloid 1-42, total tau, and P-tau181 for identifying alzheimer disease amyloid plaque pathology. *Arch. Neurol.* 68, 1137–1144.

Forman, M. S., Farmer, J., Johnson, J. K., Clark, C. M., Arnold, S. E., Coslett, H. B., et al. (2006). Frontotemporal dementia: clinicopathological correlations. *Ann. Neurol.* 59, 952–962.

Foulds, P., McAuley, E., Gibbons, L., Davidson, Y., Pickering-Brown, S. M., Neary, D., et al. (2008). TDP-43 protein in plasma may index TDP-43 brain pathology in Alzheimer's disease and frontotemporal lobar degeneration. *Acta Neuropathol.* 116, 141–146.

Gabelle, A., Roche, S., Geny, C., Bennys, K., Labauge, P., Tholance, Y., et al. (2011). Decreased sAbetaPPbeta, Abeta38, and Abeta40 cerebrospinal fluid levels in frontotemporal dementia. *J. Alzheimers Dis.* 26, 553–563.

Geser, F., Brandmeir, N. J., Kwong, L. K., Martinez-Lage, M., Elman, L., McCluskey, L., et al. (2008). Evidence of multisystem disorder in whole-brain map of pathological TDP-43 in amyotrophic lateral sclerosis. *Arch. Neurol.* 65, 636–641.

Geser, F., Martinez-Lage, M., Robinson, J., Uryu, K., Neumann, M., Brandmeir, N. J., et al. (2009). Clinical and pathological continuum of multisystem TDP-43 proteinopathies. *Arch. Neurol.* 66, 180–189.

Ghidoni, R., Benussi, L., Glionna, M., Franzoni, M., and Binetti, G. (2008). Low plasma progranulin levels predict progranulin mutations in frontotemporal lobar degeneration. *Neurology* 71, 1235–1239.

Gorno-Tempini, M. L., Brambati, S. M., Ginex, V., Ogar, J., Dronkers, N. F., Marcone, A., et al. (2008). The logopenic/phonological variant of primary progressive aphasia. *Neurology* 71, 1227–1234.

Gorno-Tempini, M. L., Dronkers, N. F., Rankin, K. P., Ogar, J. M., Phengrasamy, L., Rosen, H. J., et al. (2004). Cognition and anatomy in three variants of primary progressive aphasia. *Ann. Neurol.* 55, 335–346.

Gorno-Tempini, M. L., Hillis, A. E., Weintraub, S., Kertesz, A., Mendez, M., Cappa, S. F., et al. (2011). Classification of primary progressive aphasia and its variants. *Neurology* 76, 1006–1014.

Green, A. J., Harvey, R. J., Thompson, E. J., and Rossor, M. N. (1999). Increased tau in the cerebrospinal fluid of patients with frontotemporal dementia and Alzheimer's disease. *Neurosci. Lett.* 259, 133–135.

Grossman, M. (2010). Primary progressive aphasia: clinicopathological correlations. *Nat. Rev. Neurol.* 6, 88–97.

Grossman, M., Eslinger, P. J., Troiani, V., Anderson, C., Avants, B., Gee, J. C., et al. (2010). The role of ventral medial prefrontal cortex in social decisions: converging evidence from fMRI and frontotemporal lobar degeneration. *Neuropsychologia* 48, 3505–3512.

Grossman, M., Farmer, J., Leight, S., Work, M., Moore, P., Van Deerlin, V., et al. (2005). Cerebrospinal fluid profile in frontotemporal dementia and Alzheimer's disease. *Ann. Neurol.* 57, 721–729.

Grossman, M., Powers, J., Ash, S., McMillan, C., Burkholder, L., Irwin, D., et al. (2012). Disruption of large-scale neural networks in non-fluent/agrammatic variant primary progressive aphasia associated with frontotemporal degeneration pathology. *Brain Lang.* doi: 10.1016/j.bandl.2012.10.005. [Epub ahead of print].

Grossman, M., Xie, S. X., Libon, D. J., Wang, X., Massimo, L., Moore, P., et al. (2008). Longitudinal decline in autopsy-defined frontotemporal lobar degeneration. *Neurology* 70, 2036–2045.

Gunawardena, D., Ash, S., McMillan, C., Avants, B., Gee, J., and Grossman, M. (2010). Why are patients with progressive nonfluent aphasia nonfluent? *Neurology* 75, 588–594.

Hampel, H., Blennow, K., Shaw, L. M., Hoessler, Y. C., Zetterberg, H., and Trojanowski, J. Q. (2010). Total and phosphorylated tau protein as biological markers of Alzheimer's disease. *Exp. Gerontol.* 45, 30–40.

Hesse, C., Rosengren, L., Vanmechelen, E., Vanderstichele, H., Jensen, C., Davidsson, P., et al. (2000). Cerebrospinal fluid markers for Alzheimer's disease evaluated after acute ischemic stroke. *J. Alzheimers Dis.* 2, 199–206.

Hodges, J. R., Davies, R. R., Xuereb, J. H., Casey, B., Broe, M., Bak, T. H., et al. (2004). Clinicopathological correlates in frontotemporal dementia. *Ann. Neurol.* 56, 399–406.

Hodges, J. R., and Patterson, K. (2007). Semantic dementia: a unique clinicopathological syndrome. *Lancet Neurol.* 6, 1004–1014.

Hoglinger, G. U., Melhem, N. M., Dickson, D. W., Sleiman, P. M., Wang, L. S., Klei, L., et al. (2011). Identification of common variants influencing risk of the tauopathy progressive supranuclear palsy. *Nat. Genet.* 43, 699–705.

Hu, W. T., Chen-Plotkin, A., Arnold, S. E., Grossman, M., Clark, C. M., Shaw, L. M., et al. (2010a). Biomarker discovery for Alzheimer's disease, frontotemporal lobar degeneration, and Parkinson's disease. *Acta Neuropathol.* 120, 385–399.

Hu, W. T., Chen-Plotkin, A., Grossman, M., Arnold, S. E., Clark, C. M., Shaw, L. M., et al. (2010b). Novel CSF biomarkers for frontotemporal lobar degenerations. *Neurology* 75, 2079–2086.

Hu, W. T., McMillan, C., Libon, D., Leight, S., Forman, M., Lee, V. M., et al. (2010c). Multimodal predictors for Alzheimer disease in nonfluent primary progressive aphasia. *Neurology* 75, 595–602.

Hu, W. T., Trojanowski, J. Q., and Shaw, L. M. (2011). Biomarkers in frontotemporal lobar degenerations–progress and challenges. *Prog. Neurobiol.* 95, 636–648.

Hutton, M., Lendon, C. L., Rizzu, P., Baker, M., Froelich, S., Houlden, H., et al. (1998). Association of missense and 5'-splice-site mutations in tau with the inherited dementia FTDP-17. *Nature* 393, 702–705.

Irwin, D. J., Cohen, T. J., Grossman, M., Arnold, S. E., Xie, S. X., Lee, V. M., et al. (2012a). Acetylated tau, a novel pathological signature in Alzheimer's disease and other tauopathies. *Brain* 135, 807–818.

Irwin, D. J., McMillan, C. T., Toledo, J. B., Arnold, S. E., Shaw, L. M., Wang, L. S., et al. (2012b). Comparison of cerebrospinal fluid levels of tau and Abeta 1-42 in Alzheimer disease and frontotemporal degeneration using 2 analytical platforms. *Arch. Neurol.* 69, 1018–1025.

Irwin, D. J., McMillan, C. T., Brettschneider, J., Libon, D. J., Powers, J., Rascovsky, K., et al. (2013). Cognitive decline and reduced survival in C9orf72 expansion frontotemporal degeneration and amyotrophic lateral sclerosis. *J. Neurol. Neurosurg. Psychiatry*. 84, 163–169.

Jack, C. R. Jr., Knopman, D. S., Jagust, W. J., Shaw, L. M., Aisen, P. S., Weiner, M. W., et al. (2010). Hypothetical model of dynamic biomarkers of the Alzheimer's pathological cascade. *Lancet Neurol.* 9, 119–128.

Jack, C. R. Jr., Vemuri, P., Wiste, H. J., Weigand, S. D., Lesnick, T. G., Lowe, V., et al. (2012). Shapes of the trajectories of 5 major biomarkers of Alzheimer disease. *Arch. Neurol.* 69, 856–867.

Jin, K., Takeda, A., Shiga, Y., Sato, S., Ohnuma, A., Nomura, H., et al. (2006). CSF tau protein: a new prognostic marker for Guillain-Barre syndrome. *Neurology* 67, 1470–1472.

Josephs, K. A. (2008). Frontotemporal dementia and related disorders: deciphering the enigma. *Ann. Neurol.* 64, 4–14.

Josephs, K. A., Duffy, J. R., Strand, E. A., Whitwell, J. L., Layton, K. F., Parisi, J. E., et al. (2006a). Clinicopathological and imaging correlates of progressive aphasia and apraxia of speech. *Brain* 129, 1385–1398.

Josephs, K. A., Whitwell, J. L., Jack, C. R., Parisi, J. E., and Dickson, D. W. (2006b). Frontotemporal lobar degeneration without lobar atrophy. *Arch. Neurol.* 63, 1632–1638.

Kapaki, E., Paraskevas, G. P., Papageorgiou, S. G., Bonakis, A., Kalfakis, N., Zalonis, I., et al. (2008). Diagnostic value of CSF biomarker profile in frontotemporal lobar degeneration. *Alzheimer Dis. Assoc. Disord.* 22, 47–53.

Kasai, T., Tokuda, T., Ishigami, N., Sasayama, H., Foulds, P., Mitchell, D. J., et al. (2009). Increased TDP-43 protein in cerebrospinal fluid of patients with amyotrophic lateral sclerosis. *Acta Neuropathol.* 117, 55–62.

Kertesz, A., McMonagle, P., Blair, M., Davidson, W., and Munoz, D. G. (2005). The evolution and pathology of frontotemporal dementia. *Brain* 128, 1996–2005.

Kipps, C. M., Hodges, J. R., and Hornberger, M. (2010). Nonprogressive behavioural frontotemporal dementia: recent developments and clinical implications of the 'bvFTD phenocopy syndrome'. *Curr. Opin. Neurol.* 23, 628–632.

Knibb, J. A., Xuereb, J. H., Patterson, K., and Hodges, J. R. (2006). Clinical and pathological characterization of progressive aphasia. *Ann. Neurol.* 59, 156–165.

Knopman, D. S., Boeve, B. F., Parisi, J. E., Dickson, D. W., Smith, G. E., Ivnik, R. J., et al. (2005). Antemortem diagnosis of

frontotemporal lobar degeneration. *Ann. Neurol.* 57, 480–488.

Knopman, D. S., Kramer, J. H., Boeve, B. F., Caselli, R. J., Graff-Radford, N. R., Mendez, M. F., et al. (2008). Development of methodology for conducting clinical trials in frontotemporal lobar degeneration. *Brain* 131, 2957–2968.

Koedam, E. L., Van Der Vlies, A. E., Van Der Flier, W. M., Verwey, N. A., Koene, T., Scheltens, P., et al. (2012). Cognitive correlates of cerebrospinal fluid biomarkers in frontotemporal dementia. *Alzheimers Dement.* doi: 10.1016/j.jalz.2011.12.007. [Epub ahead of print].

Koopman, K., Le Bastard, N., Martin, J. J., Nagels, G., De Deyn, P. P., and Engelborghs, S. (2009). Improved discrimination of autopsy-confirmed Alzheimer's disease (AD) from non-AD dementias using CSF P-tau(181P). *Neurochem. Int.* 55, 214–218.

Koric, L., Felician, O., Guedj, E., Hubert, A. M., Mancini, J., Boucraut, J., et al. (2010). Could clinical profile influence CSF biomarkers in early-onset Alzheimer disease? *Alzheimer Dis. Assoc. Disord.* 24, 278–283.

Krut, J. J., Zetterberg, H., Blennow, K., Cinque, P., Hagberg, L., Price, R. W., et al. (2013). Cerebrospinal fluid Alzheimer's biomarker profiles in CNS infections. *J. Neurol.* 260, 620–626.

Lee, S. E., Rabinovici, G. D., Mayo, M. C., Wilson, S. M., Seeley, W. W., Dearmond, S. J., et al. (2011). Clinicopathological correlations in corticobasal degeneration. *Ann. Neurol.* 70, 327–340.

Lewczuk, P., Zimmermann, R., Wiltfang, J., and Kornhuber, J. (2009). Neurochemical dementia diagnostics: a simple algorithm for interpretation of the CSF biomarkers. *J Neural Transm* 116, 1163–1167.

Libon, D. J., Rascovsky, K., Gross, R. G., White, M. T., Xie, S. X., Dreyfuss, M., et al. (2011). The Philadelphia Brief Assessment of Cognition (PBAC): a validated screening measure for dementia. *Clin. Neuropsychol.* 25, 1314–1330.

Luk, C., Compta, Y., Magdalinou, N., Marti, M. J., Hondhamuni, G., Zetterberg, H., et al. (2012). Development and assessment of sensitive immuno-PCR assays for the quantification of cerebrospinal fluid three- and four-repeat tau isoforms in tauopathies. *J. Neurochem.* 123, 396–405.

Mackenzie, I. R., Neumann, M., Baborie, A., Sampathu, D. M., Du Plessis, D., Jaros, E., et al. (2011). A harmonized classification system for FTLD-TDP pathology. *Acta Neuropathol.* 122, 111–113.

Mackenzie, I. R., Neumann, M., Bigio, E. H., Cairns, N. J., Alafuzoff, I., Kril, J., et al. (2010). Nomenclature and nosology for neuropathologic subtypes of frontotemporal lobar degeneration: an update. *Acta Neuropathol.* 119, 1–4.

Massimo, L., Libon, D. J., Chandrasekaran, K., Dreyfuss, M., McMillan, C. T., Rascovsky, K., et al. (2013). Self-appraisal in behavioural variant frontotemporal degeneration. *J. Neurol. Neurosurg. Psychiatry*, 84, 148–153.

Massimo, L., Powers, C., Moore, P., Vesely, L., Avants, B., Gee, J., et al. (2009). Neuroanatomy of apathy and disinhibition in frontotemporal lobar degeneration. *Dement. Geriatr. Cogn. Disord.* 27, 96–104.

Matsuo, E. S., Shin, R. W., Billingsley, M. L., Van Devoorde, A., O'Connor, M., Trojanowski, J. Q., et al. (1994). Biopsy-derived adult human brain tau is phosphorylated at many of the same sites as Alzheimer's disease paired helical filament tau. *Neuron* 13, 989–1002.

Mattsson, N., Andreasson, U., Persson, S., Arai, H., Batish, S. D., Bernardini, S., et al. (2011). The Alzheimer's association external quality control program for cerebrospinal fluid biomarkers. *Alzheimers Dement.* 7, 386–395. e386.

Mattsson, N., Ruetschi, U., Pijnenburg, Y. A., Blankenstein, M. A., Podust, V. N., Li, S., et al. (2008). Novel cerebrospinal fluid biomarkers of axonal degeneration in frontotemporal dementia. *Mol. Med. Report.* 1, 757–761.

McMillan, C. T., Avants, B., Irwin, D. J., Toledo, J. B., Wolk, D. A., Van Deerlin, V. M., et al. (2013). Can MRI screen for CSF biomarkers in neurodegenerative disease? *Neurology*, 80, 132–138.

McMillan, C. T., Brun, C., Siddiqui, S., Churgin, M., Libon, D., Yushkevich, P., et al. (2012a). White matter imaging contributes to the multimodal diagnosis of frontotemporal lobar degeneration. *Neurology* 78, 1761–1768.

McMillan, C. T., Rascovsky, K., Khella, M. C., Clark, R., and Grossman, M. (2012b). The neural basis for establishing a focal point in pure coordination games. *Soc. Cogn. Affect. Neurosci.* 7, 881–887.

Mesulam, M., Wicklund, A., Johnson, N., Rogalski, E., Leger, G. C., Rademaker, A., et al. (2008). Alzheimer and frontotemporal pathology in subsets of primary progressive aphasia. *Ann. Neurol.* 63, 709–719.

Mesulam, M. M. (1982). Slowly progressive aphasia without generalized dementia. *Ann. Neurol.* 11, 592–598.

Mesulam, M. M. (2001). Primary progressive aphasia. *Ann. Neurol.* 49, 425–432.

NLM/NIH. 2012. Available online at: http://www.ncbi.nlm.nih.gov/pubmed/ [Accessed 10/27/12 2012].

Olsson, A., Vanderstichele, H., Andreasen, N., De Meyer, G., Wallin, A., Holmberg, B., et al. (2005). Simultaneous measurement of beta-amyloid(1-42), total tau, and phosphorylated tau (Thr181) in cerebrospinal fluid by the xMAP technology. *Clin. Chem.* 51, 336–345.

Ost, M., Nylen, K., Csajbok, L., Ohrfelt, A. O., Tullberg, M., Wikkelso, C., et al. (2006). Initial CSF total tau correlates with 1-year outcome in patients with traumatic brain injury. *Neurology* 67, 1600–1604.

Otto, M., Wiltfang, J., Tumani, H., Zerr, I., Lantsch, M., Kornhuber, J., et al. (1997). Elevated levels of tau-protein in cerebrospinal fluid of patients with Creutzfeldt-Jakob disease. *Neurosci. Lett.* 225, 210–212.

Patel, S., Lee, E. B., Xie, S. X., Law, A., Jackson, E. M., Arnold, S. E., et al. (2012). Phosphorylated tau/amyloid beta 1-42 ratio in ventricular cerebrospinal fluid reflects outcome in idiopathic normal pressure hydrocephalus. *Fluids Barriers CNS* 9:7. doi: 10.1186/2045-8118-9-7

Pijnenburg, Y. A., Schoonenboom, N. S., Rosso, S. M., Mulder, C., Van Kamp, G. J., Van Swieten, J. C., et al. (2004). CSF tau and Abeta42 are not useful in the diagnosis of frontotemporal lobar degeneration. *Neurology* 62, 1649.

Pijnenburg, Y. A., Schoonenboom, S. N., Mehta, P. D., Mehta, S. P., Mulder, C., Veerhuis, R., et al. (2007). Decreased cerebrospinal fluid amyloid beta (1-40) levels in frontotemporal lobar degeneration. *J. Neurol. Neurosurg. Psychiatry* 78, 735–737.

Rabinovici, G. D., Jagust, W. J., Furst, A. J., Ogar, J. M., Racine, C. A., Mormino, E. C., et al. (2008). Abeta amyloid and glucose metabolism in three variants of primary progressive aphasia. *Ann. Neurol.* 64, 388–401.

Rascovsky, K., Hodges, J. R., Knopman, D., Mendez, M. F., Kramer, J. H., Neuhaus, J., et al. (2011). Sensitivity of revised diagnostic criteria for the behavioural variant of frontotemporal dementia. *Brain* 134, 2456–2477.

Rascovsky, K., Salmon, D. P., Hansen, L. A., and Galasko, D. (2008). Distinct cognitive profiles and rates of decline on the Mattis Dementia Rating Scale in autopsy-confirmed frontotemporal dementia and Alzheimer's disease. *J. Int. Neuropsychol. Soc.* 14, 373–383.

Renton, A. E., Majounie, E., Waite, A., Simon-Sanchez, J., Rollinson, S., Gibbs, J. R., et al. (2011). A hexanucleotide repeat expansion in C9ORF72 is the cause of chromosome 9p21-linked ALS-FTD. *Neuron* 72, 257–268.

Riemenschneider, M., Wagenpfeil, S., Diehl, J., Lautenschlager, N., Theml, T., Heldmann, B., et al. (2002). Tau and Abeta42 protein in CSF of patients with frontotemporal degeneration. *Neurology* 58, 1622–1628.

Rosso, S. M., Van Herpen, E., Pijnenburg, Y. A., Schoonenboom, N. S., Scheltens, P., Heutink, P., et al. (2003). Total tau and phosphorylated tau 181 levels in the cerebrospinal fluid of patients with frontotemporal dementia due to P301L and G272V tau mutations. *Arch. Neurol.* 60, 1209–1213.

Schmidt, M. L., Gur, R. E., Gur, R. C., and Trojanowski, J. Q. (1988). Intraneuronal and extracellular neurofibrillary tangles exhibit mutually exclusive cytoskeletal antigens. *Ann. Neurol.* 23, 184–189.

Schoonenboom, N. S., Pijnenburg, Y. A., Mulder, C., Rosso, S. M., Van Elk, E. J., Van Kamp, G. J., et al. (2004). Amyloid beta(1-42) and phosphorylated tau in CSF as markers for early-onset Alzheimer disease. *Neurology* 62, 1580–1584.

Schoonenboom, N. S., Reesink, F. E., Verwey, N. A., Kester, M. I., Teunissen, C. E., Van De Ven, P. M., et al. (2012). Cerebrospinal fluid markers for differential dementia diagnosis in a large memory clinic cohort. *Neurology* 78, 47–54.

Seguin, J., Formaglio, M., Perret-Liaudet, A., Quadrio, I., Tholance, Y., Rouaud, O., et al. (2011). CSF biomarkers in posterior cortical atrophy. *Neurology* 76, 1782–1788.

Seppala, T. T., Nerg, O., Koivisto, A. M., Rummukainen, J., Puli, L., Zetterberg, H., et al. (2012). CSF biomarkers for Alzheimer disease correlate with cortical brain biopsy findings. *Neurology* 78, 1568–1575.

Shaw, L. M., Vanderstichele, H., Knapik-Czajka, M., Clark, C. M., Aisen, P. S., Petersen, R. C.,

et al. (2009). Cerebrospinal fluid biomarker signature in Alzheimer's disease neuroimaging initiative subjects. *Ann. Neurol.* 65, 403–413.

Shaw, L. M., Vanderstichele, H., Knapik-Czajka, M., Figurski, M., Coart, E., Blennow, K., et al. (2011). Qualification of the analytical and clinical performance of CSF biomarker analyses in ADNI. *Acta Neuropathol.* 121, 597–609.

Shi, J., Shaw, C. L., Du Plessis, D., Richardson, A. M., Bailey, K. L., Julien, C., et al. (2005). Histopathological changes underlying frontotemporal lobar degeneration with clinicopathological correlation. *Acta Neuropathol.* 110, 501–512.

Sjogren, M., Davidsson, P., Tullberg, M., Minthon, L., Wallin, A., Wikkelso, C., et al. (2001). Both total and phosphorylated tau are increased in Alzheimer's disease. *J. Neurol. Neurosurg. Psychiatry* 70, 624–630.

Sjogren, M., Minthon, L., Davidsson, P., Granerus, A. K., Clarberg, A., Vanderstichele, H., et al. (2000a). CSF levels of tau, beta-amyloid(1-42) and GAP-43 in frontotemporal dementia, other types of dementia and normal aging. *J. Neural Transm.* 107, 563–579.

Sjogren, M., Rosengren, L., Minthon, L., Davidsson, P., Blennow, K., and Wallin, A. (2000b). Cytoskeleton proteins in CSF distinguish frontotemporal dementia from AD. *Neurology* 54, 1960–1964.

Snowden, J., Neary, D., and Mann, D. (2007). Frontotemporal lobar degeneration: clinical and pathological relationships. *Acta Neuropathol.* 114, 31–38.

Sperling, R. A., Aisen, P. S., Beckett, L. A., Bennett, D. A., Craft, S., Fagan, A. M., et al. (2011). Toward defining the preclinical stages of Alzheimer's disease: recommendations from the National Institute on Aging-Alzheimer's Association workgroups on diagnostic guidelines for Alzheimer's disease. *Alzheimers Dement.* 7, 280–292.

Steinacker, P., Hendrich, C., Sperfeld, A. D., Jesse, S., Von Arnim, C. A., Lehnert, S., et al. (2008). TDP-43 in cerebrospinal fluid of patients with frontotemporal lobar degeneration and amyotrophic lateral sclerosis. *Arch. Neurol.* 65, 1481–1487.

Tapiola, T., Alafuzoff, I., Herukka, S. K., Parkkinen, L., Hartikainen, P., Soininen, H., et al. (2009). Cerebrospinal fluid {beta}-amyloid 42 and tau proteins as biomarkers of Alzheimer-type pathologic changes in the brain. *Arch. Neurol.* 66, 382–389.

Toledo, J. B., Brettschneider, J., Grossman, M., Arnold, S. E., Hu, W. T., Xie, S. X., et al. (2012). CSF biomarkers cutoffs: the importance of coincident neuropathological diseases. *Acta Neuropathol.* 124, 23–35.

Trojanowski, J. Q., and Growdon, J. H. (1998). A new consensus report on biomarkers for the early antemortem diagnosis of Alzheimer disease: current status, relevance to drug discovery, and recommendations for future research. *J. Neuropathol. Exp. Neurol.* 57, 643–644.

Trojanowski, J. Q., Vandeerstichele, H., Korecka, M., Clark, C. M., Aisen, P. S., Petersen, R. C., et al. (2010). Update on the biomarker core of the Alzheimer's Disease Neuroimaging Initiative subjects. *Alzheimers Dement.* 6, 230–238.

Turner, R. S., Kenyon, L. C., Trojanowski, J. Q., Gonatas, N., and Grossman, M. (1996). Clinical, neuroimaging, and pathologic features of progressive nonfluent aphasia. *Ann. Neurol.* 39, 166–173.

Van Deerlin, V. M., Sleiman, P. M., Martinez-Lage, M., Chen-Plotkin, A., Wang, L. S., Graff-Radford, N. R., et al. (2010). Common variants at 7p21 are associated with frontotemporal lobar degeneration with TDP-43 inclusions. *Nat. Genet.* 42, 234–239.

Van Harten, A. C., Kester, M. I., Visser, P. J., Blankenstein, M. A., Pijnenburg, Y. A., Van Der Flier, W. M., et al. (2011). Tau and p-tau as CSF biomarkers in dementia: a meta-analysis. *Clin. Chem. Lab. Med.* 49, 353–366.

Vanmechelen, E., Vanderstichele, H., Davidsson, P., Van Kerschaver, E., Van Der Perre, B., Sjogren, M., et al. (2000). Quantification of tau phosphorylated at threonine 181 in human cerebrospinal fluid: a sandwich ELISA with a synthetic phosphopeptide for standardization. *Neurosci. Lett.* 285, 49–52.

Verwey, N. A., Kester, M. I., Van Der Flier, W. M., Veerhuis, R., Berkhof, H., Twaalfhoven, H., et al. (2010). Additional value of CSF amyloid-beta 40 levels in the differentiation between FTLD and control subjects. *J. Alzheimers Dis.* 20, 445–452.

Wang, L. S., Leung, Y. Y., Chang, S. K., Leight, S., Knapik-Czajka, M., Baek, Y., et al. (2012). Comparison of xMAP and ELISA assays for detecting cerebrospinal fluid biomarkers of Alzheimer's disease. *J. Alzheimers Dis.* 31, 439–445.

Weiner, M. W., Aisen, P. S., Jack, C. R. Jr., Jagust, W. J., Trojanowski, J. Q., Shaw, L., et al. (2010). The Alzheimer's disease neuroimaging initiative: progress report and future plans. *Alzheimers Dement.* 6, 202-211 e207.

Whitwell, J. L., Weigand, S. D., Boeve, B. F., Senjem, M. L., Gunter, J. L., Dejesus-Hernandez, M., et al. (2012). Neuroimaging signatures of frontotemporal dementia genetics: C9ORF72, tau, progranulin and sporadics. *Brain* 135, 794–806.

Zhukareva, V., Sundarraj, S., Mann, D., Sjogren, M., Blenow, K., Clark, C. M., et al. (2003). Selective reduction of soluble tau proteins in sporadic and familial frontotemporal dementias: an international follow-up study. *Acta Neuropathol.* 105, 469–476.

Zhukareva, V., Vogelsberg-Ragaglia, V., Van Deerlin, V. M., Bruce, J., Shuck, T., Grossman, M., et al. (2001). Loss of brain tau defines novel sporadic and familial tauopathies with frontotemporal dementia. *Ann. Neurol.* 49, 165–175.

Conflict of Interest Statement: Dr. John Q. Trojanowski reports single consulting services to Pfizer, J&J, MetLife, and BMS; Royalty payments through Penn licenses; and research support from AstraZeneca and BMS. The other authors declare that the research was conducted in the absence of any commercial or financial relationships that could be construed as a potential conflict of interest.

Received: 06 January 2013; paper pending published: 30 January 2013; accepted: 05 February 2013; published online: 21 February 2013.

*Citation: Irwin DJ, Trojanowski JQ and Grossman M (2013) Cerebrospinal fluid biomarkers for differentiation of frontotemporal lobar degeneration from Alzheimer's disease. Front. Aging Neurosci. **5**:6. doi: 10.3389/fnagi.2013.00006*

frontiers in
AGING NEUROSCIENCE

MINI REVIEW ARTICLE
published: 02 July 2013
doi: 10.3389/fnagi.2013.00025

Is abeta a sufficient biomarker for monitoring anti-abeta clinical studies? A critical review

Jens Moreth , Chrystelle Mavoungou and Katharina Schindowski*

Faculty for Biotechnology, Institute of Applied Biotechnology, Biberach University of Applied Science, Biberach/Riss, Germany

Edited by:
Manuel Menéndez-González, Hospital Álvarez-Buylla, Spain

Reviewed by:
Eugenia Rota, Ospedale Guglielmo da Saliceto di Piacenza, Italy
Xue Hua, University of California, Los Angeles, USA
Sandra A. Acosta, University of South Florida, USA

***Correspondence:**
Katharina Schindowski, Faculty for Biotechnology, Institute of Applied Biotechnology, Biberach University of Applied Science, Karlstrasse 11, D-88400 Biberach/Riss, Germany
e-mail: zimmermann@hochschule-bc.de

Amyloid-beta (Aβ) in Alzheimer's disease (AD) appeared to be a promising target for disease-modifying therapeutic strategies like passive immunotherapy with anti-Aβ monoclonal antibodies (mAbs). Biochemical markers in cerebrospinal fluid (CSF) include alterations of Aβ that allow the diagnosis of AD. Biomarker strategies, such as the levels of Aβ in CSF and plasma, currently play an important role in early clinical trials for AD. Indeed, these strategies have a relevant impact on the outcome of such studies, since the biomarkers are used to monitor the bioactivity of anti-Aβ mAbs. The clinical trials of Solanezumab were mainly based on the readout of Aβ levels in CSF and plasma, whereas those of Bapineuzumab were based on cognition; however, little is known about the mechanisms altering these biomarker levels, and no biomarker has yet been proven to be a successful predictor for AD therapy. In addition, the Aβ biomarkers allow for the determination of free and bound anti-Aβ mAb in order to monitor the available amount of bioactive drug and could give hints to the mechanism of action. In this review, we discuss clinical Aβ biomarker data and the latest regulatory strategies.

Keywords: passive immunization, dementia, therapeutic monoclonal antibodies, regulatory strategy, CSF, plasma increase, mode of action, pharmacogenetics and pharmacogenomics

Aβ-AGGREGATES AND THEIR IMPLICATIONS ON IMMUNIZATION

With about 70% of all cases, Alzheimer's disease (AD) is the most-common form of dementia (Alzheimer's Disease International, 2009) and countries in demographic transition will experience the greatest growth. AD is defined as a multifactorial disease with the pathogenic cerebral deposition of the aggregated proteins Amyloid-β (Aβ) and hyper-phosphorylated tau (phospho-tau). Despite the well-accepted pathogenic role of Aβ (Selkoe, 2001), the underlying pathogenic mechanism is still elusive (Broersen et al., 2010). Aβ-aggregates—majorly derived from $Aβ_{40}$ and $Aβ_{42}$—are generated from amyloid precursor protein by sequential proteolysis (Haass and Selkoe, 2007) followed by self-association from monomeric to soluble oligomeric and protofibrillar Aβ. Protofibrillar Aβ further aggregates into insoluble Aβ-fibrils and deposits in the brain as amyloid plaques. Since the number of these plaques does not correlate well with the severity of dementia (Terry, 2006)—as opposed to soluble Aβ-aggregates (McDonald et al., 2010)—the amyloid hypothesis has been reformulated, positioning soluble Aβ aggregates as hallmark in AD pathology (Walsh and Selkoe, 2007; Broersen et al., 2010). A plethora of different Aβ-species with overlapping size and morphology have been described (Broersen et al., 2010; Benilova et al., 2012): Aβ-dimers (Shankar et al., 2008; O'Nuallain et al., 2010), low-molecular weight oligomers comprising dimeric to tetrameric Aβ (Walsh et al., 2005), pentamers and hexamers (Ahmed et al., 2010), dodecameric Aβ56* (Lesne et al., 2006; Reed et al., 2011), globulomers (Barghorn et al., 2005), Aβ-oligomers (Kayed et al., 2003), Alzheimer-derived diffusible ligands (ADDLs; Lambert et al., 1998), protofibrils (Walsh et al., 1999), and amylospheroids (Hoshi et al., 2003). Although, the size and molecular weight of these Aβ-species have predominantly been used for differentiation, the peptide source, either synthetic or endogenous, and the applied methods for characterization—e.g., SDS-PAGE, TEM, AFM, Ultracentrifugation—hamper a direct comparison (Moreth et al., 2013). Despite the pathological relevance of endogenous Aβ-species, low protein concentrations and protein heterogeneity elude a precise characterization of the molecular identity. The synthetic Aβ-aggregate is applicable to a more-precise characterization, but still retains limited relevance, since the variety of reported Aβ-aggregates has yet to be proven to be present in AD brain. Furthermore, the identification of Aβ-aggregates is hampered owing to their meta-stability and the ability for inter-conversion in different aggregation pathways (Moreth et al., 2013), which was also mentioned by Bitan et al. (2005). This is of great importance for immunization, since the fate of the pre-aggregated Aβ is elusive after injection.

Abbreviations: aa, amino acid; Aβ, amyloid-beta; AβO, Aβ oligomers; AD, Alzheimer's disease; ADAS-Cog, Alzheimer's Disease Assessment Scale-cognitive subscale; ADDLs, Alzheimer derived diffusible ligands; ADNI, Alzheimer's disease neuroimaging initiative; AFM, atomic force microscopy; ApoE4, ApolipoproteinE4; CSF, cerebrospinal fluid; DAD, disability assessment for dementia; EMA, European Medicine Agency; FDA, food and drug administration; J&J, Johnson&Johnson; LRP, low density lipoprotein receptor-related protein; MRI, magnetic resonance imaging; PET, positron emission tomography; phospho-tau, hyperphosphorylated tau; PK, pharmacokinetic; SDS-PAGE, sodium dodecyl sulfate polyacrylamide gel electrophoresis; TEM, transmission electron microscopy.

OCCURRENCE OF Aβ SPECIES IN PLASMA AND CSF

From a set of upcoming biomarkers (Fagan and Perrin, 2012), the most-established biomarkers for AD diagnosis in cerebrospinal

fluid (CSF) are still the determination of $A\beta_{42}$, total-Tau and phospho-Tau_{181} (Di Carlo et al., 2012). Only a combination of these three CSF biomarkers increases the validity of the diagnosis with a combined sensitivity of 95% (Blennow et al., 2010). In AD, CSF-$A\beta_{42}$ is significantly decreased, which is believed to be due to decreased clearance of aggregated $A\beta_{42}$ from the brain. The $A\beta_{40}$ levels seem to be constant and therefore the increased $A\beta_{42}/A\beta_{40}$ ratio has been suggested to improve early AD-diagnosis. However, this is still controversial and for plasma-derived Aβ reports are even more contradictory (Zetterberg, 2008; Zetterberg et al., 2010). To mention the prefibrillar Aβ-aggregates as the prime toxic agents in AD, one might address these as potential biomarkers. However, there is still a lack of a robust method for the detection of larger Aβ-aggregates *in vivo* (e.g., ADDL, Aβ-oligomers). Some recent reports showed methods for Aβ-aggregate detection based on ELISA, IP western blotting and Aβ-aggregate capture assays. All of these methods are based on conformation-specific antibodies, which do not detect monomeric or fibrillar, but rather the prefibrillar aggregates (Funke et al., 2009), even though the most relevant Aβ-aggregate for AD diagnosis is still elusive. Furthermore, based on the described meta-stability of Aβ-aggregates (Moreth et al., 2013), it might be misleading to focus on a single aggregate species if the whole spectrum of aggregates from the dimer up to protofibrillar Aβ are present in the brain and of importance in AD-progression.

PLASMA AND CSF Aβ AS BIOMARKERS TO MONITOR PASSIVE ANTI-Aβ IMMUNOTHERAPY CLINICAL STUDIES

Aβ has a complex pharmacokinetic profile, as it is permanently produced in brain as well as in the periphery, and transported back and forth between both pharmacokinetic compartments (Zlokovic et al., 1993; Ghersi-Egea et al., 1996; Shibata et al., 2000). Soluble Aβ is either degraded by proteases (Iwata et al., 2005), transported via the blood-brain barrier by receptors like LRP (Sagare et al., 2007), RAGE (Deane et al., 2003), and P-glycoprotein (Ito et al., 2006), or aggregates to multimers and plaques. Likewise, plaque Aβ is in steady-state equilibrium with soluble Aβ (Kawarabayashi et al., 2001). Finally, Aβ is rapidly eliminated by hepatic and renal degradation (Ghiso et al., 2004). PET scanning with the Pittsburgh compound (PiB) detects fibrillar Aβ. CSF $A\beta_{42}$ and PET measures of fibrillar Aβ are significantly inversely correlated with each other, likely to reflect Aβ deposition in the brain (Fagan et al., 2006).

Proteins in plasma, like antibodies that capture soluble Aβ, are capable of sequestering soluble forms of Aβ from their bound and circulating forms. Total Aβ plasma levels will therefore increase while free Aβ levels reduce due to the longer half-life of protein-complexed Aβ [see **Figure 1A**; (Park et al., 2012)]. The elimination of the Aβ-protein complex is according to the complex's half-life, which is rather long in the case of FcRn-recycled monoclonal antibodies (mAbs). Complexed Aβ is predictably not transported across the blood brain barrier, does not form multimers, and influences the equilibrium between soluble Aβ and plaque Aβ that appears to result in improved clearance of cerebral Aβ, e.g., CSF Aβ. The Aβ-binding proteins should have an affinity to Aβ high enough to compete with endogenous Aβ-binding proteins and transporters. Free Aβ drops rapidly after Aβ is sequestered, but due to its rapid synthesis in various tissues, it is restored to basal endogenous levels rather quickly (Barten et al., 2005).

Peripherally-administered mAbs that sequester soluble Aβ result in an increase of plasma Aβ (DeMattos et al., 2002) that is correlated to its affinity; some mAbs are even capable of reducing CSF Aβ (Mavoungou and Schindowski, 2013). Several studies used these biomarkers as clinical strategy (**Table 1**). Solanezumab caused a sharp, sustained, and dose-dependent increase of plasma $A\beta_{1-40}$ and $A\beta_{1-42}$ (Farlow et al., 2012). CSF $A\beta_{1-40}$ and $A\beta_{1-42}$ increased in the mild to moderate AD patients with 0.1% of plasma levels of Solanezumab found in the CSF. The rise in level of total Aβ in plasma and CSF is assumed to be related to target engagement (Strobel and Bowman Rogers, 2012). Free CSF Aβ was determined by protein G sepharose immunoprecipitation to deplete immunoglobins and subsequent ELISA (Farlow et al., 2012). Therefore, this method was used for CSF samples only, since immunoglobulin plasma concentrations are too high for this method. In a rather small cohort of patients, free CSF $A\beta_{1-40}$ decreased with treatment, while free $A\beta_{1-42}$ did not. It is suspected that the higher amount of free CSF $A\beta_{1-42}$ is related to the dissolution of plaques that were mainly composed of $A\beta_{42}$. However, PiB scans of another subcohort showed no significant change between the groups, although treated patients with mild AD had a trend toward less amyloid, this lacked statistical significance (Matthews and Bader, 2012).

The clinical biomarker data from Bapineuzumab are more difficult to interpret, due to the fact that Bapineuzumab binds both soluble and plaque Aβ, and the methodological strategy is rather unclear. $A\beta_{1-40}$ and $A\beta_{x-42}$ were detected by a sandwich ELISA using 4G8 for capture and a C-terminal mAb for detection (**Figure 1B**). 4G8 does not interfere with Bapineuzumab binding (Johnson-Wood et al., 1997; Clarke and Shearman, 2000). Interestingly, $A\beta_{1-42}$ was determined with an ELISA using 3D6 as capture. 3D6 is the parental molecule of Bapineuzumab and therefore these two mAbs compete with each other when binding Aβ. Consequently, Bapineuzumab-Aβ complexes in CSF will predictably not be detected in this assay, though according to PK data Bapineuzumab occurs in CSF with 0.3% incidence of plasma levels (Blennow et al., 2012). Hence, the clinical data reveal no changes in CSF $A\beta_{1-42}$ levels with Bapineuzumab treatment, while Solanezumab treatment revealed an increase in $A\beta_{1-42}$ detected with the C-terminal mAb 21F12 and the N-terminal 3D6. Moreover, to avoid signal suppression due to steric hindrance, the authors of the Solanezumab study spiked an excess of Solanezumab in the assay buffer (Farlow et al., 2012). Furthermore, Bapineuzumab treatment decreased CSF phospho-tau (Salloway et al., 2012; Sperling et al., 2012). Like Solanezumab, Bapineuzumab was not active on patient's cognition and activities of daily living unless subsequent post-test of subcohorts were considered for re-analysis (Salloway et al., 2009; Lilly, 2012; Matthews and Bader, 2012). In summary, both antibodies engaged their target, but they hardly improved clinical signs (Strobel and Bowman Rogers, 2012). Bapineuzumab's clinical development was discontinued for AD in 2012 (Johnson & Johnson, 2012), AAB-003/PF-0523681 an engineered 3D6

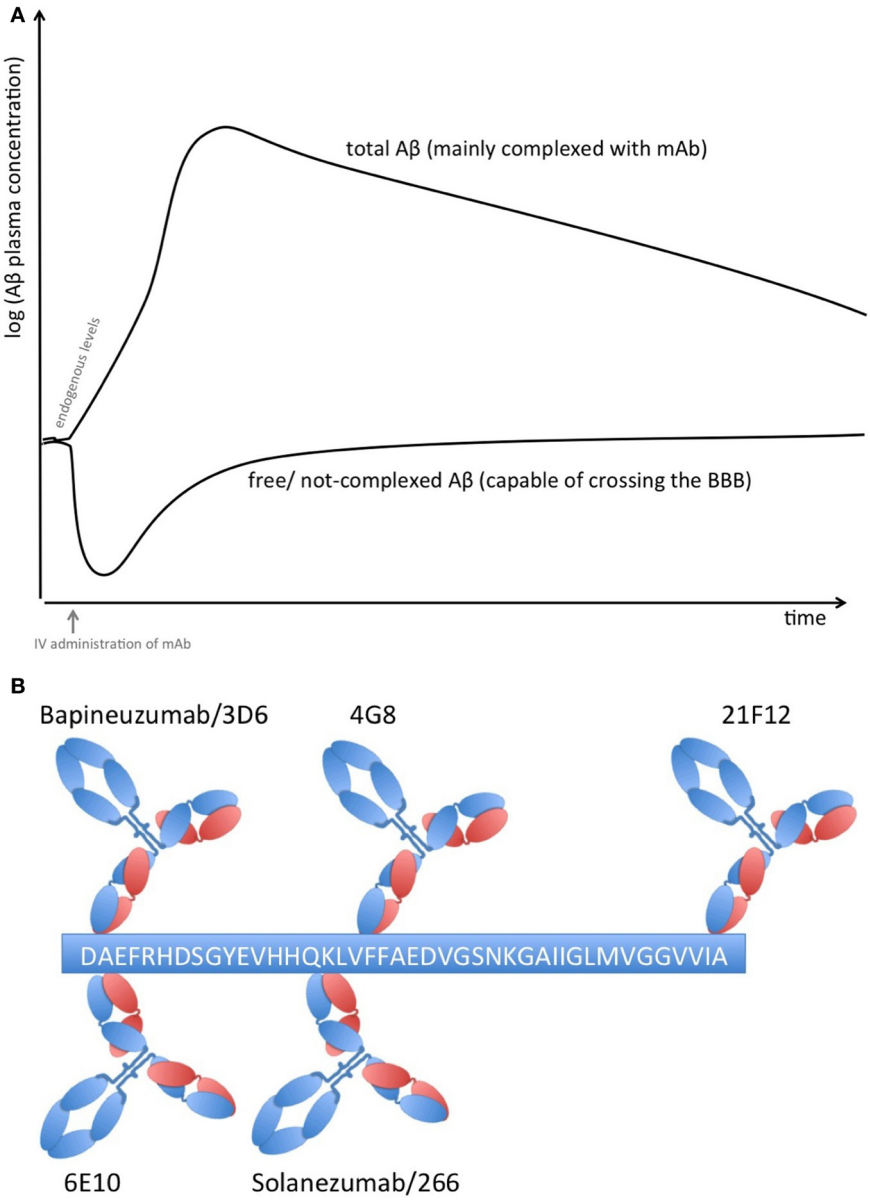

FIGURE 1 | (A) Plasma Aβ levels after treatment with an Aβ sequestering compound. Anti-Aβ mAbs capture soluble Aβ and form Aβ-mAb complexes, which have a much longer half-life than free Aβ alone. Therefore, total Aβ (i.e., free and bound) plasma levels rise while free Aβ levels drop rapidly but return rather quickly to normal levels due to its rapid synthesis in many tissues. **(B)** Binding sites on $Aβ_{1-42}$ of therapeutic and diagnostic mAbs. Adapted from Johnson-Wood et al. (1997); Clarke and Shearman (2000).

replaced Bapineuzumab in the sponsor's pipeline (Pfizer, 2013). Dose-dependent plasma total Aβ increases were reported from GSK933776 and Crenezumab with decreased free plasma Aβ levels (GlaxoSmithKline, 2011; Adolfsson et al., 2012).

THE IMPORTANCE OF AN APPROPRIATE BIOMARKER STRATEGY FOR AD

In an ideal world with a successful anti-AD therapy, the detection of AD biomarkers should indicate appropriate patient selection likely to derive therapeutic benefit. The EMA tried first to get closer to this ideal world, at least from the regulatory side, and introduced research diagnostic criteria that added specificity to the prevailing concept of mild cognitive impairment (Dubois et al., 2007). This set the stage for new types of trials (Strobel and Bowman Rogers, 2012). The criteria are closer to the disease, combining a mild but measurable memory impairment with a biomarker change. The EMA considered firstly that a pathological signature based on CSF $Aβ_{42}$ and phospho-tau was acceptable for identifying prodromal-stage patients who are at risk of developing AD (European Medicines Agency, 2011b), secondly, using

Table 1 | Clinical effects of anti-Aβ mAbs on CSF and plasma Aβ, adapted from Mavoungou and Schindowski (2013).

Study/cohort	Subcohort size for biomarker evaluation	Evaluated biomarker	Clinical effect of treatment on biomarker	Clinical effect on cognition	PK data of mAb	References
BAPINEUZUMAB (HUMANIZED 3D6)						
201 Phase II	Placebo: $n = 14$ BAPI: $n = 20$	CSF $A\beta_{x-42}$ Total CSF tau CSF phospho-tau	No changes No changes Trend to reduction ($p = 0.056$)	In small cohort 6% less loss of ADAS-Cog scores after 18 months	Approximately 0.3% CSF-plasma ratio	Salloway et al., 2009
Phase II: pooled 201 and 202	Placebo: $n = 19$ BAPI: $n = 26$–27	CSF $A\beta_{1-40}$ CSF $A\beta_{x-42}$ CSF $A\beta_{1-42}$ Total CSF tau CSF phospho-tau	No changes Decrease from baseline No changes No changes Reduction ($p = 0.03$)	Not determined	Not determined	Blennow et al., 2012
Phase III: 301 (*ApoE4* carrier)	Placebo: $n = 77$ 0.5 mg/kg: $n = 47$ 1.0 mg/kg: $n = 54$	CSF phospho-tau CSF phospho-tau	No changes at 0.5 mg/kg Reduction at 1.0 mg/kg	In a subcohort of mild cases at 1.0 mg/kg ∼30% less loss of DAD scores after 18 months	Not determined	Salloway et al., 2012
Phase III: 302 (*ApoE4* non-carrier)	Placebo: $n = 85$ 0.5 mg/kg: $n = 127$	CSF phospho-tau	Reduction at 0.5 mg/kg	No effect on cognition after 18 months, even not for mild cases	Not determined	Sperling et al., 2012
SOLANEZUMAB (HUMANIZED m266)						
Phase II	Placebo: $n = 8$; SOLA: $n = 10$–11 per dose group	CSF total $A\beta_{40}$ CSF total $A\beta_{42}$ CSF free $A\beta_{40}$ CSF free $A\beta_{42}$ Plasma total $A\beta_{40}$ Plasma total $A\beta_{42}$	Increase at high dose Increase at high dose Decrease at high dose Increase at high dose Dose-dependent increase Dose-dependent decrease	No significant cognitive benefit on the ADAS-cog score over after 12-weeks	0.1% CSF-plasma ratio	Farlow et al., 2012
GSK933776 (DISCONTINUED FOR AD)						
Phase I	Placebo: $n = 14$; GSK933776: $n = 3$–6 per dose group	Plasma total Aβ Plasma free Aβ CSF $A\beta_{1-38}$ tau/phospho-tau	Dose-dependent increase Dose-dependent decrease Increase at the highest dose No changes	Not determined	>0.2% CSF-plasma ratio	GlaxoSmithKline, 2011
CRENEZUMAB (MABT5102A)						
Phase I	MABT: $n = 25$–31 per regime group	Plasma total $A\beta_{40}$ Plasma total $A\beta_{40}$	Dose-dependent increase Dose-dependent increase	Not determined	Not determined	Adolfsson et al., 2012

hippocampal volume (European Medicines Agency, 2011a), and thirdly, using amyloid PET as a biomarker to enrich pre-dementia trials (European Medicines Agency, 2011c). Likewise, the FDA revised its criteria as well. Nevertheless, evidence is needed that a surrogate marker predicts a subsequent clinical outcome. Qualifying disease- and disorder-specific biomarkers for AD can still be considered "exploratory" from a regulatory point of view, therefore making an accurate validation and qualification questionable. Nevertheless, biomarkers, in particular those appropriate to guide selection of patients for clinical trials as well as those used as surrogate endpoint for drug efficacy, have reached the status of "probable valid biomarker" within the scope of investigation drugs along with an effective clinical trial strategy. In conclusion, the results show that CSF biomarkers are better predictors of progression to AD than plasma Aβ isoforms (Hansson et al., 2010).

Florbetapir, which binds Aβ plaques like PiB, was fast-track reviewed by the FDA and is currently the first granted and therefore qualified imaging agent for clinical use (Food and Drug Administration, 2012a). Following the results of the evaluation, even though a positive scan indicates moderate to frequent plaques, a positive Florbetapir scan is not AD specific, indicating that it is not appropriate to establish an accurate diagnosis of AD (Food and Drug Administration, 2012b). In fact, nobody currently knows why cognitively normal people accumulate Aβ in their brains, and what that might mean for their future brain health. The AD Neuroimaging Initiative (ADNI) belongs to one of the instruments to gain more information on the disease by means of PET and MRI linked to genetic disposition, cognitive impairment as well as CSF and plasma biomarkers. The use of such information obviously is crucial to set future clinical designs for AD (Food and Drug Administration, 2012a) but also

as prophylactic examination for physicians in case of genetic predisposition for AD. On the other hand, exploring a set of imaging and biochemical biomarkers helps to develop regulatory guidelines to change diagnostic criteria, their validation and finally to support the potential use of biomarkers in different stages of drug development.

While the expressed view is that CSF biomarkers indicate the pathologic processes underlying AD, it is also important to keep in mind that specific genotypes like *ApoE4* and presenilin mutations affect the degree of pathological change. Therefore, using pharmacogenetics will enrich clinical drug development. From the presented data it seems that use of CSF markers is an unavoidable step for a correct and early diagnosis. However, the data reported show only the positive results, with no negative comments or discussion on potential pitfalls. Uncritical support without showing areas of uncertainty or controversy could be misleading, in helping to improve the design of subsequent randomized controlled clinical trials. The hazard ratio in longitudinal studies shows an extremely large confidence interval, which is not that supportive for the utility of monitoring. The specifications of the confidence interval for such a multifactorial disease like AD might be nowadays too tight in the light of the recent findings about the disease. That means it is understandable that the confidence interval cannot be met for most of the cases. A combination of biomarkers to boost the sensitivity and reliability for tracking AD progression at different stage and widening the current specification limits with respect to confidential interval would better match with the variability of the results.

CONCLUSION

To summarize, Aβ-aggregates reveal a remarkable metastability and the ability for reorganization within different aggregate equilibria. One might assume that the whole spectrum of prefibrillar Aβ-aggregates is of relevance in AD. Thus, targeting one specific species of Aβ with immunotherapy and using Aβ as preclinical and clinical biomarker is based on tentative, though countless data that apparently do not reflect the clinical reality. Therefore, the clinical biomarker data from the phase II and III studies of the most-advanced anti-Aβ mAbs are not appropriate to predict the cognitive outcome, even though the results show that CSF Aβ appears to be more relevant than plasma Aβ. This stresses the urgent need to understand the molecular basis of AD and to find adequate surrogate biomarkers. From a regulatory point of view, the approval of a highly-innovative active substance for the treatment for AD still remains a challenge. Although biomarker strategies have been taken more and more into account, the current study designs for AD superficially address the silent pathogenesis of the disease. The EMA and FDA are looking forward to qualifying new surrogate endpoints that encompass appropriate biomarker concepts in support of a robust biomarker strategy, which would enable the discovery of medicinal products that are active in interfering with AD pathogenesis.

AUTHORS CONTRIBUTIONS

Jens Moreth supported with novel data on Aβ conformation and aggregation, Chrystelle Mavoungou supported with insight from regulatory affairs and Katharina Schindowski supported with insight on Aβ immunotherapy und neuroimmunology. All authors drafted the manuscript. All authors read and approved the final manuscript.

ACKNOWLEDGMENTS

The authors thank Owen Scudamore for language editing and help with the manuscript.

REFERENCES

Adolfsson, O., Pihlgren, M., Toni, N., Varisco, Y., Buccarello, A. L., Antoniello, K., et al. (2012). An effector-reduced anti-β-amyloid (Aβ) antibody with unique Aβ binding properties promotes neuroprotection and glial engulfment of Aβ. *J. Neurosci.* 32, 9677–9689. doi: 10.1523/JNEUROSCI.4742-11.2012

Ahmed, M., Davis, J., Aucoin, D., Sato, T., Ahuja, S., Aimoto, S., et al. (2010). Structural conversion of neurotoxic amyloid-beta(1-42) oligomers to fibrils. *Nat. Struct. Mol. Biol.* 17, 561–567. doi: 10.1038/nsmb.1799

Alzheimer's Disease International. (2009). *World Alzheimer Report 2009*. Available online at: http://www.alz.co.uk/research/world-report

Barghorn, S., Nimmrich, V., Striebinger, A., Krantz, C., Keller, P., Janson, B., et al. (2005). Globular amyloid beta-peptide oligomer a homogenous and stable neuropathological protein in Alzheimer's disease. *J. Neurochem.* 95, 834–847. doi: 10.1111/j.1471-4159.2005.03407.x

Barten, D. M., Guss, V. L., Corsa, J. A., Loo, A., Hansel, S. B., Zheng, M., et al. (2005). Dynamics of beta-amyloid reductions in brain, cerebrospinal fluid, and plasma of beta-amyloid precursor protein transgenic mice treated with a gamma-secretase inhibitor. *J. Pharmacol. Exp. Ther.* 312, 635–643. doi: 10.1124/jpet.104.075408

Benilova, I., Karran, E., and De Strooper, B. (2012). The toxic Abeta oligomer and Alzheimer's disease: an emperor in need of clothes. *Nat. Neurosci.* 15, 349–357. doi: 10.1038/nn.3028

Bitan, G., Fradinger, E. A., Spring, S. M., and Teplow, D. B. (2005). Neurotoxic protein oligomers what you see is not always what you get. *Amyloid* 12, 88–95. doi: 10.1080/13506120500106958

Blennow, K., Hampel, H., Weiner, M., and Zetterberg, H. (2010). Cerebrospinal fluid and plasma biomarkers in Alzheimer disease. *Nat. Rev. Neurol.* 6, 131–144. doi: 10.1038/nrneurol.2010.4

Blennow, K., Zetterberg, H., Rinne, J. O., Salloway, S., Wei, J., Black, R., et al. (2012). Effect of immunotherapy with bapineuzumab on cerebrospinal fluid biomarker levels in patients with mild to moderate Alzheimer Disease. *Arch. Neurol.* 69, 1002–1010. doi: 10.1001/archneurol.2012.90

Broersen, K., Rousseau, F., and Schymkowitz, J. (2010). The culprit behind amyloid beta peptide related neurotoxicity in Alzheimer's disease: oligomer size or conformation. *Alzheimers Res. Ther.* 2, 12. doi: 10.1186/alzrt36

Clarke, E. E., and Shearman, M. S. (2000). Quantitation of amyloid-beta peptides in biological milieu using a novel homogeneous time-resolved fluorescence (HTRF) assay. *J. Neurosci. Methods* 102, 61–68. doi: 10.1016/S0165-0270(00)00280-6

Deane, R., Du Yan, S., Submamaryan, R. K., LaRue, B., Jovanovic, S., Hogg, E., et al. (2003). RAGE mediates amyloid-beta peptide transport across the blood-brain barrier and accumulation in brain. *Nat. Med.* 9, 907–913. doi: 10.1038/nm890

DeMattos, R. B., Bales, K. R., Cummins, D. J., Paul, S. M., and Holtzman, D. M. (2002). Brain to plasma amyloid-β efflux: a measure of brain amyloid burden in a mouse model of Alzheimer's disease. *Science* 295, 2264–2267. doi: 10.1126/science.1067568

Di Carlo, M., Giacomazza, D., and San Biagio, P. L. (2012). Alzheimer's disease: biological aspects, therapeutic perspectives and diagnostic tools. *J. Phys. Condens. Matter* 24:244102. doi: 10.1088/0953-8984/24/24/244102

Dubois, B., Feldman, H., Jacova, C., Dekosky, S., Barberger-Gateau,

P., Cummings, J., et al. (2007). Research criteria for the diagnosis of Alzheimer's disease: revising the NINCDS-ADRDA criteria. *Lancet* 6, 734–746. doi: 10.1016/S1474-4422(07)70178-3

European Medicines Agency. (2011a). *European Medicines Agency Releases Qualification Opinion on Diagnosis of Pre-Dementia Alzheimer's for Public Consultation*. Available online at: http://www.ema.europa.eu/ema/index.jsp?curl=pages/news_and_events/news/2011/10/news_detail_001359.jspandmid=WC0b01ac058004d5c1. (Accessed January 30, 2013).

European Medicines Agency. (2011b). *First Clinical Biomarker Qualification Released for Public Consultation*. Available online at: http://www.ema.europa.eu/ema/index.jsp?curl=pages/news_and_events/news/2011/02/news_detail_001207.jspandmid=WC0b01ac058004d5c1. (Accessed March 3, 2013).

European Medicines Agency. (2011c). *Qualification Opinion of Alzheimer's Disease Novel Methodologies/Biomarkers for the use of CSF AB 1-42 and t-tau Signature and/or PET-Amyloid Imaging (Positive/Negative) as a Biomarkers for Enrichment, for use in Regulatory Clinical Trials in Mild*. Available online at: http://www.ema.europa.eu/docs/en_GB/document_library/Regulatory_and_procedural_guideline/2011/12/WC500118365.pdf. (Accessed January 30, 2013).

Fagan, A. M., Mintun, M. A., Mach, R. H., Lee, S.-Y., Dence, C. S., Shah, A. R., et al. (2006). Inverse relation between *in vivo* amyloid imaging load and cerebrospinal fluid Abeta42 in humans. *Ann. Neurol.* 59, 512–519. doi: 10.1002/ana.20730

Fagan, A. M., and Perrin, R. J. (2012). Upcoming candidate cerebrospinal fluid biomarkers of Alzheimer's disease. *Biomark. Med.* 6, 455–476. doi: 10.2217/bmm.12.42

Farlow, M., Arnold, S. E., Van Dyck, C. H., Aisen, P. S., Snider, B. J., Porsteinsson, A. P., et al. (2012). Safety and biomarker effects of solanezumab in patients with Alzheimer's disease. *Alzheimer's Dement.* 8, 261–271. doi: 10.1016/j.jalz.2011.09.224

Food and Drug Administration. (2012a). *FDA Approves Imaging Drug Amyvid*. Available online at: http://www.fda.gov/NewsEvents/Newsroom/PressAnnouncements/ucm299678.htm. (Accessed January 30, 2013).

Food and Drug Administration. (2012b). *FY 2012 Innovative Drug Approvals*. Available online at: http://www.fda.gov/downloads/aboutfda/reportsmanualsforms/reports/ucm330859.pdf. (Accessed March 27, 2013).

Funke, S. A., Birkmann, E., and Willbold, D. (2009). Detection of Amyloid-beta aggregates in body fluids: a suitable method for early diagnosis of Alzheimer's disease. *Curr. Alzheimer Res.* 6, 285–289. doi: 10.2174/156720509788486536

Ghersi-Egea, J. F., Gorevic, P. D., Ghiso, J., Frangione, B., Patlak, C. S., and Fenstermacher, J. D. (1996). Fate of cerebrospinal fluid-borne amyloid beta-peptide: rapid clearance into blood and appreciable accumulation by cerebral arteries. *J. Neurochem.* 67, 880–883. doi: 10.1046/j.1471-4159.1996.67020880.x

Ghiso, J., Shayo, M., Calero, M., Ng, D., Tomidokoro, Y., Gandy, S., et al. (2004). Systemic catabolism of Alzheimer's Abeta40 and Abeta42. *J. Biol. Chem.* 279, 45897–45908. doi: 10.1074/jbc.M407668200

GlaxoSmithKline. (2011). *A Randomised, Single-Blind, Placebo-Controlled Study to Investigate the Safety, Tolerability, Immunogenicity, Pharmacokinetics and Pharmacodynamics of Intravenous Infusion of GSK933776 in Patients with Alzheimer's Disease*. Available online at: http://www.gsk-clinicalstudyregister.com/result_comp_list.jsp?phase=AllandstudyType=Allandpopulation=Allandmarketing=Noandcompound=GSK933776. (Accessed June 1, 2012).

Haass, C., and Selkoe, D. J. (2007). Soluble protein oligomers in neurodegeneration: lessons from the Alzheimer's amyloid β-peptide. *Nat. Rev. Mol. Cell Biol.* 8, 101–112. doi: 10.1038/nrm2101

Hansson, O., Zetterberg, H., Vanmechelen, E., Vanderstichele, H., Andreasson, U., Londos, E., et al. (2010). Evaluation of plasma Abeta40 and Abeta42 as predictors of conversion to Alzheimer's disease in patients with mild cognitive impairment. *Neurobiol. Aging* 31, 357–367. doi: 10.1016/j.neurobiolaging.2008.03.027

Hoshi, M., Sato, M., Matsumoto, S., Noguchi, A., Yasutake, K., Yoshida, N., et al. (2003). Spherical aggregates of beta-amyloid (amylospheroid) show high neurotoxicity and activate tau protein kinase I/glycogen synthase kinase-3beta. *Proc. Natl. Acad. Sci. U.S.A.* 100, 6370–6375. doi: 10.1073/pnas.1237107100

Ito, S., Ohtsuki, S., and Terasaki, T. (2006). Functional characterization of the brain-to-blood efflux clearance of human amyloid-beta peptide (1-40) across the rat blood-brain barrier. *Neurosci. Res.* 56, 246–252. doi: 10.1016/j.neures.2006.07.006

Iwata, N., Higuchi, M., and Saido, T. C. (2005). Metabolism of amyloid-h peptide and Alzheimer' s disease. *Brain* 108, 403–430.

Johnson & Johnson. (2012). *Johnson & Johnson Announces Discontinuation Of Phase 3 Development of Bapineuzumab Intravenous (IV) In Mild-To-Moderate Alzheimer's Disease. 2012*. Available online at: http://www.jnj.com/connect/news/product/johnson-and-johnson-announces-discontinuation-of-phase-3-development-of-bapineuzumab-intravenous-iv-in-mild-to-moderate-alzheimers-disease

Johnson-Wood, K., Lee, M., Motter, R., Hu, K., Gordon, G., Barbour, R., et al. (1997). Amyloid precursor protein processing and Aβ42 deposition in a transgenic mouse model of Alzheimer disease. *Proc. Natl. Acad. Sci. U.S.A.* 94:1550. doi: 10.1073/pnas.94.4.1550

Kawarabayashi, T., Younkin, L. H., Saido, T. C., Shoji, M., Ashe, K. H., and Younkin, S. G. (2001). Age-dependent changes in brain, CSF, and plasma amyloid (beta) protein in the Tg2576 transgenic mouse model of Alzheimer's disease. *J. Neurosci.* 21, 372–381.

Kayed, R., Head, E., Thompson, J. L., McIntire, T. M., Milton, S. C., Cotman, C. W., et al. (2003). Common structure of soluble amyloid oligomers implies common mechanism of pathogenesis. *Science* 300, 486–489. doi: 10.1126/science.1079469

Lambert, M. P., Barlow, A. K., Chromy, B. A., Edwards, C., Freed, R., Liosatos, M., et al. (1998). Diffusible, nonfibrillar ligands derived from Abeta1-42 are potent central nervous system neurotoxins. *Proc. Natl. Acad. Sci. U.S.A.* 95, 6448–6453. doi: 10.1073/pnas.95.11.6448

Lesne, S., Koh, M. T., Kotilinek, L., Kayed, R., Glabe, C. G., Yang, A., et al. (2006). A specific amyloid-beta protein assembly in the brain impairs memory. *Nature* 440, 352–357. doi: 10.1038/nature04533

Lilly, E. (2012). *Lilly Announces Detailed Results of the Phase 3 Solanezumab Expedition Studies Following a Presentation of the Independent Analyses by the Alzheimer's Disease Cooperative Study (ADCS)*. Available online at: http://newsroom.lilly.com/releasedetail.cfm?ReleaseID=702211

Matthews, G., and Bader, V. (2012). *Indipendent Analysis of Solanezumab Provides Evidence that Compound may remove Amyloid from Brain in Alzheimer's Disease. Clinical Trials on Alzheimer's Disease* (Press Release). Available online at: http://www.ctad.fr/07-download/Congres2012/PressRelease/Sola-Release_29Oct2012.pdf. (Accessed November 5, 2012).

Mavoungou, C., and Schindowski, K. (2013). "Immunotherapy with anti-Amyloid-beta antibodies in Alzheimer's disease: a critical review on the molecules in the pipelines with regulatory considerations," in *Frontiers in Clinical Drug Research - Alzheimer Disorders,* Vol. 1, ed A. U. Rahman (Oak Park: Bentham Science Publishers), 3–85.

McDonald, J. M., Savva, G. M., Brayne, C., Welzel, A. T., Forster, G., Shankar, G. M., et al. (2010). The presence of sodium dodecyl sulphate-stable abeta dimers is strongly associated with alzheimer-type dementia. *Brain J. Neurol.* 133, 1328–1341.

Moreth, J., Kroker, K. S., Schwanzar, D., Schnack, C., Von Arnim, C. A. F., Hengerer, B., et al. (2013). Globular and protofibrillar Aβ aggregates impair neurotransmission by different mechanisms. *Biochemistry* 52, 1466–1476. doi: 10.1021/bi3016444

O'Nuallain, B., Freir, D. B., Nicoll, A. J., Risse, E., Ferguson, N., Herron, C. E., et al. (2010). Amyloid beta-protein dimers rapidly form stable synaptotoxic protofibrils. *J. Neurosci.* 30, 14411–14419. doi: 10.1523/JNEUROSCI.3537-10.2010

Park, J. E., Dorner-Ciossek, C., Hoerer, S., Kussmaul, L., Lenter, M., Zimmermann, K., et al. (2012). A-Beta binding polypeptides. *U.S. Patent 8337845 B2 filed*, 2012.

Pfizer. (2013). *Pfizer Pipeline our Medicines in Development*. Available online at: http://www.pfizer.com/research/product_pipeline/product_pipeline.jsp. (Accessed March 27, 2013).

Reed, M. N., Hofmeister, J. J., Jungbauer, L., Welzel, A. T., Yu, C., Sherman, M. A., et al. (2011). Cognitive effects of cell-derived and synthetically derived Abeta oligomers. *Neurobiol. Aging* 32, 1784–1794. doi: 10.1016/j.neurobiolaging.2009.11.007

Sagare, A., Deane, R., Bell, R. D., Johnson, B., Hamm, K., Pendu, R., et al. (2007). Clearance of amyloid-beta by circulating lipoprotein receptors. *Nat. Med.* 13, 1029–1031. doi: 10.1038/nm1635

Salloway, S., Sperling, R., Gilman, S., Fox, N. C., Blennow, K., Raskind, M., et al. (2009). A phase 2 multiple ascending dose trial of bapineuzumab in mild to moderate Alzheimer disease. *Neurology* 73, 2061–2070. doi: 10.1212/WNL.0b013e3181c67808

Salloway, S., Sperling, R., Honig, L., Porsteinsson, A., Sabbagh, M., Liu, E., et al. (2012). A randomized, double-blind, placebo-controlled clinical trial of intravenous bapineuzumab in patients with Alzheimer's disease who are apolipoprotein E ε4 non-carriers. *Eur. J. Neurol.* 19, SC312.

Selkoe, D. J. (2001). Alzheimer's disease: genes, proteins, and therapy. *Physiol. Rev.* 81, 741–766.

Shankar, G. M., Li, S., Mehta, T. H., Garcia-Munoz, A., Shepardson, N. E., Smith, I., et al. (2008). Amyloid-beta protein dimers isolated directly from Alzheimer's brains impair synaptic plasticity and memory. *Nat. Med.* 14, 837–842. doi: 10.1038/nm1782

Shibata, M., Yamada, S., Kumar, S. R., Calero, M., Bading, J., Frangione, B., et al. (2000). Clearance of Alzheimer's amyloid-ss(1-40) peptide from brain by LDL receptor-related protein-1 at the blood-brain barrier. *J. Clin. Invest.* 106, 1489–1499. doi: 10.1172/JCI10498

Sperling, R., Salloway, S., Raskind, M., Ferris, S., Liu, E., Yuen, E., et al. (2012). A randomized, double-blind, placebo-controlled clinical trial of intravenous bapineuzumab in patients with Alzheimer's disease who are apolipoprotein E ε4 carriers. *Eur. J. Neurol.* 19, SC3012.

Strobel, G., and Bowman Rogers, M. (2012). *CTAD (2012) in Monte Carlo: Getting Preclinical Trials Ship Shape. Alzheimer Research Forum.* Available online at: http://www.alzforum.org/new/pdf/CTAD2012.pdf. (Accessed January 14, 2013).

Terry, R. D. (2006). Alzheimer's disease and the aging brain. *J. Geriatric Psychiatry Neurol.* 19, 125–128. doi: 10.1177/0891988706291079

Walsh, D. M., Hartley, D. M., Kusumoto, Y., Fezoui, Y., Condron, M. M., Lomakin, A., et al. (1999). Amyloid beta-protein fibrillogenesis. Structure and biological activity of protofibrillar intermediates. *J. Biol. Chem.* 274, 25945–25952. doi: 10.1074/jbc.274.36.25945

Walsh, D. M., and Selkoe, D. J. (2007). A beta oligomers - a decade of discovery. *J. Neurochem.* 101, 1172–1184. doi: 10.1111/j.1471-4159.2006.04426.x

Walsh, D. M., Townsend, M., Podlisny, M. B., Shankar, G. M., Fadeeva, J. V., El Agnaf, O., et al. (2005). Certain inhibitors of synthetic amyloid beta-peptide (Abeta) fibrillogenesis block oligomerization of natural Abeta and thereby rescue long-term potentiation. *J. Neurosci.* 25, 2455–2462. doi: 10.1523/JNEUROSCI.4391-04.2005

Zetterberg, H. (2008). Is plasma amyloid-beta a reliable biomarker for Alzheimer's disease. *Recent Pat. CNS Drug Discov.* 3, 109–111. doi: 10.2174/157488908784534595

Zetterberg, H., Blennow, K., and Hanse, E. (2010). Amyloid beta and APP as biomarkers for Alzheimer's disease. *Exp. Gerontol.* 45, 23–29. doi: 10.1016/j.exger.2009.08.002

Zlokovic, B. V., Ghiso, J., Mackic, J. B., McComb, J. G., Weiss, M. H., and Frangione, B. (1993). Blood-brain barrier transport of circulating Alzheimer's amyloid beta. *Biochem. Biophys. Res. Commun.* 197, 1034–1040. doi: 10.1006/bbrc.1993.2582

Conflict of Interest Statement: The authors declare that the research was conducted in the absence of any commercial or financial relationships that could be construed as a potential conflict of interest.

Received: 31 March 2013; accepted: 12 June 2013; published online: 02 July 2013.

*Citation: Moreth J, Mavoungou C and Schindowski K (2013) Is abeta a sufficient biomarker for monitoring anti-abeta clinical studies? A critical review. Front. Aging Neurosci. **5**:25. doi: 10.3389/fnagi.2013.00025*

frontiers in
AGING NEUROSCIENCE

ORIGINAL RESEARCH ARTICLE
published: 01 April 2013
doi: 10.3389/fnagi.2013.00011

The role of apolipoprotein E (*APOE*) genotype in early mild cognitive impairment (E-MCI)

Shannon L. Risacher[1], Sungeun Kim[1,2], Li Shen[1,2], Kwangsik Nho[1], Tatiana Foroud[3], Robert C. Green[4], Ronald C. Petersen[5], Clifford R. Jack Jr.[6], Paul S. Aisen[7], Robert A. Koeppe[8], William J. Jagust[9], Leslie M. Shaw[10], John Q. Trojanowski[10], Michael W. Weiner[11,12] and Andrew J. Saykin[1,2,3]*, for the Alzheimer's Disease Neuroimaging Initiative (ADNI)[†]

[1] *Department of Radiology and Imaging Sciences, Center for Neuroimaging, Indiana University School of Medicine, Indianapolis, IN, USA*
[2] *Center for Computational Biology and Bioinformatics, Indiana University School of Medicine, Indianapolis, IN, USA*
[3] *Department of Medical and Molecular Genetics, Indiana University School of Medicine, Indianapolis, IN, USA*
[4] *Division of Genetics, Department of Medicine, Brigham and Women's Hospital and Harvard Medical School, Boston, MA, USA*
[5] *Department of Neurology, Mayo Clinic, Rochester, MN, USA*
[6] *Department of Radiology, Mayo Clinic, Rochester, MN, USA*
[7] *Department of Neurology, University of California, San Diego, San Diego, CA, USA*
[8] *Department of Radiology, University of Michigan, Ann Arbor, MI, USA*
[9] *Department of Neurology, University of California, Berkeley, Berkeley, CA, USA*
[10] *Department of Pathology and Laboratory Medicine, University of Pennsylvania School of Medicine, Philadelphia, PA, USA*
[11] *Departments of Radiology, Medicine, and Psychiatry, University of California, San Francisco, San Francisco, CA, USA*
[12] *Department of Veterans Affairs Medical Center, San Francisco, CA, USA*
[†] *Data used in preparation of this article were obtained from the Alzheimer's Disease Neuroimaging Initiative (ADNI) database (adni.loni.ucla.edu). As such, the investigators within the ADNI contributed to the design and implementation of ADNI and/or provided data but did not participate in analysis or writing of this report. A complete listing of ADNI investigators can be found at: http://adni.loni.ucla.edu/wp-content/uploads/how_to_apply/ADNI_Acknowledgement_List.pdf*

Edited by:
Manuel Menéndez-González, Hospital Álvarez-Buylla, Spain

Reviewed by:
Gregory A. Jicha, University of Kentucky, USA
Maria S. M. Palomo, Centro de Especialidades de la Avenida de Portugal y guardias de Neurología, Spain
Marwan N. Sabbagh, Banner Sun Health Research Institute, USA

****Correspondence:***
Andrew J. Saykin, Department of Radiology and Imaging Sciences, Center for Neuroimaging, Indiana University School of Medicine, IU Health Neuroscience Center, Suite 4100, 355 West 16th Street, Indianapolis, IN 46202, USA.
e-mail: asaykin@iupui.edu.

Objective: Our goal was to evaluate the association of *APOE* with amyloid deposition, cerebrospinal fluid levels (CSF) of Aβ, tau, and p-tau, brain atrophy, cognition and cognitive complaints in E-MCI patients and cognitively healthy older adults (HC) in the ADNI-2 cohort.

Methods: Two-hundred and nine E-MCI and 123 HC participants from the ADNI-2 cohort were included. We evaluated the impact of diagnostic status (E-MCI vs. HC) and *APOE* ε4 status (ε4 positive vs. ε4 negative) on cortical amyloid deposition (AV-45/Florbetapir SUVR PET scans), brain atrophy (structural MRI scans processed using voxel-based morphometry and Freesurfer version 5.1), CSF levels of Aβ, tau, and p-tau, and cognitive performance and complaints.

Results: E-MCI participants showed significantly impaired cognition, higher levels of cognitive complaints, greater levels of tau and p-tau, and subcortical and cortical atrophy relative to HC participants ($p < 0.05$). Cortical amyloid deposition and CSF levels of Aβ were significantly associated with *APOE* ε4 status but not E-MCI diagnosis, with ε4 positive participants showing more amyloid deposition and lower levels of CSF Aβ than ε4 negative participants. Other effects of *APOE* ε4 status on cognition and CSF tau levels were also observed.

Conclusions: *APOE* ε4 status is associated with amyloid accumulation and lower CSF Aβ, as well as increased CSF tau levels in early prodromal stages of AD (E-MCI) and HC. Alternatively, neurodegeneration, cognitive impairment, and increased complaints are primarily associated with a diagnosis of E-MCI. These findings underscore the importance of considering *APOE* genotype when evaluating biomarkers in early stages of disease.

Keywords: apolipoprotein E (APOE), early mild cognitive impairment (E-MCI), Florbetapir/AV-45/Amyvid, positron emission tomography (PET), magnetic resonance imaging (MRI), cerebrospinal fluid (CSF), Alzheimer's disease neuroimaging initiative (ADNI)

INTRODUCTION

Alzheimer's disease (AD) is the most common age-related neurodegenerative disease, featuring cognitive decline, accumulation of amyloid plaques and neurofibrillary tangles, and extensive neurodegeneration (Alzheimer's Association, 2011; McKhann et al., 2011). The most commonly accepted prodromal AD stage is mild cognitive impairment (MCI), which is characterized by clinically-relevant cognitive dysfunction in the absence of significant interference with daily functioning (Petersen et al., 1999; Albert et al., 2011). Amnestic MCI features marked memory impairments which are predictive of progression to clinical AD. Recently, MCI patients have been classified into two forms based

on severity: early MCI (E-MCI) and late MCI (L-MCI). Relative to an age-appropriate normative level, E-MCI patients show an approximately 1–1.5 standard deviation (SD) decline in memory, while L-MCI patients show a 1.5 SD or greater decline. These designated cut-offs for E-MCI and L-MCI have not been fully explored to date. However, the identification of participants with a 1–1.5 SD deficit in memory as E-MCI may be more sensitive for identifying participants in the earliest stages of cognitive decline. However, the specificity of these diagnostic criteria has yet to be determined and may be lower than the L-MCI cut-offs, allowing participants with more diverse causal factors of cognitive decline (other than prodromal AD) to be included in this diagnostic category. Future studies examining these clinical criteria and clinical and pathological outcomes of identified E-MCI patients relative to L-MCI patients will be important for understanding the cognitive changes observed in these patients. Importantly, these new guidelines provide an opportunity to evaluate the role of AD biomarkers and other potential disease-causing factors in a very early clinical stage. In fact, a recent study demonstrated increased amyloid binding measured using [^{18}F]Florbetapir positron emission tomography (PET) in patients with E-MCI relative to HC, but no alterations in metabolism as assessed using [^{18}F]FDG PET (Wu et al., 2012).

The most common genetic variant associated with late-onset AD is the apolipoprotein E (*APOE*) ε4 allele (Corder et al., 1993; Bertram et al., 2010). The presence of an ε4 allele confers a significantly higher likelihood of developing AD. *APOE* genotype is also associated with AD biomarkers, with the presence of an *APOE* ε4 allele associated with greater amyloid deposition (Drzezga et al., 2009; Morris et al., 2010; Fleisher et al., 2011), a higher degree and faster rate of neurodegeneration (Moffat et al., 2000; Caroli and Frisoni, 2010), alterations in brain function and glucose metabolism (Bookheimer et al., 2000; Bondi et al., 2005; Langbaum et al., 2009), changes in cerebrospinal fluid (CSF) measures of amyloid and tau (Vemuri et al., 2010; Tosun et al., 2011), as well as more impaired cognition (Mayeux et al., 2001; Farlow et al., 2004; Caselli et al., 2011) in patients with L-MCI and AD and cognitively healthy older adults (HC). However, the role of *APOE* genotype in E-MCI has not been assessed. Therefore, the goal of this study is to evaluate the effect of *APOE* ε4 status on amyloid deposition, neurodegeneration, and cognition in patients diagnosed with E-MCI, the earliest clinically-defined prodromal stage of AD.

MATERIALS AND METHODS

ALZHEIMER'S DISEASE NEUROIMAGING INITIATIVE (ADNI)

ADNI was launched in 2004 by the National Institute on Aging (NIA), the National Institute of Biomedical Imaging and Bioengineering (NIBIB), the Food and Drug Administration (FDA), pharmaceutical companies, and non-profit organizations, as a multi-year public-private partnership. The Principal Investigator is Michael W. Weiner, MD, VA Medical Center and UCSF. ADNI is a longitudinal study, ultimately including more than 1200 participants (aged 55–90) recruited from over 50 sites across the United States and Canada. Further information can be found at http://www.adni-info.org/ and in previous reports (Jack et al., 2010; Jagust et al., 2010; Petersen et al., 2010; Saykin et al., 2010; Trojanowski et al., 2010; Weiner et al., 2010). Appropriate Institutional Review Boards approval occurred at each ADNI site and informed consent was obtained from each participant or authorized representative.

PARTICIPANTS

Participants were selected if they were designated as E-MCI or HC (continuing participants or newly enrolled) at the initial visit of the ADNI-GO or ADNI-2 phases and had *APOE* genotype data. The sample included 209 E-MCI patients and 123 HC. Patients were diagnosed with E-MCI using criteria described in the ADNI-2 procedures manual (http://www.adni-info.org/). Briefly, patients were diagnosed with E-MCI using the following criteria:

1. Subject must have a subjective memory concern as reported by subject, study partner, or clinician.
2. Abnormal memory function documented by scoring within the education adjusted ranges on the Logical Memory II subscale (Delayed Paragraph Recall, Paragraph A only) from the Wechsler Memory Scale—Revised (the maximum score is 25):
   a. 9–11 for 16 or more years of education.
   b. 5–9 for 8–15 years of education.
   c. 3–6 for 0–7 years of education.
3. Mini-Mental State Exam score between 24 and 30 (inclusive) (Exceptions may be made for subjects with less than 8 years of education at the discretion of the project director).
4. Clinical Dementia Rating = 0.5; Memory Box score must be at least 0.5.
5. General cognition and functional performance sufficiently preserved such that a diagnosis of Alzheimer's disease cannot be made by the site physician at the time of the screening visit.

In addition, all participants met ADNI inclusion and exclusion criteria which have been described previously (Weiner et al., 2010) and can be found at http://www.adni-info.org/.

APOE genotyping for all participants was performed as previously described (Saykin et al., 2010). In the present study, we sought to evaluate the impact of the presence or absence of an *APOE* ε4 allele on imaging and non-imaging phenotypes. Therefore, all participants were divided into two groups based on *APOE* ε4 status, including participants with one or more ε4 allele (*APOE* ε4 positive (ε4+); 85 E-MCI, 30 HC) and participants without an ε4 allele (*APOE* ε4 negative (ε4−); 124 E-MCI, 93 HC).

CLINICAL AND NEUROPSYCHOLOGICAL ASSESSMENTS

All clinical and neuropsychological test performance data for included participants was downloaded from the ADNI clinical data repository on the Laboratory of Neuro Imaging (LONI) site. Specifically, we evaluated participant performance on the Mini-Mental State Exam (MMSE), Alzheimer's Disease Assessment Scale (ADAS), Montreal Cognitive Assessment (MoCA; Total and all sub-scores), Rey Auditory Verbal Learning Test (RAVLT; Total score, delayed recall score, delayed recognition score), Weschler's Logical Memory Scale—Revised (LM; Immediate and Delayed), Clock Drawing Test (CDT), Trailmaking Test A and B (TMT-A,

TMT-B), Boston Naming Test (BNT), Animal Fluency, and the American National Adult Reading Test (ANART). We also evaluated clinical measures, including a measure of dementia severity [Clinical Dementia Rating Scale (CDR), Sum of Boxes score], general functioning [Functional Assessment Questionnaire (FAQ)], depression [Geriatric Depression Scale (GDS)], and stroke/vascular incident history (Modified Hachinski Scale). Cognitive complaints were assessed using the Measure of Everyday Cognition (E-Cog) from both the patient and an informant. The total level of complaints on the E-Cog (overall and within each domain) for both the participant and the informant were assessed as percentage of items endorsed as either "2 = questionably or occasionally worse," "3 = consistently a little worse," or "4 = consistently much worse." Items endorsed as "9 = I don't know" were excluded.

STRUCTURAL MRI SCANS

All available baseline 3 Tesla structural magnetic resonance imaging (MRI) scans were downloaded from LONI for included E-MCI and HC participants. Scans were corrected prior to download as previously described (Jack et al., 2008, 2010). Most participants had a minimum of two scans from the baseline visit. All available scans were processed using voxel-based morphometry (VBM) implemented in Statistical Parametric Mapping 8 (SPM8) (Ashburner and Friston, 2000) and Freesurfer version 5.1 (Dale et al., 1999; Fischl et al., 1999), as described in previous reports (Dale et al., 1999; Fischl et al., 1999; Ashburner and Friston, 2000; Risacher et al., 2009, 2010) and briefly below:

VBM

Scans were co-registered to a T1-weighted template, segmented into grey matter (GM), white matter (WM), and CSF compartments with bias correction, unmodulated normalized to Montreal Neurologic Institute (MNI) space as $1 \times 1 \times 1$ mm voxels, and smoothed with an 8 mm Gaussian kernel. All scans underwent extensive quality control. Mean GM density was extracted from all available baseline scans for target regions of interest (ROIs) using MarsBaR (Brett et al., 2002). Since most participants had two or more baseline MRI scans, an average GM density measure was calculated for each ROI using the mean GM density values extracted from each of the available baseline scans. Eighteen participants (5 HC ε4−, 2 HC ε4+, 5 E-MCI ε4−, 6 E-MCI ε4+) were excluded from the GM density analyses for missing data or failed processing.

Automated parcellation

Freesurfer version 5.1 was used to extract volumetric and cortical thickness measures. Similar to the VBM ROI data, values from all available baseline scans were averaged to create a mean volumetric or cortical thickness value for each ROI. Seven participants (2 HC ε4−, 1 HC ε4+, 2 E-MCI ε4−, 2 E-MCI ε4+) were excluded from the cortical thickness and volumetric analyses for incomplete data or failed processing.

AMYLOID PET SCANS ([^{11}C]FLORBETAPIR)

Pre-processed [^{11}C]Florbetapir PET scans (Coregistered, Averaged, Standardized Image and Voxel Size, Uniform Resolution) were downloaded from LONI (http://adni.loni.ucla.edu/). Before download, images were averaged, aligned to a standard space, re-sampled to a standard image and voxel size, smoothed to a uniform resolution and normalized to a cerebellar GM reference region resulting in standardized uptake value ratio (SUVR) images as previously described (Jagust et al., 2010). After downloading, the images were aligned to each participant's same visit MRI scan and normalized to MNI space as $2 \times 2 \times 2$ mm voxels using parameters from the MRI segmentation. The normalized scans were evaluated for the effect of *APOE* ε4 status on a voxel-wise basis using a two-sample *t*-test, masked using a whole-brain mask, and covaried for age, gender, education, and handedness. Significant results were displayed at a voxel-wise threshold of $p < 0.01$ [family-wise error (FWE) correction for multiple comparisons] with a minimum cluster size (k) of 50 voxels. SPM8 was used for all processing and voxel-wise analysis. Mean regional SUVR values were also extracted for target ROIs using MarsBaR. Fourteen participants (6 HC ε4−, 5 HC ε4+, 3 E-MCI ε4−) were excluded from [^{11}C]Florbetapir analyses for missing scan data or failed processing.

CSF BIOMARKERS

Levels of amyloid-beta 1-42 (Aβ), total tau, and phosphorylated tau (p-tau) were measured from all available CSF samples as previously described (Shaw et al., 2009, 2011; Trojanowski et al., 2010). CSF data was downloaded from the LONI site and extracted for all included participants. Of the 332 included participants, 44 participants (25 E-MCI and 19 HC) were missing all CSF data. 4 additional participants (2 E-MCI, 3 HC) were missing CSF tau data and 2 additional HC participants were missing CSF p-tau data. Furthermore, participants with CSF levels outside 3 SDs above or below the mean were excluded, including 6 E-MCI participants with tau levels more than 3 SDs above the mean and 2 E-MCI participants with p-tau levels more than 3 SDs above the mean. Thus, the final samples for CSF analyses included 288 participants in the CSF Aβ analysis, 278 participants in the CSF tau analysis, and 284 participants in the CSF p-tau analysis.

STATISTICAL ANALYSES

We evaluated the effect of diagnosis and *APOE* ε4 status on demographics, cognition, cognitive complaints, amyloid deposition, atrophy, and CSF biomarkers using two-way analysis of covariance (ANCOVA) for continuous variables and a chi-square test for categorical variables implemented in SPSS 19.0 (SPSS, Inc., Chicago, IL). Specifically, the effect of diagnosis (HC vs. E-MCI), *APOE* ε4 status (ε4+ vs. ε4−), and the interaction of diagnosis and ε4 status on performance on clinical and psychometric tests, cognitive complaints, amyloid deposition (mean SUVR from target ROIs), CSF levels of Aβ, tau, and p-tau, and brain atrophy (volume, cortical thickness, and GM density from target ROIs) were assessed. All ANCOVA analyses were covaried for age, gender, education, and handedness. The analysis of neurodegenerative measures was also covaried for total intracranial volume (ICV). The frequency of having one or more *APOE* ε4 alleles was also compared between diagnostic groups (HC vs. E-MCI) using a chi-square test.

Table 1 | Demographics, neuropsychological and clinical test performance, and cognitive complaints [Mean (Standard Error)].

		HC: ε4− ($n = 93$)	HC: ε4+ ($n = 30$)	E-MCI: ε4− ($n = 124$)	E-MCI: ε4+ ($n = 85$)	*p*-values		
						DX	*APOE*	Interaction
Demographics	Age (years)	74.1 (0.72)	73.67 (1.27)	71.47 (0.62)	70.26 (0.75)	0.0007	0.3506	0.6572
	Education (years)	16.47 (0.27)	16.37 (0.48)	15.9 (0.24)	15.78 (0.28)	0.0810	0.7251	0.9756
	Gender (M, F)	49, 44	13, 17	64, 60	52, 33	0.3686	0.4394	0.3258
	Handedness (R, L)	85, 8	28, 2	109, 15	79, 6	0.5619	0.2777	0.5831
Clinical performance	CDR-Sum of Boxes	0.04 (0.06)	0.08 (0.11)	1.15 (0.05)	1.34 (0.06)	0.0000	0.0979	0.2989
	FAQ Total[a]	0.17 (0.25)	0.05 (0.45)	1.66 (0.21)	2.22 (0.26)	0.0000	0.4699	0.2637
	Modified Hachinski Total	0.59 (0.07)	0.37 (0.12)	0.77 (0.06)	0.58 (0.07)	0.0257	0.0164	0.8585
	GDS Total[b]	0.80 (0.14)	0.53 (0.25)	1.87 (0.12)	1.55 (0.15)	0.0000	0.0901	0.8687
Reading	ANART Errors[c]	10.61 (0.83)	9.05 (1.47)	11.22 (0.71)	12.35 (0.88)	0.0606	0.8320	0.1832
General cognition	MMSE Total Score	29.05 (0.14)	28.91 (0.25)	28.57 (0.12)	28.06 (0.15)	0.0002	0.0565	0.2847
	ADAS Cognitive Subtotal[d]	6.25 (0.36)	6.76 (0.63)	7.77 (0.30)	8.60 (0.37)	0.0002	0.1211	0.7147
	ADAS Total Score[e]	9.63 (0.51)	10.38 (0.90)	11.99 (0.44)	13.98 (0.53)	0.0000	0.0266	0.3168
	MoCA Total Score[f]	25.64 (0.27)	24.90 (0.47)	24.12 (0.22)	23.57 (0.28)	0.0000	0.0446	0.7835
Memory	Logical Memory - Immediate	14.78 (0.29)	13.26 (0.50)	10.84 (0.24)	10.85 (0.30)	0.0000	0.0273	0.0267
	Logical Memory - Delayed	13.89 (0.23)	12.51 (0.39)	8.76 (0.19)	8.97 (0.24)	0.0000	0.0318	0.0036
	RAVLT Total Score[d]	44.99 (0.93)	42.48 (1.65)	39.98 (0.79)	37.63 (0.97)	0.0000	0.0320	0.9459
	RAVLT Delayed Recall[d]	7.26 (0.39)	6.61 (0.70)	6.18 (0.33)	5.24 (0.41)	0.0128	0.0976	0.7601
	RAVLT Delayed Recognition[d]	12.82 (0.27)	12.20 (0.48)	11.98 (0.23)	12.01 (0.28)	0.1249	0.3687	0.3238
	MoCA Delayed Memory[g]	2.36 (0.16)	1.67 (0.29)	1.40 (0.14)	1.49 (0.17)	0.0061	0.1356	0.0509
Language and naming	Boston Naming Test Total[e]	28.24 (0.31)	28.64 (0.55)	27.08 (0.26)	27.34 (0.32)	0.0015	0.3790	0.8413
	Animal Fluency Total[d]	21.07 (0.49)	21.63 (0.87)	18.98 (0.42)	18.62 (0.51)	0.0000	0.8704	0.4444
	MoCA Naming[d]	2.90 (0.03)	3.01 (0.06)	2.83 (0.03)	2.89 (0.04)	0.0311	0.0374	0.5251
	MoCA Language[d]	2.52 (0.08)	2.57 (0.13)	2.45 (0.06)	2.34 (0.08)	0.1150	0.7619	0.3858
Visuospatial and executive function	Clock Drawing Score[d]	4.62 (0.06)	4.63 (0.11)	4.69 (0.05)	4.60 (0.07)	0.8319	0.5891	0.4899
	Clock Drawing - Copy Score[d]	4.86 (0.04)	4.93 (0.08)	4.80 (0.04)	4.84 (0.05)	0.2157	0.3119	0.7972
	Trailmaking A[d]	33.40 (1.16)	34.28 (2.05)	34.52 (0.99)	39.06 (1.21)	0.0418	0.0542	0.1943
	Trailmaking B[h]	81.07 (4.34)	79.47 (7.85)	90.52 (3.76)	107.64 (4.58)	0.0007	0.1469	0.0807
	Trailmaking B-A[h]	47.66 (3.99)	45.54 (7.21)	55.94 (3.45)	68.52 (4.2)	0.0021	0.2868	0.1347
	MoCA Visuospatial-Executive[a]	4.29 (0.09)	4.37 (0.16)	4.28 (0.08)	4.04 (0.10)	0.1440	0.4833	0.1444
	MoCA Attention[d]	5.77 (0.07)	5.55 (0.12)	5.64 (0.06)	5.47 (0.07)	0.2040	0.0123	0.7272
	MoCA Abstraction[d]	1.80 (0.06)	1.79 (0.11)	1.69 (0.05)	1.56 (0.06)	0.0276	0.3399	0.4321
	MoCA Orientation[d]	5.94 (0.04)	5.94 (0.08)	5.83 (0.04)	5.74 (0.04)	0.0040	0.3920	0.4418

(Continued)

Table 1 | Continued

		HC: ε4− ($n = 93$)	HC: ε4+ ($n = 30$)	E-MCI: ε4− ($n = 124$)	E-MCI: ε4+ ($n = 85$)	*p*-values		
						DX	*APOE*	Interaction
Patient complaints	E-Cog Patient: Total[d,k]	27.01 (2.59)	28.00 (4.52)	49.04 (2.18)	52.10 (2.67)	0.0000	0.5147	0.7396
	E-Cog Patient: Memory[d,k]	43.09 (2.92)	45.91 (5.11)	73.03 (2.46)	77.60 (3.02)	0.0000	0.2932	0.8033
	E-Cog Patient: Language[d,k]	32.59 (3.16)	33.39 (5.52)	56.31 (2.66)	55.96 (3.26)	0.0000	0.9520	0.8805
	E-Cog Patient: Visuospatial[d,k]	11.55 (3.11)	13.91 (5.43)	28.44 (2.61)	33.46 (3.20)	0.0000	0.3222	0.7216
	E-Cog Patient: Planning[d,k]	12.94 (3.33)	11.29 (5.82)	32.82 (2.80)	38.40 (3.43)	0.0000	0.6230	0.3654
	E-Cog Patient: Organization[d,k]	20.69 (3.56)	17.07 (6.22)	38.33 (2.99)	38.16 (3.67)	0.0000	0.6576	0.6858
	E-Cog Patient: Divided Attention[d,k]	36.55 (4.10)	41.95 (7.16)	59.36 (3.44)	64.13 (4.23)	0.0000	0.3011	0.9485
Informant complaints	E-Cog Informant: Total[i,k]	11.38 (2.39)	14.83 (4.18)	40.00 (2.01)	45.78 (2.47)	0.0000	0.1087	0.6866
	E-Cog Informant: Memory[i,k]	21.04 (2.98)	25.77 (5.21)	61.73 (2.51)	64.77 (3.08)	0.0000	0.2778	0.8138
	E-Cog Informant: Language[i,k]	8.71 (2.95)	15.11 (5.16)	38.32 (2.48)	44.24 (3.05)	0.0000	0.0829	0.9454
	E-Cog Informant: Visuospatial[j,k]	5.42 (2.78)	4.18 (4.86)	21.23 (2.35)	32.97 (2.87)	0.0000	0.1166	0.0528
	E-Cog Informant: Planning[i,k]	7.44 (3.25)	10.97 (5.68)	31.80 (2.73)	37.94 (3.35)	0.0000	0.2155	0.7375
	E-Cog Informant: Organization[i,k]	7.62 (3.25)	9.34 (5.68)	32.36 (2.73)	37.20 (3.35)	0.0000	0.4009	0.6891
	E-Cog Informant: Divided Attention[i,k]	18.38 (4.07)	23.69 (7.12)	56.69 (3.43)	57.89 (4.20)	0.0000	0.5051	0.6736

[a] *2 HC (1 ε4+, 1 ε4−) missing data.*

[b] *2 E-MCI (1 ε4+, 1 ε4−) missing data.*

[c] *2 HC (1 ε4+, 1 ε4−), 5 E-MCI (2 ε4+, 3 ε4−) missing data.*

[d] *1 HC (ε4+) missing data.*

[e] *1 HC (ε4+), 1 E-MCI (ε4−) missing data.*

[f] *3 HC (1 ε4+, 2 ε4−), 1 E-MCI (ε4+) missing data.*

[g] *2 HC (1 ε4+, 1 ε4−), 1 E-MCI (ε4+) missing data.*

[h] *2 HC (2 ε4+), 4 E-MCI (1 ε4+, 3 ε4−) missing data.*

[i] *4 HC (1 ε4+, 3 ε4−) missing data.*

[j] *4 HC (ε4+), 1 E-MCI (ε4−) missing data.*

[k] *Patient and informant E-Cog values are expressed as a percentage of items endorsed (total and within each domain); see text for additional description.*

RESULTS

DEMOGRAPHICS, PSYCHOMETRIC PERFORMANCE, AND COGNITIVE COMPLAINTS

Significantly more E-MCI were *APOE* ε4+ than HC ($p = 0.003$), with 85 of 209 E-MCI participants (40.7%) showing one or more ε4 alleles relative to only 30 of 123 HC participants (24.4%). Demographics and psychometric performance variables for E-MCI and HC participants stratified by *APOE* ε4 status are shown in **Table 1**. The effect of diagnosis, ε4 status, and the interaction between diagnosis and ε4 status are displayed. Age was significantly different between diagnostic groups ($p < 0.05$) but not *APOE* ε4 groups. A significant interaction between diagnosis and ε4 status on LM Immediate and Delayed performance was observed, with ε4+ HC showing worse performance on both measures than ε4− HC participants but no difference by ε4 status in E-MCI participants. A trend for a significant interaction on the MoCA delayed recall sub-score ($p = 0.05$) was also observed, again with a significant effect of ε4 status in HC but not E-MCI participants. Finally, a marginally significant interaction of diagnosis and ε4 status for informant complaints in the visuospatial domain ($p = 0.05$) was also seen, with ε4 status having an effect only in E-MCI participants.

Significant effects of diagnosis on the CDR-SB, FAQ, Modified Hachinski Total, and GDS were observed ($p < 0.05$), with E-MCI participants showing a greater CDR-SB, as well as higher scores on the FAQ, Modified Hachinski, and GDS. Differences in psychometric performance by diagnosis were observed for nearly every test ($p < 0.05$), except for the RAVLT Delayed Recognition, CDT (Total and Copy Scores), and the MoCA language, executive-visuospatial function, and attention sub-scores. Significant differences in cognitive complaints from both the participant and the informant by diagnosis were also observed in all domains ($p < 0.001$). In all cases, E-MCI participants had worse cognition and more cognitive complaints than HC participants.

Vascular risk factors and/or stroke history was significantly different by *APOE* ε4 status ($p < 0.05$), with ε4+ participants showing lower Modified Hachinski Total scores. In addition, ε4 status was significantly associated with performance on a number of psychometric tests, including the ADAS Total score, MoCA Total score, RAVLT Total score, and the MoCA naming and attention sub-scores ($p < 0.05$). The effect of ε4 status was also significant at a trend level for TMT-A ($p = 0.05$). For these comparisons, ε4+ participants demonstrated worse performance than ε4−.

VOXEL-BASED COMPARISONS OF AMYLOID DEPOSITION

ε4+ E-MCI showed significantly greater amyloid deposition upon voxel-wise analysis than ε4− (**Figure 1**; voxel-wise threshold: $p < 0.01$ (FWE), $k = 50$ voxels). The most significant cluster was observed in the left orbitofrontal cortex (**Figure 1A**). Additional significant clusters were observed in the medial frontal

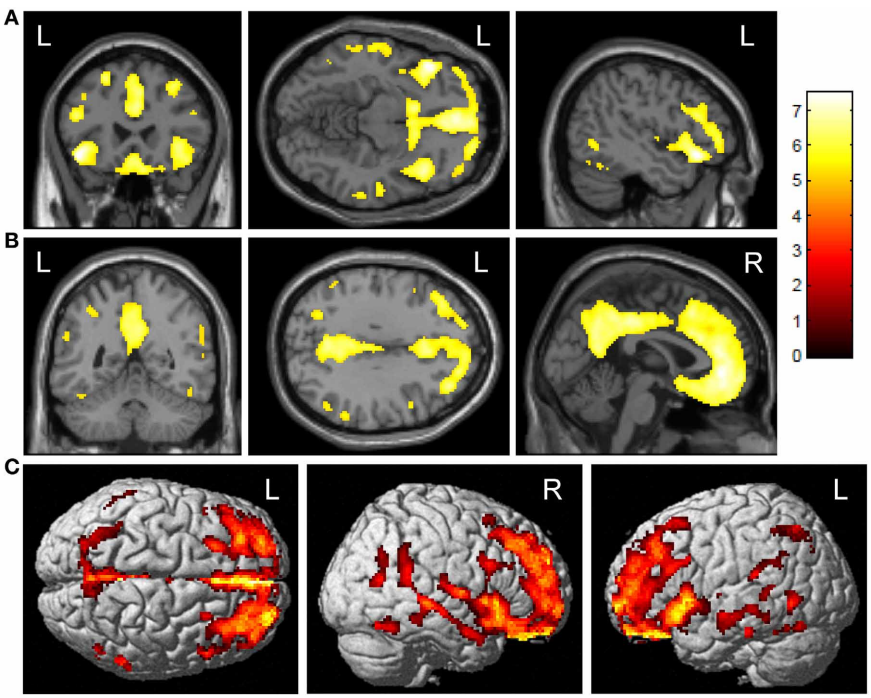

FIGURE 1 | Voxel-wise association of *APOE* ε4 status and amyloid deposition in E-MCI participants. Greater cortical amyloid deposition was observed in *APOE* ε4+ ($n = 85$) relative to *APOE* ε4− ($n = 121$) E-MCI participants. Significant clusters were observed in the medial and lateral frontal lobes **(A)**, anterior and posterior cingulate **(B)**, and lateral temporal lobes. Surface renderings show the diffuse pattern of significant clusters **(C)**. All analyses were covaried for age, gender, education, and handedness and a voxel-wise threshold of $p < 0.01$ (FWE correction for multiple comparisons) and minimum cluster size (k) of 50 voxels was considered significant.

lobe/anterior cingulate cortex, the right orbitofrontal cortex, and the posterior cingulate/precuneus (**Figure 1B**). The surface rendering also reflects the widespread pattern of significant differences with significant clusters throughout the frontal, parietal, and temporal lobes (**Figure 1C**). No significant clusters were observed in the reverse comparison (ε4− > ε4+; *data not shown*).

ROI COMPARISONS OF AMYLOID DEPOSITION

ROI results were consistent with voxel-wise findings demonstrating significantly greater global and regional amyloid deposition in ε4+ relative to ε4− E-MCI participants in the global cortex, mean frontal lobe, anterior cingulate, and precuneus (**Figure 2**). A significant effect of ε4 status ($p < 0.001$) but not diagnosis was observed in all ROI measures, with ε4+ participants showing greater amyloid than ε4− participants regardless of diagnosis (HC or E-MCI). Overall, amyloid PET results indicate that ε4+ individuals showed greater amyloid deposition than ε4− regardless of cognitive impairment in the earliest stages of decline.

ROI COMPARISONS OF NEURODEGENERATION

Hippocampal neurodegeneration (volume and GM density) was associated with diagnosis ($p < 0.001$; **Figures 3A,B**) but not *APOE* ε4 status. E-MCI participants showed more hippocampal atrophy than HC. However, a significant interaction effect of diagnosis and ε4 status on mean temporal lobe cortical thickness was observed ($p = 0.008$; **Figure 3C**), with ε4+ HC participants showing thicker mean temporal lobes than all other groups. Mean temporal lobe GM density was also significantly associated with diagnosis ($p = 0.005$) and ε4 status ($p = 0.047$; **Figure 3D**), as E-MCI patients showed smaller mean temporal lobe GM density than HC and ε4− participants showed smaller mean temporal lobe GM density than ε4+ participants.

CSF LEVELS OF Aβ, TAU, AND p-tau

CSF levels of Aβ, tau, and p-tau were significantly affected by diagnosis and *APOE* ε4 status (**Figure 4**). Levels of CSF Aβ were significantly associated with ε4 status ($p < 0.001$), with ε4+ participants showing lower levels of Aβ than ε4− participants (**Figure 4A**). CSF tau levels were significantly affected by

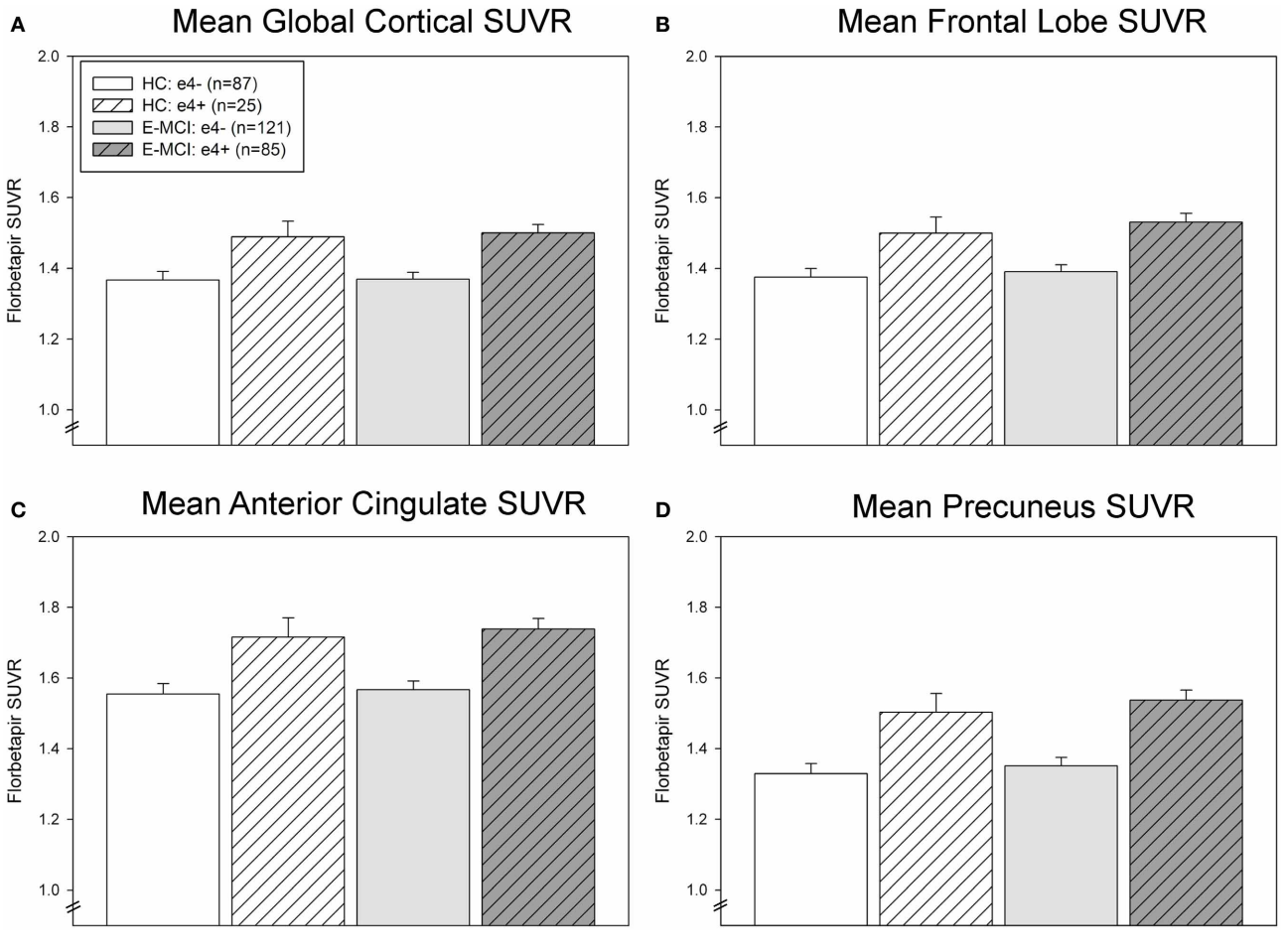

FIGURE 2 | Regional effects of *APOE* ε4 status on amyloid deposition in E-MCI and HC participants. A significant effect of *APOE* ε4 status on regional amyloid deposition was observed ($p < 0.001$), including in the global cortical mean amyloid **(A)**, mean bilateral frontal lobes **(B)**, anterior cingulate **(C)**, and precuneus **(D)**. In all evaluated regions, *APOE* ε4+ E-MCI ($n = 85$) and HC ($n = 25$) participants showed a higher mean standardized uptake value ratio (SUVR) than *APOE* ε4− E-MCI ($n = 121$) and HC ($n = 87$) participants. No significant effect of diagnostic status was observed.

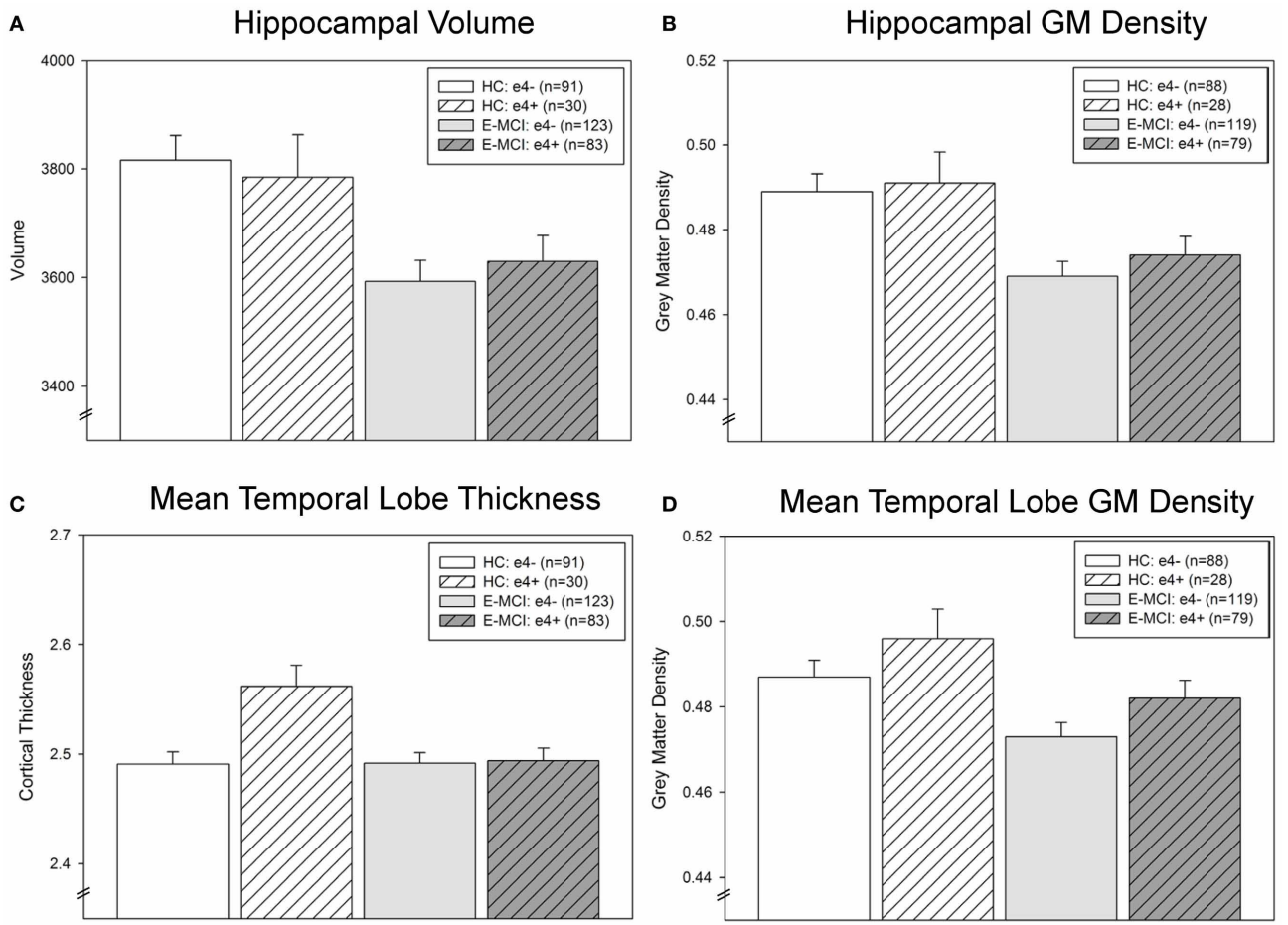

FIGURE 3 | Temporal lobe atrophy is associated with *APOE* ε4 status and diagnostic group in E-MCI and HC participants. A significant effect of diagnosis on neurodegeneration in the temporal lobe was observed ($p < 0.05$), including in hippocampal volume **(A)** and grey matter (GM) density **(B)**, mean temporal lobe cortical thickness **(C)**, and mean temporal lobe GM density **(D)**. In all evaluated regions, E-MCI participants showed more temporal lobe atrophy than HC participants. In addition, *APOE* ε4 status was significantly associated with mean temporal lobe GM density, with *APOE* ε4− participants showing smaller mean temporal lobe GM density than *APOE* ε4+ participants. Finally, a significant interaction effect of diagnosis and *APOE* ε4 status was observed in mean temporal lobe cortical thickness, with ε4− HC participants showing thicker mean temporal lobes than all other groups. All analyses were covaried for age, gender, education, handedness, and total intracranial volume (ICV). The total number of participants for each analysis is indicated on each graph (Panels **A–D**). Note: Thirteen participants were excluded from the GM density analyses, but not the cortical thickness and volumetric analyses, for failed VBM segmentation (3 HC ε4−, 2 HC ε4+, 4 E-MCI ε4−, 4 E-MCI ε4+).

both diagnosis ($p = 0.041$) and ε4 status ($p < 0.001$; **Figure 4B**). E-MCI patients had higher tau levels than HC participants and ε4+ participants had higher levels than ε4− participants. Finally, an interaction between diagnosis and ε4 status on p-tau was also observed ($p = 0.046$), primarily driven by a higher level of p-tau in ε4+ HC and E-MCI participants (**Figure 4C**).

DISCUSSION

This study provides a comprehensive evaluation of the impact of *APOE* ε4 status on cognition, cognitive complaints, amyloid deposition, neurodegeneration, and CSF Aβ, tau, and p-tau levels in E-MCI and HC. As expected, we observed a significant association of diagnosis with clinical and cognitive status. Furthermore, diagnosis was associated with neurodegeneration and CSF tau and p-tau levels but not with amyloid deposition. Cognitive performance, amyloid deposition, temporal lobe atrophy, and CSF tau and p-tau levels were significantly associated with ε4 status, with ε4+ participants showing poorer cognition, less temporal lobe atrophy, and higher CSF tau and p-tau levels. ε4+ participants also showed greater cortical amyloid deposition and lower CSF Aβ levels. Finally, an interaction between diagnosis and ε4 status was observed for memory performance, temporal lobe cortical thickness, and CSF p-tau levels. Overall, the results suggest that *APOE* ε4 status impacts AD-related pathological and clinical changes in E-MCI and HC.

The effect of *APOE* genotype on amyloid deposition has been shown previously, including in middle-aged and older cognitively healthy adults, as well as patients with L-MCI and AD (Drzezga et al., 2009; Shaw et al., 2009; Morris et al., 2010; Fleisher et al., 2011; Tosun et al., 2011). Biochemically, *APOE* genotype has

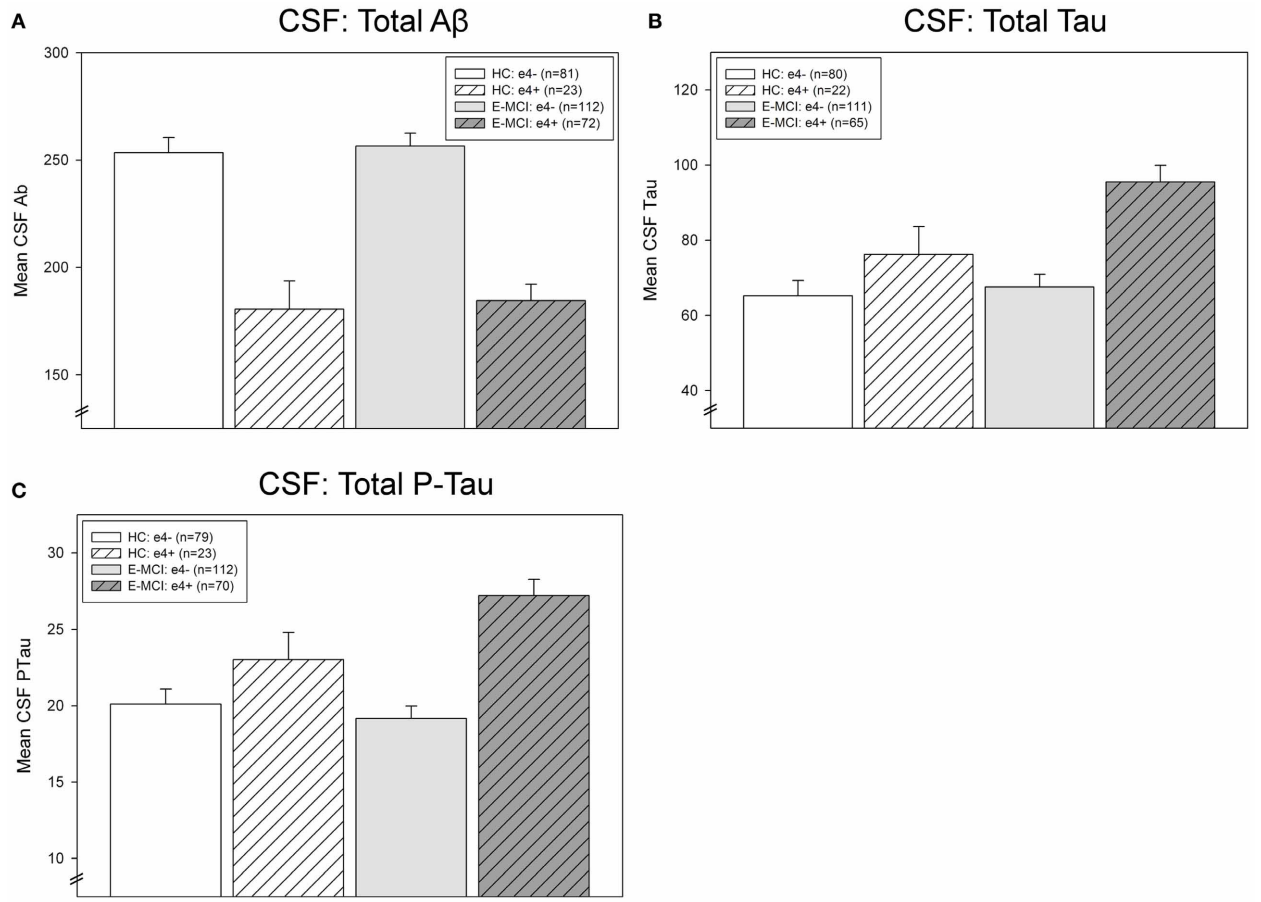

FIGURE 4 | Effects of *APOE* ε4 status and diagnosis on CSF protein levels in E-MCI and HC participants. Diagnostic group and *APOE* ε4 status significantly affected CSF levels of Aβ **(A)**, total tau **(B)**, and p-tau **(C)**. CSF Aβ was significantly associated to *APOE* ε4 status ($p < 0.001$), with *APOE* ε4+ E-MCI and HC participants showing lower levels of Aβ than *APOE* ε4− E-MCI and HC participants, regardless of diagnosis. Total tau levels were significantly affected by both diagnosis ($p < 0.05$) and *APOE* ε4 status ($p < 0.001$), with E-MCI patients showing higher total tau levels than HC participants and *APOE* ε4+ showing higher levels than *APOE* ε4− participants. Finally, an interaction between diagnostic status and *APOE* ε4 status on CSF p-tau levels was also observed ($p < 0.05$), primarily driven by a higher level of p-tau in *APOE* ε4+ HC and E-MCI participants relative to *APOE* ε4− HC and E-MCI participants. The total number of participants in each analysis is shown for each graph (Panels **A–C**). Note: See text for description of participants excluded from the CSF analysis.

been shown to affect Aβ clearance rate, with the APOE ε4 isoform showing significantly slower clearance (Deane et al., 2008; Castellano et al., 2011; Holtzman et al., 2012). The lack of diagnostic effect on amyloid deposition in this study suggests that in the earliest stages of cognitive change, *APOE* ε4 status has a stronger relationship to amyloid deposition than cognitive status.

The additional findings of a diagnostic effect on cognition, cognitive complaints, neurodegeneration, and CSF tau and p-tau levels underscore the importance of E-MCI as a diagnostic entity. Thus, this report has notable clinical implications, particularly in the potential implementation and utilization of E-MCI as a clinical diagnostic entity. Patients with E-MCI show changes in cognition and selected biomarkers, suggesting that these individuals may have a higher likelihood of clinical progression. The association of cognition and complaints to atrophic changes, rather than amyloid levels, supports E-MCI as an intermediate stage with pathology beyond amyloid accumulation.

These results further support the Jack et al. model of AD biomarkers, suggesting that changes in cognition and neurodegeneration occur after measurable amyloid accumulation (Saykin et al., 2010; Jack et al., 2011). Additionally, *APOE* ε4 genotype may alter the hypothesized sigmoidal curves, in particular amyloid accumulation. These results also indicate the importance of genetic background in determining likelihood and extent of amyloid accumulation, even in preclinical stages, which may be particularly important in clinical trial enrollment. Further, in the era of personalized medicine, the implications of *APOE* genotype disclosure to patients in a clinical setting must be carefully considered, given the impact of *APOE* on AD risk and amyloid deposition (Green et al., 2009; Roberts et al., 2011).

The observed greater temporal lobe cortical thickness and GM density in ε4+ participants, particularly in HC, is somewhat unexpected and may be related to the modest sample size of the ε4+ HC group. However, previous studies have observed

increased cortical thickness, including in middle-aged *APOE* ε4 positive participants (Espeseth et al., 2008), in cognitively HC who are transitioning to become CSF Aβ biomarker positive (Fortea et al., 2011), and in asymptomatic patients positive for a *PSEN1* mutation more than 9 years prior to the clinical onset (Fortea et al., 2010). Thus, future studies including longitudinal follow-up with an expanded sample will be important in determining the significance of this finding.

The present study has a few notable limitations. First, we evaluated the effect of *APOE* ε4 status on AD biomarkers in only HC and E-MCI rather than across the disease spectrum. Although our goal was to evaluate *APOE* in the earliest stages of AD, future studies assessing the full clinical spectrum are warranted. In addition, we did not evaluate all known biomarkers of AD, including FDG PET or advanced MRI techniques (i.e., diffusion tensor imaging, resting-state functional MRI, etc.). These measures are available in subsets of the ADNI-GO/2 cohort and thus, future studies evaluating these measures would augment the findings of the present report. Thirdly, genome-wide genetic data for this cohort was recently released. Future studies assessing other variants may provide information about the role of genetics in very early stages of AD. Finally, the present study evaluates only cross-sectional measures. Future studies using longitudinal and clinical outcome data will allow assessment of the role of *APOE* in progression of HC and E-MCI.

In summary, we assessed the role of *APOE* ε4 status on clinical and cognitive measures, cognitive complaints, and imaging and CSF biomarkers in HC and E-MCI participants from the ADNI-GO/2 cohort. We determined that *APOE* ε4 status is associated with increased amyloid deposition in both HC and E-MCI, while diagnostic category is associated with measures of cognition and cognitive complaints, as well as neurodegeneration. Therefore, we conclude that *APOE* is an important mediator of amyloid pathology in the earliest stages of AD-associated clinical decline.

ACKNOWLEDGMENTS

Data collection and sharing for this project was funded by the Alzheimer's Disease Neuroimaging Initiative (ADNI) [National Institutes of Health (NIH) Grant U01 AG024904 (PI: MW Weiner)]. ADNI is funded by the National Institute on Aging (NIA), the National Institute of Biomedical Imaging and Bioengineering (NIBIB), and through generous contributions from the following: Abbott; Alzheimer's Association; Alzheimer's Drug Discovery Foundation; Amorfix Life Sciences Ltd.; AstraZeneca; Bayer HealtHCare; BioClinica, Inc.; Biogen Idec Inc.; Bristol-Myers Squibb Company; Ei6sai Inc.; Elan Pharmaceuticals Inc.; Eli Lilly and Company; F. Hoffmann-La Roche Ltd. and its affiliated company Genentech, Inc.; GE HealtHCare; Innogenetics, N.V.; IXICO Ltd.; Janssen Alzheimer Immunotherapy Research & Development, LLC.; Johnson & Johnson Pharmaceutical Research & Development LLC.; Medpace, Inc.; Merck & Co., Inc.; Meso Scale Diagnostics, LLC.; Novartis Pharmaceuticals Corporation; Pfizer Inc.; Servier; Synarc Inc.; and Takeda Pharmaceutical Company, with participation from the US FDA. The Canadian Institutes of Health Research is providing funds to support ADNI clinical sites in Canada. Private sector contributions are facilitated by the Foundation for the National Institutes of Health (www.fnih.org). The grantee organization is the Northern California Institute for Research and Education, and the study is coordinated by the Alzheimer's Disease Cooperative Study at the University of California, San Diego. ADNI data are disseminated by Laboratory for Neuro Imaging at the University of California, Los Angeles. ADNI was also supported by NIH grants P30 AG010129, K01 AG030514, and the Dana Foundation. Additional support for analyses included in the present report was provided by the following sources: NIA R01 AG19771 (to Andrew J. Saykin), NIA P30 AG10133-18S1 (to Dr. Bernardino Ghetti and Andrew J. Saykin), NLM R01 LM011360 (to Li Shen and Andrew J. Saykin), K24 AG027841 (to Robert C. Green), an Indiana CTSI Predoctoral Fellowship (TL1 RR025759 to Shannon L. Risacher), NIA U01-AG10483 [to Paul S. Aisen (PI)], NIA U01-AG024904 [to Paul S. Aisen (Coordinating Center Director)], NIA R01-AG030048 [to Paul S. Aisen (PI)], NIA R01-AG16381 [to Paul S. Aisen (Co-I)], NIH AG027859 [to William J. Jagust (PI)], NIH AG027984 [to William J. Jagust (PI)], and NIH AG 024904 [William J. Jagust (Co-I)].

REFERENCES

Albert, M. S., Dekosky, S. T., Dickson, D., Dubois, B., Feldman, H. H., Fox, N. C., et al. (2011). The diagnosis of mild cognitive impairment due to Alzheimer's disease: recommendations from the National Institute on Aging-Alzheimer's Association workgroups on diagnostic guidelines for Alzheimer's disease. *Alzheimers Dement.* 7, 270–279.

Ashburner, J., and Friston, K. J. (2000). Voxel-based morphometry–the methods. *Neuroimage* 11, 805–821.

Association, A. S. (2011). 2011 Alzheimer's disease facts and figures. *Alzheimers Dement.* 7, 208–244.

Bertram, L., Lill, C. M., and Tanzi, R. E. (2010). The genetics of Alzheimer disease: back to the future. *Neuron* 68, 270–281.

Bondi, M. W., Houston, W. S., Eyler, L. T., and Brown, G. G. (2005). fMRI evidence of compensatory mechanisms in older adults at genetic risk for Alzheimer disease. *Neurology* 64, 501–508.

Bookheimer, S. Y., Strojwas, M. H., Cohen, M. S., Saunders, A. M., Pericak-Vance, M. A., Mazziotta, J. C., et al. (2000). Patterns of brain activation in people at risk for Alzheimer's disease. *N. Engl. J. Med.* 343, 450–456.

Brett, M., Anton, J.-L., Valabregue, R., and Poline, J.-B. (2002). "Region of interest analysis using an SPM toolbox [abstract]," in *Presented at the 8th International Conference on Functional Mapping of the Human Brain, June 2–6, 2002.* (Sendai, Japan).

Caroli, A., and Frisoni, G. B. (2010). The dynamics of Alzheimer's disease biomarkers in the Alzheimer's Disease Neuroimaging Initiative cohort. *Neurobiol. Aging* 31, 1263–1274.

Caselli, R. J., Dueck, A. C., Locke, D. E., Hoffman-Snyder, C. R., Woodruff, B. K., Rapcsak, S. Z., et al. (2011). Longitudinal modeling of frontal cognition in APOE epsilon4 homozygotes, heterozygotes, and noncarriers. *Neurology* 76, 1383–1388.

Castellano, J. M., Kim, J., Stewart, F. R., Jiang, H., Dematteis, R. B., Patterson, B. W., et al. (2011). Human apoE isoforms differentially regulate brain amyloid-beta peptide clearance. *Sci. Transl. Med.* 3, 89ra57.

Corder, E. H., Saunders, A. M., Strittmatter, W. J., Schmechel, D. E., Gaskell, P. C., Small, G. W., et al. (1993). Gene dose of apolipoprotein E type 4 allele and the risk of Alzheimer's disease in late onset families. *Science* 261, 921–923.

Dale, A., Fischl, B., and Sereno, M. (1999). Cortical surface-based analysis. I. Segmentation and surface reconstruction. *Neuroimage* 9, 179–194.

Deane, R., Sagare, A., Hamm, K., Parisi, M., Lane, S., Finn, M. B., et al. (2008). apoE isoform-specific disruption of amyloid beta peptide

clearance from mouse brain. *J. Clin. Invest.* 118, 4002–4013.

Drzezga, A., Grimmer, T., Henriksen, G., Muhlau, M., Perneczky, R., Miederer, I., et al. (2009). Effect of APOE genotype on amyloid plaque load and gray matter volume in Alzheimer disease. *Neurology* 72, 1487–1494.

Espeseth, T., Westlye, L. T., Fjell, A. M., Walhovd, K. B., Rootwelt, H., and Reinvang, I. (2008). Accelerated age-related cortical thinning in healthy carriers of apolipoprotein E epsilon 4. *Neurobiol. Aging* 29, 329–340.

Farlow, M. R., He, Y., Tekin, S., Xu, J., Lane, R., and Charles, H. C. (2004). Impact of APOE in mild cognitive impairment. *Neurology* 63, 1898–1901.

Fischl, B., Sereno, M., and Dale, A. (1999). Cortical surface-based analysis. II: Inflation, flattening, and a surface-based coordinate system. *Neuroimage* 9, 195–207.

Fleisher, A. S., Chen, K., Liu, X., Roontiva, A., Thiyyagura, P., Ayutyanont, N., et al. (2011). Using positron emission tomography and florbetapir F18 to image cortical amyloid in patients with mild cognitive impairment or dementia due to Alzheimer disease. *Arch. Neurol.* 68, 1404–1411.

Fortea, J., Sala-Llonch, R., Bartres-Faz, D., Bosch, B., Llado, A., Bargallo, N., et al. (2010). Increased cortical thickness and caudate volume precede atrophy in PSEN1 mutation carriers. *J. Alzheimers Dis.* 22, 909–922.

Fortea, J., Sala-Llonch, R., Bartres-Faz, D., Llado, A., Sole-Padulles, C., Bosch, B., et al. (2011). Cognitively preserved subjects with transitional cerebrospinal fluid ss-amyloid 1-42 values have thicker cortex in Alzheimer's disease vulnerable areas. *Biol. Psychiatry* 70, 183–190.

Green, R. C., Roberts, J. S., Cupples, L. A., Relkin, N. R., Whitehouse, P. J., Brown, T., et al. (2009). Disclosure of APOE genotype for risk of Alzheimer's disease. *N. Engl. J. Med.* 361, 245–254.

Holtzman, D. M., Herz, J., and Bu, G. (2012). Apolipoprotein e and apolipoprotein e receptors: normal biology and roles in Alzheimer disease. *Cold Spring Harb. Perspect. Med.* 2:a006312. doi: 10.1101/cshperspect.a006312

Jack, C. R. Jr., Bernstein, M. A., Borowski, B. J., Gunter, J. L., Fox, N. C., Thompson, P. M., et al. (2010). Update on the magnetic resonance imaging core of the Alzheimer's disease neuroimaging initiative. *Alzheimers Dement.* 6, 212–220.

Jack, C. R. Jr., Bernstein, M. A., Fox, N. C., Thompson, P., Alexander, G., Harvey, D., et al. (2008). The Alzheimer's Disease Neuroimaging Initiative (ADNI): MRI methods. *J. Magn. Reson. Imaging* 27, 685–691.

Jack, C. R. Jr., Vemuri, P., Wiste, H. J., Weigand, S. D., Aisen, P. S., Trojanowski, J. Q., et al. (2011). Evidence for ordering of Alzheimer disease biomarkers. *Arch. Neurol.* 68, 1526–1535.

Jagust, W. J., Bandy, D., Chen, K., Foster, N. L., Landau, S. M., Mathis, C. A., et al. (2010). The Alzheimer's Disease Neuroimaging Initiative positron emission tomography core. *Alzheimers Dement.* 6, 221–229.

Langbaum, J. B., Chen, K., Lee, W., Reschke, C., Bandy, D., Fleisher, A. S., et al. (2009). Categorical and correlational analyses of baseline fluorodeoxyglucose positron emission tomography images from the Alzheimer's Disease Neuroimaging Initiative (ADNI). *Neuroimage* 45, 1107–1116.

Mayeux, R., Small, S. A., Tang, M., Tycko, B., and Stern, Y. (2001). Memory performance in healthy elderly without Alzheimer's disease: effects of time and apolipoprotein-E. *Neurobiol. Aging* 22, 683–689.

McKhann, G. M., Knopman, D. S., Chertkow, H., Hyman, B. T., Jack, C. R. Jr., Kawas, C. H., et al. (2011). The diagnosis of dementia due to Alzheimer's disease: recommendations from the National Institute on Aging-Alzheimer's Association workgroups on diagnostic guidelines for Alzheimer's disease. *Alzheimers Dement.* 7, 263–269.

Moffat, S. D., Szekely, C. A., Zonderman, A. B., Kabani, N. J., and Resnick, S. M. (2000). Longitudinal change in hippocampal volume as a function of apolipoprotein E genotype. *Neurology* 55, 134–136.

Morris, J. C., Roe, C. M., Xiong, C., Fagan, A. M., Goate, A. M., Holtzman, D. M., et al. (2010). APOE predicts amyloid-beta but not tau Alzheimer pathology in cognitively normal aging. *Ann. Neurol.* 67, 122–131.

Petersen, R. C., Aisen, P. S., Beckett, L. A., Donohue, M. C., Gamst, A. C., Harvey, D. J., et al. (2010). Alzheimer's Disease Neuroimaging Initiative (ADNI): clinical characterization. *Neurology* 74, 201–209.

Petersen, R. C., Smith, G. E., Waring, S. C., Ivnik, R. J., Tangalos, E. G., and Kokmen, E. (1999). Mild cognitive impairment: clinical characterization and outcome. *Arch. Neurol.* 56, 303–308.

Risacher, S. L., Saykin, A. J., West, J. D., Shen, L., Firpi, H. A., and McDonald, B. C. (2009). Baseline MRI predictors of conversion from MCI to probable AD in the ADNI cohort. *Curr. Alzheimer Res.* 6, 347–361.

Risacher, S. L., Shen, L., West, J. D., Kim, S., McDonald, B. C., Beckett, L. A., et al. (2010). Longitudinal MRI atrophy biomarkers: relationship to conversion in the ADNI cohort. *Neurobiol. Aging* 31, 1401–1418.

Roberts, J. S., Christensen, K. D., and Green, R. C. (2011). Using Alzheimer's disease as a model for genetic risk disclosure: implications for personal genomics. *Clin. Genet.* 80, 407–414.

Saykin, A. J., Shen, L., Foroud, T. M., Potkin, S. G., Swaminathan, S., Kim, S., et al. (2010). Alzheimer's Disease Neuroimaging Initiative biomarkers as quantitative phenotypes: genetics core aims, progress, and plans. *Alzheimers Dement.* 6, 265–273.

Shaw, L. M., Vanderstichele, H., Knapik-Czajka, M., Clark, C. M., Aisen, P. S., Petersen, R. C., et al. (2009). Cerebrospinal fluid biomarker signature in Alzheimer's disease neuroimaging initiative subjects. *Ann. Neurol.* 65, 403–413.

Shaw, L. M., Vanderstichele, H., Knapik-Czajka, M., Figurski, M., Coart, E., Blennow, K., et al. (2011). Qualification of the analytical and clinical performance of CSF biomarker analyses in ADNI. *Acta Neuropathol.* 121, 597–609.

Tosun, D., Schuff, N., Shaw, L. M., Trojanowski, J. Q., and Weiner, M. W. (2011). Relationship between CSF biomarkers of Alzheimer's disease and rates of regional cortical thinning in ADNI data. *J. Alzheimers Dis.* 26(Suppl. 3), 77–90.

Trojanowski, J. Q., Vandeerstichele, H., Korecka, M., Clark, C. M., Aisen, P. S., Petersen, R. C., et al. (2010). Update on the biomarker core of the Alzheimer's Disease Neuroimaging Initiative subjects. *Alzheimers Dement.* 6, 230–238.

Vemuri, P., Wiste, H. J., Weigand, S. D., Knopman, D. S., Shaw, L. M., Trojanowski, J. Q., et al. (2010). Effect of apolipoprotein E on biomarkers of amyloid load and neuronal pathology in Alzheimer disease. *Ann. Neurol.* 67, 308–316.

Weiner, M. W., Aisen, P. S., Jack, C. R. Jr., Jagust, W. J., Trojanowski, J. Q., Shaw, L., et al. (2010). The Alzheimer's disease neuroimaging initiative: progress report and future plans. *Alzheimers Dement.* 6, 202 e207–211 e207.

Wu, L., Rowley, J., Mohades, S., Leuzy, A., Dauar, M. T., Shin, M., et al. (2012). Dissociation between Brain Amyloid Deposition and Metabolism in Early Mild Cognitive Impairment. *PLoS ONE* 7:e47905. doi: 10.1371/journal.pone.0047905

Conflict of Interest Statement: Dr. Jack serves as a consultant for Janssen, Bristol-Meyer-Squibb, General Electric, Siements, and Johnson & Johnson; is involved in clinical trials sponsored by Allon and Baxter, Inc.; receives research funding from the NIH and the Alexander Family Alzheimer's Disease Research Professorship of the Mayo Foundation. Dr. Aisen serves on a scientific advisory board for NeuroPhage; serves as a consultant to Elan Corporation, Wyeth, Eisai Inc., Schering-Plough Corp., Bristol-Myers-Squibb, Eli Lilly and Company, NeuroPhage, Merck & Co., Roche, Amgen, Genentech, Inc., Abbott, Pfizer Inc., Novartis, Bayer, Astellas, Dainippon, Biomarin, Solvay, Otsuka, Daiichi, AstraZeneca, Janssen and Medivation, Inc.; and receives research support from Pfizer Inc., Eli Lilly and Company, and Baxter International Inc. Dr. Jagust has served on a scientific advisory board for Genentech, Inc.; has served as a consultant for Synarc, Janssen Alzheimer Immunotherapy, Genentech, Inc., Siemens, and TauRx. Dr. Shaw has served on a technical advisory board for Innogenetics and Saladax; serves as a consultant for Janssen; is involved in clinical trials sponsored by Eisai, Inc., and Baxter, Inc.; and receives research funding from the NIH and MJ Fox Foundation for Parkinson's research. Dr. Trojanowski may accrue revenue in the future on patents submitted by the University of Pennsylvania wherein he is co-Inventor and he received revenue from the sale of Avid to Eli Lily as co-inventor on imaging related patents submitted by the University of Pennsylvania; and receives research support from the NIH, Bristol Myer Squib, AstraZenica and several non-profits. Dr. Weiner has served on scientific advisory boards for Eli Lilly, Araclon, Institut Catala de Neurociencies Aplicades, the Gulf War Veterans Illnesses Advisory Committee, Biogen Idec, and Pfizer; has served as a consultant to Astra Zeneca, Araclon, Medivation/Pfizer, Ipsen, TauRx Therapeutics LDT, Bayer Healthcare, Biogen Idec, Exonhit Therapeutics,

Servier, Synarc, Janssen, Harvard University, and KLJ Associates; has received funding for travel from NeuroVigil, Inc., CHRU Hopital Roger Salengro, Siemens, AstraZeneca, Geneva University Hospitals, Eli Lilly, Paris University, Institut Catala de Neurociencies Aplicades, University of New Mexico School of Medicine, Ipsen, Clinical Trials on Alzheimer's Disease, the AD/PD Meeting, Paul Sabatier University, Novartis, Tohoku University, Fundacio ACE, and Travel eDreams, Inc.; has received honoraria from NeuroVigil, Inc., Institut Catala de Neurociencies Aplicades, PMDA/Japanese Ministry of Health, Labour, and Welfare, Tohoku University, and the Alzheimer's Drug Discovery Foundation; has received research support from Merck and Avid; and has stock options for Synarc and Elan. Dr. Saykin has received investigator-initiated research funding from Welch Allyn and Siemens Healthcare; has served as a consultant or advisory board member for Siemens Healthcare and Eli Lilly. Drs. Risacher, Shen, Kim, Nho, Foroud, Petersen, and Koeppe declare that the research was conducted in the absence of any commercial or financial relationships that could be construed as a potential conflict of interest.

Received: 19 December 2012; paper pending published: 17 January 2013; accepted: 01 March 2013; published online: 01 April 2013.

*Citation: Risacher SL, Kim S, Shen L, Nho K, Foroud T, Green RC, Petersen RC, Jack Jr. CR, Aisen PS, Koeppe RA, Jagust WJ, Shaw LM, Trojanowski JQ, Weiner MW and Saykin AJ (2013) The role of apolipoprotein E (APOE) genotype in early mild cognitive impairment (E-MCI). Front. Aging Neurosci. **5**:11. doi: 10.3389/fnagi.2013.00011*

frontiers in
AGING NEUROSCIENCE

ORIGINAL RESEARCH ARTICLE
published: 23 November 2012
doi: 10.3389/fnagi.2012.00032

Is the subcallosal medial prefrontal cortex a common site of atrophy in Alzheimer's disease and frontotemporal lobar degeneration?

Olof Lindberg[1]*, Eric Westman[1], Sari Karlsson[2], Per Östberg[3], Leif A. Svensson[4], Andrew Simmons[5,6] and Lars-Olof Wahlund[1]

[1] *Department of Neurobiology, Care Sciences and Society, Karolinska Institutet, Stockholm, Sweden*
[2] *Aging Research Centre, Karolinska Institutet, Stockholm, Sweden*
[3] *Division of Speech and Language Pathology, Department of Clinical Science, Intervention and Technology, Karolinska Institutet, Stockholm, Sweden*
[4] *Department of Medical Physics, Karolinska University Hospital, Stockholm, Sweden*
[5] *Institute of Psychiatry, King's College London, London, UK*
[6] *NIHR Biomedical Research Centre for Mental Health, London, UK*

Edited by:
Manuel Menendez Gonzalez, Hospital Álvarez-Buylla, Spain

Reviewed by:
Manuel Menendez Gonzalez, Hospital Álvarez-Buylla, Spain
Sandro M. Krieg, Technical University Munich, Germany

****Correspondence:***
Olof Lindberg, Clinical Geriatrics, Department of Neurobiology, Care Sciences and Society, Karolinska Institutet, Novum, Plan 5, Stockholm SE-141 86, Sweden.
e-mail: olof.lindberg@ki.se

Regions affected late in neurodegenerative disease are thought to be anatomically connected to regions affected earlier. The subcallosal medial prefrontal cortex (SMPC) has connections with the dorsolateral prefrontal cortex (DLPFC), orbitofrontal cortex (OFC), and hippocampus (HC), which are regions that may become atrophic in frontotemporal lobar degeneration (FTLD) and Alzheimer's disease (AD). We hypothesized that the SMPC is a common site of frontal atrophy in the FTLD subtypes and in AD. The volume of the SMPC, DLPFC, OFC, HC, and entorhinal cortex (EC) were manually delineated for 12 subjects with frontotemporal dementia (FTD), 13 with semantic dementia (SD), 9 with progressive nonfluent aphasia (PNFA), 10 AD cases, and 13 controls. Results revealed significant volume loss in the left SMPC in FTD, SD, and PNFA, while the right SMPC was also atrophied in SD and FTD. In AD a non significant tendency of volume loss in the left SMPC was found ($p = 0.08$), with no volume loss on the right side. Results indicated that volume loss reflected the degree of brain connectivity. In SD and AD temporal regions displayed most atrophy. Among the frontal regions, the SMPC (which receives the strongest temporal projections) demonstrated most volume loss, the OFC (which receives less temporal projections) less volume loss, while the DLPFC (which is at multisynaptic distance from the temporal regions) demonstrated no volume loss. In PNFA, the left SMPC was atrophic, possibly reflecting progression from the left anterior insula, while FTD patients may have had SMPC atrophy at the initial stages of the disease. Atrophy of the SMPC may thus be affected by either initial temporal or initial frontal atrophy, making it a common site of frontal atrophy in the dementia subtypes investigated.

Keywords: Alzheimer's disease, frontotemporal dementia, subcallosal medial prefrontal cortex, MRI

INTRODUCTION

In recent years the view that regional atrophy in dementia results from damage to particular brain networks has received increased attention. This view not only relates regional damage to impairment of mental functions, dependent on different brain networks, but also allows inference as to how and where atrophy develops during the course of disease. The assumption is that "later-affected regions bear known anatomical connections with the sites of earlier injury" (Seeley et al., 2009, p. 42). We will refer to this as the "connection hypothesis." The basic mechanism of the connection hypothesis has previously been demonstrated in monkey brain (Woolsey, 1947; Jones and Powell, 1970) and in neuropathological postmortem studies of Alzheimer's disease (AD) (Pearson et al., 1985; De Lacoste and White, 1993).

The underlying mechanism of the connection hypothesis is that molecular pathologies such as β-amyloid, tau, α-synuclein, and TDP-43 aggregate and progress through specific anatomical connections or brain networks (Seeley et al., 2009; Raj et al., 2012). Support for this assumption in both AD and FTLD has been presented in a large study by Seeley et al. (2009). In another study a model of brain connectivity was derived from whole brain tractography on diffusion MRI scans on 14 healthy young controls. On the basis of the strength of connectivity found in this model several networks were proposed that in subsequent analysis was shown to correspond well with Seeley's assumption of network-specific progression of atrophy in FTLD and AD (Raj et al., 2012).

AD and semantic dementia (SD), which is a subtype of frontotemporal lobar degeneration (FTLD), are characterized by severe hippocampal and temporal lobe pathology while the frontal lobes are initially largely spared. This could be interpreted as support for the connection hypothesis because most frontal

regions are at a "multisynaptic" distance from the temporal regions first affected. Most regions in the frontal lobe interact with the hippocampus (HC) through the cingulate and posterior parahippocampal gyri and entorhinal cortices (Goldman-Rakic et al., 1984). Disease processes emanating from the temporal cortex must thus progress through a number of synaptic connections to reach the frontal parts of the brain.

Two regions in the frontal lobe, the subcallosal medial prefrontal cortex (SMPC), and to a lesser extent the orbitofrontal cortex (OFC), are exceptions to the multisynaptic communication pattern described above. Studies with retrograde and anterograde tracers on the rhesus monkey brain show that these frontal regions receive direct projections from the hippocampal formation (Goldman-Rakic et al., 1984; Barbas and Blatt, 1995; Carmichael and Price, 1996). Such direct connections also exist in humans (Kahn et al., 2008). The direct projections from the HC to the SMPC and ORB originate mainly from the CA1 field and the subiculum, and contrary to many brain connections, they are strictly ipsilateral and unidirectional (Barbas and Blatt, 1995; Laroche et al., 2000).

Monkey studies suggest that the entorhinal cortex (EC), heavily affected in AD, also projects particularly to the OFC and the SMPC (Ongur and Price, 2000; Munoz and Insausti, 2005; Insausti and Amaral, 2008). There is, however, less convincing evidence for such direct connections between the EC and the SMPC in humans (Kahn et al., 2008).

In addition to the temporal regions, the SMPC has reciprocal connections with several regions in the frontal lobe. Brodmann areas (BA) 9 and 46 in the dorsolateral prefrontal cortex (DLPFC) are connected to BA14 in the SMPC (Carmichael and Price, 1996; Ongur and Price, 2000). It has further been demonstrated that some areas of the SMPC (such as BA25) have reciprocal connections with regions in the OFC, as well as some parts of the anterior agranular insula (Carmichael and Price, 1996; Ongur and Price, 2000).

In accordance with the connection hypothesis it can be assumed that the SMPC and the OFC become pathologically involved in dementia characterized by temporal/hippocampal pathology. This has indeed been shown in both SD (Whitwell and Jack, 2005; Schroeter et al., 2007; Rohrer et al., 2009) and AD (Thompson et al., 2007). According to the connection hypothesis, atrophy might also progress to the SMPC from a number of frontal regions. In the behavioral variant of FTLD called frontotemporal dementia (FTD), the OFC becomes atrophic early (Perry et al., 2006), while the left anterior insula may be the first area to display atrophy in progressive nonfluent aphasia (PNFA) (Rohrer et al., 2009).

The hypothesis of the current study is that the SMPC is a common site of frontal atrophy in all types of FTLD as well as AD because of its anatomical connections with regions suggested to be the first sites of atrophy in these diseases.

To study this we compared the degree of atrophy in the SMPC with atrophy in the EC, the HC, the DLPFC and the OFC in AD and in the three subtypes of FTLD (FTD, PNFA, and SD).

METHODS

PARTICIPANTS

Participants were recruited retrospectively from the Memory Clinic at the Karolinska University Hospital Huddinge, Stockholm, Sweden. All participants went through a standard investigation procedure at the memory clinic. Clinical diagnoses were determined at a multidisciplinary consensus conference with physicians, neuropsychologists, speech-language pathologists, and nurses (Andersson, 2007). FTLD syndromes were diagnosed following international consensus criteria (Neary et al., 1998). Patients with FTLD and AD at different stages of the disease were included. Diagnoses of AD were based on criteria of the ICD-10 International Classification of Diseases, Tenth Revision (ICD-10). The control group (CTL) comprised individuals referred to the memory clinic because of mild subjective forgetfulness in everyday life. Objective cognitive impairment was ruled out through comprehensive neuropsychological assessment (impairment was defined as performance 1.5 SD unit below the age-normal mean on any cognitive test). To further minimize the risk of including participants at the very early stages of neurodegenerative diseases, we included only those participants whose performance did not deteriorate over a minimum of 2-years follow-up. Volumetric MRI data were obtained from 12 FTD, 9 PNFA, 12 SD, and 10 AD patients, as well as 13 CTL subjects.

The study was approved by the Regional Ethical Review Board in Stockholm, Sweden. Demographic and neuropsychological data are presented in **Table 1**. The dementia groups did not differ in age, but all dementia groups had, as expected, significantly lower Mini-Mental State Examination scores (MMSE; Folstein et al., 1975) than the CTL group.

Table 1 | Demographic and neuropsychological characteristics of the investigated groups.

	CTL	FTD	PNFA	SD	AD
Number	13	12	9	13	10
Age (sd)	63.0 (7.4)	61.8 (7.4)	63.9 (6.7)	64.2 (7.3)	64.2 (6.8)
Years of disease (sd)	–	2.50 (2.1)#	3.5 (1.7)	3.9 (1.9)	3.0 (1.3)
MMSE (sd)	29.2 (0.9)	20.8 (6.1)*	16.9 (11.4)*	22.6 (6.9)*	22.4 (6.5)*
Female/male	7/3	9/3	6/3	9/4	7/3

*CTL, controls; FTD, frontotemporal dementia; PNFA, progressive nonfluent aphasia; SD, semantic dementia; AD, Alzheimer's Disease; MMSE, mini mental state examination; sd, standard deviation; *Significantly different from CTL on Kruskal–Wallis test with Mann–Whitney U-test post-hoc. #Significant longer illness duration than FTD in One-Way analysis of variance with a Tukey post-hoc.*

IMAGE ACQUISITION

T1-weighted MR images were acquired on a 1.5T Magnetom Vision Plus scanner (Siemens Medical Systems, Erlangen, Germany). A 3D magnetization-prepared rapid gradient echo pulse sequence (TR, 11.4 ms; TE, 4.4 ms; TI, 300 ms; flip angle, 10°; NEX, 1) was used to obtain 72 contiguous coronal 2.5-mm sections with a 512 × 144 matrix and a 230-mm FOV.

The original images were subsequently interpolated to a 1 × 1 × 1 mm resolution dataset, on which volumetric analyses were performed. Comprehensive quality control was carried out for all MR images as previously described (Simmons et al., 2009, 2011).

CORTICAL PARCELLATION AND VOLUMETRY

The software program MRIcro (Version 1.37; http://www.mricro.com, http://www.mccauslandcenter.sc.edu/mricro/mricron/) was used for parcellation of the cortex. With this software, an image can be viewed in horizontal, sagittal, and coronal directions simultaneously with a reconstruction of the surface of the brain. Measurements were subsequently performed using the HERMES MultiModality software package (Nuclear Diagnostics, Stockholm, Sweden). Regions of interest were traced manually on contiguous coronal sections. The intracranial volume (ICV) was obtained by using a stereologic point-counting technique comprising manual tracing of the ICV on every fourth slice, following landmarks proposed by Eritaia et al. (2000).

The SMPC was traced in the coronal orientation. The anterior border was defined as the first slice in which the callosal white matter connects the two hemispheres (**Figure 1A**) and the posterior border was the last slice in which the inferior part of the corpus callosum could be visualized (**Figure 1B**). Between these landmarks all gray matter on the ventromedial surface was included. Intraclass correlation coefficients (ICCs) were calculated to estimate the reliability of measurements. Tracings of other frontal regions were carried out following Suzuki et al. (2005). For DLPFC we combined the gray matter volume of the superior frontal gyrus with that of the middle frontal gyrus. The reliability of the SMPC measurements was investigated on two occasions and was >0.91 both times. The ICC for other cortical regions has been reported previously (Lindberg et al., 2009), but in short all ICCs were greater than 0.90. All statistical calculations were performed on normalized volume of measured region, derived by dividing the volume of the region by the ICV.

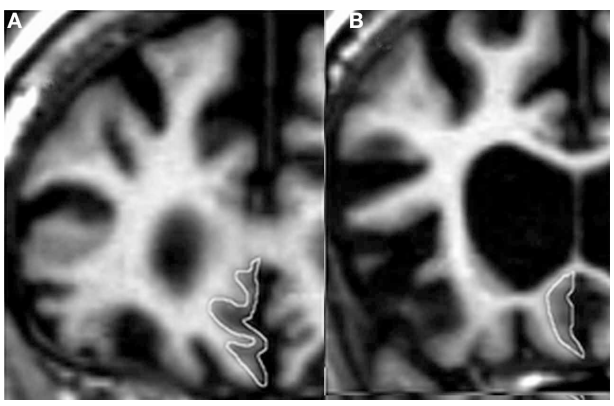

FIGURE 1 | The subcallosal medial prefrontal cortex (SMPC). (A) The anterior border of the delineated region. **(B)** The posterior border of the delineated region.

STATISTICAL ANALYSIS

Volumetric data were analyzed by One-Way analysis of variance with a Fisher LSD *post-hoc* test using Statistica 10 (StatSoft, Inc., 2011). All volumetric data were normalized by ICV by the formula volume of region/ICV. A P value less than 0.05 was considered significant.

CORRELATIONS BETWEEN REGIONAL VOLUMES

To investigate the relationship between frontal and temporal atrophy with atrophy of the SMPC, Pearson's correlation coefficient (r) was calculated for the total normalized volume (left + right side) of each region and the total normalized volume of SMPC.

MULTIVARIATE ANALYSIS

Principle component analysis (PCA) is an unsupervised method which does not use *a priori* information about groups for the analysis. The representations of a multivariate data table X, consisting of rows (observations) and columns (variables) as a low-dimensional plane, is an important feature of PCA. Statistically, PCA reduces the dimensionality and complexity of the data by finding lines and planes in the K-dimensional space (K = number of variables in the model) that approximates the data in the best way possible in the least squares sense. This provides an overview of the data and allows patterns, trends, and outliers to be observed. It is also possible to view relationships between the observations and the variables. A model usually reduces the K-dimensional space to 2–5 dimensions (Eriksson et al., 2006). The results from PCA are visualized by plotting two components in a scatter plot. Components are vectors in the multivariate space along which groups can be separated. These vectors are dominated by the input variables (x). All the components created by the models are, by definition, orthogonal to each other and span the projection plane of the points. Each point in the scatter plot represents one individual subject. Loadings plots illustrate how the original variables influence the new latent variables (components). The PCA model included all five groups (AD, SD, FTD, PNFA, and CTL) and was created to investigate the constellation of clusters that the program uses to separate dementia patients from controls, not to create a model that effectively separated different variants of dementia.

RESULTS

VOLUMETRIC ANALYSIS

The participants with FTD had significantly smaller gray matter volume than the CTL group in all regions studied. The greatest gray matter loss was found in the OFC, SMPC, and HC with a loss of approximately 25% compared to CTL subjects. The EC and right DLPFC regions had approximately 20% volume loss while left DLPFC had 15% loss relative to CTL subjects (**Figure 2**).

Participants with PNFA displayed greater volume loss on the left side. All regions had significant volume loss compared to the

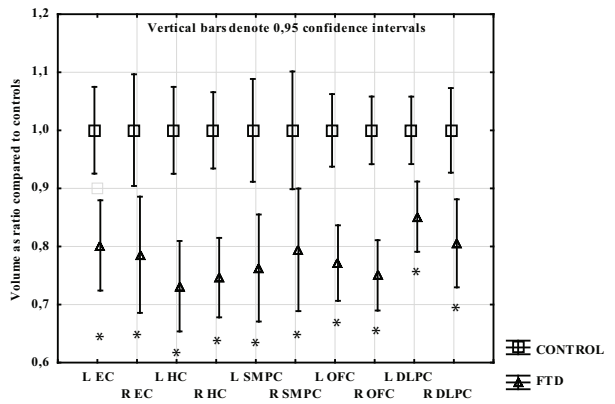

FIGURE 2 | The volume of measured region in FTD expressed as a ratio of CTL volume. CTL volume is set to 1. X-axis denotes the included regions: EC, entorhinal cortex; HC, hippocampus; OFC, orbitofrontal cortex; SMPC, subcallosal medial prefrontal cortex; DLPFC, dorsolateral prefrontal cortex. $^*p < 0.01$.

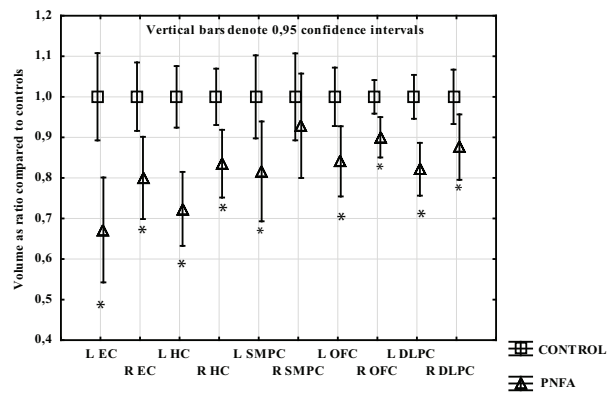

FIGURE 3 | The volume of measured region in PNFA expressed as a ratio of CTL volume. CTL volume is set to 1. X-axis denotes the included regions: EC, entorhinal cortex; HC, hippocampus; OFC, orbitofrontal cortex; SMPC, subcallosal medial prefrontal cortex; DLPFC, dorsolateral prefrontal cortex. $^*p < 0.01$.

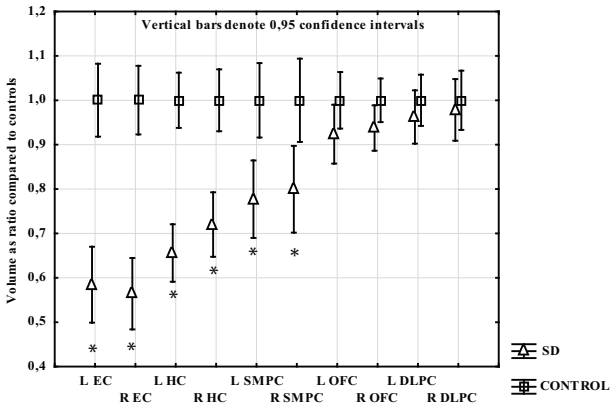

FIGURE 4 | The volume of measured region in SD expressed as a ratio of CTL volume. CTL volume is set to 1. X-axis denotes the included regions: EC, entorhinal cortex; HC, hippocampus; OFC, orbitofrontal cortex; SMPC, subcallosal medial prefrontal cortex; DLPFC, dorsolateral prefrontal cortex. $^*p < 0.01$.

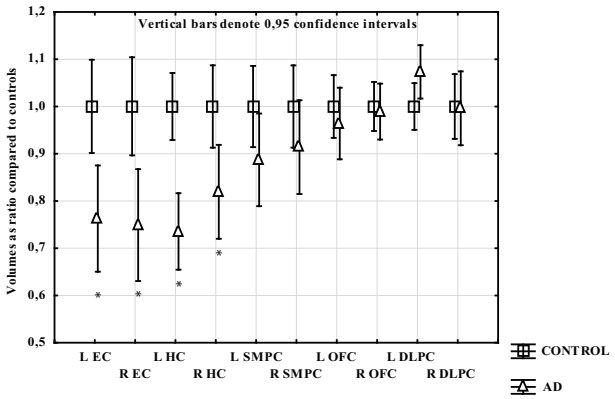

FIGURE 5 | The volume of measured region in AD expressed as a ratio of CTL volume. CTL volume is set to 1. X-axis denotes the included regions: EC, entorhinal cortex; HC, hippocampus; OFC, orbitofrontal cortex; SMPC, subcallosal medial prefrontal cortex; DLPFC, dorsolateral prefrontal cortex. $^*p < 0.01$.

CTL group except the right SMPC. The left EC displayed the greatest mean gray matter loss compared to CTL, followed by left HC, left SMPC, and left DLPFC (**Figure 3**).

All temporal regions and the SMPC displayed significant gray matter loss in participants with SD. The EC displayed most loss (around 40%) followed by HC (30%) and then SMPC (25%). No gray matter loss was found in the OFC or DLPFC (**Figure 4**).

In participants with AD only the temporal regions displayed significant gray matter loss. The greatest atrophy was found in EC and left HC (around 25%) followed by right HC (18%). In the left SMPC there was a tendency to volume loss (around 11%; $p = 0.10$), while the right SMPC, left and right OFC and DLPFC did not demonstrate a statistically significant gray matter reduction (**Figure 5**).

PRINCIPAL COMPONENT ANALYSIS (ALL GROUPS)

The PCA model containing all five groups revealed three components, accounting for 70% of the variance of the original data [$R^2(X)$] and its cross-validated predictability, $Q^2(X) = 0.48$. At the extreme left end of the X-axis on the scatter plot (**Figure 6A**), we found the dementia cases that displayed most severe frontal and temporal atrophy, while on the right end we found mostly CTL subjects. The loading plot of the PCA may indicate the relationship between frontal and temporal atrophy and the SMPC (**Figure 6B**). The first component that is plotted along the X-axis can be interpreted as an indicator of general degree of atrophy. The second component (Y-axis) may potentially be interpreted as temporal versus frontal atrophy. Notice that the EC and the HC are plotted relatively close together. The same pattern is observed for DLPFC and OFC.

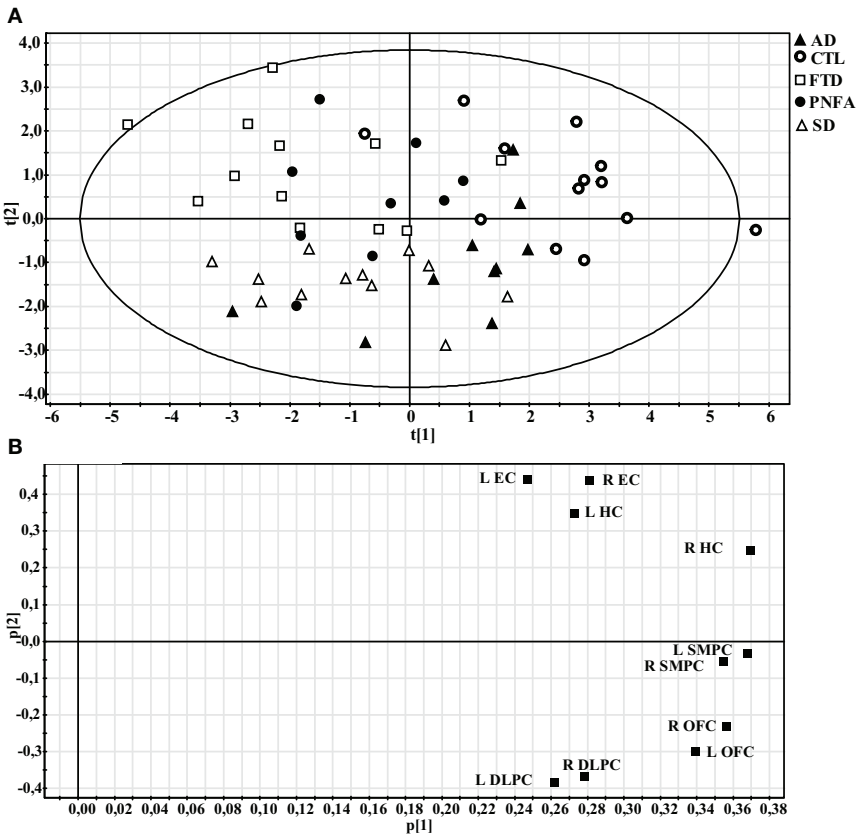

FIGURE 6 | Principal component analysis (PCA) of all subjects. (A) Scatter plot illustrating how individuals are distributed along the first two components. **(B)** Loading plot showing the influence of the regional volumes on the first two components.

CORRELATIONS BETWEEN REGIONAL VOLUMES

In FTD there was a significant correlation between the total normalized volume of OFC and the total normalized volume of SMPC, while no correlation was found between HC and SMPC (**Figures 7A,B**). The SMPC was also correlated with the total volume of DLPFC ($r = 0.76$, $p = 0.004$).

In SD there was a significant correlation between the total normalized volume of HC and the total normalized volume of SMPC, while no correlation was found between the OFC and SMPC (**Figures 7C,D**).

The total normalized volume of SMPC was not correlated with any other region in AD or in PNFA.

DISCUSSION

This study explored the hypothesis that the SMPC may be particularly vulnerable to atrophy in FTLD and AD because of its anatomical connections with frontal and temporal regions that become atrophic in these diseases. In AD and SD, the EC and the HC have been found to be early sites of atrophy (Braak et al., 1996; Rohrer et al., 2009). The SMPC may receive the densest efferent hippocampal projections in the frontal lobe (Barbas and Blatt, 1995). The OFC receives less dense projections (Munoz and Insausti, 2005) while the DLPFC is at a multiple synaptic distance from the HC. This pattern of connectivity is reflected by the volumetric data. The EC and the HC have most volume loss, followed by the SMPC and the OFC, while the DLPFC has no loss of gray matter volume in AD and SD. As discussed in the introduction, there are some differences between man and monkey in the findings concerning connectivity between the EC and the frontal lobe. If there are direct projections from the EC to the SMPC, then the atrophy of the EC could (as in HC) progress directly to the SMPC. Another possibility is that atrophy of the EC progresses to the HC as these regions are reciprocally connected (Pearson et al., 1985; De Lacoste and White, 1993), and from the HC to the SMPC.

In FTD, volumetric analyses revealed that the OFC and the HC was the most atrophic region compared to CTL. The SMPC has, however, almost as much volume loss. One previous study suggests that the OFC may be the first site of atrophy in FTD (Perry et al., 2006). Another study suggests that the so-called paralimbic network (of which the SMPC is part) becomes atrophic first (Seeley et al., 2008). We found a non-significant difference between the degree of atrophy in the OFC and the SMPC, which potentially could support the view that the SMPC is part of a network that becomes affected first in FTD.

In PNFA, left but not right SMPC was atrophic compared to controls. Volume loss in the left SMPC might reflect a progression from initial atrophy in the left anterior insula.

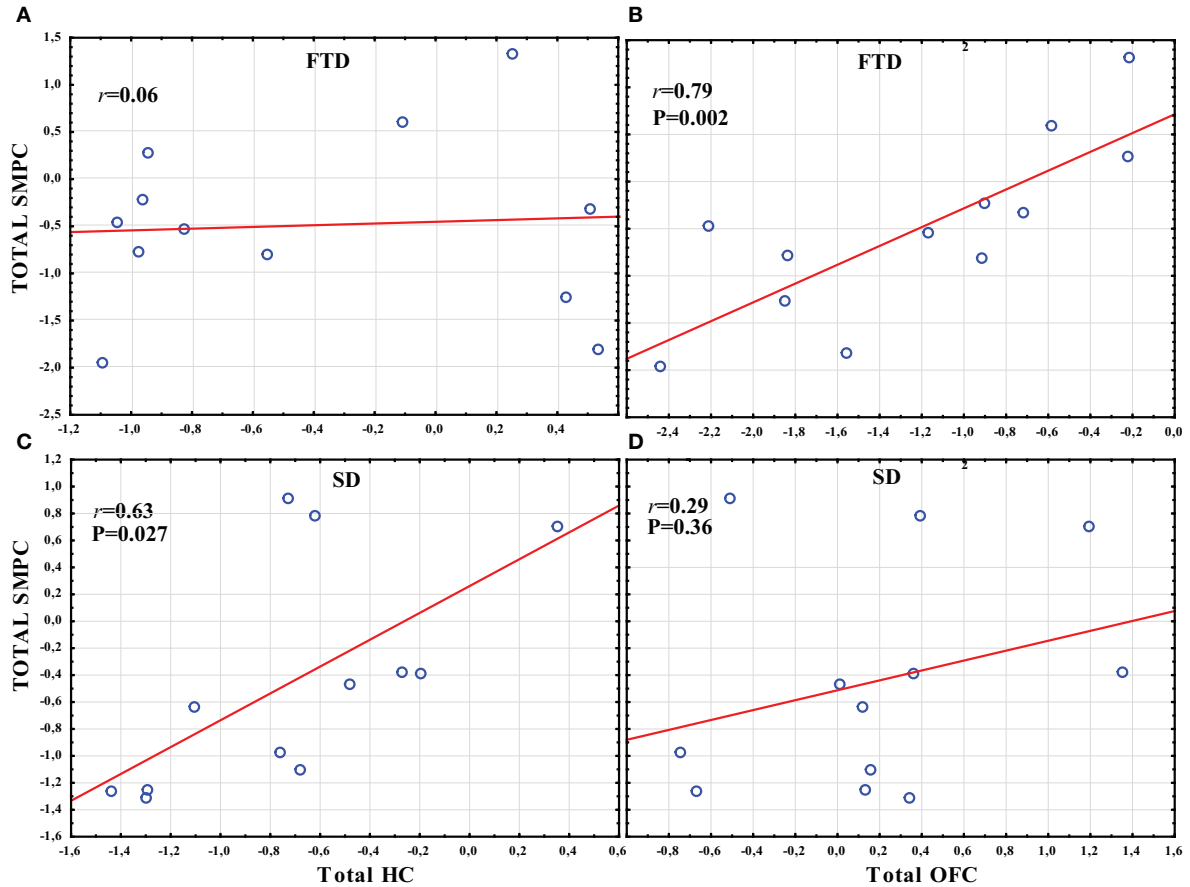

FIGURE 7 | The correlation between the total volume of SMPC, HC and OFC in SD and FTD. (A) The correlation between the total volume of SMPC and HC in FTD. **(B)** The correlation between total volume of SMPC and OFC in FTD. **(C)** The correlation between total volume SMPC and HC in SD. **(D)** The correlation between total volume of SMPC and OFC in SD.

We hypothesized that we also would find atrophy in the SMPC in AD, however only a tendency was found on the left side. The main reason for this was probably the relatively small number of cases included in this dementia group. One reason for not including more AD patients was that we wanted to have approximately the same statistical power for each dementia group. The FTLD group represents almost all patients with this rare diagnosis treated at the memory clinic at Huddinge hospital during a period of 10 years. It should also be noted that the general degree of atrophy was less severe in the AD cases than in the FTLD patients. Another strong indication that HC and SMPC atrophy may be connected is that the ratio of HC volume and SMPC volume is almost identical for AD and SD. Thus the ratio between left HC/Left SMPC is 0.85 in SD and 0.83 in AD, and the ratio between R HC/R SMPC is 0.90 for both SD and AD.

From the discussion above it could be suggested that the development of atrophy in the SMPC may be affected both by frontal as well as temporal atrophy. The results of the PCA may support this finding. As noted in the results section, the EC and the HC as well as the DLPFC and the OFC are closely plotted together in the PCA loading plot. The SMPC is plotted almost in the centre between the EC/HC and the DLPFC/OFC. This could indicate that atrophy of the SMPC may be almost as related to frontal as to temporal atrophy.

This assumption may also be supported by the findings of our correlation analyses. FTD was the dementia subtype that displayed most frontal atrophy (centered in the OFC). In this subtype the total volume of SMPC was correlated with the total volume of OFC, but not with the total volume of HC (**Figures 7A,B**). SD is the subtype that displayed most temporal atrophy centered on HC and EC. Here the total volume of the SMPC was correlated with the total volume of HC, but not with the total volume of OFC (**Figures 7C,D**). Thus the volume of SMPC is correlated to a region with severe frontal atrophy in FTD and to a region with severe temporal atrophy in SD.

Atrophy and laterality of atrophy of the SMPC may also be relevant for behavioral and neuropsychiatric alteration in the variants of dementia included in this investigation. The SMPC is the most posterior part of the ventromedial prefrontal cortex (VMPC). The VMPC has for example been associated with the ability to infer other persons' thoughts and feelings often referred to as "theory of mind" (Gregory et al., 2002), the construct of empathy (Shamay-Tsoory, 2010) and the broad concept of "emotional intelligence," which encompasses a number of social

or emotional abilities that enable individuals to smoothly interact in or adapt to a social environment (Bar-On et al., 2003). The right VMPC may be particulary important for certain social abilities, such as theory of mind (Shamay-Tsoory et al., 2005) and empathy (Shamay-Tsoory et al., 2003). Rosen et al. (2005) also found that right SMPC atrophy was associated with disinhibition in dementia, while atrophy of the more anterior parts of the right VMPC was associated with apathy. They have further shown that the right SMPC is important for self-appraisal (the ability to assess one's own abilities) (Rosen et al., 2010).

Our data suggest that the left SMPC may become atrophic in PNFA and AD, while the right side is also involved in FTD and SD. Considering the relative importance of the right side for behavior symptoms (Rosen et al., 2005; Shamay-Tsoory et al., 2005; Rosen et al., 2010) it could be hypothesized that FTD and SD display more frequent alteration of behavior than PNFA and AD. Indeed this has been described in the international consensus criteria for diagnosing the subtypes of FTLD. FTD patients may display "decline in social interpersonal conduct" and SD patients may show "loss of sympathy and empathy" (Neary, 1999). PNFA on the other hand is described as having "early preservation of social skills." For the diagnosis of AD the American Psychiatric Association ([*DSM-IV-TR*], 2000) does not include deficits in social interaction skills, focusing on memory deficits as a core diagnostic feature, in addition to at least one of the following symptoms: aphasia, apraxia, agnosia or defecits in executive functioning.

The fact that the left SMPC may become more involved in AD may potentially also be explained by the connection hypothesis. Several previous studies have found that hippocampal atrophy at initial stages of AD may be more severe on the left side (Shi et al., 2009). Thus pathology may first progress to the left SMPC/VMPC and then as the disease develops to the right temporal lobe and right SMPC/VMPC. Thus the right VMPC may initially be relatively spared in AD and PNFA which may preserve these patients social interaction skills longer than in SD and FTD.

The most important limitation of this study is the lack of longitudinal data to provide direct evidence for how atrophy develops in the brain. The main point of this work is however that brain connectivity in cross-sectional data may provide important clues as to how and where atrophy may develop during the progression of neurodegenerative diseases.

Another limitation is that only structural 3D images were available in this study. Other MRI-techniques such as diffusion tensor imaging (Catani et al., 2012) or resting state MRI (Yi et al., 2012) could potentially reveal signs of pathology in brain networks before atrophy of regions that belong to these networks become detectable.

A third factor that needs to be considered in the interpretation of our results is the characteristics of our control group who sought consultation at the memory clinic because of subjective feelings of forgetfulness. While objective memory deficits were neither found at baseline investigation nor at follow up (with a minimal interval of 2 years), this does not exclude that these individuals may develop a neurodegenerative disorder later than two years after first examination. Differences between the investigated neurodegenerative disease and controls may thus potentially be even larger if subjects without subjective memory complaints had been used as controls.

CONCLUSIONS

Our finding supports the view that the SMPC, owing to its anatomical connections, may become a common site of frontal pathology in AD and FTLD. This supports the assumption that progression of atrophy in dementia may be predicted on the basis of the anatomical connectivity of the first atrophic region. Knowledge of the regional connectivity of the brain may thus help to predict in which regions atrophy will appear in the progression of neurodegenerative diseases.

AUTHOR CONTRIBUTIONS

Olof Lindberg and Eric Westman substantially contributed to conception and design, or acquisition of data, or analysis and interpretation of data. Olof Lindberg, Eric Westman, Sari Karlsson, Per Östberg, Andrew Simmons, Leif A. Svensson, Lars-Olof Wahlund to the drafting of the article or revising it critically for important intellectual content.

ACKNOWLEDGMENTS

This work was supported by Swedish Brain Power, the Strategic Research Programme in Neuroscience at Karolinska Institutet (StratNeuro), Stockholm Medical Image Laboratory and Education (SMILE), the Foundation of: "Gamla tjänarinnor" and the Foundation of: "Ragnhild och Einar Lundströms Minne." Andrew Simmons was supported by funds from NIHR Biomedical Research Centre for Mental Health at the South London and Maudsley NHS Foundation Trust and Institute of Psychiatry, Kings College London, the NIHR Biomedical Research Unit for Dementia at the South London and Maudsley NHS Foundation Trust and Institute of Psychiatry, Kings College London and Alzheimer's Research UK.

REFERENCES

Andersson, C. (2007). *Predictors of Cognitive Decline in Memory Clinic Patients.* Doctoral dissertation. Stockholm: Karolinska Institutet.

Barbas, H., and Blatt, G. J. (1995). Topographically specific hippocampal projections target functionally distinct prefrontal areas in the rhesus monkey. *Hippocampus* 5, 511–533.

Bar-On, R., Tranel, D., Denburg, N. L., and Bechara, A. (2003). Exploring the neurological substrate of emotional and social intelligence. *Brain* 126, 1790–1800.

Braak, H., Braak, E., Yilmazer, D., De Vos, R. A., Jansen, E. N., and Bohl, J. (1996). Pattern of brain destruction in Parkinson's and Alzheimer's diseases. *J. Neural Transm.* 103, 455–490.

Carmichael, S. T., and Price, J. L. (1996). Connectional networks within the orbital and medial prefrontal cortex of macaque monkeys. *J. Comp. Neurol.* 371, 179–207.

Catani, M., dell'Aqua, F., Bizzi, A., Forkel, S., Williams, S., Simmons, A., et al. (2012). Beyond cortical localization in clinico-anatomical correlation. *Cortex* 48, 1262–1287.

De Lacoste, M. C., and White, C. L. 3rd. (1993). The role of cortical connectivity in Alzheimer's disease pathogenesis: a review and model system. *Neurobiol. Aging* 14, 1–16.

Eriksson, L., Jonansson, E., Kettaneh-Wold, N., and Wold, S. (2006). *Multi- and Megavariate Data Analysis Part 1.* Umeå: Umetrics Academy.

Eritaia, J., Wood, S. J., Stuart, G. W., Bridle, N., Dudgeon, P., Maruff, P., et al. (2000). An optimized method for estimating intracranial volume from magnetic resonance images. *Magn. Reson. Med.* 44, 973–977.

Folstein, M. F., Folstein, S. E., and McHugh, P. R. (1975). "Mini-mental state." A practical method for grading the cognitive state of patients for the clinician. *J. Psychiatr. Res.* 12, 189–198.

Goldman-Rakic, P. S., Selemon, L. D., and Schwartz, M. L. (1984). Dual pathways connecting the dorsolateral prefrontal cortex with the hippocampal formation and parahippocampal cortex in the rhesus monkey. *Neuroscience* 12, 719–743.

Gregory, C., Lough, S., Stone, V., Erzinclioglu, S., Martin, L., Baron-Cohen, S., et al. (2002). Theory of mind in patients with frontal variant frontotemporal dementia and Alzheimer's disease: theoretical and practical implications. *Brain* 125, 752–764.

Insausti, R., and Amaral, D. G. (2008). Entorhinal cortex of the monkey: IV. Topographical and laminar organization of cortical afferents. *J. Comp. Neurol.* 509, 608–641.

Jones, E. G., and Powell, T. P. (1970). An anatomical study of converging sensory pathways within the cerebral cortex of the monkey. *Brain* 93, 793–820.

Kahn, I., Andrews-Hanna, J. R., Vincent, J. L., Snyder, A. Z., and Buckner, R. L. (2008). Distinct cortical anatomy linked to subregions of the medial temporal lobe revealed by intrinsic functional connectivity. *J. Neurophysiol.* 100, 129–139.

Laroche, S., Davis, S., and Jay, T. M. (2000). Plasticity at hippocampal to prefrontal cortex synapses: dual roles in working memory and consolidation. *Hippocampus* 10, 438–446.

Lindberg, O., Östberg, P., Zandbelt, B. B., Öberg, J., Zhang, Y., Andersen, C., et al. (2009). Cortical morphometric subclassification of frontotemporal lobar degeneration. *AJNR Am. J. Neuroradiol.* 30, 1233–1239.

Munoz, M., and Insausti, R. (2005). Cortical efferents of the entorhinal cortex and the adjacent parahippocampal region in the monkey (*Macaca fascicularis*). *Eur. J. Neurosci.* 22, 1368–1388.

Neary, D. (1999). Overview of frontotemporal dementias and the consensus applied. *Dement. Geriatr. Cogn. Disord.* 10(Suppl. 1), 6–9.

Neary, D., Snowden, J. S., Gustafson, L., Passant, U., Stuss, D., Black, S., et al. (1998). Frontotemporal lobar degeneration: a consensus on clinical diagnostic criteria. *Neurology* 51, 1546–1554.

Ongur, D., and Price, J. L. (2000). The organization of networks within the orbital and medial prefrontal cortex of rats, monkeys and humans. *Cereb. Cortex* 10, 206–219.

Pearson, R. C., Esiri, M. M., Hiorns, R. W., Wilcock, G. K., and Powell, T. P. (1985). Anatomical correlates of the distribution of the pathological changes in the neocortex in Alzheimer disease. *Proc. Natl. Acad. Sci. U.S.A.* 82, 4531–4534.

Perry, R. J., Graham, A., Williams, G., Rosen, H., Erzinclioglu, S., Weiner, M., et al. (2006). Patterns of frontal lobe atrophy in frontotemporal dementia: a volumetric MRI study. *Dement. Geriatr. Cogn. Disord.* 22, 278–287.

Raj, A., Kuceyeski, A., and Weiner, M. (2012). A network diffusion model of disease progression in dementia. *Neuron* 73, 1204–1215.

Rohrer, J. D., Warren, J. D., Modat, M., Ridgway, G. R., Douiri, A., Rossor, M. N., et al. (2009). Patterns of cortical thinning in the language variants of frontotemporal lobar degeneration. *Neurology* 72, 1562–1569.

Rosen, H. J., Alcantar, O., Rothlind, J., Sturm, V., Kramer, J. H., Weiner, M., et al. (2010). Neuroanatomical correlates of cognitive self-appraisal in neurodegenerative disease. *Neuroimage* 49, 3358–3364.

Rosen, H. J., Allison, S. C., Schauer, G. F., Gorno-Tempini, M. L., Weiner, M. W., and Miller, B. L. (2005). Neuroanatomical correlates of behavioural disorders in dementia. *Brain* 128, 2612–2625.

Schroeter, M. L., Raczka, K., Neumann, J., and Yves Von Cramon, D. (2007). Towards a nosology for frontotemporal lobar degenerations-a meta-analysis involving 267 subjects. *Neuroimage* 36, 497–510.

Seeley, W. W., Crawford, R., Rascovsky, K., Kramer, J. H., Weiner, M., Miller, B. L., et al. (2008). Frontal paralimbic network atrophy in very mild behavioral variant frontotemporal dementia. *Arch. Neurol.* 65, 249–255.

Seeley, W. W., Crawford, R. K., Zhou, J., Miller, B. L., and Greicius, M. D. (2009). Neurodegenerative diseases target large-scale human brain networks. *Neuron* 62, 42–52.

Shamay-Tsoory, S. G. (2010). The neural bases for empathy. *Neuroscientist* 17, 18–24.

Shamay-Tsoory, S. G., Tomer, R., Berger, B. D., and Aharon-Peretz, J. (2003). Characterization of empathy deficits following prefrontal brain damage: the role of the right ventromedial prefrontal cortex. *J. Cogn. Neurosci.* 15, 324–337.

Shamay-Tsoory, S. G., Tomer, R., Berger, B. D., Goldsher, D., and Aharon-Peretz, J. (2005). Impaired "affective theory of mind" is associated with right ventromedial prefrontal damage. *Cogn. Behav. Neurol.* 18, 55–67.

Shi, F., Liu, B., Zhou, Y., Yu, C., and Jiang, T. (2009). Hippocampal volume and asymmetry in mild cognitive impairment and Alzheimer's disease: meta-analyses of MRI studies. *Hippocampus* 19, 1055–1064.

Simmons, A., Westman, E., Muehlboeck, S., Mecocci, P., Vellas, B., Tsolaki, M., et al. (2009). MRI measures of Alzheimer's disease and the AddNeuroMed study. *Ann. N.Y. Acad. Sci.* 1180, 47–55.

Simmons, A., Westman, E., Muehlboeck, S., Mecocci, P., Vellas, B., Tsolaki, M., et al. (2011). The AddNeuroMed framework for multi-centre MRI assessment of Alzheimer's disease: experience from the first 24 months. *Int. J. Geriatr. Psychiatry* 26, 75–82.

Suzuki, M., Zhou, S. Y., Takahashi, T., Hagino, H., Kawasaki, Y., Niu, L., et al. (2005). Differential contributions of prefrontal and temporolimbic pathology to mechanisms of psychosis. *Brain* 128, 2109–2122.

Thompson, P. M., Hayashi, K. M., Dutton, R. A., Chiang, M. C., Leow, A. D., Sowell, E. R., et al. (2007). Tracking Alzheimer's disease. *Ann. N.Y. Acad. Sci.* 1097, 183–214.

Whitwell, J. L., and Jack, C. R. Jr. (2005). Comparisons between Alzheimer disease, frontotemporal lobar degeneration, and normal aging with brain mapping. *Top. Magn. Reson. Imaging* 16, 409–425.

Woolsey, C. N. (1947). Patterns of sensory representation in the cerebral cortex. *Fed. Proc.* 6, 437–441.

Yi, L., Wang, J., Jia, L., Zhao, Z., Lu, J., Li, K., et al. (2012). Structural and functional changes in subcortical vascular mild cognitive impairment: a combined voxel-based morphometry and resting-state FMRI study. *PLoS ONE* 7:e44758. doi: 10.1371/journal.pone.0044758

Conflict of Interest Statement: The authors declare that the research was conducted in the absence of any commercial or financial relationships that could be construed as a potential conflict of interest.

Received: 30 October 2012; paper pending published: 04 November 2012; accepted: 05 November 2012; published online: 23 November 2012.

*Citation: Lindberg O, Westman E, Karlsson S, Östberg P, Svensson LA, Simmons A and Wahlund L-O (2012) Is the subcallosal medial prefrontal cortex a common site of atrophy in Alzheimer's disease and frontotemporal lobar degeneration? Front. Ag. Neurosci. **4**:32. doi: 10.3389/fnagi.2012.00032*

frontiers in
AGING NEUROSCIENCE

METHODS ARTICLE
published: 15 July 2013
doi: 10.3389/fnagi.2013.00030

VBM with viscous fluid registration of gray matter segments in SPM

Joao M. S. Pereira[1,2]*, Julio Acosta-Cabronero[2], George Pengas[2], Li Xiong[3], Peter J. Nestor[4] and Guy B. Williams[2]

[1] Laboratory of Biostatistics and Medical Informatics, IBILI - Faculty of Medicine, University of Coimbra, Coimbra, Portugal
[2] Department of Clinical Neurosciences, School of Clinical Medicine, University of Cambridge, Cambridge, UK
[3] Neurology Department, Zhongnan Hospital of Wuhan University, Wuhan, China
[4] German Center for Neurodegenerative Diseases (DZNE), Magdeburg, Germany

Edited by:
Manuel Menéndez-González, Hospital Álvarez-Buylla, Spain

Reviewed by:
Katsutoshi Furukawa, Tohoku University, Japan
Yunfei Huang, Albany Medical College, USA

***Correspondence:**
Joao M. S. Pereira, Laboratory of Biostatistics and Medical Informatics, IBILI - Faculty of Medicine, University of Coimbra, Azinhaga de Santa Comba – Celas, 3000-548 Coimbra, Portugal
e-mail: joao.mspereira@gmail.com

Improved registration of gray matter segments in SPM has been achieved with the DARTEL algorithm. Previous work from our group suggested, however, that such improvements may not translate to studies of clinical groups. To address the registration issue in atrophic brains, this paper relaxed the condition of diffeomorphism, central to DARTEL, and made use of a viscous fluid registration model with limited regularization constraints to register the modulated gray matter probability maps to an intra-population template. Quantitative analysis of the registration results after the additional viscous fluid step showed no worsening of co-localization of fiducials compared to DARTEL or unified segmentation methods, and the resulting voxel based morphometry (VBM) analyses were able to better identify atrophic regions and to produce results with fewer apparent false positives. DARTEL showed great sensitivity to atrophy, but the resulting VBM maps presented broad, amorphous regions of significance that are hard to interpret. We propose that the condition of diffeomorphism is not necessary for basic VBM studies in atrophic populations, but also that it has disadvantages that must be taken into consideration before a study. The presented viscous fluid registration method is proposed for VBM studies to enhance sensitivity and localizing power.

Keywords: MRI, VBM, SPM, DARTEL, registration, dementia

INTRODUCTION

Imaging biomarkers are of considerable interest in dementia research. Aside from the qualities of the biomarker itself, the method with which it is analysed is crucial to consider as insensitive or unstable methods could mean that real information is lost (false negatives) or that spurious changes (false positives) are reported. Voxel-based image analysis has become a cornerstone of assessing structural imaging biomarkers, yet such methods are typically validated in simulations and the healthy population. The DARTEL algorithm (Diffeomorphic Anatomical Registration Through Exponentiated Lie Algebra) has been presented as an improvement for the registration of gray matter probability maps used in voxel based morphometry (VBM) (Ashburner, 2007) in the software package SPM (http://www.fil.ion.ucl.ac.uk/spm/). One of the key advantages of DARTEL is its explicit search for an inverse consistent, diffeomorphic transformation. This leads to very smooth, large deformation fields that follow elegant mathematical descriptors and that can be easily inverted. Although such characteristics can be useful for applications where it is important to consistently use reverse deformation fields, that is not the case with standard VBM studies of dementia, where most often scans are simply registered to standard space and nothing more is done with the deformation fields (aside from their use for modulation for volume change) (Ridgway et al., 2008). Moreover, a previously published study (Pereira et al., 2010) demonstrated variability in the registration accuracy both by region and disease categorization, raising questions about the spatially variant sensitivity of the resulting VBM significance maps. Even though DARTEL shows improved performance when using preprocessed scans (bias corrected and skull stripped), the associated VBM results showed apparent false positives when compared to the standard SPM5 results using the same scans (Pereira et al., 2010). The motivation for the present study was to explore a simpler, standard registration algorithm without diffeomorphism, in order to assess whether DARTEL's stringent mathematical approach, is in effect inappropriately regularized for use in neurodegenerative disease research. The approach taken in the present study makes use of a long established high degrees of freedom registration algorithm as an alternative: a viscous fluid registration (Christensen et al., 1996). The novelty in the current study compared to past fluid registration studies, however, is its use as an additional registration step, on top of the standard registration in SPM. The hypothesis is that by relaxing the severe regularization constraints intrinsic to DARTEL, the viscous fluid algorithm will be able to account for more anatomical variability, while also preserving structural detail post-registration. This is especially applicable to atrophic brains, which may require both finer (more local) and more extreme deformations than the ones permitted by DARTEL. The resulting VBMs will be more sensitive and more anatomically meaningful than either VBM with

DARTEL or standard VBM. As the viscous fluid methods are able to account for finer deformations than the limited degrees of freedom discrete cosine transform (DCT) used in unified segmentation (Ashburner and Friston, 2005), this study considered the utility of applying the former as an additional step to include after SPM's registration. This was implemented as a hierarchical registration model in which a low degrees of freedom algorithm (DCT in unified segmentation) is applied first in order to account for gross differences between the target and the subject, and then a high degree of freedom method (viscous fluid) is applied to address the finer details. The concept of working on top of already registered gray matter probability maps is justified by the fact that DCT registration is unable to account for all anatomical differences between the subject and the template (Ashburner and Friston, 1999). In short, rather than using a complicated, mathematically rich approach like DARTEL in order to achieve smooth deformation fields that might be of little benefit to a real clinical study, better results might be achieved by adding an extra step after the unified segmentation.

The method presented in this study was tested using real datasets from neurodegenerative studies because these are precisely the datasets where such algorithms find application as VBM studies. This is of paramount importance because other registration approaches, notably DARTEL, have been validated in abstract mathematical frameworks or on healthy volunteer data (Ashburner, 2007; Yassa and Stark, 2009) and then accepted as clinical tools without thorough testing in clinical settings. The clinical plausibility of the resulting statistical maps of VBM, as compared with known patterns of atrophy from other assessments, is a significant consideration if these methods are to be robust for clinical studies. In the current study, the results were assessed in comparison to prior knowledge of disease atrophy patterns and manual hippocampal volumetry in patient groups. Finally, fiducial markers were placed in a subset of subjects so as to directly compare the method to the standard unified segmentation and DARTEL methods.

MATERIALS AND METHODS

All algorithms presented in this section were written in Matlab7, and run on a Dual Xeon 3.2 GHz Intel X86 64 bit processor with 4GB RAM running GNU Debian Linux version 3.1, except where otherwise stated. The code of the fluid registration algorithm presented in this paper can be found in http://www.uc.pt/en/fmuc/ibili/Archives/Articles/JPereira/MiMe.

VISCOUS FLUID ALGORITHM

A viscous fluid algorithm was implemented in order to register the gray matter probability maps generated by SPM8 (http://www.fil.ion.ucl.ac.uk/spm/software/spm8/). Viscous fluid registration assumes a subject's brain *S* to behave as a viscous fluid when being registered to a target space *T*, with each point of the subject scan being deformed by the action of an external driving force field **F**. This force field is cancelled out at equilibrium by the internal forces of the fluid body, as described by the Navier-Stokes equation:

$$\mu\nabla^2\mathbf{v}(\mathbf{x},\ t) + (\mu+\lambda)\nabla(\nabla\cdot\mathbf{v}(\mathbf{x},\ t)) + \mathbf{F}(\mathbf{x},\mathbf{u}(\mathbf{x},t)) = 0 \quad (1)$$

with:

$$\mathbf{v}(\mathbf{x},t) = \frac{d\mathbf{u}(\mathbf{x},t)}{dt} \quad (2)$$

In Equation 1, $\mathbf{F}(\mathbf{x},\mathbf{u}(\mathbf{x},t))$ is the external force acting on the body deformed by the displacement field $\mathbf{u}(\mathbf{x},t)$ at location $\mathbf{x}$ at time t, ∇ is the gradient operator, ∇^2 is the Laplacian operator, and μ and λ are the viscosity constants. From this point on, dependencies will be dropped for the sake of simplicity [e.g., $\mathbf{v}(\mathbf{x},t)$ will be written as $\mathbf{v}$]. For the external forces calculation, a simple difference metric was used, based on the difference between the target and the deformed subject, multiplied by the gradient of the latter (Christensen et al., 1996).

As a linear differential equation, and using finite differences to discretize it (Press et al., 1992), Equation 1 can be written as:

$$\mathbf{L}\mathbf{v} = \mathrm{F} \quad (3)$$

where **L** is a linear operator, **v** is the velocity field and **F** is the external force field. This system can be either explicitly solved or a solution can be estimated using approximations to the linear operator **L**.

The explicit solution requires the use of the successive over-relaxation (SOR) method (Press et al., 1992; Wollny and Kruggel, 2002), which may be too time consuming. One possibility is to speed it up by using adaptive updates (SOR with adaptative updates, SORA) (Wollny and Kruggel, 2002). Another option is to approximate the linear operator **L** with an adequate convolution kernel **K**. As a consequence, the velocity response to each individual force vector can be estimated by its convolution with **K**. It is known that **K** can be a Gaussian filter (Thirion, 1998). This is a simplistic solution that has been shown to cause a decrease in registration quality (Gramkow and Bro-Nielsen, 1997). Another approximation, based on the eigenfunctions of **L**, can be used to yield more accurate results through a "viscous kernel" (Bro-Nielsen and Gramkow, 1996; Gramkow and Bro-Nielsen, 1997). We assessed all three approaches in this paper.

An Eulerian frame of reference describes the non-linear warp field variables through fixed positions **x** associated with time dependent displacement vectors $\mathbf{u}(\mathbf{x},t)$ such that the deformed position at time t is described as $\mathbf{x}-\mathbf{u}(\mathbf{x},t)$ (Christensen et al., 1996). The material derivative d/dt provides the instantaneous rate of change a point **x** of the grid observes at time t. A particle of the viscous body flowing through position **x** at that time will have a velocity **v** described by:

$$\mathbf{v} = \frac{d\mathbf{u}}{dt} = \frac{\partial\mathbf{u}}{\partial t} + \sum_{i=1}^{3} v_i\frac{\partial\mathbf{u}}{\partial x_i} \Leftrightarrow \frac{\partial\mathbf{u}}{\partial t} = \mathbf{R} = \mathbf{v} - \sum_{i=1}^{3} v_i\frac{\partial\mathbf{u}}{\partial x_i} \quad (4)$$

where $\mathbf{v} = (v_1, v_2, v_3)$ and $\mathbf{x} = (x_1, x_2, x_3)$.

The sum element in Equation 4 accounts for the deformation applied on the body and is zero when the body and the reference grid match. As a consequence, the partial derivative of the deformation **u** with respect to time yields a perturbation field **R** that is used to update the warping. The deformation field **u** is updated

for iteration $k+1$ of the registration algorithm by $\mathbf{R}$ such that:

$$\mathbf{u}^{(k+1)} = \mathbf{u}^{(k)} + \Delta\mathbf{u}^{(k)} = \mathbf{u}^{(k)} + \mathbf{R}^{(k)} \cdot \boldsymbol{\Delta} T^{(k)} \quad (5)$$

where $\Delta T^{(k)}$ is an iteration dependent time step, thus performing an explicit Euler integration of the perturbation vectors, which in themselves form a velocity field. The choice of time step will depend on the maximum value of the perturbation field, $\|\mathbf{R}^{(k)}\|_{\max}$. In the current work, $\Delta T^{(k)}$ was chosen such that a maximum displacement value m was enforced for each iteration (D'Agostino et al., 2003):

$$\Delta T^{(k)} = \frac{m}{\| \mathbf{R}^{(k)} \|_{\max}} \quad (6)$$

B. TOPOLOGY PRESERVATION

The determinant of the Jacobian of the deformation field must at all times be positive in order to ensure that topology is preserved (Christensen et al., 1996). This is ensured by regridding the deformation field every time this determinant crosses a certain threshold. Details of how this is done can be found in the supplementary material.

VISCOUS FLUID ASSESSMENT

The viscous fluid registration method was used to register gray matter probability maps in the context of VBM analyses of clinical cohorts. The first set of analyses was performed using groups of healthy controls ($n = 18$), Alzheimer's disease (AD) ($n = 19$), semantic dementia (SD) ($n = 10$) and behavioral variant frontotemporal dementia subjects (bvFTD) ($n = 8$). Subjects in each of the disease groups were diagnosed according to standard criteria (McKhann et al., 1984; Neary et al., 1998). These subjects made up Set A. This diverse set of atrophy profiles—AD, SD, and bvFTD—allowed for a thorough assessment of the proposed viscous fluid method in contrast to DARTEL and a standard SPM method. Demographic information about these groups can be found in the supplementary material (**Table S1**). Hippocampal volumes had been measured on the AD and control cohorts of Set A for a previous study (Pengas et al., 2010), and are presented in **Table 1**.

In order to not confine the assessment to a set of scans sharing the same acquisition parameters, another set of scans (designated Set B) was also used. Set B comprised controls ($n = 21$), AD subjects ($n = 16$), SD subjects ($n = 10$), and $n = 17$ patients diagnosed with mild cognitive impairment (MCI). The demographic details of these groups are listed in the supplementary material (**Table S2**). Hippocampal volumes were measured for all cohorts of Set B and are presented in **Table 2**. Details of how these volumes were obtained can be found in the supplementary material.

Set A was acquired with a 1.5 T GE Signa MRI scanner (GE Medical Systems, Milwaukee, WI). Volumetric T_1-weighted images were coronally acquired using SPGR (pixel dimensions $0.86 \times 0.86\,\text{mm}^2$, slice thickness 1.5 or 1.8 mm). Set B was acquired on a Siemens Trio 3T system (Siemens Medical Systems, Erlangen, Germany) using a 3D MPRAGE pulse sequence for the acquisition of volumetric T_1-weighted images with 144 slices, 192×192 matrix dimensions and $1.25\,\text{mm}^3$ voxel size. Scans were preprocessed according to a previously described pipeline (Acosta-Cabronero et al., 2008) (see supplementary material).

All scans were registered and segmented using the unified segmentation model provided in SPM8 (Ashburner and Friston, 2005). Probability maps of GM, WM, and CSF were also obtained in native space from all subjects for automated total intracranial volume (TIV) estimation (Pengas et al., 2008).

Subjects were also processed with the DARTEL algorithm, designated $\text{DARTEL}_{\text{pre}}$ when used with preprocessed scans, using default parameters and modulated gray matter probability maps. The output probability maps of the DARTEL algorithm were used in all subsequent analyses without any further processing.

VISCOUS FLUID REGISTRATION

Heuristic tests suggested that the eigenfunction-based kernel approximation was faster than SORA, while providing better results than the gaussian kernel approximation. As such, this was the method of choice in this paper. The others methods, however, presented similar results, which will not be discussed herein. All gray matter probability maps, normalized and resliced to an isotropic resolution of $2\,\text{mm}^3$ were registered with the viscous fluid method using the eigenfunction-based approximation to the linear operator to solve the differential equation. This viscous fluid method will be named "Fluid" from this point on.

For all sets of scans, a fixed random gray matter probability map from the control cohort was used as the target to which

Table 1 | Hippocampal volumes for subjects used in the AD VBM study of Set A, normalized to the mean total intracraneal volume (TIV) of the control cohort.

	Right hippocampus volume (mm^3)	Left hippocampus volume (mm^3)
Controls	1667 ± 301.0	1574 ± 214.4
AD	1399 ± 294.3 (−16.1%)	1270 ± 369.0 (−19.3%)

Values presented are mean ± standard deviation. Average percentage volume reduction relative to controls is shown in brackets. Values for the AD subjects are significantly lower than controls ($p < 0.05$, one-tail t-test). TIV was not statistically different between cohorts (not shown).

Table 2 | Hippocampal volumes for Controls, as well as for AD and MCI subjects in Set B, normalized to the mean TIV of the control cohort.

	Right hippocampus volume (mm^3)	Left hippocampus volume (mm^3)
Controls	1286 ± 157.5	1206 ± 209.6
AD	986 ± 192.9 (−23.4%)	886 ± 166.2 (−26.6%)
MCI	1037 ± 124.4 (−19.4%)	1008 ± 101.3 (−16.4%)

Values presented are mean ± standard deviation. Average percentage volume reduction is shown in brackets. Values are significantly lower than controls in all patient cohorts ($p < 0.05$ one-tail t-test). TIV was not statistically different between cohorts (not shown).

all other probability maps were registered. Given that these gray matter probability maps are already registered to a template, no further linear registration was performed.

VBM ANALYSES

A two-group *t*-test comparison was made between each diseased cohort and the relevant control group (i.e., with the same acquisition parameters). The control target was also included in the control group for the statistical analyses.

A relative threshold mask of 0.2 was used for all studies, except where otherwise stated. Scans were smoothed with an 8 mm full width half maximum (FWHM) Gaussian kernel. All analyses were also performed with 6 and 10 mm FWHM kernels, but as results were very similar to those obtained with the 8 mm kernel these are not shown or discussed. All tests were performed with total intracraneal volume (TIV) as a nuisance covariate.

The analyses of the scans of Set A included both gray matter probability maps from raw (not preprocessed) volumes and preprocessed volumes. Set B was only analysed using preprocessed scans. All probability maps were modulated by the Jacobian determinant of the non-linear viscous transformation. The modulation step was required for consistency with the original probability maps; moreover, the fine deformation fields result in determinant values that contain important information about local volume changes in the brain. All analyses had a statistical threshold of $p_{\text{FWE corrected}} = 0.05$, unless the resulting glass brains were blank (or showed only noise), in which case the threshold of $p_{\text{uncorrected}} = 0.001$ was used. The extent threshold k was set at 0 for all analyses. No correction was made for the differing initial voxel dimensions in Set A as this was a systematic error introduced in all studies and can be discounted when comparing the results (Pereira et al., 2008). Results of DARTEL, $\text{DARTEL}_{\text{pre}}$, Fluid and $\text{Fluid}_{\text{pre}}$ were analysed in their own template space.

REGISTRATION ASSESSMENT

Registration quality was assessed by comparing the results of the viscous fluid re-registration analyses with those of SPM8's unified segmentation and DARTEL.

A quantitative analysis of the registration performance was also performed using a subgroup of Set A that had fiducial points placed on the original scans as part of a previous study (Pereira et al., 2010). A set of 20 locations were chosen for fiducial marker placement. The consistency of location for each fiducial marker cluster was analysed with three metrics–the degree of dispersion error after warping in the direction of greatest location uncertainty (λ_1), and the extent to which dispersion was distributed along a given plane (R_1). The first metric (λ_1) is similar to a standard deviation of the registration error on a specific location—ideally, it should be zero. The second metric (R_1) is a ratio between the amount of registration misalignment in the main error direction and the total sum of errors in all directions—it complements the amount of error by providing information on the anisotropy of that error, i.e., if the misalignment has a preferential direction (anisotropic) or if it is randomly distributed in space (isotropic). The resulting λ_1 and R_1 values of the fiducial clusters from Fluid and $\text{Fluid}_{\text{pre}}$ were then compared with the corresponding results from SPM, SPM_{pre}, DARTEL, and $\text{DARTEL}_{\text{pre}}$. Further details of this method and results can be found in the supplementary material.

RESULTS

VBM RESULTS

The VBM results for Set A are presented in **Figures 1–3**, and the results for Set B are in **Figures 4–6**.

It was observed that VBMs performed with the Fluid registration algorithms showed greater sensitivity than both SPM and DARTEL. This effect was especially evident for mild atrophy scenarios, namely for the AD cohorts. In these cases, hippocampal atrophy—known to be present from the manually measured hippocampi—in Fluid was more extensive than with SPM and (especially) SPM_{pre}, without the apparent cost of localization reduction visible in the DARTEL results. In fact, the DARTEL algorithm fared better in terms of eliminating apparent extraneous results in mild atrophy cases, but at the apparent cost of eliminating true positives, a problem previously described in detail (Pereira, 2010) and seen here in **Figure 1**, where the detection of hippocampal atrophy, in DARTEL without preprocessing, was less pronounced than with the other methods.

Compared to DARTEL, the results obtained with the Fluid algorithms retained greater anatomical detail, comparable to the detail obtained with both SPM methods. DARTEL destroys the anatomical detail of the results, especially in severely atrophic regions that appear as amorphous areas, as seen in the SD analyses shown in **Figures 2**, **6**.

ASSESSMENT OF FIDUCIAL POINTS

A detailed analysis of the fiducial study has been included in the supplementary material. The λ_1 values dispersion values for Fluid (both with and without preprocessed scans) remained comparable to those of all other methods for most cases. The Fluid results were very consistent with the other methods. Also as observed previously using SPM and DARTEL (Pereira et al., 2010), there was an interaction between brain pathology and registration difficulties shown across all metrics, with severe focal atrophy still presenting the greatest challenge.

DISCUSSION

The use of viscous fluid registration algorithms to re-register gray matter probability maps demonstrates potential for VBM analyses. Overall, the VBM results from the analysis of each cohort were consistent with prior knowledge of atrophy profiles. Fluid registration enhanced the sensitivity of VBM while retaining anatomical detail. There was evidence for improvement over both standard SPM and DARTEL in several analyses.

REGISTRATION ASSESSMENT

The quantitative assessment of Fluid registration when compared to both SPM and DARTEL (further details and results can be found in the supplementary material) showed that all methods were broadly comparable. Despite the good match between target and subject, the registration algorithms seemed to be limited by the inherent variability between subjects that eludes warping. The registration performance values were quite variable across brain regions, and a disease grouping interaction for all methods was visible. The quantitative analysis of fiducial metrics closely

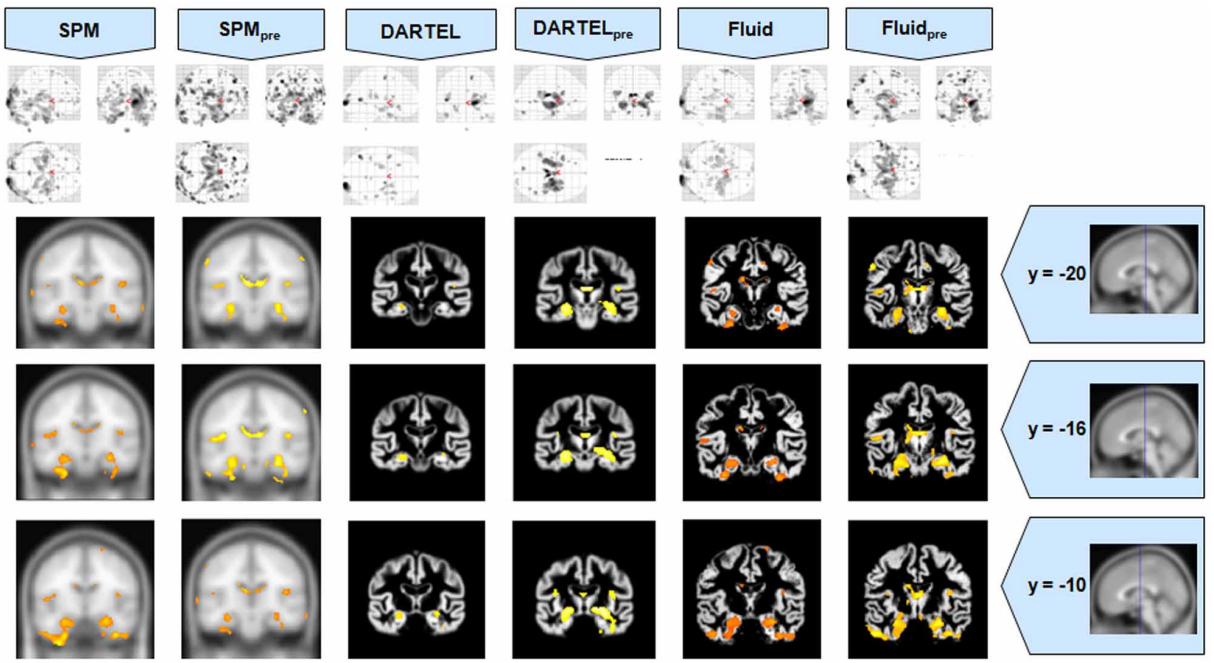

FIGURE 1 | VBM results for the AD cohort of Set A, with $p_{\text{uncorrected}} = 0.001$. The projection of the results on three coronal slices are presented, at y = −20, −16, and 0 mm, emphasizing the hippocampal region, expected to be atrophic in this pathology and visible in all methods. The entorhinal cortex, however, also likely atrophic, is lost in both DARTEL results. The MNI template was used for SPM and SPM_{pre}, and the bespoke target was used for both DARTEL results, as well as for both Fluid results. Due to the use of bespoke template spaces, the presented coronal slices are not strictly comparable across different methods.

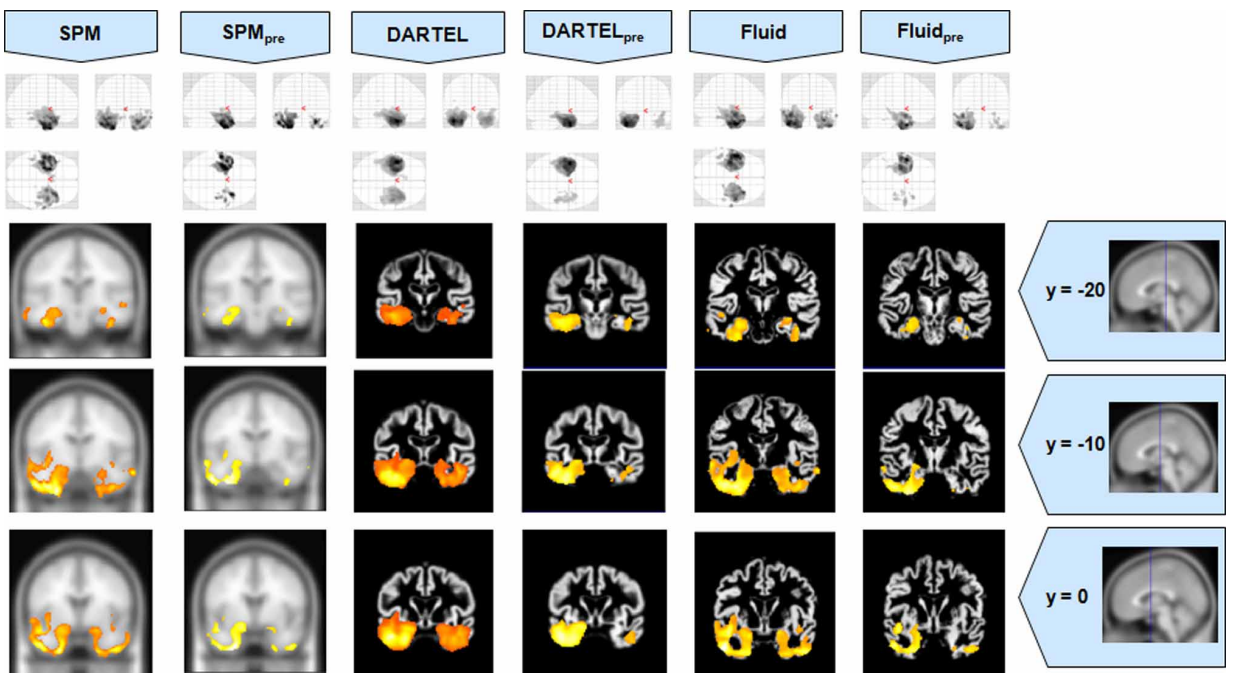

FIGURE 2 | VBM results for the SD cohort of Set A, with $p_{\text{FWEcorrected}} = 0.05$. The projection of the results on three coronal slices are presented, at y = −20, −10, and 0 mm, emphasizing the temporal lobes, expected to be atrophic in this pathology. The lack of anatomical detail in DARTEL is notable, especially around the mesial temporal lobe. This detail is regained with the Fluid methods, with an increase in sensitivity compared to the SPM methods. The MNI template was used for SPM and SPM_{pre}, and the bespoke target was used for both DARTEL results, as well as for both Fluid results. Due to the use of bespoke template spaces, the presented coronal slices are not strictly comparable across different methods.

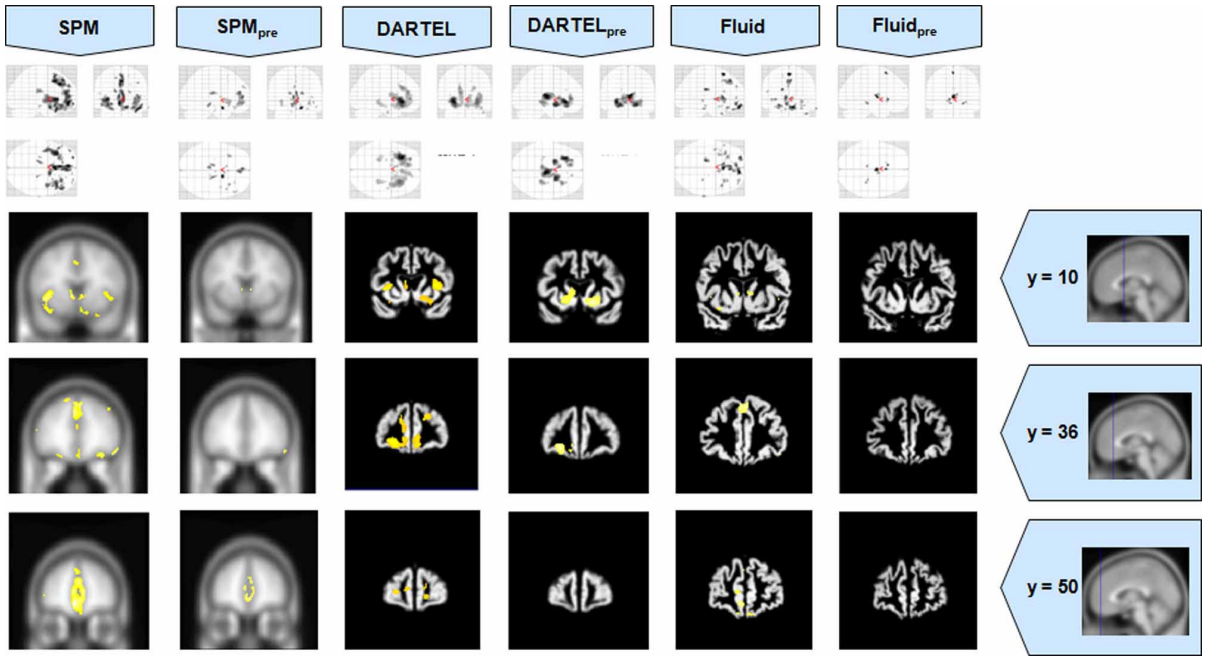

FIGURE 3 | VBM results for the bvFTD cohort of Set A, with $p_{FWEcorrected} = 0.05$. The projection of the results on three coronal slices are presented, at y = 10, 36, and 50 mm, emphasizing the frontal lobe, expected to be atrophic in this pathology. This was the only case where the use of Fluid methods did not provide tangible benefits; DARTEL was also not more informative than the SPM methods. The MNI template was used for SPM and SPM_{pre}, and the bespoke target was used for both DARTEL results, as well as for both Fluid results. Due to the use of bespoke template spaces, the presented coronal slices are not strictly comparable across different methods.

resembled the results for SPM5's unified segmentation that were reported previously (Pereira et al., 2010). This is not unexpected, as the viscous fluid registration was based on SPM8's registered probability maps (similar to SPM5's) and the algorithm was also limited to 15 iterations[1].

Importantly, the observation that the dispersion values of the fiducial markers were not significantly worsened by the Fluid methods suggesting that these registration algorithms are preserving the anatomical validity of the registration—in theory, there is a danger that geometric overfitting could lead to a loss of anatomical validity (i.e., that better fitting comes at the expense of moving anatomical structures). The quantitative results indicate that this did not occur.

VBM ANALYSES

All methods were able to identify the key abnormalities known from prior knowledge: hippocampal atrophy in AD and MCI groups (Galton et al., 2001; Du et al., 2004; Pennanen et al., 2004; Du et al., 2007); rostral temporal lobe atrophy in SD (Chan et al., 2001; Rosen et al., 2002; Williams et al., 2005; Nestor et al., 2006); and frontal atrophy in bvFTD (Rosen et al., 2002; Williams et al., 2005; Cardenas et al., 2007; Pereira et al., 2009). The preprocessed viscous registration results were, however, more concentrated on these areas of known atrophy in several of the analyses. This might suggest a reduction in false positives though it is important to highlight that, in the absence of ground-truth measurements for unexpected locations, this might also reflect lack of sensitivity to true, albeit unanticipated, abnormalities. On the other hand there was evidence to suggest that adding the viscous registration step offered superior results in detecting true positives and preserving anatomical detail, particularly in contrast to DARTEL. For instance, the AD analysis found fairly restricted hippocampal abnormalities in the temporal lobe using DARTEL. In contrast, the fluid registration method showed blobs extending into the adjacent temporal lobe (**Figure 1**). This result is far more consistent with previous manual volumetric studies of the entorhinal region (Du et al., 2004; Pennanen et al., 2004) and with knowledge of the spread of neuropathology in very early AD (Braak and Braak, 1991). It should be noted that SPM without DARTEL also detected change in this region. Regarding anatomical precision, the SD analysis also suggested superior performance with viscous registration over DARTEL. As seen in **Figures 2**, **6**, DARTEL identified the rostral temporal abnormality but the blobs were essentially amorphous. In contrast, the viscous method produced results that adhered to the gray matter and were maximal in the rostral inferior surface, again consistent with prior knowledge from manual volumetrics (Chan et al., 2001; Galton et al., 2001; Davies et al., 2004). The difficulties shown by DARTEL when analysing atrophic brains have also been made evident in a recent paper (Ashburner and Friston, 2011), where it is clear that the algorithm underperforms when large deformations are required.

[1] A more liberal convergence criterion was also tested, up to a maximum of 25 iterations, but the resulting VBM glass brains started to show false positives around the cerebellum. These results suggested that the chosen number of iterations was adequate.

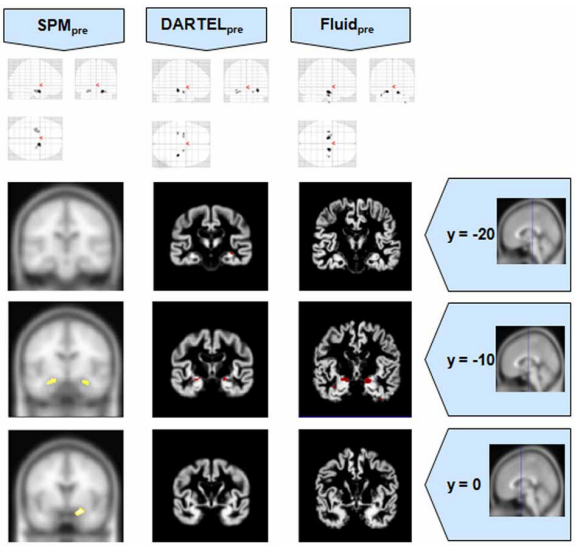

FIGURE 4 | VBM results for the MCI cohort of Set B, with $p_{FWEcorrected} = 0.05$. The projection of the results on three coronal slices are presented, at y = −20, −10, and 0 mm, emphasizing the hippocampal region, expected to be atrophic in this pathology. Whereas DARTEL detects the atrophy, the Fluid methods are also able to detect it with further anatomical detail. The loss of sensitivity with DARTEL is clear. The MNI template was used for SPM and SPM$_{pre}$, and the bespoke target was used for the DARTEL result, as well as for the Fluid result. Due to the use of bespoke template spaces, the presented coronal slices are not strictly comparable across different methods. A different colour scale was use for Fluid$_{pre}$ to highlight the detected areas.

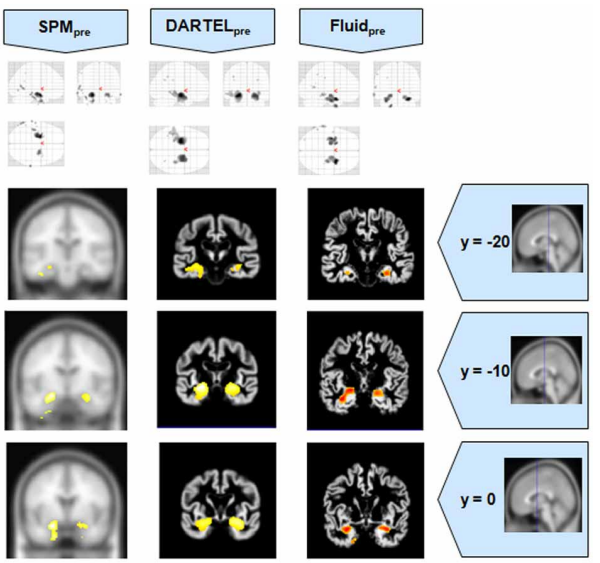

FIGURE 5 | VBM results for the AD cohort of Set B, with $p_{FWEcorrected} = 0.05$. The projection of the results on three coronal slices are presented, at y = −20, −10, and 0 mm, emphasizing the hippocampal region, expected to be atrophic in this pathology. As before, whereas DARTEL detects the atrophy, the Fluid methods are also able to detect it with further anatomical detail. The MNI template was used for SPM and SPM$_{pre}$, and the bespoke target was used for the DARTEL result, as well as for the Fluid result. Due to the use of bespoke template spaces, the presented coronal slices are not strictly comparable across different methods. A different color scale was use for Fluid$_{pre}$ to highlight the detected areas.

The loss of anatomical detail due to averaging of subjects with DARTEL is shown in **Figure 7**. Even though DARTEL iteratively builds the template in order to reduce differences between subjects and to create a sharp average, the effects of blurring were still present. The viscous fluid algorithms, in contrast, generate gray matter probability maps that are locally deformed in order to conform to precise anatomical reference structures, whereas the DARTEL probability map results are degraded, leading to loss of localization power and to VBM results that are smoother and seemingly amorphous (**Figures 2**, **6**). Moreover, DARTEL has more regularization constraints than the viscous registration method presented in this paper that prevent it from creating the very local warps that a viscous fluid method can generate. This creates smooth diffeomorphic deformation fields but leads to limited local warping capabilities.

It must be acknowledged, nevertheless, that the use of a single subject template has some potential disadvantages, namely biasing the registration result for more similar brains. The nature of the gray matter probability maps, however, bypasses some of those limitations as the registered subjects already share a space very similar to the template. To address this concern, the Fluid algorithms were also tested by using as registration target the average of all subjects in each analysis, but results were essentially the same as the ones presented. Even if the templates were similar, the Fluid methods are more lightly regularized and are able to produce fields that can flow more freely than with DARTEL. It must be also noted that the use of a bespoke template in DARTEL, based on the iterative average of the registered gray matter probability maps, is prone to errors if at least one of the probability maps is poorly segmented. Heuristic tests have shown that such an approach may lead to false positives and to the propagation of segmentation errors. This issue will be addressed in future work.

It also important to highlight that while fluid registration yielded results that were more consistent with prior knowledge and/or manual volumetry (AD and MCI) and greater preservation of anatomical detail (SD), the bvFTD analyses did not show a benefit for this technique. All three approaches showed changes in the frontal lobe as would be expected from prior knowledge, though they were least extensive with fluid registration. The frontal lobes are large, and this results suggests that in the face of a large spatial extent of atrophy, the registration step is less important. Interestingly, in this group, it was not DARTEL but rather the default SPM analysis that yielded the most significant and extensive frontal abnormalities.

Finally, in common with many previous clinical VBM studies, this work made use of low numbers of subjects per cohort in order to simulate the real world application as closely as possible. We speculate that low numbers of subjects hinder the quality of a bespoke template—this would explain why DARTEL underperformed so often in the scenarios presented in this article. Moreover, a future application of the work presented in this paper is to make single subject VBM-like analyses possible in a clinical

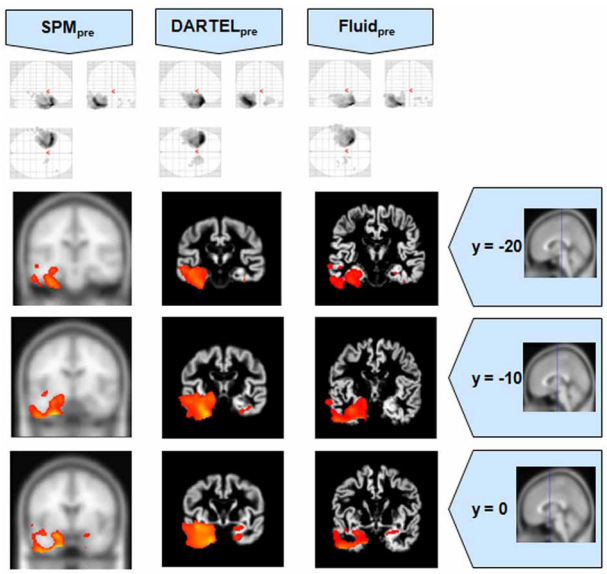

FIGURE 6 | VBM results for the SD cohort of Set B, with $p_{FWEcorrected} = 0.05$. The projection of the results on three coronal slices are presented, at y = −20, −10, and 0 mm, emphasizing the temporal lobes, expected to be atrophic in this pathology. The gain in sensitivity with the Fluid methods compared to the SPM approaches is clear; the gain in anatomical detail compared to DARTEL is again notable. The MNI template was used for SPM and SPM$_{pre}$, and the bespoke target was used for the DARTEL result, as well as for the Fluid result. Due to the use of bespoke template spaces, the presented coronal slices are not strictly comparable across different methods.

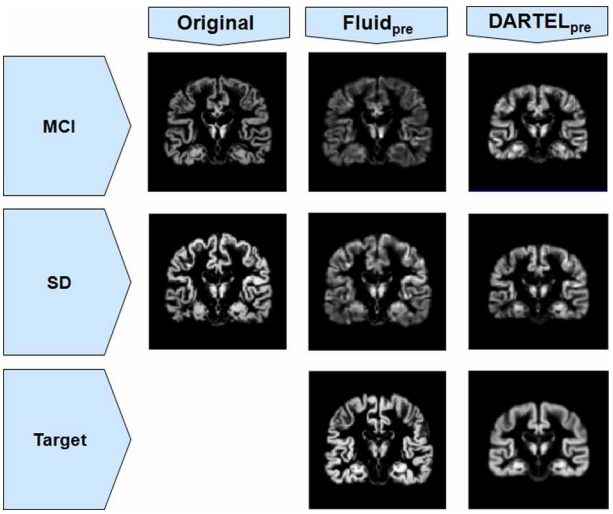

FIGURE 7 | Gray matter segments before and after registration to a target, for both MCI and SD cohorts from Set B, using both Fluid$_{pre}$ and DARTEL$_{pre}$. Notice the smoothness of DARTEL$_{pre}$'s target (for the *SD* population only, as an example) compared to the target used in Fluid$_{pre}$.

context. Understanding the practical limitations of the available methods when using low numbers of subjects is therefore fundamental to this aim.

CONCLUSIONS

The use of a viscous fluid registration algorithm to re-register the gray matter probability maps produced by the unified segmentation proved to be a useful tool, especially in terms of the qualitative assessment of VBM results. This Fluid registration method was able to provide detailed results with probability maps generated from both unpreprocessed and (especially) preprocessed scans; this was true for both a very focal atrophic cohort such as SD and in milder, more diffuse, atrophy such as AD and MCI. When compared to alternatives, especially DARTEL, which also uses a comparable methodology, the VBM outputs were more contiguous and anatomically localized with the Fluid methods. Additionally, these results suggest that most high-degree of freedom registration algorithm, with very little regularization, may be useful to re-register the probability maps in order to improve VBM results.

ACKNOWLEDGMENTS

Joao M. S. Pereira would like to acknowledge the support of his funding body, Fundação para a Ciência e a Tecnologia, Portugal. George Pengas and Julio Acosta-Cabronero were funded by the Alzheimer's Research Trust (UK). The work also received support from an MRC grant to Peter J. Nestor and from the NIHR Cambridge Biomedical Research Centre.

SUPPLEMENTARY MATERIAL

The Supplementary Material for this article can be found online at: http://www.frontiersin.org/Aging_Neuroscience/10.3389/fnagi.2013.00030/abstract

REFERENCES

Acosta-Cabronero, J., Williams, G. B., Pereira, J. M. S., Pengas, G., and Nestor, P. J. (2008). The impact of skull-stripping and radio-frequency bias correction on grey-matter segmentation for voxel-based morphometry. *Neuroimage* 39, 1654–1665. doi: 10.1016/j.neuroimage.2007.10.051

Ashburner, J. (2007). A fast diffeomorphic image registration algorithm. *Neuroimage* 38, 95–113. doi: 10.1016/j.neuroimage.2007.07.007

Ashburner, J., and Friston, K. J. (2011). Diffeomorphic registration using geodesic shooting and Gauss-Newton optimisation. *Neuroimage* 55, 954–967. doi: 10.1016/j.neuroimage.2010.12.049

Ashburner, J., and Friston, K. J. (1999). Nonlinear spatial normalisation using basis functions. *Hum. Brain Mapp.* 7, 254–266.

Ashburner, J., and Friston, K. J. (2005). Unified segmentation. *Neuroimage* 15, 839–851. doi: 10.1016/j.neuroimage.2005.02.018

Braak, H., and Braak, E. (1991). Neuropathological stageing of Alzheimer-related changes. *Acta Neuropathol.* 82, 239–259. doi: 10.1007/BF00308809

Bro-Nielsen, M., and Gramkow, C. (1996). "Fast fluid registration of medical images," in *Proceedings Visualization in Biomedical Computing (VBC'96)*, Vol. 1131, (Hamburg: Springer Lecture Notes in Computer Science), 267–276.

Cardenas, V. A., Boxer, A. L., Chao, L. L., Gorno-Tempini, M. L., Miller, B. L., Weiner, M. W., et al. (2007). Deformation-based morphometry reveals brain atrophy in frontotemporal dementia. *Arch. Neurol.* 64, 873–877. doi: 10.1001/archneur.64.6.873

Chan, D., Fox, N. C., Scahill, R. I., Crum, W. R., Whitwell, J. L., Leschziner, G., et al. (2001). Patterns of temporal lobe atrophy in semantic dementia and Alzheimer's disease. *Ann. Neurol.* 49, 433–442. doi: 10.1002/ana.92

Christensen, G. E., Rabbitt, R. D., and Miller, M. I. (1996). Deformable templates using large deformation kinematics. *IEEE Trans. Image Process.* 5, 1435–1447. doi: 10.1109/83.536892

D'Agostino, E., Maes, F., Vandermeulen, D., and Suetens, P. (2003). A viscous fluid model for multimodal non-rigid image registration using mutual information. *Med. Image Anal.* 7, 565–575. doi: 10.1016/S1361-8415(03)00039-2

Davies, R. R., Graham, K. S., Xuereb, J. H., Williams, G. B., and Hodges, J. R. (2004). The human perirhinal cortex and semantic memory. *Eur. J. Neurosci.* 20, 2441–2446. doi: 10.1111/j.1460-9568.2004.03710.x

Du, A.-T., Schuff, N., Kramer, J. H., Rosen, H. J., Gorno-Tempini, M. L., Rankin, K., et al. (2007). Different regional patterns of cortical thinning in Alzheimer's disease and frontotemporal dementia. *Brain* 130, 1159–1166. doi: 10.1093/brain/awm016

Du, A. T., Schuff, N., Kramer, J. H., Ganzer, S., Zhu, X. P., Jagust, W. J., et al. (2004). Higher atrophy rate of entorhinal cortex than hippocampus in AD. *Neurology* 62, 422–427. doi: 10.1212/01.WNL.0000106462.72282.90

Galton, C. J., Patterson, K., Graham, K., Lambon-Ralph, M. A., Williams, G., Antoun, N., et al. (2001). Differing patterns of temporal atrophy in Alzheimer's disease and semantic dementia. *Neurology* 57, 216–225. doi: 10.1212/WNL.57.2.216

Gramkow, C., and Bro-Nielsen, M. (1997). "Comparison of three filters in the solution of the navier-stokes equation in registration," in *Scandinavian Conference on Image Analysis*, (Lappenranta), 795–802.

McKhann, G., Drachman, D., Folstein, M., Katzman, R., Price, D., and Stadlan, E. M. (1984). Clinical diagnosis of Alzheimer's disease: report of the NINCDS-ADRDA Work Group under the auspices of Department of Health and Human Services Task Force on Alzheimer's Disease. *Neurology* 34, 939–944. doi: 10.1212/WNL.34.7.939

Neary, D., Snowden, J. S., Gustafson, L., Passant, U., Stuss, D., Black, S., et al. (1998). Frontotemporal lobar degeneration: a consensus on clinical diagnostic criteria. *Neurology* 51, 1546–1554. doi: 10.1212/WNL.51.6.1546

Nestor, P. J., Fryer, T. D., and Hodges, J. (2006). Declarative memory impairments in Alzheimer's disease and semantic dementia. *Neuroimage* 30, 1010–1020. doi: 10.1016/j.neuroimage.2005.10.008

Pengas, G., Hodges, J. R., Watson, P., and Nestor, P. J. (2010). Focal posterior cingulate atrophy in incipient Alzheimer's disease. *Neurobiol. Aging* 31, 25–33. doi: 10.1016/j.neurobiolaging.2008.03.014

Pengas, G., Pereira, J. M. S., Williams, G. B., and Nestor, P. J. (2008). Comparative reliability of total intracranial volume estimation methods and the influence of atrophy in a longitudinal semantic dementia cohort. *J. Neuroimag.* 19, 37–46. doi: 10.1111/j.1552-6569.2008.00246.x

Pennanen, C., Kivipelto, M., Tuomainen, S., Hartikainen, P., Hanninen, T., Laakso, M. P., et al. (2004). Hippocampus and entorhinal cortex in mild cognitive impairment and early AD. *Neurobiol. Aging* 25, 303–310. doi: 10.1016/S0197-4580(03)00084-8

Pereira, J. M., Nestor, P. J., and Williams, G. B. (2008). Impact of inconsistent resolution on VBM studies. *Neuroimage* 40, 1711–1717. doi: 10.1016/j.neuroimage.2008.01.031

Pereira, J. M. S. (2010). *Characterisation, Optimisation and Application of Voxel Based Morphometry in MRI Studies of Dementia.* Ph.D. thesis. Cambridge: University of Cambridge.

Pereira, J. M. S., Williams, G. B., Acosta-Cabronero, J., Pengas, G., Spillantini, M. G., Xuereb, J. H., et al. (2009). Atrophy patterns in histologic vs clinical groupings of frontotemporal lobar degeneration. *Neurology* 72, 1653–1660. doi: 10.1212/WNL.0b013e3181a55fa2

Pereira, J. M. S., Xiong, L., Acosta-Cabronero, J., Pengas, G., Williams, G. B., and Nestor, P. J. (2010). Registration accuracy for VBM studies varies according to region and degenerative disease grouping. *Neuroimage* 49, 2205–2215. doi: 10.1016/j.neuroimage.2009.10.068

Press, W. H., Teukolsky, S. A., Vetterling, W. T., and Flannery, B. P. (1992). "Numerical recipes," in *C: the Art of Scientific Computing, 2nd Edn*. Cambridge: Cambridge University Press.

Ridgway, G. R., Henley, S. M. D., Rohrer, J. D., Scahill, R. I., Warren, J. D., and Fox, N. C. (2008). Ten simple rules for reporting voxel-based morphometry studies. *Neuroimage* 40, 1429–1435. doi: 10.1016/j.neuroimage.2008.01.003

Rosen, H., Gorno-Tempini, M., Goldman, W., Perry, R., Schuff, N., Weiner, M., et al. (2002). Patterns of brain atrophy in frontotemporal dementia and semantic dementia. *Neurology* 58, 198–208. doi: 10.1212/WNL.58.2.198

Thirion, J.-P. (1998). Image matching as a diffusion process: an analogy with Maxwell's Demons. *Med. Image Anal.* 2, 243–260. doi: 10.1016/S1361-8415(98)80022-4

Williams, G. B., Nestor, P. J., and Hodges, J. R. (2005). Neural correlates of semantic and behavioural deficits in frontotemporal dementia. *Neuroimage* 24, 1042–1051. doi: 10.1016/j.neuroimage.2004.10.023

Wollny, G., and Kruggel, F. (2002). Computational cost of nonrigid registration algorithms based on fluid dynamics. *IEEE Trans. Med. Imag.* 21, 946–952. doi: 10.1109/TMI.2002.803113

Yassa, M. A., and Stark, C. E. L. (2009). A quantitative evaluation of cross-participant registration techniques for MRI studies of the medial temporal lobe. *Neuroimage* 44, 319–327. doi: 10.1016/j.neuroimage.2008.09.016

Conflict of Interest Statement: The authors declare that the research was conducted in the absence of any commercial or financial relationships that could be construed as a potential conflict of interest.

Received: 04 April 2013; accepted: 21 June 2013; published online: 15 July 2013.

*Citation: Pereira JMS, Acosta-Cabronero J, Pengas G, Xiong L, Nestor PJ and Williams GB (2013) VBM with viscous fluid registration of gray matter segments in SPM. Front. Aging Neurosci. **5**:30. doi: 10.3389/fnagi.2013.00030*

frontiers in
AGING NEUROSCIENCE

METHODS ARTICLE
published: 24 March 2014
doi: 10.3389/fnagi.2014.00023

MTA index: a simple 2D-method for assessing atrophy of the medial temporal lobe using clinically available neuroimaging

Manuel Menéndez-González[1,2,3]*, Alfonso López-Muñiz[2,3], José A. Vega[2], José M. Salas-Pacheco[4] and Oscar Arias-Carrión[5,6]*

[1] Unidad de Neurología, Hospital Álvarez-Buylla, Mieres, Spain
[2] Departamento de Morfología y Biología Celular, Universidad de Oviedo, Oviedo, Spain
[3] Instituto de Neurociencias, Universidad de Oviedo, Oviedo, Spain
[4] Instituto de Investigación Científica, Universidad Juárez del Estado de Durango, Durango, México
[5] Unidad de Trastornos del Movimiento y Sueño (TMS), Hospital General Dr. Manuel Gea González/UNAM, México DF, Mexico
[6] Unidad de Trastornos del Movimiento y Sueño (TMS), Hospital General Ajusco Medio, México DF, Mexico

Edited by:
Gemma Casadesus, Case Western Reserve University, USA

Reviewed by:
Andrea Bozoki, Michigan State University, USA
Eugenia Rota, Ospedale Guglielmo da Saliceto di Piacenza, Italy

***Correspondence:**
Manuel Menéndez-González, Unidad de Neurología, Hospital Álvarez-Buylla, CP 33616, Mieres, Asturias Spain
e-mail: manuelmenendezgonzalez@gmail.com;
Oscar Arias-Carrión, Unidad de Trastornos del Movimiento y Sueno (TMS), Hospital General Dr. Manuel Gea González, Calzada de Tlalpan 4800, Delegación Tlalpan, 14080 México DF, México
e-mail: arias@ciencias.unam.mx

Background and purpose: Despite a strong correlation to severity of AD pathology, the measurement of medial temporal lobe atrophy (MTA) is not being widely used in daily clinical practice as a criterion in the diagnosis of prodromal and probable AD. This is mainly because the methods available to date are sophisticated and difficult to implement for routine use in most hospitals—volumetric methods—or lack objectivity—visual rating scales. In this pilot study we aim to describe a new, simple and objective method for measuring the rate of MTA in relation to the global atrophy using clinically available neuroimaging and describe the rationale behind this method.

Description: This method consists of calculating a ratio with the area of 3 regions traced manually on one single coronal MRI slide at the level of the interpeduncular fossa: (1) the medial temporal lobe (MTL) region (A); (2) the parenchima within the medial temporal region, that includes the hippocampus and the parahippocampal gyrus—the fimbria taenia and plexus choroideus are excluded—(B); and (3) the body of the ipsilateral lateral ventricle (C). Therefrom we can compute the ratio "Medial Temporal Atrophy index" at both sides as follows: $MTAi = (A - B) \times 10/C$.

Conclusions: The MTAi is a simple 2D-method for measuring the relative extent of atrophy in the MTL in relation to the global brain atrophy. This method can be useful for a more accurate diagnosis of AD in routine clinical practice. Further studies are needed to assess the usefulness of MTAi in the diagnosis of early AD, in tracking the progression of AD and in the differential diagnosis of AD with other dementias.

Keywords: medial temporal lobe atrophy, biomarker, Alzheimer, mild cognitive impairment, MRI, neuroimaging, diagnosis

BACKGROUND

Alzheimer's disease's (AD) pathology accumulates for years and may be even decades before it is typically diagnosed (Morris et al., 1996). Sensitive biomarker techniques may be able to pick up signs of neurodegeneration presymptomatically. Recently proposed criteria for research purposes for prodromal AD (Sperling et al., 2011), mild cognitive impairment (MCI) due to AD (Albert et al., 2011), and probable AD dementia (McKhann et al., 2011) incorporate evidence of AD pathology including molecular changes and brain structure and function as supportive biomarkers. MRI-based biomarkers are among the supportive evidence for a diagnosis of early AD and MCI due to AD. By focusing on cortical regions known to be affected in AD dementia, subtle but reliable atrophy is identifiable in asymptomatic individuals nearly a decade before dementia, making this measure a potentially important imaging biomarker of early diagnosis (Dickerson et al., 2011). Volume losses in the medial temporal lobe (MTL) region—composed by the hippocampus and the parahippocampal gyrus—and posterior cingulated and orbitofrontal regions have been observed in AD and confirmed in many studies (Kesslak et al., 1991; Parnetti et al., 1996; Smith and Jobst, 1996; de Leon et al., 1997; Jack et al., 1997; Nagy et al., 1999; Bouwman et al., 2007; Eckerstrom et al., 2010; Jack et al., 2010; Zhang et al., 2010; Apostolova et al., 2012; Ewers et al., 2012; Leung et al., 2013; Heister et al.). This leads to a predictable pattern of brain atrophy that could be very useful to improve diagnosis and follow up and help making a better assessment of the neuroprotective effects of a therapy. The quantification of atrophy in the MTL (MTA) has been attempted using several different neuroimaging measurements, including rating scales, linear measurements, and volumetric methods.

Visual assessment rating scales are quick, and can be performed on large numbers of scans in a clinical setting, the disadvantage being that there is a loss of accuracy compared

with objective analysis and are subjected to interrater variability (Westman et al., 2011). Some studies found that visual rating assessment of the MTL gave similar prediction accuracy to multivariate classification and manual hippocampal volumes (Ringman et al., 2010; Duara et al., 2013) while others reported the visual rating assessment failed to detect patients at high risk, such as people carrying mutations of familial AD and also failed to detect progression over time (Ridha et al., 2007; Pereira et al., 2013). In addition, clinical, demographic, and genetic variables can influence the classification of MTA cut-off scores, leading to misdiagnosis in some cases. These variables, in addition to the differential sensitivity and specificity of each cut-off, should be carefully considered when performing visual MTA assessment (Scheltens et al., 1992).

Linear measures of brain regions are easy to take using clinically available neuroimaging. Some studies attempted to define sentinel changes that will allow the use of linear measurements of the hippocampus or the temporal horn to support clinical decision making. These studies have yielded variable results, with sensitivities ranging from 33 to 93% and specificity of approximately 95% (Dahlbeck et al., 1991; Erkinjuntti et al., 1993; Frisoni et al., 2002).

Volumetric analysis provides an accurate and detailed measure of a predetermined circumscribed area or region of interest. For AD, the most used structure is the whole hippocampus. Some indices comparing the extent of atrophy in the hippocampus with the whole brain atrophy are also being described (http://brainatrophyindices.blogspot.com). Manual volumetry is considered the gold standard but it has some drawbacks. First it requires training since the tracer must learn to delineate the hippocampus's boundaries and anterior- and posterior-limits. Then segmentation of the hippocampus takes approximately 20–30 min, depending on user experience (Soininen et al., 1994; Petrella et al., 2003), which limits routine clinical use. Some groups automated segmentation techniques and protocols for multi-atlas driven automatic segmentation of the hippocampus (Morra et al., 2008; Brewer et al., 2009; Kovacevic et al., 2009). Results of a study comparing manual and automated determination of hippocampal volumes in MCI and early AD indicated that these two methods derived highly correlated results with strong agreement (Shen et al., 2010). Albeit homogenization efforts are under development (Frisoni and Jack, 2011; Boccardi et al., 2013), the complexity and diversity of protocols used for volumetry keeps being a limitation today.

In summary, despite convenience and strong correlation to severity of AD pathology, MTA is not being used in daily clinical practice for diagnosing prodromal and probable AD yet, as it is in clinical trials and research studies. This is mainly because the methods already described lack accuracy (visual methods) or are not convenient enough to be routinely used by clinicians in busy departments (volumetric methods).

PURPOSE

In this report we aim to describe a new, objective and simple 2D-method for measuring atrophy of the MTL using clinically available neuroimaging. We also aim to explain the rationale behind this method. However, we do not seek to describe here the validity of this parameter for diagnosing AD since these researches are being conducted currently and results will be addressed in future publications.

PROTOCOL DESCRIPTION

This method consists of measuring the area of 3 brain regions on one single MRI slide and then use these data for calculating a simple ratio. First, we take the coronal slide at the level of the interpeduncular fossa on the TIR sequence. Then, regions are traced manually, simply using the pointer-rule tool of any software for visualizing DICOM images. As guidelines to draw structures and boundaries we followed the atlases by Mai et al. (1997) and Duvernoy (1998). The three areas are: (1) the MTL region (A), defined in a coronal brain slide as the four-sided space bordered in its inferior side by the tentorium cerebelli, in its medial side by the cerebral peduncles, in its upper side by the roof of the temporal horn of the lateral ventricle and in its lateral side by the collateral sulcus and a straight-line linking the collateral sulcus with the lateral edge of the temporal horn of the lateral ventricle; (2) the parenchima within the medial temporal region, that includes the hippocampus and the parahippocampal gyrus—the fimbria taenia and plexus choroideus are excluded—(B); and (3) the body of the ipsilateral lateral ventricle (C) (**Figure 1**). Therefrom, we can compute the ratio "Medial Temporal Atrophy index (MTAi)" at both sides as follows: $MTAi = (A - B) \times 10/C$. An example is shown in **Figure 2**.

If we have two MRI studies from different times (1 = first one, 2 = second one), we can also compute the yearly rate of MTA as follows: $yrMTA = (A2 - B2) - (A1 - B1) \times 120/(\#months\ between\ MRI\ studies)$ and the yearly rate of relative MTA as follows: $(yrMTAr) = (A2 - B2) - (A1 - B1) \times 120/(C2 - C1) \times (\#months\ between\ MRI\ studies)$.

EXPRESSING THE MEDIAL TEMPORAL ATROPHY INDEX

When we compute the MTAi we obtain 2 values, one for each hemisphere. In addition, it is also interesting to compute the median of these 2 values, and the index of asymmetry (IA). We determine the IA using formula $IA = (lMTAi - dMTAi)/(lMTAi + dMTAi) \times 100$. Small positive or negative IA values of magnitude less than $\sim \pm 3\%$ indicate that there is not a significant hemispheric asymmetry and the median MTAi can be used alone as a parameter of the global relative MTA. Higher IA values indicate significant hemispheric asymmetry and the median value should not be used alone since it is not a good representative value of the extent of relative MTA. Thus, the MTAi can be presented directly as the absolute right/left MTAi values or as the median MTAi with the IA (**Table 1**).

RATIONALE BEHIND THE MEDIAL TEMPORAL ATROPHY INDEX

The rationale behind this method is based on two premises: First, AD is a disease affecting the hippocampus, not a disease of the hippocampus. From a neuropathological point of view it is evident that that the characteristic pathological changes in AD begin outside the hippocampus, with development of neurofibrillary tangles in the transentorhinal and entorhinal cortex, spreading subsequently to the subiculum and CA1 regions of the

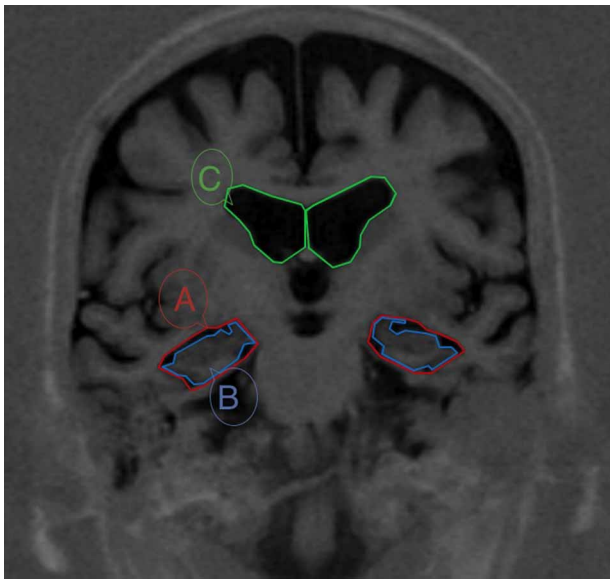

FIGURE 1 | MRI from a patient with MCI with boundaries of the three areas needed for calculating the Medial Temporal Atrophy index (MTAi). The section passes through the interpeduncular fosae. The three areas are: (1) the medial temporal lobe region **(A)**, defined in a coronal brain slide as the space bordered in its inferior side by the tentorium cerebelli, in its medial side by the cerebral peduncles, in its upper side by the roof of the temporal horn of the lateral ventricle and in its lateral side by the colateral sulcus and a straight-line linking the colateral sulcus with the lateral edge of the temporal horn of the lateral ventricle; (2) the parenchima within the medial temporal region, that includes the hippocampus and the parahippocampal girus **(B)**; and (3) the body of the ipsilateral lateral ventricle **(C)**.

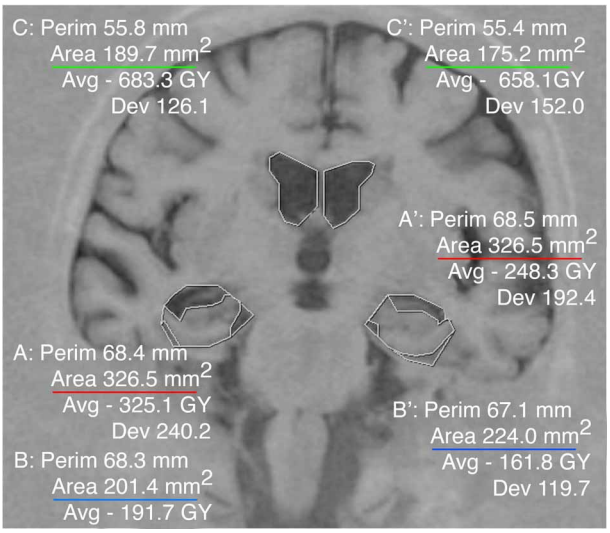

FIGURE 2 | Example of the Medial Temporal Atrophy index (MTAi) in a patient with mild AD. The three areas were traced manually on each hemisphere using the software for visualizing radiological images IMPAX. The data needed to compute the index are displayed automatically. We have underlined the different areas in colors as in **Figure 1**. The MTAi in the right hemisphere is: rMTAi = (326.5 − 201.4) ×10/189.7 = 6.59. The MTAi in the left hemisphere is: lMTAi = (326.5 − 224.0) ×10/175.2 = 5.85. Note how in spite of the coincidence of this case with exactly the same medial temporal region **(A and A')** in both hemispheres, the right MTAi is clearly higher than the left MTAi. Indeed when we calculate the Index of Asymmetry (IA), it is higher than 3: IA = (5, 85 − 6.59)/(5, 85 + 6.59) ×100 = −5, 15%.

Table 1 | Mean of the mean Medial Temporal Atrophy index (mMTAi) and Index of Asymmetry (IA) values in short series of patients with MCI (3), mild AD (3), moderate AD (3), severe AD (3), FTLD -not staged- (3), LBD -not staged- (3) and 5 healthy controls. Values are merely illustrative -not informative-.

	Mean mMTAi	Mean AI
Healthy control	2, 4	1, 8
MCI	3, 1	2, 4
Mild AD	4, 6	2, 6
Moderate AD	5, 2	2, 8
Severe AD	5, 8	3, 4
FTLD	3, 8	8, 2
DLB	2, 7	3, 7

hippocampus (Jack et al., 1992; Braak and Braak, 1985; Convit et al., 2000; Kerchner et al., 2010; Lim et al., 2012) and later to limbic, and ultimately to neocortical regions, such as the precuneus, middle frontal gyrus, and posterior cingulate gyrus. The severity of this atrophy, at least in the medial temporal regions, correlates with the severity of underlying neuropathological changes seen on postmortem studies (Echávarri et al., 2011). The second premise is that, despite most volumetric methods focus on the hippocampus and disregard the parahippocampal gyrus, many studies have shown that parahippocampal atrophy is as good indicator of AD as the hippocampus atrophy is (Nestor et al., 2008; Burgmans et al., 2011; Smith et al., 2012; Zarei et al., 2012). Thus, the entorinal cortex, the hippocampus, and the parahippocampal gyrus may be considered as the "epicentrum" of the neurodegenerative process. Therefore, in order to pick up the disease early we do not need to find out the volume of the whole hippocampus but detect atrophy at "the point" where the pathology is visible first.

THE SLICE SELECTED

Functionally, the hippocampus can be segmented into three distinct anatomical and functional subregions (head, body, and tail), according to the morphology and relative connectivity with prefrontal cortex (PFC), posterior cingulate cortex (PCC), and thalamus, respectively. The AD group show stronger hippocampus–PFC and weaker hippocampus–PCC functional connectivity, the magnitudes of which correlate with cognitive performance (Convit et al., 2000; Dickerson et al., 2011; Libby et al., 2012). In line with this fact and in order to assess the body of the hippocampus we have taken the coronal section passing through the interpeduncular fossa where the body of the hippocampus can be clearly viewed. However, this index might be performed on any other coronal slide where the MTL structures are viewed.

THE AREAS SELECTED

Age-associated differences are detected in the MTL (Parnetti et al., 1996; Jack et al., 1997; Apostolova et al., 2012; Leung et al., 2013)

with an acceleration of MTA starting around 72 years of age in healthy people (Jack et al., 1997). However, these changes are modest and their rate of progression over time is relatively slow with a mean rate of about 1.6% per year (Leung et al., 2013). Accelerated MTA is a consistent finding in AD and MCI with rates of about 2.8% in stable MCI, 3.7% in MCI transitioning to AD (MCI progressors), and up to 4.0% in AD (Kesslak et al., 1991; Parnetti et al., 1996; Jack et al., 1997; Bouwman et al., 2007; Eckerstrom et al., 2010; Jack et al., 2010; Apostolova et al., 2012; Ewers et al., 2012; Leung et al., 2013; Heister et al.). Frontotemporal dementia may also lead to MTA, but in a different pattern: frontotemporal dementia and semantic dementia show atrophy in the anterior portion of the hippocampus, and in semantic dementia the atrophy is asymmetrical, with the left hippocampus being affected more severely. No significant hippocampal atrophy is detected in non-fluent progressive aphasia (Barber et al., 1999; Schacter and Wagner, 1999; Chan et al., 2001; van de Pol et al., 2006). Other diseases such as dementia with Lewy bodies do not show MTA or it is much milder (Hashimoto et al., 1998; Whitwell et al., 2007; Chou et al., 2010).

In contrast to MTA, ventricular enlargement (body of lateral ventricles) in old people lacks specificity representing a measure of global brain atrophy due to aging or any neurodegenerative disorder. Global ventricular enlargement correlates with decline in cognitive performance and with cerebrospinal fluid pathologic markers of AD (Thompson et al., 2004; Apostolova et al., 2010). Absolute ventricular volumes and ventricular enlargement are greater in subjects with AD and MCI compared to age-matched controls. Ventricular enlargement also demonstrated sensitivity to disease progression by way of discriminating between subjects with stable MCI and those that progressed to AD (Nestor et al., 2008). However, it is important to note that all these studies were made using absolute ventricular volumes, without differentiation among the different portions of the lateral ventricles, while the lateral (temporal) horns are the portion contributing most to the ventricular enlargement in early AD (Giesel et al., 2006). It is well-known that enlargement of lateral ventricles is a measure of unspecific global brain atrophy since it is strongly associated both with aging in healthy and with neurodegeneration (Apostolova et al., 2012). Almost any neurodegenerative disorder affecting the brain hemispheres leads to some degree of ventricular enlargement, including Parkinson's disease (Meyer et al., 2007; Apostolova et al., 2010; Dalaker et al., 2011), Lewy-Bodies Dementia (Meyer et al., 2007), Frontotemporal Lobe Dementia (Galton et al., 2001; Gordon et al., 2010), and Corticobasal Degeneration (Hauser et al., 1996) and so do some psychiatric conditions (Swayze et al., 1990; Mathalon et al., 2001). Thus, it would be interesting to compare the extent of atrophy in the MTL with the extent of global brain atrophy (**Table 1**).

THE RATIO

This index reflects the rate of atrophy in the MTL—that is a value rather specific of AD since its early stages—in relation to the global unspecific atrophy represented by ventricular enlargement. Thus, it is a measure estimative of the contribution of the atrophy in the MTL to the whole brain atrophy.

ADVANTAGES AND LIMITATIONS OF THE MTA INDEX

From the clinician's point of view, the MTA index has the following advantages over other methods: (1) Measurement and scoring of MTA index is objective and reliable, providing a distinct advantage over visual techniques. (2) Volumetric measurements require the use of special software, and much greater technical stringency in the acquisition of the MRI scans and are far more prone to a variety of measurement errors. Delineating the areas needed for calculating the MTA index is fast and easy; little training is needed. Therefore, it can be implemented for daily clinical practice using basic neuroimaging facilities currently available in most hospitals with busy clinical settings. (3) An additional advantage of using MTA index over volumetric measures is that regional brain volumes are variable across individuals and need to be normalized by conversion to a ratio of the absolute volumes to intracranial volume, whereas the MTA index has built-in normalization and thus avoids multiplicative errors inherent in using ratios of two quantitative variables. (4) The same way, as aging affects both the hippocampus and lateral ventricles independent of AD pathology, aging should be included as covariate in methods providing absolute volumes or scores. The MTA index is an "intra-patient" ratio comparing the MTL and lateral ventricles, so it will probably not need cut-off scores adjusted by age. For the yearly rate of MTA and the yearly rate of relative MTA, normalization is not necessary neither because each subject serves as their own control.

On the other hand, the main limitation of the MTA index is that scoring is based on measurements performed on a single coronal slice, thereby providing a limited perspective of overall brain pathology. It is also expected that other conditions affecting the ventricular morphology, such as hydrocephalus, will probably alter the interpretation of the MTAi in these cases.

This paper is a methodological description only. Cut-off scores have to be calculated and its use as a parameter for diagnosing AD in research and clinical practice has to be validated. Particularly, prospective studies are needed to assess the usefulness of MTA index in the diagnosis of early AD, in tracking the progression of AD and in the differential diagnosis of AD with other dementias.

CONCLUSIONS

We report a new, manual method for assessing medial temporal lobe atrophy (MTA) that is objective and easy to apply using clinically available neuroimaging. It may have some advantages over visual and volumetric methods that still need to be evaluated.

REFERENCES

Albert, M. S., Dekosky, S. T., Dickson, D., Dubois, B., Feldman, H. H., Fox, N. C., et al. (2011). The diagnosis of mild cognitive impairment due to Alzheimer's disease: recommendations from the National Institute on Aging and Alzheimer's Association workgroup. *Alzheimers Dement.* 7, 270–279. doi: 10.1016/j.jalz.2011.03.008

Apostolova, L. G., Beyer, M., Green, A. E., Hwang, K. S., Morra, J. H., Chou, Y. Y., et al. (2010). Hippocampal, caudate, and ventricular changes in Parkinson's disease with and without dementia. *Mov. Disord.* 25, 687–695. doi: 10.1002/mds.22799

Apostolova, L. G., Green, A. E., Babakchanian, S., Hwang, K. S., Chou, Y. Y., Toga, A. W., et al. (2012). Hippocampal atrophy and ventricular enlargement in normal aging, mild cognitive impairment (MCI), and Alzheimer disease. *Alzheimer Dis. Assoc. Disord.* 26, 17–27. doi: 10.1097/WAD.0b013e3182163b62

Barber, R., Gholkar, A., Scheltens, P., Ballard, C., McKeith, I. G., and O'Brien, J. T. (1999). Medial temporal lobe atrophy on MRI in dementia with Lewy bodies. *Neurology* 52, 1153–1158. doi: 10.1212/WNL.52.6.1153

Boccardi, M., Bocchetta, M., Apostolova, L. G., Preboske, G., Robitaille, N., Pasqualetti, P., et al. (2013). Establishing magnetic resonance images orientation for the EADC-ADNI manual hippocampal segmentation protocol. *J. Neuroimaging*. doi: 10.1111/jon.12065. [Epub ahead of print].

Bouwman, F. H., Schoonenboom, S. N., van der Flier, W. M., van Elk, E. J., Kok, A., Barkhof, F., et al. (2007). CSF biomarkers and medial temporal lobe atrophy predict dementia in mild cognitive impairment. *Neurobiol. Aging* 28, 1070–1074. doi: 10.1016/j.neurobiolaging.2006.05.006

Braak, H., and Braak, E. (1985). On areas of transition between entorhinal allocortex and temporal isocortex in the human brain. Normal morphology and lamina-specific pathology in Alzheimer's disease. *Acta Neuropathol.* 68, 325–332. doi: 10.1007/BF00690836

Brewer, J. B., Magda, S., Airriess, C., and Smith, M. E. (2009). Fully automated quantification of regional brain volumes for improved detection of focal atrophy in Alzheimer disease. *AJNR Am. J. Neuroradiol.* 30, 578–580. doi: 10.3174/ajnr.A1402

Burgmans, S., van Boxtel, M. P., van den Berg, K. E., Gronenschild, E. H., Jacobs, H. I., Jolles, J., et al. (2011). The posterior parahippocampal gyrus is preferentially affected in age-related memory decline. *Neurobiol. Aging* 32, 1572–1578. doi: 10.1016/j.neurobiolaging.2009.09.008

Chan, D., Fox, N. C., Scahill, R. I., Crum, W. R., Whitwell, J. L., Leschziner, G., et al. (2001). Patterns of temporal lobe atrophy in semantic dementia and Alzheimer's disease. *Ann. Neurol.* 49, 433–442. doi: 10.1002/ana.92

Chou, Y. Y., Leporé, N., Saharan, P., Madsen, S. K., Hua, X., Jack, C. R., et al. (2010). Alzheimer's disease neuroimaging initiative. Ventricular maps in 804 ADNI subjects: correlations with CSF biomarkers and clinical decline. *Neurobiol. Aging* 31, 1386–1400. doi: 10.1016/j.neurobiolaging.2010.05.001

Convit, A., de Asis, J., de Leon, M. J., Tarshish, C. Y., De Santi, S., and Rusinek, H. (2000). Atrophy of the medial occipitotemporal, inferior, and middle temporal gyri in non-demented elderly predict decline to Alzheimer's disease. *Neurobiol. Aging* 21, 19–26. doi: 10.1016/S0197-4580(99)00107-4

Dahlbeck, J. W., McCluney, K. W., Yeakley, J. W., Fenstermacher, M. J., Bonmati, C., Van Horn, G., et al. (1991). The interuncal distance: a new MR measurement for the hippocampal atrophy of Alzheimer disease. *AJNR Am. J. Neuroradiol.* 12, 931–932.

Dalaker, T. O., Zivadinov, R., Ramasamy, D. P., Beyer, M. K., Alves, G., Bronnick, K. S., et al. (2011). Ventricular enlargement and mild cognitive impairment in early Parkinson's disease. *Mov. Disord.* 26, 297–301. doi: 10.1002/mds.23443

de Leon, M. J., George, A. E., Golomb, J., Tarshish, C., Convit, A., Kluger, A., et al. (1997). Frequency of hippocampal formation atrophy in normal aging and Alzheimer's disease. *Neurobiol. Aging* 18, 1–11. doi: 10.1016/S0197-4580(96)00213-8

Dickerson, B. C., Stoub, T. R., Shah, R. C., Sperling, R. A., Killiany, R. J., Albert, M. S., et al. (2011). Alzheimer-signature MRI biomarker predicts AD dementia in cognitively normal adults. *Neurology* 76, 1395–1402. doi: 10.1212/WNL.0b013e3182166e96

Duara, R., Loewenstein, D. A., Shen, Q., Barker, W., Varon, D., Greig, M. T., et al. (2013). Volumetric and visual ratings of medical temporal atrophy in AD and MCI: comparison of age-specific cut-offs. *Front. Aging Neurosci*. 5:47. doi: 10.3389/fnagi.2013.00047

Duvernoy, H. M. (1998). *The Human Hippocampus: Functional Anatomy, Vascularization and Serial Sections with MRI*. Berlin: Springer-Verlag. doi: 10.1007/978-3-662-03628-0

Echávarri, C., Aalten, P., Uylings, H. B., Jacobs, H. I., Visser, P. J., Gronenschild, E. H., et al. (2011). Atrophy in the parahippocampal gyrus as an early biomarker of Alzheimer's disease. *Brain Struct. Funct.* 215, 265–271. doi: 10.1007/s00429-010-0283-8

Eckerstrom, C., Andreasson, U., Olsson, E., Rolstad, S., Blennow, K., Zetterberg, H., et al. (2010). Combination of hippocampal volume and cerebrospinal fluid biomarkers improves predictive value in mild cognitive impairment. *Dement. Geriatr. Cogn. Disord.* 29, 294–300. doi: 10.1159/000289814

Erkinjuntti, T., Lee, D. H., Gao, F., Steenhuis, R., Eliasziw, M., Fry, R., et al. (1993). Temporal lobe atrophy on magnetic resonance imaging in the diagnosis of early Alzheimer's disease. *Arch. Neurol.* 50, 305–310. doi: 10.1001/archneur.1993.00540030069017

Ewers, M., Walsh, C., Trojanowski, J. Q., Shaw, L. M., Petersen, R. C., Jack, C. R., et al. (2012). Prediction of conversion from mild cognitive impairment to Alzheimer's disease dementia based upon biomarkers and neuropsychological test performance. *Neurobiol. Aging* 33, 1203–1214. doi: 10.1016/j.neurobiolaging.2010.10.019

Frisoni, G. B., Geroldi, C., Beltramello, A., Bianchetti, A., Binetti, G., Bordiga, G., et al. (2002). Radial width of the temporal horn: a sensitive measure in Alzheimer disease. *AJNR Am. J. Neuroradiol.* 23, 35–47.

Frisoni, G. B., and Jack, C. R. (2011). Harmonization of magnetic resonance-based manual hippocampal segmentation: a mandatory step for wide clinical use. *Alzheimers Dement.* 7, 171–174. doi: 10.1016/j.jalz.2010.06.007

Galton, C. J., Gomez-Anson, B., Antoun, N., Scheltens, P., Patterson, K., Graves, M., et al. (2001). Temporal lobe rating scale: application to Alzheimer's disease and frontotemporal dementia. *J. Neurol. Neurosurg. Psychiatr.* 70, 165–173. doi: 10.1136/jnnp.70.2.165

Giesel, F. L., Hahn, H. K., Thomann, P. A., Widjaja, E., Wignall, E., von Tengg-Kobligk, H., et al. (2006). Temporal horn index and volume of medial temporal lobe atrophy using a new semiautomated method for rapid and precise assessment. *AJNR Am. J. Neuroradiol.* 27, 1454–1458.

Gordon, E., Rohrer, J. D., Kim, L. G., Omar, R., Rossor, M. N., Fox, N. C., et al. (2010). Measuring disease progression in frontotemporal lobar degeneration: a clinical and MRI study. *Neurology* 74, 666–673. doi: 10.1212/WNL.0b013e3181d1a879

Hashimoto, M., Kitagaki, H., Imamura, T., Hirono, N., Shimomura, T., Kazui, H., et al. (1998). Medial temporal and whole-brain atrophy in dementia with Lewy bodies: a volumetric MRI study. *Neurology* 51, 357–362. doi: 10.1212/WNL.51.2.357

Hauser, R. A., Murtaugh, F. R., Akhter, K., Gold, M., and Olanow, C. W. (1996). Magnetic resonance imaging of corticobasal degeneration. *J. Neuroimaging* 6, 222–226.

Heister, D., Brewer, J. B., Magda, S., Blennow, K., McEvoy, L. K., and Alzheimer's Disease Neuroimaging Initiative. (2011). Predicting MCI outcome with clinically available MRI and CSF biomarkers. *Neurology* 77, 1619–1628. doi: 10.1212/WNL.0b013e3182343314

Jack, C. R. Jr., Petersen, R. C., O'Brien, P. C., and Tangalos, E. G. (1992). MR-based hippocampal volumetry in the diagnosis of Alzheimer's disease. *Neurology* 42, 183–188.

Jack, C. R. Jr., Petersen, R. C., Xu, Y. C., Waring, S. C., O'Brien, P. C., Tangalos, E. G., et al. (1997). Medial temporal atrophy on MRI in normal aging and very mild Alzheimer's disease. *Neurology* 49, 786–794. doi: 10.1212/WNL.49.3.786

Jack, C. R. Jr., Wiste, H. J., Vemuri, P., Weigand, S. D., Senjem, M. L., Zeng, G., et al. (2010). Brain beta-amyloid measures and magnetic resonance imaging atrophy both predict time-to-progression from mild cognitive impairment to Alzheimer's disease. *Brain* 133, 3336–3348. doi: 10.1093/brain/awq277

Kerchner, G. A., Hess, C. P., Hammond-Rosenbluth, K. E., Xu, D., Rabinovici, G. D., Kelley, D. A., et al. (2010). Hippocampal CA1 apical neuropil atrophy in mild Alzheimer disease visualized with 7-T MRI. *Neurology* 75, 1381–1387. doi: 10.1212/WNL.0b013e3181f736a1

Kesslak, J. P., Nalcioglu, O., and Cotman, C. W. (1991). Quantification of magnetic resonance scans for hippocampal and parahippocampal atrophy in Alzheimer's disease. *Neurology* 41, 51–54. doi: 10.1212/WNL.41.1.51

Kovacevic, S., Rafii, M. S., and Brewer, J. B. (2009). High-throughput, fully automated volumetry for prediction of MMSE and CDR decline in mild cognitive impairment. *Alzheimer Dis. Assoc. Disord.* 23, 139–145. doi: 10.1097/WAD.0b013e318192e745

Leung, K. K., Bartlett, J. W., Barnes, J., Manning, E. N., Ourselin, S., and Fox, N. C. (2013). Azheimer's disease neuroimaging initiative. Cerebral atrophy in mild cognitive impairment and Alzheimer disease: rates and acceleration. *Neurology* 80, 648–654. doi: 10.1212/WNL.0b013e318281ccd3

Libby, L., Ekstrom, A., Ragland, J. D., and Ranganath, C. (2012). Differential connectivity of perirhinal and parahippocampal cortices within human hippocampal subregions revealed by high-resolution functional imaging. *J. Neurosci.* 32, 6550–6560. doi: 10.1523/JNEUROSCI.3711-11.2012

Lim, H. K., Jung, W. S., Ahn, K. J., Won, W. Y., Hahn, C., Lee, S. Y., et al. (2012). Relationships between hippocampal shape and cognitive performances in drug-naïve patients with Alzheimer's disease. *Neurosci. Lett.* 516, 124–129. doi: 10.1016/j.neulet.2012.03.072

Mai, J. K., Assheuer, J., and Paxinos, G. (1997). *Atlas of the Human Brain*. San Diego, CA: Academic Press.

Mathalon, D. H., Sullivan, E. V., Lim, K. O., and Pfefferbaum, A. (2001). Progressive brain volume changes and the clinical course of Schizophrenia in men: a longitudinal magnetic resonance imaging study. *Arch. Gen. Psychiatry* 58, 148–157. doi: 10.1001/archpsyc.58.2.148

McKhann, G. M., Knopman, D. S., Chertkow, H., Hyman, B. T., Jack, C. R. Jr., Kawas, C. H., et al. (2011). The diagnosis of dementia due to Alzheimer's disease: recommendations from the National Institute on Aging-Alzheimer's Association workgroups on diagnostic guidelines for Alzheimer's disease. *Alzheimers Dement*. 7, 263–269. doi: 10.1016/j.jalz.2011.03.005

Meyer, J. S., Huang, J., and Chowdhury, M. H. (2007). MRI confirms mild cognitive impairments prodromal for Alzheimer's, vascular and Parkinson-Lewy body dementias. *J. Neurol. Sci.* 257, 97–104. doi: 10.1016/j.jns.2007.01.016

Morra, J. H., Tu, Z., Apostolova, L. G., Green, A. E., Avedissian, C., Madsen, S. K., et al. (2008). Alzheimer's disease neuroimaging initiative. Validation of a fully automated 3D hippocampal segmentation method using subjects with Alzheimer's disease mild cognitive impairment, and elderly controls. *Neuroimage* 43, 59–68. doi: 10.1016/j.neuroimage.2008.07.003

Morris, J. C., Storandt, M., McKeel, D. W. Jr., Rubin, E. H., Price, J. L., Grant, E. A., et al. (1996). Cerebral amyloid deposition and diffuse plaques in "normal" aging: evidence for presymptomatic and very mild Alzheimer's disease. *Neurology* 46, 707–719. doi: 10.1212/WNL.46.3.707

Nagy, Z., Hindley, N. J., Braak, H., Braak, E., Yilmazer-Hanke, D. M., Schultz, C., et al. (1999). The progression of Alzheimer's disease from limbic regions to the neocortex: clinical, radiological and pathological relationships. *Dement. Geriatr. Cogn. Disord.* 10, 115–120. doi: 10.1159/000017111

Nestor, S. M., Rupsingh, R., Borrie, M., Smith, M., Accomazzi, V., Wells, J. L., et al. (2008). Alzheimer's disease neuroimaging initiative. Ventricular enlargement as a possible measure of Alzheimer's disease progression validated using the Alzheimer's disease neuroimaging initiative database. *Brain* 131, 2443–2454. doi: 10.1093/brain/awn146

Parnetti, L., Lowenthal, D. T., Presciutti, O., Pelliccioli, G. P., Palumbo, R., Gobbi, G., et al. (1996). 1H-MRS, MRI-based hippocampal volumetry, and 99mTc-HMPAO-SPECT in normal aging, age-associated memory impairment, and probable Alzheimer's disease. *J. Am. Geriatr. Soc.* 44, 133–138.

Pereira, J. B., Cavallin, L., Spulber, G., Aguilar, C., Mecocci, P., Vellas, B., et al. (2013). Influence of age, disease onset and ApoE4 on visual medial temporal lobe atrophy cut-offs. *J. Intern. Med.* doi: 10.1111/joim.12148. [Epub ahead of print].

Petrella, J. R., Coleman, R. E., and Doraiswamy, P. M. (2003). Neuroimaging and early diagnosis of Alzheimer disease: a look to the future. *Radiology* 226, 315–336. doi: 10.1148/radiol.2262011600

Ridha, B. H., Barnes, J., van de Pol, L. A., Schott, J. M., Boyes, R. G., Siddique, M. M., et al. (2007). Application of automated medial temporal lobe atrophy scale to Alzheimer disease. *Arch. Neurol.* 64, 849–854. doi: 10.1001/archneur.64.6.849

Ringman, J. M., Pope, W., and Salamon, N. (2010). Insensitivity of visual assessment of hippocampal atrophy in familial Alzheimer's disease. *J. Neurol.* 257, 839–842. doi: 10.1007/s00415-009-5436-4

Schacter, D. L., and Wagner, A. D. (1999). Medial temporal lobe activations in fMRI and PET studies of episodic encoding and retrieval. *Hippocampus* 9, 7–24. doi: 10.1002/(SICI)1098-1063(1999)9:1%3C7::AID-HIPO2%3E3.0.CO;2-K

Scheltens, P., Leys, D., Barkhof, F., Huglo, D., Weinstein, H. C., Vermersch, P., et al. (1992). Atrophy of medial temporal lobes on MRI in "probable" Alzheimer's disease and normal ageing: diagnostic value and neuropsychological correlates. *J. Neurol. Neurosurg. Psychiatr.* 55, 967–972. doi: 10.1136/jnnp.55.10.967

Shen, L., Saykin, A. J., Kim, S., Firpi, H. A., West, J. D., Risacher, S. L., et al. (2010). Comparison of manual and automated determination of hippocampal volumes in MCI and early AD. *Brain Imaging Behav.* 4, 86–95. doi: 10.1007/s11682-010-9088-x

Smith, A. D., and Jobst, K. A. (1996). Use of structural imaging to study the progression of Alzheimer's disease. *Br. Med. Bull.* 52, 575–586. doi: 10.1093/oxfordjournals.bmb.a011568

Smith, C. D., Andersen, A. H., and Gold, B. T. (2012). Structural brain alterations before mild cognitive impairment in ADNI: validation of volume loss in a predefined antero-temporal region. *J. Alzheimers. Dis.* 31, S49–S58. doi: 10.3233/JAD-2012-120157

Soininen, H. S., Partanen, K., Pitkanen, A., Vainio, P., Hanninen, T., Hallikainen, M., et al. (1994). Volumetric MRI analysis of the amygdala and the hippocampus in subjects with age-associated memory impairment: correlation to visual and verbal memory. *Neurology* 44, 1660–1668. doi: 10.1212/WNL.44.9.1660

Sperling, R. A., Aisen, P. S., Beckett, L. A., Bennett, D. A., Craft, S., Fagan, A. M., et al. (2011). Toward defining the preclinical stages of Alzheimer's disease: recommendations from the National Institute on Aging-Alzheimer's Association workgroups on diagnostic guidelines for Alzheimer's disease. *Alzheimers Dement.* 7, 280–292. doi: 10.1016/j.jalz.2011.03.003

Swayze, V. W. II., Andreasen, N. C., Alliger, R. J., Ehrhardt, J. C., and Yuh, W. C. (1990). Structural brain abnormalities in bipolar affective disorder: ventricular enlargement and focal signal hyperintensities. *Arch. Gen. Psychiatry* 47, 1054–1059. doi: 10.1001/archpsyc.1990.01810230070011

Thompson, P. M., Hayashi, K. M., De Zubicaray, G. I., Janke, A. L., Rose, S. E., Semple, J., et al. (2004). Mapping hippocampal and ventricular change in Alzheimer disease. *Neuroimage* 22, 1754–1766. doi: 10.1016/j.neuroimage.2004.03.040

van de Pol, L. A., Hensel, A., van der Flier, W. M., Visser, P. J., Pijnenburg, Y. A., Barkhof, F., et al. (2006). Hippocampal atrophy on MRI in frontotemporal lobar degeneration and Alzheimer's disease. *J. Neurol. Neurosurg. Psychiatr.* 77, 439–442. doi: 10.1136/jnnp.2005.075341

Westman, E., Cavallin, L., Muehlboeck, J. S., Zhang, Y., Mecocci, P., Vellas, B., et al. (2011). AddNeuroMed consortium. Sensitivity and specificity of medial temporal lobe visual ratings and multivariate regional MRI classification in Alzheimer's disease. *PLoS ONE* 6:e22506. doi: 10.1371/journal.pone.0022506

Whitwell, J. L., Weigand, S. D., Shiung, M. M., Boeve, B. F., Ferman, T. J., Smith, G. E., et al. (2007). Focal atrophy in dementia with Lewy bodies on MRI: a distinct pattern from Alzheimer's disease. *Brain* 130(Pt 3), 708–719. doi: 10.1093/brain/awl388

Zarei, M., Beckmann, C. F., Binnewijzend, M. A., Schoonheim, M. M., Oghabian, M. A., Sanz-Arigita, E. J., et al. (2012). Functional segmentation of the hippocampus in the healthy human brain and in Alzheimer's disease. *Neuroimage* 66C, 28–35. doi: 10.1016/j.neuroimage.2012.10.071

Zhang, Y., Qiu, C., Lindberg, O., Bronge, L., Aspelin, P., Bäckman, L., et al. (2010). Acceleration of hippocampal atrophy in a non-demented elderly population: the SNAC-K study. *Int. Psychogeriatr.* 22, 14–25. doi: 10.1017/S1041610209991396

Conflict of Interest Statement: The authors declare that the research was conducted in the absence of any commercial or financial relationships that could be construed as a potential conflict of interest.

Received: 27 August 2013; accepted: 11 February 2014; published online: 24 March 2014.

*Citation: Menéndez-González M, López-Muñiz A, Vega JA, Salas-Pacheco JM and Arias-Carrión O (2014) MTA index: a simple 2D-method for assessing atrophy of the medial temporal lobe using clinically available neuroimaging. Front. Aging Neurosci. **6**:23. doi: 10.3389/fnagi.2014.00023*

This article was submitted to the journal Frontiers in Aging Neuroscience.

frontiers in
AGING NEUROSCIENCE

ORIGINAL RESEARCH ARTICLE
published: 18 September 2013
doi: 10.3389/fnagi.2013.00047

The utility of age-specific cut-offs for visual rating of medial temporal atrophy in classifying Alzheimer's disease, MCI and cognitively normal elderly subjects

***Ranjan Duara*[1,2,3,4,5,6]*, *David A. Loewenstein*[1,3], *Qian Shen*[1,7], *Warren Barker*[1], *Daniel Varon*[1,4], *Maria T. Greig*[1], *Rosie Curiel*[3], *Joscelyn Agron*[1], *Isael Santos*[1] and *Huntington Potter*[5†]**

[1] *Wien Center for Alzheimer's Disease and Memory Disorders, Mount Sinai Medical Center, Miami Beach, FL, USA*
[2] *Departments of Medicine and Neurology, Miller School of Medicine, University of Miami, Miami, FL, USA*
[3] *Department of Psychiatry and Behavioral Sciences, Miller School of Medicine, University of Miami, Miami, USA*
[4] *Department of Neurology, Florida International University College of Medicine, Miami, FL, USA*
[5] *Departments of Molecular Medicine and Neurology, University of South Florida, Tampa, FL, USA*
[6] *Johnnie B. Byrd, Sr. Alzheimer's Center and Research Institute, Tampa, FL, USA*
[7] *Department of Biomedical Engineering, University of Miami, Coral Gables, FL, USA*

Edited by:
Manuel Menéndez-González, Hospital Álvarez-Buylla, Spain

Reviewed by:
Katsutoshi Furukawa, Tohoku University, Japan
Elizabeth J. Coulthard, University of Bristol, UK

****Correspondence:***
Ranjan Duara, Mount Sinai Medical Center, Wien AD Research Center, 4300 Alton Road, Miami Beach, FL 33140, USA
e-mail: duara@msmc.com

†Present address:
Huntington Potter, Department of Neurology and Linda Crnic Institute for Down Syndrome, School of Medicine, University of Colorado, Anschutz Medical Campus, Aurora, USA

Background: New research criteria for diagnosing Alzheimer's disease (AD) in the mild cognitive impairment stage (MCI-AD) incorporate biomarkers to assign a level of certainty to the diagnosis. Structural MRI is widely available but greatly under-utilized for assessing atrophy of structures affected in early AD, such as the hippocampus (HP), because the quantification of HP volumes (HP-v) requires special expertise, and normative values have not been established.

Methods: Elderly subjects ($n = 273$) from the Florida ADRC were classified as having no cognitive impairment (cognitively normal, CN), amnestic mild cognitive impairment (aMCI) or AD. Volumes for the hippocampus (HP-v) were measured on structural MRI scans. A validated visual rating system for measuring medial temporal atrophy (VRS-MTA), including hippocampal, entorhinal cortex and perirhinal cortex atrophy was employed. The participants were subdivided into younger (less than or equal to 75 years of age) and older (greater than 75 years of age) subgroups.

Results: Volumetric and VRS-MTA measures were equivalent in predicting classification of CN vs. aMCI for older (area under the receiver operator curves [aROC]: 0.652 vs. 0.723) and younger subjects (aROC: 0.764 vs. 0.736). However, for younger AD subjects, aROC values were significantly higher for VRS-MTA measures (0.920) than for volumetric measures (0.847). Relative to HP-v, VRS-MTA score was significantly more correlated to impairment on a range of memory tests and was more associated with progression of aMCI to AD than HP-v.

Conclusion: Structural MRI with VRS-MTA assessment can serve as a biomarker for supporting the diagnosis of MCI-AD. Age-adjusted VRS-MTA scores are at least as effective as HP-v for distinguishing aMCI and AD from CN and for predicting progression from aMCI to AD. VRS-MTA is convenient for use in the clinic as well as for clinical trials and can readily be incorporated into a standardized radiological report.

Keywords: volumetric measures, hippocampus, visual rating, medial temporal atrophy, aMCI, Alzheimer's disease

INTRODUCTION

Recently revised criteria for diagnosing an early clinical stage of AD ("Mild Cognitive Impairment, or MCI, due to AD"; MCI-AD) (Albert et al., 2011) and "Prodromal AD" (Sperling et al., 2011) incorporate biomarkers to increase the certainty of the diagnosis. One such biomarker, atrophy of the hippocampus (HP) and other medial temporal lobe (MTL) structures on structural MRI, increase the likelihood of a neurodegenerative disorder, such as AD, as the cause of MCI. In spite of the widespread use of MRI scans for the assessment of individuals with various forms of cognitive impairment, this biomarker is used primarily for excluding causes of cognitive impairment other than AD, such as hydrocephalus, vascular and space-occupying lesions. However, MRI can be used to confirm the presence of neurodegenerative pathology among patients presenting with MCI and dementia (Frisoni et al., 2010) and is greatly underutilized for this purpose by clinicians and radiologists. Although prodromal forms of AD are in a continuum with, and may be clinically indistinguishable from what is described as "Probable AD," current diagnostic research standards incorporate a biomarker to support the

diagnosis of prodromal AD or MCI-AD It is clear that the diagnosis of both Probable AD and Prodromal AD/MCI-AD would be more secure in the presence of a positive biomarker which provides further evidence of the presence of a neurodegenerative disease (Albert et al., 2011; Sperling et al., 2011).

Neurodegenerative changes such as atrophy which are characteristic of Alzheimer's disease (AD), and occasionally of other dementing diseases, such as Fronto-temporal Lobar Dementia (FTLD) or Hippocampal Sclerosis, may be detected using volumetric analysis or, more conveniently, using visual rating of MRI scans. Nevertheless, the incorporation of MRI for confirming the diagnosis of neurodegenerative disease has yet to receive widespread utility, in part because of (a) lack of awareness of the value and accuracy of MRI for this purpose, (b) automated, quantitative volumetric methods for measuring hippocampal volume are unwieldy, expensive and not easily adapted for routine clinical use, and (c) the lack of widely accepted age-adjusted norms and cut-scores for hippocampal volume (HP-v) and medial temporal atrophy (MTA).

The goal of this study was to evaluate user-friendly methods to evaluate structural MRI scans and to provide appropriate age-adjusted cut scores for both visually rated MTA measures and HP-v structures, which best distinguish normal elderly subjects from those who have AD. Accordingly, we compared hippocampal volumes (HP-v) to a refinement of the semiquantitative visual rating method, initially developed by Scheltens et al. (1995). This new visual rating system for assessing medial temporal atrophy (VRS-MTA) (Duara et al., 2008; Urs et al., 2009) provides a total MTA score by combining atrophy levels in individual medial temporal structures, including the HP, the entorhinal cortex (ERC), and the perirhinal cortex (PRC). We established appropriate age-related cut-offs for both volumetric measures of the HP and VRS-MTA measures, which correctly classified 70–80% of cognitively normal [CN] subjects without cognitive impairment. We chose these levels of specificity because at least 20–30% of CN subjects are known to harbor the pathology of AD on post-mortem evaluation (Morris, 2006). We then compared the accuracy of these two methods for distinguishing CN from subjects with aMCI and AD, the associations of these two measures with neuropsychological measures of cognition and the ability to predict progression from aMCI to dementia.

METHODS

SUBJECT RECRUITMENT

The current sample was recruited from a group of 273 subjects (107 CN, who were enrolled in the Florida Alzheimer's Disease Research Center Clinical Core (FADRC-CC) in Miami Beach FL between 2005 and 2009 (Duara et al., 2010). Subjects were diagnosed as cognitively normal (CN) or having amnestic MCI (aMCI) or dementia. The study was approved by the Institutional Review Board at Mount Sinai Medical Center, Miami Beach, and the University of South Florida, Tampa. All subjects or a legal representative provided informed consent.

EVALUATIONS

The following were completed on all subjects: (1) full clinical history, obtained from a reliable informant; (2) neurological evaluation; (3) psychiatric evaluation, including administration of the Geriatric Depression scale (Sheikh and Yesavage, 1986) and the Neuropsychiatric Inventory (Cummings et al., 1994); (4) Clinical Disease Rating scale (CDR-SB; Morris, 1993); (5) Mini-Mental State Examination (MMSE; Folstein et al., 1975); (6) a neuropsychological test battery, as described below; (7) Unified Parkinson Disease Rating Scale (UPDRS, motor section; Fahn and Elton, 1987) which has been documented as a sensitive tool for quantifying motor dysfunction and parkinsonism in patients with various forms of MCI and dementia.

Cardiovascular Risk (CVR) Score was calculated as the sum of 10 independent risk factors (14) selected from the National Alzheimer's Coordinating Center (NACC) Uniform Data Set (UDS) Subject Health History assessment protocol (Appel et al., 2009).

DIAGNOSTIC PROCEDURES

DETERMINING A CONSENSUS DIAGNOSIS FOR COGNITIVELY NORMAL, DIFFERENT MCI SUBTYPES AND DEMENTIA

The physician assigned a cognitive diagnosis of CN, MCI, or Dementia, as described previously (Duara et al., 2010). Briefly, the PhyDx was based on the subject's entire clinical history and functional status, which was derived from the history itself, CDR rating, functional activity questionnaire, MMSE score and subscores, taking into account the subjects' educational and cultural background, sensory (especially visual and hearing) and motor deficits, language and speech disorders, medical and psychiatric conditions and the perceived reliability of the informant. In addition to the physician's diagnosis, an independent neuropsychological diagnosis was rendered by a neuropsychologist.

NEUROPSYCHOLOGICAL DIAGNOSIS (NPDx)

All neuropsychological tests were administered in the subjects' native language (English or Spanish) and compared to age and education adjusted normative data, as described previously (Loewenstein et al., 2009). The tests included all of those outlined in the NACC protocol (Beekly et al., 2007), as well as additional tests, including the Three Trial Fuld Object Memory Evaluation (FOME; Fuld, 1981), and the Hopkins Verbal Learning Test-Delayed Recall (HVLT; Benedict et al., 1998). Memory measures were: the FOME, HVLT, and Delayed Visual Reproduction of the Wechsler Memory Scale-R (Wechsler, 1987). Non-memory tests included: category fluency (Monsch et al., 1992), letter fluency (language; Monsch et al., 1992), Block Design-WAIS-III (visuospatial; Wechsler, 1997), Trails B (Executive; Army Individual Test Battery, 1944), and Similarities-WAIS-R (Executive; Wechsler, 1997). Neuropsychological classification were made as follows: (a) a test score of 1.5 SD or greater below expected normative values on any single test for MCI syndromes; and (b) 2.0 SD or greater below expected normative values in one memory and one non-memory test for dementia (corresponding to NINCDS-ADRDA criteria; (McKhann et al., 1984). Nomenclature used for NPDx was Normal, Non-Amnestic MCI (naMCI; single or multi-domain), amnestic MCI (aMCI; single or multi-domain) and Dementia.

ALGORITHMIC CONSENSUS COGNITIVE DIAGNOSES (AlgDx)

An algorithmic approach to consensus diagnosis (Duara et al., 2010) combined the PhyDx with the NPDx, as follows: (a) a

PhyDx and a NPDx of Normal received an AlgDx of cognitively normal (CN); (b) a PhyDx diagnosis of MCI and a NPDx of aMCI received an AlgDx of aMCI; (c) a PhyDx of dementia and a NPDx of aMCI or Dementia received an AlgDx of Dementia. Patients diagnosed with aMCI met Petersen criteria for MCI (Petersen et al., 1999). Probable AD was diagnosed according to National Institute of Neurological and Communicative Disorders and Stroke (NINCDS)–Alzheimer's Disease and Related Disorders Association (ADRDA) criteria for AD (McKhann et al., 1984) and the criteria set forth by the National Alzheimer's Coordinating Center.

MRI Scans were acquired using a proprietary 3-D volumetric protocol on a Siemens Symphony, 1.5 Tesla machine (Iselin, NJ) or a GE 1.5 T machine, using proprietary three-dimensional magnetization-prepared rapid-acquisition gradient echo (Siemens) or the three-dimensional spoiled gradient recalled echo (General Electric) sequences; MRI scans were acquired in the coronal plane, and contiguous slices with thickness of 1.5 mm or less were reconstructed.

VOLUMETRIC ANALYSIS OF BRAIN MRIs

Volumetric analysis is performed using Individual Brain Atlas and Statistical Parametric Mapping (IBASPM; Alemán-Gómez et al., 2006). In IBAPSM, the volume of brain regions is calculated after normalization or spatial transformation to Montreal Neurological Institute (MNI; McGill University, 2009) templates. The scans are segmented into three types of tissue in each hemisphere: gray matter, white matter, and cerebrospinal fluid. An individual brain atlas for each subject is created with the transformation matrix obtained from the normalization step, and anatomical automatic labeling (AAL) to specify 116 regions. Hippocampal volume (HP-vol) was calculated as the ratio of the volume of each HP (right and left) to the total intracranial volume (Shen et al., 2011).

VISUAL RATING METHODS ASSESSING BRAIN MRIs

The scope and utility of Scheltens' system was expanded by Duara et al. (2008) and Urs et al. (2009), to provide reliable visual ratings of individual MTL regions, i.e., hippocampus (HPC), ERC, and PRC. Reliability and accuracy were achieved using very thin coronal slices (1.2 to 1.5 mm thickness), perpendicular to the AC-PC line and intersecting the mammillary bodies (Urs et al., 2009). We have previously reported excellent inter-rater reliability for measuring individual MTL structures; kappa values among two raters ranged between 0.75 and 0.94 for inter-rater reliability and 0.87 and 0.93 for intra-rater reliability. (Urs et al., 2009). With VRS-MTA, semi-quantitative assessments of atrophy of the HP, ERC, and PRC were assigned as follows: a score of Grade 0 corresponded to no atrophy, Grade 1 to minimal atrophy, Grade 2 to mild atrophy, Grade 3 to moderate atrophy and Grade 4 to severe atrophy (**Figure 1**). The VRS-MTA program provides a library of drop-down images, depicting the anatomical boundaries of these structures as well as each grade of atrophy for the ERC, HP, and PRC.

ApoE genotype was determined using standard methods (Wenham et al., 1991). ApoEε4 frequencies were subsequently calculated for each diagnostic group.

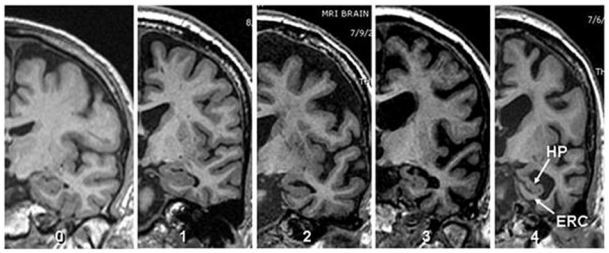

FIGURE 1 | Visual rating scale. Image depicting four degrees of atrophy in Hippocampus and Entorhinal cortex according to visual rating scale where 0 = no atrophy, 1 = minimal atrophy, 2 = mild atrophy, 3 = moderate atrophy and 4 = server atrophy (Score shown corresponds to both structure).

DERIVING CUT-OFFS FOR HP-VOL AND VRS-MTA VALUES FOR DIFFERENT AGE GROUPS AND BOTH BRAIN SIDES

To derive cut-scores for HP-vol (measured as percentage of intracranial volume) for the older CN group we used the scores of 20 subjects, aged 76 years and above (mean age = 79.64 years; *SD* = 3.2 years range = 76–90 years), who had an algorithmic diagnosis of CN. The cut-off scores for the lowest 20% (liberal cut score ≤0.0249%) and 30% (conservative cut score ≤0.0224%) of HP-vol, for each side, which was then used to identify hippocampal atrophy for all diagnostic groups aged 76 or greater. Similarly, we determined the approximate cut score (range of 0–12 points for each side), for highest 20–30% (liberal cut score ≥4) or 30–40% (conservative cut score ≥5) of combined HP, ERC, and PRC ratings on the left and right sides. These cut scores were then used to identify threshold levels of MTA for all diagnostic groups, aged 76 years or greater, separately for the right and left sides in each subject.

To derive a cut-score for the younger CN group, we took the scores of 87 cognitively normal individuals aged 63–75 years (mean age = 68.33 years; *SD* = 3.2 years) and used a similar procedure as for the older CN. The derived cut scores for HP-v (liberal cut score ≤0.027; conservative cut score ≤0.0257) and VRS-MTA ratings (liberal cut score ≥2.0; conservative cut score ≥3) for the right and left sides for each subject. In addition, so as to identify localized atrophy within the medial temporal region on each side, independent of the total VRS-MTA score, we determined the highest VRS scores for the right and left HP and ERC for each subject. For these measures a liberal (≤1.5) and a conservative (≤2.0) cut score were determined that would classify not more than 20 or 33% of both young and old CN group as having abnormal atrophy. These cut scores were also applied to subjects diagnosed with amnestic MCI and dementia.

LONGITUDINAL EVALUATION PROCEDURES

A total of 72 of the 103 subjects had at least one-annual follow-up evaluation (mean = 33.1 months; *SD* = 14.1 months), including neurological, psychiatric and neuropsychological evaluations, and re-diagnosis by the AlgDx. The mean age of this sample was 76.8 (*SD* = 5.8 years) and mean MMSE scores of were 26.1 (*SD* = 2.4) making the sample comparable to the aMCI patients who were originally diagnosed at baseline.

STATISTICAL ANALYSIS

Group comparisons of demographic variables across three study groups were analyzed using analyses of variance (ANOVA) or chi-square tests, as appropriate. *Post-hoc* tests of means were examined by the Tukey-Kramer procedure at $p < 0.05$. Comparative analyses of VRS-MTA and HP-v measures were assessed using receiver operator (ROC) curves. HP-v and MTA-VRS scores were correlated to a broad array of cognitive measures among memory impaired patients. Comparisons between correlation coefficients were tested statistically using SISA binomials (Uitenbroek, 1997). Finally, differences in progression rates across groups were assessed using chi-square procedures.

RESULTS

DEMOGRAPHICS

In the entire sample of subjects (age range = 63–93 years; mean age = 75.0 ± 7.2 years) there were statistically significant demographic differences between CN, aMCI, and AD groups, with regards to age, gender and educational attainment as well as on MMSE scores [$F_{(2,\ 269)} = 172.05$; $p < 0.001$] (**Table 1**). *Post-hoc* tests revealed that CN patients were younger, better educated, had higher MMSE scores and were more frequently female compared to the other two groups. AD subjects were older and had lower MMSE scores than aMCI subjects. There were significant group differences with regards to Spanish vs. English-speaking subjects or percentage of subjects carrying one or more ApoE ϵ4 allele. As indicated in **Table 1**, CN subjects scored higher than aMCI and AD subjects on all neuropsychological measures, and demonstrated less atrophy in comparison to aMCI and AD subjects on VRS-MTA and HP-v scores. AD subjects had more atrophy than aMCI subjects on VRS-MTA and HP-v measures, as well as impairment on all neuropsychological measures, with the exception of the Block Design test, in which there was no difference in scores between AD and aMCI subjects.

PERFORMANCE OF VRS-MTA vs. HP-v

For the discrimination of amnestic MCI from CN, in both the younger and older age groups, there was no difference in the areas under receiver operating curve (aROC) between HP-v measures and VRS-MTA measures ($Z = 1.26$; $p < 0.27$) (**Table 2**). For the discrimination of AD from CN, among the younger age group (63–75 years), VRS-MTA performed better than HP-v (aROC: 0.92 vs. 0.847, $p < 0.046$). The corresponding sensitivity/specificity values for VRS-MAT and HP-v were: 89.2/82.1% and 75.7/82.1% for the more liberal cutoffs described in the methods. There was no difference between the performance of VRS-MTA and HP-v in the older group, for the classification of AD vs. CN. Considering the correct age-associated cut-offs for impairment for the total sample, 63% of those subjects who did not meet criteria for impairment using HP-v, did meet criteria for impairment using VRS-MTA, and conversely, only 30% of those who were VRS-MTA negative were HP-v positive.

CORRELATIONS WITH COGNITIVE MEASURES

In a combined group of aMCI and AD subjects, who had adequate cognitive testing data, both HPv and VRS-MTA measures were strongly correlated with scores on various memory tests and with the category fluency test (a measure of speed of search from semantic lexicon) (**Table 3**). Tests of visuospatial function (block design), processing speed and attention (Trails A) and executive

Table 1 | Demographics and MRI measures.

	CN ($n = 107$)	aMCI ($n = 105$)	AD ($n = 56$)	*f*-value
Age	71.1^{c} (5.8)	77.9^{b} (5.3)	79.5^{a} (6.8)	42.59***
Education	15.0^{a} (3.2)	12.4^{b} (3.9)	12.4^{b} (4.1)	16.71***
Gender (Female)	75.7%	50.0%	53.7%	X^2= 16.93***
Hispanic%	47.4%	48.0%	57.4%	X^2= 1.64***
ApoE%	24.7%	30.6%	42.9%	X^2= 4.13 ***
MMSE	29.0^{a} (1.1)	25.9^{b} (2.5)	22.4^{c} (3.1)	172.05***
Fuld OME	25.7^{a} (2.0)	18.9^{b} (4.8)	10.6^{c}(6.5)	195.35***
HVLT-Total Recall	25.3^{a} (4.3)	17.4^{b} (4.5)	13.2^{c} (4.7)	159.48***
HVLT-DEL	9.2^{a} (1.7)	3.7^{b} (2.9)	1.3^{c} (2.2)	258.75***
Semantic interference test (SIT) score	13.3^{a} (2.9)	8.2^{b} (3.2)	3.1^{c}(3.0)	209.04***
Visual reproduction test-delayed	23.0^{a} (7.9)	8.3^{b} (7.2)	3.4^{c} (5.7)	149.08***
Memory for Passages (Delayed)	11.5^{a} (3.5)	5.6^{b} (3.7)	2.2^{c} (3.0)	149.92***
Two Category Fluency	34.2^{a} (7.3)	24.1^{b} (6.2)	17.2^{c} (5.9)	134.24***
Block Design- WAIS-IV	31.5$_{a}$ (9.4)	19.11^{b} (7.9)	18.8^{b} (7.8)	64.39***
Trails A	35.9^{a} (11.3)	54.5^{b} (23.9)	73.5^{c} (33.5)	55.04***
Trails B	95.1^{a} (48.2)	199.4^{b} (88.6)	254.1^{c} (73.7)	106.58***
HP-v (most impaired side)	0.00275^{a} (0.0003)	0.00240^{b} (0.004)	0.00208^{c} (0.005)	60.3***
VRS-MTA score (most impaired side)	1.7^{a} (1.8)	4.2^{b} (2.7)	6.9^{c} (3.3)	81.31***

CN, Cognitively normal; aMCI, amnestic cognitive impairment; MMSE, Mini-mental status exam; HVLT, Hopkins verbal learning test; HP-v, Hippocampal volume; VRS-MTA, Visual rating scale-mdial temporal atrophy. $^{***}p < 0.001$; means with different superscripts are statistically different at $p < 0.05$ by the Tukey-Kramer test.

Table 2 | HP-v and VRS-MTA measures in the classification of subjects with Amnestic MCI and Alzheimer's disease.

Diagnostic comparison and age group	Sensitivity/Specificity (%) for HP-v	aROC for HP-v measure	Sensitivity/Specificity (%) for VRS-MTA	aROC for VRS-MTA measure	Comparison of aROCs for Hp-v and VRS-MTA
AMNESTIC MILD COGNITIVE IMPAIRMENT VERSUS ELDERLY NORMAL					
63–75 years ($n = 60$)	35.0/82.1	0.652 ($SE = 0.06$)	55.0/82.1	0.723 ($SE = 0.06$)	$Z = 1.38$; $p > 0.26$
76+ years ($n = 45$)	60.0/81.6	0.764 ($SE = 0.05$)	51.1 /78.2	0.736 ($SE = 0.05$)	$Z = 0.60$; $p > 0.54$
ALZHEIMER'S DISEASE VERSUS ELDERLY NORMAL					
63–75 years ($n = 37$)	75.7/82.1	0.847 ($SE = 0.05$)	89.2/82.1	0.920 ($SE = 0.03$)	$Z = 2.00$; $p < 0.046$
76+ years ($n = 19$)	63.2/81.6	0.713 ($SE = 0.08$)	68.4/78.2	0.853 ($SE = 0.04$)	$Z = 1.66$; $p < 0.10$

HP-v, hippocampal volume; VRS-MTA, Visual rating system- medial temporal atrophy; aROC, Area under the receiver operating curve; AD, Alzheimer's disease; MCI, amnestic MCI; CN, Cognitively normal.

Table 3 | Comparative correlations between volumetric and VRS-MTA measures among 129 cognitively impaired patients.

	Correlation with HP-v	Correlation with VRS-MTA	Test of difference in correlations coefficients[#]	*p*-value
Fuld object memory evaluation	0.35***	−0.51***	2.33	<0.011
HVLT (Delayed Recall)	0.15	−0.29***	1.91	<0.030
WMS- memory for passages (Delayed Recall)	0.20*	−0.36***	2.27	<0.013
WMS-visual reproduction (Delay Recall)	0.33***	−0.47***	1.96	<0.027
Two word category fluency	0.31***	−0.32***	0.14	446
Trails A	−0.14	0.07	NA	NA
Trails B	−0.05	0.11	NA	NA
Block-design WAIS-II	0.05	−0.09	NA	NA
Similarities WAIS-R	−0.10	0.09	NA	NA

*HP-v, hippocampal volume; VRS-MTA, Visual rating system-medial temporal atrophy. [#] Difference in correlations tested using SISA polynomials (Uitenbroek, 1997)/ *$p < 0.05$, ***$p < 0.001$.*

function (Trails B) were not correlated significantly with HP-v or VRS-MTA imaging measures. In most instances the memory measures (using the Fuld OME, for example) were more strongly correlated with VRS-MTA ($r = -0.51$) than with HP-v ($r = -0.35$) ($t = 2.33$; $p < 0.02$) (**Table 3**).

PROGRESSION FROM aMCI TO AD

Among a sample of aMCI subjects ($n = 72$; mean age $= 76.8 \pm 5.8$ years: educational attainment $= 12.83 \pm 3.6$ years) with adequate follow-up data (mean follow-up period $= 33.1 \pm 14.1$ months) the percentage of progressors vs. non-progressors to AD was predicted using both stringent and liberal VRS-MTA cut-off scores (**Table 4**). Using stringent VRS-MTA criteria, 51% of aMCI subjects scoring at or above the impairment cut-off were found to be progressors, as compared to 21% scoring at or above the impairment cut-off being non-progressors ($\chi^2 = 5.51$; $p = 0.019$). In contrast, for HP-v 41 % of aMCI subjects scoring at or above the impairment cut-off were found to be progressors, as compared to 29% scoring at or above the stringent impairment cut-offs being non-progressors ($\chi^2 = 1.19$; $p = 0.28$).

Table 4 | VRS-MTA score, HP-v and progression from aMCI to AD.

	Progressors to AD	Non-progressors	Chi-square	*p*-value
VRS-MTA score (Conservative criteria)	50.7%	20.6%	5.51	0.019
HP-v (Conservative criteria)	44.1%	28.9%	1.19	0.275

HP-v, hippocampal volume; VRS-MTA, Visual rating system-medial temporal atrophy.

DISCUSSION

In this study, we showed that VRS-MTA is superior to volumetric assessment of the HP (HP-v) for distinguishing aMCI patients and normal elderly controls. When we divided the subjects into "young-old" (63–75 years) and "older-old" (76 years+) subgroups, our previous findings hold true, in much smaller groups of subjects (Duara et al., 2008; Shen et al., 2011). We have also shown that VRS-MTA ratings correlate more strongly than do HP-v with memory measures and CDR ratings (Shen et al., 2011). In this study, we have additionally provided age-corrected cut-scores for HP-v and VRS–MTA scores for classifying subjects with

aMCI and AD and have shown that VRS-MTA scores, but not HP-v scores in this cohort, were predictors of progression from aMCI to AD.

The use of structural MRI scans as biomarkers, in association with clinical criteria, for distinguishing CN subjects from those with incipient or Probable AD requires the use of age-adjusted cut- scores for research and for clinical practice. For the first time, to our knowledge, we have shown that specific age-related cut-scores for VRS-MTA and HP-v measures can be used for distinguishing CN from AD subjects. By deriving scores for the most impaired hemisphere, based upon age-related norms, we may have further enhanced the overall sensitivity of VRS-MTA. Indeed, almost two thirds of those subjects who did not meet criteria for impairment using HP-v, did meet criteria for impairment using VRS-MTA, and conversely, less than a third of those who were VRS-MTA negative were HP-v positive. Thus, each measure provides unique information, most notably VRS MTA, which includes independent and additive measures of the HP, ERC, and PRC.

An advantage of using VRS-MTA over HP-v is that regional brain volumes are variable across individuals and need to be normalized by conversion to a ratio of the absolute volume of the HP to intracranial volume, whereas VRS-MTA has built–in normalization and thus avoids multiplicative errors inherent in using ratios of two quantitative variables. From the clinician's vantage point, VRS-MTA has the following additional desirable attributes: (1) measurement and scoring of VRS-MTA is quick and reliable by the clinician, providing a distinct advantage over traditional volumetric techniques; (2) HP-v measurements, as compared to VRS-MTA measurements, require much greater technical stringency in the acquisition of the MRI scans and are far more vulnerable to a variety of measurement errors; (3) HP-v measurements require a technical interface for obtaining quantitative assessment whereas VRS-MTA does not (Duara et al., 2008; Shen et al., 2011). Although volumetric analysis of regional brain atrophy can be performed by a variety of programs which are widely available, they have been used almost exclusively in research applications, and not in clinical practice. Currently, measurement of HP-v is inconvenient and expensive in time and money and technical problems that often occur during the image acquisition protocol may invalidate the use of a substantial proportion of MRI scans performed in the community.

From a biological standpoint it is clear that hippocampal atrophy is non-specific and that the characteristic pathological changes in AD (Braak and Braak, 1985; Braak et al., 2006) begin outside the HP, with development of neurofibrillary tangles in the transentorhinal and entorhinal cortex, spreading subsequently to the subiculum and CA1 regions of the HP. Subsequent spread of pathology occurs to limbic, and ultimately to neocortical regions, such as the precuneus, middle frontal gyrus and posterior cingulate gyrus. The severity of this atrophy, at least in the medial temporal regions, correlates with the severity of underlying AD-related neuropathological changes seen on postmortem (Jack et al., 2002).

The use of VRS-MTA methodology affords a unique perspective, not available to those using quantitative HP-v measures, of the presence and severity of the neurodegenerative process in AD. Atrophy of the entorhinal and perirhinal cortices and the HP, widening of the collateral sulcus and atrophy of the white matter band between the subiculum and the ERC are well known pathological features of AD and are readily visible on appropriately obtained MRI scans acquired or reconstructed in the coronal plane in thin, contiguous brain slices. This information often times serves to confirm the clinical diagnosis, especially in a patient in which non-neurodegenerative causes of cognitive impairment, such as cerebrovascular disease or psychiatric conditions are also under consideration. The absence of confirmatory neurodegenerative findings on the MRI scan alerts the clinician to alternative causes of impaired cognitive performance, such as systemic disorders, attention deficit disorders, sleep-apnea syndrome, depression, anxiety, and cultural or language related factors.

The current investigation has the following advantages over previous studies: (1) Optimal age- related cut-scores for VRS-MTA and HP-v have been derived for normal subjects and then applied to aMCI and AD cases; (2) the importance of frequently-observed asymmetrical atrophy in medial temporal regions and HP-v volumes has been recognized and incorporated into the algorithm for distinguishing CN from aMCI and AD subjects, using either VRS-MTA or HP-v measures (typically, rather than using the most atrophic side in the algorithm, bilateral regions are combined into a single score). Using these methods our results indicate that VRS-MTA is at least as good, and more likely better than using HP-v for distinguishing both younger and older aMCI and AD subjects from CN subjects. VRS-MTA scores are also better correlated than are HP-v measures with memory and functional indices. Finally, VRS-MTA measures are better than HP-v measures in predicting progression to AD or dementia over a defined period of time. This suggests that VRS-MTA may provide a clearer indication of neurodegenerative pathology related to AD than merely HP-v.

Some of the limitations of using VRS-MTA include the fact that ratings are based on assessments performed on a single coronal slice, thereby providing a limited perspective of overall brain pathology (this limitation can be easily overcome by evaluating multiple adjacent coronal slices). In addition, atrophy in the medial temporal regions may not be specific to AD, but in some cases may be indicative of hippocampal sclerosis, frontotemporal lobar dementias, Lewy body dementia, vascular dementia, or cognitive impairment (Jack et al., 2002; Barkhof et al., 2007). Also, a larger and more diverse group of elderly normals will be required to extend age-related cut-off scores further than we have been able to do in this study. Age is a risk factor for AD and other neurodegenerative disorders and up to 30% elderly adults with underlying brain pathology may have sufficient cognitive reserve so that they do not present with cognitive symptoms. Hence, it is likely that among elderly volunteers, who are cognitively normal, substantial AD pathology is present, which may be reflected in their VRS-MTA scores, thereby apparently reducing the specificity of VRS-MTA cut-off scores.

At present, the primary utility of structural MRI, in the diagnosis of disorders causing cognitive impairment, is to rule out specific pathologies such as pathologies as hydrocephalus, vascular, inflammatory or demyelinating, and space-occupying lesions as the cause of the cognitive syndrome, but not for confirming the presence of AD-like pathology and its severity. Our results suggest that VRS-MTA, which could readily be incorporated into the routine assessment of patients presenting with memory symptoms, will likely assist in strengthening the diagnosis of AD or ruling it out, thereby improving both sensitivity and specificity of a clinical diagnosis of probable and prodromal AD. Moreover, VRS-MTA need not be used exclusively for clinical purposes; it could also serve as a research tool, especially in clinical trials when accuracy of the clinical diagnosis is a major requirement.

ACKNOWLEDGMENTS

Research was supported by the National Institute of Aging, NIH 5R01AG020094-03 and NIH 1P50AG025711-03, & Byrd Alzheimer Center and Research Institute grants. Statistical analysis was performed by David A. Loewenstein, Ph.D., University of Miami.

REFERENCES

Albert, M. S., Dekosky, S. T., Dickson, D., Dubois, B., Feldman, H. H., Fox, N. C., et al. (2011). The diagnosis of mild cognitive impairment due to Alzheimer's disease: recommendations from the National Institute on Aging-Alzheimer's Association workgroups on diagnostic guidelines for Alzheimer's disease. *Alzheimers Dement.* 7, 270–279. doi: 10.1016/j.jalz.2011.03.008

Alemán-Gómez, Y., Melie-García, L., and Valdés-Hernandez, P. (2006). "IBASPM: Toolbox for automatic parcellation of brain structures," in *Presented at the 12th Annual Meeting of the Organization for Human Brain Mapping* (Florence). Available on CD-Rom in NeuroImage, Vol. 27, No.1.

Appel, J., Potter, E., Bhatia, N., Shen, Q., Zhao, W., Greig, M. T., et al. (2009). Association of white matter hyperintensity measurements on brain MR imaging with cognitive status, medial temporal atrophy, and cardiovascular risk factors. *AJNR Am. J. Neuroradiol.* 30, 1870–1876. doi: 10.3174/ajnr.A1693

Army Individual Test Battery (1944). *Manual of Directions And Scoring.* Washington, DC: War Department, Adjutant General's Office.

Barkhof, F., Polvikoski, T. M., van Straaten, E. C., Kalaria, R. N., Sulkava, R., Aronen, H. J., et al. (2007). The significance of medial temporal lobe atrophy: a postmortem MRI study in the very old. *Neurology* 69, 1521–1527. doi: 10.1212/01.wnl.0000277459.83543.99

Beekly, D. L., Ramos, E. M., Lee, W. W., Deitrich, W. D., Jacka, M. E., Wu, J., et al. (2007). NIA Alzheimer's Disease Centers. The National Alzheimer's Coordinating Center (NACC) database: the Uniform Data Set. *Alzheimer Dis. Assoc. Disord.* 21, 249–158. doi: 10.1097/WAD.0b013e318142774e

Benedict, R. H. B., Schretlen, D., Groninger, L., and Brandt, J. (1998). Hopkins verbal learning test-revised: normative data and analysis of inter-form and test-retest reliability. *Clin. Neuropsychol.* 12, 43–55. doi: 10.1076/clin.12.1.43.1726

Braak, H., and Braak, E. (1985). On areas of transition between entorhinal allocortex and temporal isocortex in the human brain. Normal morphology and lamina-specific pathology in Alzheimer's disease. *Acta Neuropathol. (Berl.)* 68, 325–332. doi: 10.1007/BF00690836

Braak, H., Alafuzoff, I., Arzberger, T., Kretzschmar, H., and Del Tredici, K. (2006). Acta Staging of Alzheimer disease-associated neurofibrillary pathology using paraffin sections and immunocytochemistry. *Neuropathol.* 112, 389–404. doi: 10.1007/s00401-006-0127-z

Cummings, J. L., Mega, M., Gray, K., Rosenberg-Thompson, S., Carusi, D. A., and Gornbein, J. (1994). The neuropsychiatric inventory: comprehensive assessment of neuropathology in dementia. *Neurology* 44, 2308–2314. doi: 10.1212/WNL.44.12.2308

Duara, R., Loewenstein, D. A., Greig, M., Acevedo, A., Potter, E., Appel, J., et al. (2010). Reliability and validity of an algorithm for the diagnosis of normal cognition, MCI and dementia: implications for multi-center research studies. *Am. J. Geriatr. Psychiatry*. 18, 363–370. doi: 10.1097/JGP.0b013e3181c534a0

Duara, R., Loewenstein, D. A., Potter, E., Appel, A., Greig, M. T., Urs, R., et al. (2008). Medial temporal lobe atrophy on MRI scans and the diagnosis of Alzheimer disease. *Neurology* 71, 1986–1992. doi: 10.1212/01.wnl.0000336925.79704.9f

Fahn, S., and Elton, R. (1987). "Unified Parkinson's disease rating scale," in *Recent Developments in Parkinson Diseases*, eds S. Fahn, D. Marsden, and D. Calne (London: Macmillan), 153–163.

Folstein, M., Folstein, S., and McHugh, P. (1975). Mini-mental state. A practical method for grading the cognitive state of patients for the physician. *J. Psychiatr. Res.* 12, 189–198. doi: 10.1016/0022-3956(75)90026-6

Frisoni, G. B., Fox, N. C., Jack, C. R. Jr., Scheltens, P., and Thompson, P. M. (2010). The clinical use of structural MRI in Alzheimer disease. *Nat. Rev. Neurol.* 6, 67–77. doi: 10.1038/nrneurol.2009.215

Fuld, P. A. (1981). *Fuld Object-Memory Evaluation*. Illinois, IL: Stoelting Co.

Jack, C. R., Dickson, D. W., Parisin, J. E., Xu, Y. C., Cha, R. H., O'Brien, P. C., et al. (2002). Antemortem MRI findings correlate with hippocampal neuropathology in typical aging and dementia. *Neurology* 58, 750–757. doi: 10.1212/WNL.58.5.750

Loewenstein, D. A., Acevedo, A., Potter, E., Schinka, J. A., Raj, A., Greig, M. T., et al. (2009). Severity of medial temporal atrophy and amnestic mild cognitive impairment: selecting type and number of memory tests. *Am. J. Geriatr. Psychiatry* 17, 1050–1058. doi: 10.1097/JGP.0b013e3181b7ef42

McGill University. (2009). Montreal, QC. Available online at: http://www.bic.mni.mcgill.ca/brainweb/ (Accessed June 12, 2006; July 1, 2009).

McKhann, G., Drachman, D. A., Folstein, M. F., Katzman, R., Price, D. L., and Stadlan, E. (1984). Clinical diagnosis of Alzheimer's disease: report of the NINCDS-ADRDA Work Group under the auspices of the Department of Health and Human Services Task Force on Alzheimer's disease. *Neurology* 34, 939–944. doi: 10.1212/WNL.34.7.939

Monsch, A. Y., Bondi, M. W., Butters, N., Salmon, D. P., Katzman, R., and Thal, L. (1992). Comparison of verbal fluency tasks in the detection of dementia of the Alzheimer's type. *Arch. Neurol.* 49, 1253–1258. doi: 10.1001/archneur.1992.00530360051017

Morris, J. C. (1993). The clinical dementia rating (CDR), Current version and scoring rules. *Neurology* 43, 2412–2414. doi: 10.1212/WNL.43.11.2412-a

Morris, J. C. (2006). Mild cognitive impairment is early-stage Alzheimer disease: time to revise diagnostic criteria. *Arch. Neurol.* 63, 15–16. doi: 10.1001/archneur.63.1.15

Petersen, R. C., Smith, G. E., Waring, S. C., Ivnik, R. J., Tangalos, E. G., and Kokmen, E. (1999). Mild cognitive impairment: clinical characterization and outcome. *Arch. Neurol.* 56, 303–308. doi: 10.1001/archneur.56.3.303

Scheltens, P., Launer, L. J., Barkhof, F., Weinstein, H. C., and van Gool, W. A. (1995). Visual assessment of medial temporal lobe atrophy on magnetic resonance imaging: interobserver reliability. *J. Neurol.* 242, 557–560. doi: 10.1007/BF00868807

Sheikh, J. I., and Yesavage, J. A. (1986). "Geriatric Depression Scale (GDS): recent evidence and development of a shorter version," in *Clinical Gerontology: A Guide to Assessment and Interventions*, ed T. L. Brink (New York, NY: The Haworth Press), 165–173.

Shen, Q., Loewenstein, D., Potter, E., Zhao, W., Appel, J., Greig, M., et al. (2011). Volumetric and visual rating of MRI scans in the diagnosis of amnestic MCI and Alzheimer's Disease. *Alzheimers Dement.* 7, 101–108. doi: 10.1016/j.jalz.2010.07.002

Sperling, R. A., Aisen, P. S., Beckett, L. A., Bennett, D. A., Craft, S., Fagan, A. M., et al. (2011). Toward defining the preclinical stages of Alzheimer's disease: recommendations from the National Institute on Aging-Alzheimer's Association workgroups on diagnostic guidelines for Alzheimer's disease. *Alzheimers Dement.* 7, 280–292. doi: 10.1016/j.jalz.2011.03.003

Urs, R., Potter, E., Barker, W., Appel, J., Loewenstein, D. A., Zhao, W., et al. (2009). Visual rating system (VRS) for assessing magnetic resonance images (MRIs): a tool in the diagnosis of MCI and

Alzheimer's disease. *J. Comput. Assist. Tomogr.* 33, 73–78. doi: 10.1097/RCT.0b013e31816373d8

Uitenbroek, D. G. (1997). *SISA Binomial.* Southampton: D.G. Uitenbroek. Available online at: http://www.quantitativeskills.com/sisa/distributions/binomial.htm (Accessed January 01, 2004)

Wechsler, D. (1987). *The Wechsler Memory Scale-Revised.* San Antonio, TX: The Psychological Corporation.

Wechsler, D. (1997). *The Wechsler Adult Intelligence Scale*, *3rd Edn.* San Antonio, TX: The Psychological Corporation.

Wenham, P. R., Price, W. H., and Blandell, G. (1991). Apolipoprotein E genotyping by one-stage PCR. *Lancet* 337, 1158–1159. doi: 10.1016/0140-6736(91)92823-K

Conflict of Interest Statement: The authors declare that the research was conducted in the absence of any commercial or financial relationships that could be construed as a potential conflict of interest.

Received: 21 June 2013; accepted: 20 August 2013; published online: 18 September 2013.
*Citation: Duara R, Loewenstein DA, Shen Q, Barker W, Varon D, Greig MT, Curiel R, Agron J, Santos I and Potter H (2013) The utility of age-specific cut-offs for visual rating of medial temporal atrophy in classifying Alzheimer's disease, MCI and cognitively normal elderly subjects. Front. Aging Neurosci. **5**:47. doi: 10.3389/fnagi.2013.00047*
This article was submitted to the journal Frontiers in Aging Neuroscience.

frontiers in
AGING NEUROSCIENCE

ORIGINAL RESEARCH ARTICLE
published: 02 April 2013
doi: 10.3389/fnagi.2013.00012

Refining the diagnosis of Huntington disease: the PREDICT-HD study

Kevin M. Biglan[1], Ying Zhang[2], Jeffrey D. Long[3], Michael Geschwind[4], Gail A. Kang[4], Annie Killoran[1], Wenjing Lu[2], Elizabeth McCusker[5], James A. Mills[3], Lynn A. Raymond[6], Claudia Testa[7], Joanne Wojcieszek[8], Jane S. Paulsen[3]*, and the PREDICT-HD Investigators of the Huntington Study Group

[1] *Department of Neurology, University of Rochester, Rochester, NY, USA*
[2] *Department Biostatistics, University of Iowa, Iowa City, IA, USA*
[3] *Department of Psychiatry, University of Iowa, Iowa City, IA, USA*
[4] *Department of Neurology, University of California San Francisco, San Francisco, CA, USA*
[5] *Department of Neurology, Westmead Hospital, Sydney, NSW, Australia*
[6] *Division of Psychiatry, University of British Columbia, Vancouver, BC, Canada*
[7] *VCU Parkinson's and Movement Disorders Center Virginia Commonwealth University, Richmond, VA, USA*
[8] *Department of Neurology, Indiana University, Indianapolis, IN, USA*

Edited by:
Manuel Menéndez-González, Hospital Álvarez-Buylla, Spain

Reviewed by:
Hiroshi Morita, Sinshu University, Japan
Katsutoshi Furukawa, Tohoku University, Japan
Diego Ruano, University of Sevilla, Spain
Andrea Ciarmiello, S. Andrea Hospital ASL5 Spezzino, Italy

***Correspondence:**
Jane S. Paulsen, Department of Psychiatry, Roy J. and Lucille A. Carver College of Medicine Research, The University of Iowa, 1-305 Medical Education Building, Iowa City, IA 52242-1000, USA.
e-mail: jane-paulsen@uiowa.edu

Participants with the gene expansion for Huntington disease (HD) but not yet diagnosed were evaluated annually. Unidimensional diagnosis (UD) was a motor diagnosis defined as a diagnostic confidence level (DCL) of 4 (unequivocal motor signs, ≥99% confidence) on the standardized motor exam of the Unified Huntington Disease Rating Scale (UHDRS). Multidimensional diagnosis (MD) was defined as answering yes on Question 80 (Q80) of the UHDRS, ≥99% confidence of manifest HD based on the *entire* UHDRS. Motor, cognitive, and behavioral measures of phenotype at first diagnosis were compared by t-tests between participants diagnosed via motor exam (UD) and those diagnosed via multidimensional input (MD). Cluster analysis identified clusters based on UHDRS domains.186 participants received a diagnosis of HD during a maximum of 6.4 years of follow-up. In 108 (58.1%) the diagnosis by MD and UD occurred simultaneously, while in 69 (37.1%) the diagnosis by MD occurred prior to UD. Participants who were diagnosed by MD prior to UD were less impaired on motor (12.2 ± 6.7 vs. 22.4 ± 9.3, $p < 0.0001$), and cognitive (290.7 ± 56.2 vs. 258.0 ± 53.7, $p = 0.0002$), but not behavioral measures (16.3 ± 21.2 vs. 18.6 ± 22.1, $p = 0.49$) when compared with those diagnosed simultaneously. Cluster analysis identified three clusters that represented primarily cognitively impaired, behaviorally impaired, and cognitively preserved phenotypes. A multidimensional method results in an earlier diagnosis with less motor and cognitive impairment than a motor diagnosis. Findings have implications for designing preventive trials and providing clinical care in prodromal HD.

Keywords: Huntington's disease, trinucleotide repeat diseases, cohort studies, natural history studies, outcome research

INTRODUCTION

Huntington disease (HD) is an adult-onset, autosomal dominant, progressive, and fatal neurodegenerative disease characterized by the clinical triad of a movement disorder, cognitive decline, and behavioral disturbances caused by a cytosine-adenine-guanine (CAG) repeat in the 5′-translated region of the gene on the short arm of chromosome 4 (Duyao et al., 1993). The precise point of disease diagnosis is poorly characterized, with clinical abnormalities emerging gradually over many years during a "pre-manifest" or prodromal phase (Huntington Study Group, 2006; Paulsen et al., 2006).

A challenge of therapeutic research is in the identification of treatments that impact the manifestation of disease in individuals at varying stages of disease progression. For the neurodegenerative diseases, much effort has been devoted to early identification and staging using clinical outcome measures or biomarkers. For instance, there are widespread efforts to detect "mild cognitive impairment" prior to dementia so that therapeutics might be considered before extensive cell death has occurred. Even in HD, in which a cohort can be identified years prior to diagnosis, challenges remain in designing trials aimed at delaying illness progression. The Neurobiological Predictors of Huntington's Disease (PREDICT-HD) study is a longitudinal prospective evaluation in individuals at risk for HD with known gene status.

Abbreviations: AD, Alzheimer disease; CAG, cytosine-adenine-guanine; DCL, diagnostic confidence level; HD, Huntington disease; PREDICT-HD, Neurobiological Predictors of Huntington's Disease; Q80, Question 80; SDM, symbol digit modalities; TFC, Total Functional Capacity; UHDRS, Unified Huntington Disease Rating Scale.

The PREDICT-HD study should help identify outcomes for use in trials aimed at delaying the manifestation of illness in prodromal HD. However, in order to show that an intervention can delay disease, there needs to be consensus on how to best define the clinical diagnosis of HD. The traditional method of HD diagnosis rests on the motor manifestation of disease though the cognitive and psychiatric aspects of HD have been recognized for decades. Efforts toward more refined disease staging may be improved with a more comprehensive consideration of HD. Therefore, we compared two methods of diagnosis in the PREDICT-HD cohort: a multidimensional diagnosis (MD) and a unidimensional diagnosis (UD) or motor diagnosis.

MATERIALS AND METHODS

All aspects of the study were approved by the Institutional Review Board at each participating institution. Participants signed consents for participation and to release their de-identified data for analyses.

OVERVIEW OF PREDICT-HD

The PREDICT-HD study is designed to prospectively characterize refined clinical, neurobiological, and neurobehavioral markers of HD prior to the point of traditional motor diagnosis in a population known to carry the HD CAG expansion (Paulsen et al., 2006). Participants at risk for HD were recruited from 32 sites in the United States, Canada, Australia, and Europe beginning in 2001. All participants were required to have voluntarily undergone genetic testing for the HD CAG expansion independent from the study. Participants were evaluated annually with standardized assessments of motor, cognition, behavior, function, and clinical diagnosis.

Only individuals with the HD CAG expansion and without manifest disease (prodromal HD) as defined by the absence of unequivocal motor signs (diagnostic confidence level of less than 4 on question 17 of the UHDRS, **Table 1A**) on their initial examination were included in the current analysis. Control subjects were those participants who had tested negative for the HD CAG expansion and had participated in at least two visits. For purposes of this analysis, the last visit in controls was used for comparison with cases.

Table 1 | The Unified Huntington Disease Rating Scale diagnostic confidence level and Q80 diagnostic criteria.

A. Diagnostic confidence level

To what degree are you confident that this person meets the operational definition of the unequivocal presence of an otherwise unexplained extrapyramidal movement disorder (e.g., chorea, dystonia, bradykinesia, rigidity) in a subject at risk for HD?

0 = normal (no abnormalities)
1 = non-specific motor abnormalities (less than 50% confidence)
2 = motor abnormalities that may be signs of HD (50–89% confidence)
3 = motor abnormalities that are likely signs of HD (90–98% confidence)
4 = motor abnormalities that are unequivocal signs of HD (≥99% confidence)

B. Q80 diagnostic criteria

Based on the entire UHDRS (Motor, Cognitive, Behavioral, and Functional components) do you believe with a confidence level ≥99% that this participant has manifest HD? (0 = No, 1 = Yes)

CLINICAL ASSESSMENTS

Huntington disease clinical diagnosis

Motor Diagnosis: The Huntington Disease Rating Scale (UHDRS) diagnostic confidence level (DCL) is the standard measure used for clinical diagnosis in at-risk individuals and is based solely on the motor evaluation. It is a categorical scale (**Table 1A**) with a range from 0 (normal) to 4 (unequivocal signs of HD, ≥99% confidence ≥ on the part of the examiner). The DCL has previously shown fair inter-rater reliability (weighted kappa = 0.67, SE = 0.09) (Hogarth et al., 2005). Participants had a clinical diagnosis of HD at the time of the first rating of a DCL = 4.

Multidimensional Diagnosis: Question 80 (Q80) of the UHDRS asks raters to take into account all aspects of the UHDRS (motor, cognitive, behavioral, and functional) and to make a decision (yes or no) whether a subject has a diagnosis of HD with a confidence level 99% (**Table 1B**). The first occurrence of Q80 = yes was the multidimensional diagnostic criteria used for the current analyses.

The primary analysis compared participants who were diagnosed by MD prior to receiving a diagnosis by UD with participants who received a diagnosis of MD and UD simultaneously. A small proportion of individuals received a diagnosis by UD prior to MD and these participants were not included in the analysis.

UNIFIED HUNTINGTON DISEASE RATING SCALE OUTCOMES

The current analyses focused solely on the UHDRS assessments, since UD is rated on the motor UHDRS only and MD specifically asks raters to make a determination based on the entirety of the Hungtington Study Group (1996). The motor UHDRS assessed for the presence and severity of motor features (Hungtington Study Group, 1996). The motor UHDRS is a standardized assessment consisting of 31 items rated on a scale from 0 to 4 with a score of 0 indicating no abnormalities and 4 indicating the most severe impairment. The maximum possible total score is 124. Previously motor scores have been shown to distinguish controls from prodromal HD cases and subtle motor abnormalities were associated with closer estimated diagnosis of disease (Biglan et al., 2009). In manifest HD, oculomotor, rigidity, chorea, dystonia, and bradykinesia domains have been identified and were used to clarify if specific motor features were associated with specific clusters at time of clinical diagnosis (Marder et al., 2000).

The cognitive section of the UHDRS includes verbal fluency, symbol digit modalities test, and Stroop word, color, and interference tests (Hungtington Study Group, 1996; Biglan et al., 2009). Each of these cognitive tests has been shown to distinguish gene mutation carriers from controls in prodromal HD (Paulsen et al., 2008; Stout et al., 2011). Total cognitive scores are calculated by summing the five individual scores in the UHDRS cognitive domain.

The behavioral section of the UHDRS consists of 11 items evaluating various behavioral signs and symptoms. Individuals are

ranked on both severity and frequency on a 0 to 4 scale with 0 being not present and 4 being severe and frequent (Hungtington Study Group, 1996). Total behavioral scores are calculated by summing the severity and frequency items and ranges from 0 (no behavioral symptoms) to 88 (most severe behavioral symptoms).

The functional section of the UHDRS includes the Functional Assessment Scale, Independence Scale, and the Total Functional Capacity (TFC) (Hungtington Study Group, 1996). The TFC is a standard assessment of overall function in HD and has a demonstrated reliability for indexing progression in various diagnosed HD populations (Marder et al., 2000; Huntington Study Group, 2001). The TFC rates individuals' function on the following domains: occupation, handling finances, domestic chores, and activities of daily living. The TFC ranges from 13 (normal function) to 0 (complete loss of function). In prodromal HD, there is a strong tendency for participants to have the maximum score, as most have normal function; thus the TFC was treated as a dichotomous variable (TFC < 13) to indicate whether an individual has some kind of impairment in functionality for daily living (Paulsen et al., 2010). For assessment of employment status UHDRS item #43 (ability to work at accustomed employment) and item #44 (ability to work at any employment) were used.

STATISTICAL ANALYSIS

Kaplan-Meier curves were generated to describe the probability of being diagnosis-free over time and to evaluate the temporal relationship between incident diagnoses using the different diagnostic criteria.

UHDRS total motor, total cognitive, and total behavioral scores at the time of incident diagnosis were compared between the different diagnostic groups using *t*-tests.

Chi-square tests were used to compare differences in the frequency of diagnosis by the same vs. different raters between the different diagnostic groups.

To evaluate the factors associated with diagnosis in those participants who received a diagnosis of MD prior to UD, K-mean clustering with the pseudo-F statistic criterion was performed to identify categories of participants (clusters) at the time of diagnosis. The UHDRS total motor score, total cognitive score, and total behavior score at diagnosis were used in the cluster analysis. In order to ascertain if raters utilized participants' functional status in the diagnostic decision, TFC, and employment status were compared across the clusters. To determine if specific motor features were associated with different clusters, the sum of each motor domain was compared across clusters. The ANOVA, Fisher Exact Tests, or Kruskall-Wallis Test were performed as appropriate to determine the difference between the clusters and the control group and *post-hoc* pairwise comparisons using *t*-tests or chi-square tests, corrected for multiple comparisons (alpha < 0.01) to determine the statistical ordering among the groups.

RESULTS

Since 2001, a total of 1054 individuals have been enrolled in the PREDICT-HD study. Of these participants, 821 (78%) carried the CAG expansion and were considered prodromal (DCL < 4) at baseline. A total of 233 (22%) of the participants enrolled did not carry the CAG expansion (controls); of these, 194 had at least two follow-up visits.

Over a mean follow-up of 3.1 years (SD $= 1.4$ years and range $= 6.4$ years) a total of 186 CAG expanded participants (23% of total CAG expanded) received a first diagnosis of manifest HD by either diagnostic criteria (MD or UD). Of these diagnosed individuals, 108 (58.1%) received a diagnosis by UD and MD simultaneously, 69 (37.1%) by MD prior to UD, and 9 (4.8%) by UD prior to MD. **Figure 1** shows the Kaplan-Meier estimates of the diagnosis-free probability curves over 6 years of follow-up for diagnosis based on the UD and MD criteria.

Of those diagnosed, 148 (79.6%) had the same rater, whereas 38 (20.4%) had different raters for UD and MD. DCL $= 4$ and Q80 diagnoses were more likely to occur simultaneously when the rater was the same (89.8%). Q80 diagnosis also preceded DCL $=$ 4 diagnosis more often when the rater was the same (73.9%) (**Table 2**).

Table 3 demonstrates the clinical features at the time of diagnosis by the different criteria. Participants who were diagnosed by MD prior to UD were less impaired on UHDRS total motor scores (12.2 ± 6.7 vs. 22.4 ± 9.3, $p < 0.0001$) and on total cognitive scores (290.7 ± 56.2 vs. 258.0 ± 53.7, $p = 0.0002$) compared with individuals who received the diagnoses simultaneously.

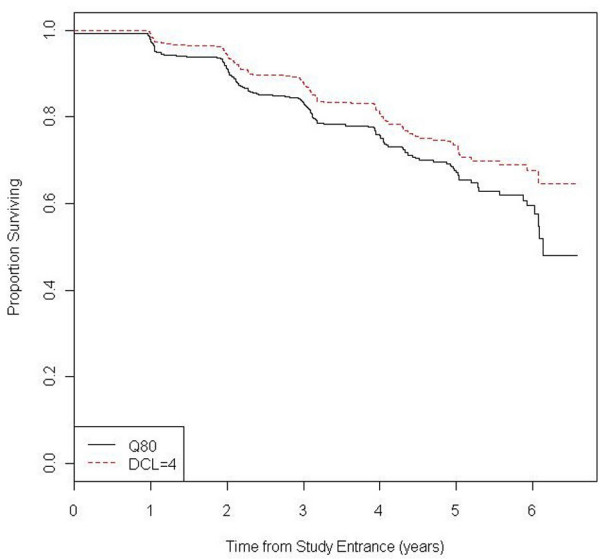

FIGURE 1 | Kaplan-Meier estimate of the probability of being diagnosis-free during follow-up by type of diagnosis (UHDRS Q80 = yes and UHDRS DCL = 4).

Table 2 | Diagnostic agreement between by same vs. different raters*,†.

Diagnosis	Same rater	Different rater	Total
Simultaneous Q80/DCL = 4	97 (89.8%)	11 (10.2%)	108
Q80 before DCL = 4	51 (73.9%)	18 (26.1%)	69
Total	148 (83.6%)	29 (16.4%)	177

*$p = 0.005$ for the comparison of clinical diagnosis by rater category.

†Does not include the 9 participants where DCL = 4 occurred before Q80.

There was no statistical difference on UHDRS behavioral scores (16.3 ± 21.2 vs. 18.6 ± 22.1, $p = 0.49$) between the two groups.

A cluster analysis using *K*-mean clustering in the participants that received MD prior to UD was performed and a three cluster solution was identified based on the pseudo-*F* statistic criterion. **Table 4** shows the mean total motor, cognitive, and behavioral scores by clusters and controls. Cluster 1 identifies a predominantly cognitively impaired phenotype because it had the lowest UHDRS cognitive mean, but the second highest behavior mean and the highest total motor mean (Cluster 1 might also be labeled as predominantly cognitive/motor). Cluster 2 identifies a predominantly behaviorally impaired phenotype as it had the highest behavior mean, but had the second highest cognitive mean and the lowest total motor mean among the gene-expanded participants. Cluster 3 represents a cognitively preserved group because the cluster had the highest cognitive mean (even higher than controls), the lowest behavior mean, and the second highest total motor mean among gene-expanded participants. All clusters had significantly worse motor scores compared with controls. A more detailed assessment of motor features using the motor sub-domains (**Table 4**) suggests that cluster 3 (cognitively preserved) had the most chorea while cluster 1 (cognitively impaired) performed the worst on the bradykinesia domain. A cluster analysis of the participants that received simultaneous diagnoses identified a three-cluster solution that was qualitatively similar (i.e., cognitive, behavioral, and preserved phenotypes), except that participants performed worse on motor and cognitive measures than the same clusters in participants with MD prior to UD (results not shown). All three clusters were more likely than controls to have greater functional impairment as measured

Table 3 | Clinical features at time of diagnosis.

Variables	Q80 before DCL = 4 ($n = 69$)	Simultaneous Q80/DCL = 4 ($n = 108$)	Controls† ($n = 194$)	*p*-value*
Gender (%F)	65.7	66.7	66.0	0.89
Age (mean ± SD)	46.3 ± 9.2	46.7 ± 10.3	46.7 ± 11.1	0.81
CAG (mean ± SD)	43.1 ± 3.1	43.5 ± 3.1	20.1 ± 3.5	0.43
UHDRS motor (mean ± SD)	12.2 ± 6.7	22.4 ± 9.3	2.8 ± 3.1	<0.001
UHDRS cognition (mean ± SD)	290.5 ± 56.5	258.0 ± 53.7	341.4 ± 47.4	<0.001
UHDRS behavior (mean ± SD)	16.3 ± 21.2	18.6 ± 22.1	5.7 ± 9.3	0.49
UHDRS TFC (%<13)	31.9	48.1	7.0	0.03

**p-values are for the comparison between Q80 diagnosis before DCL = 4 and simultaneous diagnosis.*

†The values of controls were taken at the last visit.

Table 4 | Group comparisons between clusters.

Variables	Control ($n = 194$)	Cluster 1 ($n = 21$)	Cluster 2 ($n = 32$)	Cluster 3 ($n = 15$)	ANOVA *p*-value	Pair-wise comparisons (alpha 0.01)
Age						
(mean ± SD)	46.75 ± 11.13	45.70 ± 9.32	47.26 ± 9.97	44.70 ± 7.70	0.85	–
CAG						
(mean ± SD)	20.12 ± 3.45	43.58 ± 2.59	43.22 ± 3.66	42.73 ± 2.09	<0.001	Control < C1, C2, C3
UHDRS						
Total motor						
(mean ± SD)	2.75 ± 3.08	16.52 ± 5.60	9.56 ± 6.03	11.86 ± 6.78	<0.001	Control < C2, C3 < C1
Motor domains						
Oculo (mean ± SD)	0.65 ± 1.23	4.52 ± 2.36	2.34 ± 2.89	3.57 ± 3.06	<0.001	Control < C2 < C1; Control < C3
Brady (mean ± SD)	1.44 ± 1.91	6.67 ± 3.12	4.03 ± 3.10	3.79 ± 2.81	<0.001	Control < C2, C3 < C1
Rigidity (mean ± SD)	0.31 ± 0.68	0.67 ± 1.15	0.53 ± 0.72	0.92 ± 1.07	0.004	Control < C3
Dystonia (mean ± SD)	0.06 ± 0.34	1.05 ± 1.56	0.38 ± 0.87	0.43 ± 0.76	<0.001	Control < C2 < C1; C3 < C1
Chorea (mean ± SD)	0.29 ± 0.69	3.62 ± 2.52	2.28 ± 2.05	3.14 ± 2.28	<0.001	Control < C1, C3; C2 < C1
Cognition						
(mean ± SD)	341.4 ± 47.4	224.0 ± 25.7	303.8 ± 19.4	361.8 ± 22.6	<0.001	C1 < C2 < Control, C3
Behavior						
(mean ± SD)	5.69 ± 9.29	12.65 ± 18.63	20.25 ± 21.28	7.47 ± 10.05	<0.001	Control, C3 < C2

Cluster 1, predominantly cognitive; Cluster 2, predominantly behavioral; Cluster 3, cognitively preserved.

by TFC. Whereas participants in cluster 3 were more likely to be employable compared to the other clusters, this did not meet the threshold for significance and all clusters were less likely to be employable compared with controls (see Supplementary **Table e-1**).

There was no statistical difference between the clusters in the proportion of raters that were the same vs. raters who were different (see Supplementary **Table e-2**).

DISCUSSION

In participants with prodromal HD enrolled in the PREDICT-HD study, a multidimensional diagnosis occurs earlier and with less motor and cognitive impairment than a diagnosis based on the motor examination. Given the results of our analysis, a diagnosis that considers cognitive and behavioral features in addition to motor features has face validity. Therefore, compared to the traditional motor diagnosis, a multidimensional diagnosis may be a preferable outcome for use in future trials aimed at delaying the manifestation of HD.

The current analysis also identified different phenotypes in HD at the time of diagnosis: predominantly cognitively impaired (with motor impairments), predominantly behaviorally impaired, and cognitively preserved. These phenotypic clusters had motor impairments greater than controls at diagnosis despite marked differences among the clusters in cognitive and behavioral performance. Thus, while the traditional motor diagnosis selects for the identification of a predominantly motor phenotype, a multidimensional diagnosis may identify predominantly non-motor presentations.

It is unclear why certain participants were given a multidimensional diagnosis in the absence of significant impairment in cognition or behavior in cluster 3 (cognitively preserved). This was not related to worse functional performance in this group. It may be that worse chorea in this group influenced raters to make a diagnosis even when the overall motor impairment was not deemed sufficient to make a motor diagnosis; or this could reflect differences in how raters diagnose HD. In the future it may be useful to ask raters what factors influenced their diagnostic decision. It may also be beneficial to establish objective methods for diagnosis, such as the establishment of certain cut-off scores on the UHDRS.

Despite these findings, even individuals receiving a multidimensional diagnosis are being identified relatively late after the accumulation of significant clinical signs. PREDICT-HD and other studies suggest that striatal atrophy and clinical features may develop decades prior to diagnosis (Aylward et al., 2000; Thieben et al., 2002; Paulsen et al., 2008). Recently, Sperling et al. published recommendations from the National Institute for Aging and the Alzheimer's Association Working Group for the research diagnosis of preclinical Alzheimer disease (AD) (Sperling et al., 2011). They proposed a staged diagnosis for preclinical AD with the earliest stage being associated with biomarkers of AD pathophysiology (A-beta on PET or in CSF), followed by biomarker evidence of neuronal injury (atrophy on MRI) and finally the presence of subtle clinical signs that did not meet criteria for mild cognitive impairment (Albert et al., 2011). Using a similar strategy in prodromal HD, many CAG expanded individuals at the time of enrollment in PREDICT-HD already had evidence of subtle motor, cognitive, and behavioral features and would have fallen into the last preclinical stage using the AD model (Solomon et al., 2007; Beglinger et al., 2008; Biglan et al., 2009; Duff et al., 2010; Stout et al., 2011).

While HD does not yet have the same breadth of valid and specific biomarkers as the AD research community, the identification of a similar staged categorization of prodromal HD could be considered using neuroimaging biomarkers. Thus in stage 1, CAG expanded individuals would have no evidence of neuronal injury using volumetric MRI imaging or clinical signs of HD on examination; in stage 2, there would be evidence of neuronal injury as suggested by striatal atrophy on volumetric MRI but no clinical signs of HD; finally in stage 3, individuals would have subtle clinical signs but would not yet meet criteria for diagnosis. Ultimately, clinical trials aimed at delaying manifestation in prodromal HD could evaluate the impact of interventions on the progression through the proposed stages, changes in volumetric imaging variables, changes in clinical measures and finally the impact on a multidimensional diagnosis of HD.

The current analysis has many limitations and caveats. Foremost is the use of different raters for the motor and multidimensional diagnoses. This introduced bias with a higher likelihood of discrepant diagnoses when the raters were different. However, different raters were relatively Uncommon (see **Table 2**), and there was no difference in rater type amongst the three phenotypic clusters identified. Future studies using multidimensional diagnosis should either have the rater making the diagnostic rating complete all the appropriate assessments or, if multiple individuals are doing the assessments, the multidimensional diagnosis should be based on consensus after reviewing all the data.

Another limitation was that raters were not specifically trained on how to answer Q80. Differences in the timing of diagnosis and the observed clinical phenotypes may relate to differences in how raters make the assessment of a multidimensional diagnosis. Some raters may be comfortable with diagnosing HD based on the combination of subtle motor, cognitive, and behavioral signs, whereas others may put more weight solely on the motor exam. Future studies utilizing a multidimensional diagnosis will have to standardize this decision process.

The significance of a clinical diagnosis is unclear. Striatal atrophy and subtle clinical features develop decades before traditional diagnosis. In addition, while subjects at diagnosis were more functionally impaired compared with controls, most individuals continued to work full-time and have minimal functional impairment by the measures used in this study even at the time of diagnosis. It remains to be seen whether regulatory bodies will consider a delay in diagnosis as sufficient to show that an intervention is effective or whether it will be necessary to show a slowing in functional decline. If the latter proves to be true, more refined measures of function in prodromal HD will be necessary.

Finally, it is important to emphasize that the proposed diagnostic criteria is for research purposes only and not necessarily

for the clinical diagnosis of patients. The decision to render a clinical diagnosis in individuals at risk for HD is a complicated one based on clinical features of disease, patient preferences, and a detailed understanding of relevant psychosocial factors. The potential clinical and emotional impact on patients and their families of diagnosing individuals earlier and with less motor impairment remains unknown.

A multidimensional diagnosis occurs earlier and with less motor and cognitive impairment than the traditional motor diagnosis and identifies clinical phenotypes that may have predominant non-motor features. A staging system in prodromal HD, similar to that proposed in AD, may be of value. A better understanding of diagnostic decision making may allow for better standardization of diagnosis, and the development of clear criteria for research and clinical diagnoses that may be utilized as an outcome measure in future trials aimed at delaying diagnosis in prodromal HD.

ACKNOWLEDGMENTS

We thank the PREDICT-HD sites, the study participants, and the National Research Roster for Huntington Disease Patients and Families. We would also like to thank the following PREDICT-HD Contributors for their support with this research study.

Steering Committee: Jane Paulsen, Ph.D., Principal Investigator, Eric A. Epping, MD, Ph.D., Hans Johnson, Ph.D., Megan Smith, Ph.D., Janet Williams, Ph.D., RN, FAAN, Leigh Beglinger, Ph.D., Jeffrey D. Long, Ph.D., James A. Mills, MS (University of Iowa, Iowa City, IA); Elizabeth Aylward, Ph.D. (Seattle Children's Research Institute, WA); Kevin Biglan, MD (University of Rochester, Rochester, NY); Blair Leavitt, MD (University of British Columbia, Vancouver, BC, Canada); Marcy MacDonald, Ph.D. (Massachusetts General Hospital); Martha Nance, MD (Hennepin County Medical Center, Minneapolis, MN); and Cheryl Erwin, JD, Ph.D. (University of Texas Medical School at Houston).

Scientific Sections

Bio Markers: Blair Leavitt, MDCM, FRCPC (Chair) and Michael Hayden, Ph.D. (University of British Columbia); Stefano DiDonato, MD (Neurological Institute "C. Besta," Italy); Ken Evans, Ph.D. (Ontario Cancer Biomarker Network); Wayne Matson, Ph.D. (VA Medical Center, Bedford, MA); Asa Peterson, MD, Ph.D. (Lund University, Sweden), Sarah Tabrizi, MD, Ph.D. (National Hospital for Neurology and Neurology and Neurosurgery, London); Beth Borowsky, Ph.D. (CHDI); Andrew Juhl, BS, James A. Mills, MS, Kai Wang, Ph.D. (University of Iowa); and David Weir, BSc (University of British Columbia). **Brain:** Jean Paul Vonsattell, Ph.D. (Chair), and Carol Moskowitz, ANP, MS (Columbia University Medical Center); Anne Leserman, MSW, LISW, Lynn Schaul, BA, and Stacie Vik, BA (University of Iowa). **Cognitive:** Deborah Harrington, Ph.D. (Chair), Gabriel Castillo, BS, Jessica Morison, BS, and Jason Reed, BS (University of California, San Diego), Michael Diaz, Ph.D., Ian Dobbins, Ph.D., Tamara Hershey, Ph.D., Erin Foster, OTD, and Deborah Moore, BA (Washington University Cognitive Science Battery Development); Holly Westervelt, Ph.D. (Chair, Quality Control and Training, Alpert Medical School of Brown University), Jennifer Davis, Ph.D., and Geoff Tremont, Ph.D., MS (Scientific Consultants, Alpert Medical School of Brown University); Megan Smith, Ph.D. (Chair, Administration), David J. Moser, Ph.D., Leigh J. Beglinger, Ph.D., Kelly Rowe, Gloria Wenman, and Danielle Theriault, BS (University of Iowa); Carissa Gehl, Ph.D. (VA Medical Center, Iowa City, IA); Kirsty Matheson (University of Aberdeen); Karen Siedlecki, Ph.D. (Fordham University); Marleen Van Walsem (EHDN); Susan Bonner, BA, Greg Elias, BA, Mary Gover, Rachel Bernier, and Melanie Faust, BS (Rhode Island Hospital); Beth Borowski, Ph.D. (CHDI); Noelle Carlozzi (University of Michigan); Kevin Duff, Ph.D. (University of Utah); Nellie Georgiou-Karistianis (St. Vincent's Hospital, The University of Melbourne, Australia); Julie Stout, Ph.D. (Monash University, Melbourne, Australia); Herwig Lange (Air-Rahazentrum); and Kate Papp (University of Connecticut). **Functional**: Janet Williams, Ph.D. (Chair), Leigh J. Beglinger, Ph.D., Anne Leserman, MSW, LISW, Eunyoe Ro, MA, Lee Anna Clark, Nancy Downing, RN, Ph.D., Joan Laing, Ph.D., Kristine Rees, BA, Michelle Harreld, BS, and Stacie Vik, BA (University of Iowa); Rebecca Ready, Ph.D. (University of Massachusetts); Anthony Vaccarino, Ph.D. (Ontario Cancer Biomarker Network); Sarah Farias, Ph.D. (University of California, Davis); Noelle Carlozzi, Ph.D. (University of Michigan); and Carissa Gehl, Ph.D. (VA Medical Center, Iowa City, IA). **Genetics:** Marcy MacDonald, Ph.D. (Co-Chair), Jim Gusella, Ph.D., and Rick Myers, Ph.D. (Massachusetts General Hospital); Michael Hayden, Ph.D. (University of British Columbia); Tom Wassink, MD (Co-Chair) Eric A. Epping, MD, Ph.D., Andrew Juhl, BA, James Mills, MS, and Kai Wang, Ph.D. (University of Iowa); Zosia Miedzybrodzka, MD, Ph.D. (University of Aberdeen); and Christopher Ross, MD, Ph.D. (Johns Hopkins University). **Imaging:** *Administrative:* Ron Pierson, Ph.D. (Chair), Kathy Jones, BS, Jacquie Marietta, BS, William McDowell, AA, Greg Harris, BS, Eun Young Kim, MS, Hans Johnson, Ph.D., and Thomas Wassink, MD (University of Iowa); John Ashburner, Ph.D. (Functional Imaging Lab, London); Steve Potkin, MD (University of California, Irvine); and Arthur Toga, Ph.D. (University of California, Los Angeles). *Striatal:* Elizabeth Aylward, Ph.D. (Chair, Seattle Children's Research Institute). *Surface Analysis:* Peg Nopoulos, MD (Chair), and Eric Axelson, BSE (University of Iowa). *Shape Analysis:* Christopher A. Ross (Chair), MD, Ph.D., Michael Miller, Ph.D., and Sarah Reading, MD (Johns Hopkins University); Mirza Faisal Beg, Ph.D. (Simon Fraser University). *DTI:* Vincent A. Magnotta, Ph.D. (Chair, University of Iowa); Karl Helmer, Ph.D. (Massachusetts General Hospital); Kelvin Lim, MD (University of Ulm, Germany); Mark Lowe, Ph.D. (Cleveland Clinic); Sasumu Mori, Ph.D. (Johns Hopkins University); Allen Song, Ph.D. (Duke University); and Jessica Turner, Ph.D. (University of California, Irvine). *fMRI:* Steve Rao, Ph.D. (Chair), Erik Beall, Ph.D., Katherine Koenig, Ph.D., Michael Phillips, MD, Christine Reece, BS, and Jan Zimbelman, Ph.D., PT (Cleveland Clinic); April Bryant, Andrew Juhl, BS, Kathy Jones, and Gloria Wenman (University of Iowa). **Motor:** Kevin Biglan, MD (Chair) (University of Rochester); Karen Marder, MD (Columbia University); Jody Corey-Bloom, MD, Ph.D. (University of California, San Diego); Michael Geschwind,

MD, Ph.D. (University of California, San Francisco); Ralf Reilmann, MD and Zerka Unds (Muenster, Germany); and Andrew Juhl, BS (University of Iowa). **Psychiatric:** Eric A. Epping, MD, Ph.D. (Chair), Nancy Downing, RN, Ph.D., Jess Fiedorowicz, MD, Robert Robinson, MD, Megan Smith, Ph.D., Leigh Beglinger, Ph.D., James Mills, MS, Kristine Rees, BA, Michelle Harreld, BS, Adam Ruggle, Stacie Vik, BA, Janet Williams, Ph.D., Dawei Liu, Ph.D., David Moser, Ph.D., and Kelly Rowe (University of Iowa); Karen Anderson, MD (University of Maryland); David Craufurd, MD (University of Manchester); Mark Groves, MD (Columbia University); Anthony Vaccarino, Ph.D. and Ken Evans, Ph.D. (Ontario Cancer Biomarker Network); Hugh Rickards, MD (Queen Elizabeth Psychiatric Hospital); Eric van Duijn, MD (Leiden University Medical Center, Netherlands); Phyllis Chua (The University of Melbourne, Royal Melbourne Hospital); and Kimberly Quaid, Ph.D. (Indiana University).

Core Sections
Statistics: Jeffrey D. Long, Ph.D., Ji-In Kim, Ph.D., James A. Mills, MS, Ying Zhang, Ph.D., Dawei Liu, Ph.D., Wenjing Lu, and Spencer Lourens (University of Iowa).

Recruitment/Retention: Martha Nance, MD (Chair, University of Minnesota); Anne Leserman, MSW, LISW, Nicholas Doucette, BA, Mycah Kimble, BA, Patricia Ryan, MSW, LISW, MA, Kelli Thumma, BA, Elijah Waterman, BA, and Jeremy Hinkel, BA (University of Iowa). **Ethics:** Cheryl Erwin, JD, Ph.D., (Chair, McGovern Center for Health, Humanities and the Human Spirit); Eric A. Epping, MD, Ph.D. Janet Williams, Ph.D., Nicholas Doucette, BA, Anne Leserman, MSW, LISW, James Mills, MS, Lynn Schaul, BA, and Stacie Vik, BA (University of Iowa); Martha Nance, MD (University of Minnesota); and Lisa Hughes, MEd (University of Texas Medical School at Houston). **IT/Management:** Hans Johnson, Ph.D. (Chair), R.J. Connell, BS, Karen Pease, BS, Ben Rogers, BA, BSCS, Jim Smith, AS, Shuhua Wu, MCS, Roland Zschiegner, Erin Carney, Bill McKirgan, Mark Scully, and Ryan Wyse (University of Iowa); Jeremy Bockholt (AMBIGroup).

Program Management
Administrative: Chris Werling-Witkoske (Chair), Greg Ennis, MA, Stacie Vik, BA, Karla Anderson, BS, Kristine Bjork, BA, Sean Thompson, BA, Leann Davis, Machelle Henneberry, Ann Dudler, Jamy Schumacher, and Craig Stout (University of Iowa). **Financial:** Steve Blanchard, MSHA, Kelsey Montross, BA, and Phil Danzer (University of Iowa).

STUDY FUNDING

This research is supported by the National Institutes for Health, National Institute of Neurological Disorders and Stroke (NS40068) and CHDI Foundation, Inc.

SUPPLEMENTARY MATERIAL

The Supplementary Material for this article can be found online at: http://www.frontiersin.org/Aging_Neuroscience/10.3389/fnagi.2013.00012/abstract

Table e-1 | Functional status by clusters.
Table e-2 | Proportion of same versus different raters by cluster*.

REFERENCES

Albert, M. S., Dekosky, S. T., Dickson, D., Dubois, B., Feldman, H. H., Fox, N. C., et al. (2011). The diagnosis of mild cognitive impairment due to Alzheimer's disease: recommendations from the National Institute on Aging-Alzheimer's Association workgroups on diagnostic guidelines for Alzheimer's disease. *Alzheimers Dement.* 7, 270–279.

Aylward, E. H., Codori, A. M., Rosenblatt, A., Sherr, M., Brandt, J., Stine, O. C., et al. (2000). Rate of caudate atrophy in presymptomatic and symptomatic stages of Huntington's disease. *Mov. Disord.* 15, 552–560.

Beglinger, L. J., Paulsen, J. S., Watson, D. B., Wang, C., Duff, K., Langbehn, D. R., et al. (2008). Obsessive and compulsive symptoms in prediagnosed Huntington's disease. *J. Clin. Psychiatry* 69, 1758–1765.

Biglan, K. M., Ross, C. A., Langbehn, D. R., Aylward, E. H., Stout, J. C., Queller, S., et al. (2009). Motor abnormalities in premanifest persons with Huntington's disease: the PREDICT-HD study. *Mov. Disord.* 24, 1763–1772.

Duff, K., Paulsen, J. S., Beglinger, L. J., Langbehn, D. R., Wang, C., Stout, J. C., et al. (2010). "Frontal" behaviors before the diagnosis of Huntington's disease and their relationship to markers of disease progression: evidence of early lack of awareness. *J. Neuropsychiatry Clin. Neurosci.* 22, 196–207.

Duyao, M., Ambrose, C., Myers, R., Novelletto, A., Persichetti, F., Frontali, M., et al. (1993). Trinucleotide repeat length instability and age of onset in Huntington's disease. *Nat. Genet.* 4, 387–392.

Hogarth, P., Kayson, E., Kieburtz, K., Marder, K., Oakes, D., Rosas, D., et al. (2005). Interrater agreement in the assessment of motor manifestations of Huntington's disease. *Mov. Disord.* 20, 293–297.

Hungtington Study Group. (1996). Unified Huntington's Disease Rating Scale: reliability and consistency. *Mov. Disord.* 11, 136–142.

Huntington Study Group. (2001). A randomized, placebo-controlled trial of coenzyme Q10 and remacemide in Huntington's disease. *Neurology* 57, 397–404.

Huntington Study Group PHAROS Investigators. (2006). At risk for Huntington disease: the PHAROS (Prospective Huntington At Risk Observational Study) cohort enrolled. *Arch. Neurol.* 63, 991–996.

Marder, K., Zhao, H., Myers, R. H., Cudkowicz, M., Kayson, E., Kieburtz, K., et al. (2000). Rate of functional decline in Huntington's disease. Huntington Study Group. *Neurology* 54, 452–458.

Paulsen, J. S., Hayden, M., Stout, J. C., Langbehn, D. R., Aylward, E., Ross, C. A., et al. (2006). Preparing for preventive clinical trials: the Predict-HD study. *Arch. Neurol.* 63, 883–890.

Paulsen, J. S., Langbehn, D. R., Stout, J. C., Aylward, E., Ross, C. A., Nance, M., et al. (2008). Detection of Huntington's disease decades before diagnosis: the Predict-HD study. *J. Neurol. Neurosurg. Psychiatry* 79, 874–880.

Paulsen, J. S., Wang, C., Duff, K., Barker, R., Nance, M., Beglinger, L., et al. (2010). Challenges assessing clinical endpoints in early Huntington disease. *Mov. Disord.* 25, 2595–2603.

Solomon, A. C., Stout, J. C., Johnson, S. A., Langbehn, D. R., Aylward, E. H., Brandt, J., et al. (2007). Verbal episodic memory declines prior to diagnosis in Huntington's disease. *Neuropsychologia* 45, 1767–1776.

Sperling, R. A., Aisen, P. S., Beckett, L. A., Bennett, D. A., Craft, S., Fagan, A. M., et al. (2011). Toward defining the preclinical stages of Alzheimer's disease: recommendations from the National Institute on Aging-Alzheimer's Association workgroups on diagnostic guidelines for Alzheimer's disease. *Alzheimers Dement.* 7, 280–292.

Stout, J. C., Paulsen, J. S., Queller, S., Solomon, A. C., Whitlock, K. B., Campbell, J. C., et al. (2011). Neurocognitive signs in prodromal Huntington disease. *Neuropsychology* 25, 1–14.

Thieben, M. J., Duggins, A. J., Good, C. D., Gomes, L., Mahant, N., Richards, F., et al. (2002). The distribution of structural neuropathology in pre-clinical Huntington's disease. *Brain* 125, 1815–1828.

Conflict of Interest Statement: Dr. Biglan receives grant funding from the MJFF, NINDS, NPF, HDSA, Lundbeck, Google Inc., Marvell Inc., Excellus-Blue Cross Consultant for Theravance, and Lundbeck; he also has contracts with Presbyterian Home for Central NY and the Parkinson Support Group for Central NY, and Susquehanna Nursing Home and Rehabilitation Center. Dr. Geschwind does consulting for Medacoro Consultant, Clinical Advisors, and Gerson Lehman Group and is on the Editorial Board of Dementia Cognition. Dr. Raymond's research is supported by operating grants from the Canadian Institutes of Research, the Cure Huntington Disease Initiative Foundation, Inc., and the Michael J Fox Foundation. Dr. Testa received research support from the Huntington Society of Canada (principal investigator), as well as the Tremor Research Group, HighQ Foundation, and Huntington Study Group (site principal investigator subcontracts). The Tremor Research Group subcontract sponsor is GlaxoSmithKline. Huntington Study Group subcontract sponsors are NIH/NINDS or Medivation. She was a co-investigator on NIH/NCRR 2R24RR018827-05A1. Dr. Wojcieszek receives clinical trial funding from Medivation, Novartis, Scheering Plough, and TEVA; she is also part of the TEVA speaker's bureau. All other authors report no disclosures or potential conflicts of interest.

Received: 13 December 2012; accepted: 02 March 2013; published online: 02 April 2013.

*Citation: Biglan KM, Zhang Y, Long JD, Geschwind M, Kang GA, Killoran A, Lu W, McCusker E, Mills JA, Raymond LA, Testa C, Wojcieszek J, Paulsen JS and the PREDICT-HD Investigators of the Huntington Study Group (2013) Refining the diagnosis of Huntington disease: the PREDICT-HD study. Front. Aging Neurosci. **5**:12. doi: 10.3389/fnagi.2013.00012*

frontiers in
AGING NEUROSCIENCE

ORIGINAL RESEARCH ARTICLE
published: 11 October 2013
doi: 10.3389/fnagi.2013.00055

Biomarker-based prediction of progression in MCI: comparison of AD signature and hippocampal volume with spinal fluid amyloid-β and tau

Bradford C. Dickerson[1,2,3,4]* and David A. Wolk[5,6,7] for the Alzheimer's Disease Neuroimaging Initiative[†]

[1] *Frontotemporal Dementia Unit, Massachusetts General Hospital and Harvard Medical School, Boston, MA, USA*
[2] *Department of Neurology, Massachusetts General Hospital and Harvard Medical School, Boston, MA, USA*
[3] *Massachusetts Alzheimer's Disease Research Center, Massachusetts General Hospital and Harvard Medical School, Boston, MA, USA*
[4] *Athinoula A. Martinos Center for Biomedical Imaging, Massachusetts General Hospital and Harvard Medical School, Boston, MA, USA*
[5] *Department of Neurology, University of Pennsylvania, Philadelphia, PA, USA*
[6] *Alzheimer's Disease Core Center, University of Pennsylvania, Philadelphia, PA, USA*
[7] *Penn Memory Center, University of Pennsylvania, Philadelphia, PA, USA*

Edited by:
Manuel Menéndez-González, Hospital Álvarez-Buylla, Spain

Reviewed by:
Luísa Alves, Universidade Nova de Lisboa and Centro Hospitalar de Lisboa Ocidental, Portugal
Seong An, Gachon University, South Korea

****Correspondence:***
Bradford C. Dickerson, Frontotemporal Dementia Unit, Massachusetts General Hospital and Harvard Medical School, 149, 13th Street, Suite 2691, Charlestown, Boston, MA 02129, USA
e-mail: bradd@nmr.mgh.harvard.edu

[†]Data used in preparation of this article were obtained from the Alzheimer's Disease Neuroimaging Initiative (ADNI) database (adni.loni.ucla.edu). As such, the investigators within the ADNI contributed to the design and implementation of ADNI and/or provided data but did not participate in analysis or writing of this report. A complete listing of ADNI investigators can be found at: http://adni.loni.ucla.edu/wp-content/uploads/how_to_apply/ADNI_Acknowledgement_List.pdf

Objective: New diagnostic criteria for mild cognitive impairment (MCI) due to Alzheimer's disease (AD) have been developed using biomarkers aiming to establish whether the clinical syndrome is likely due to underlying AD. We investigated the utility of magnetic resonance imaging (MRI) and cerebrospinal fluid (CSF) biomarkers in predicting progression from amnesic MCI to dementia, testing the hypotheses that (1) markers of amyloid and neurodegeneration provide distinct and complementary prognostic information over different time intervals, and that (2) evidence of neurodegeneration in amyloid-negative MCI individuals would be useful prognostically.

Methods: Data were obtained from the ADNI-1 (Alzheimer's Disease Neuroimaging Initiative Phase 1) database on all individuals with a baseline diagnosis of MCI, baseline MRI and CSF data, and at least one follow-up visit. MRI data were processed using a published set of *a priori* regions of interest to derive a measure known as the "AD signature," as well as hippocampal volume. The CSF biomarkers amyloid-β, total tau, and phospho tau were also examined. We performed logistic regression analyses to identify the best baseline biomarker predictors of progression to dementia over 1 or 3 years, and Cox regression models to test the utility of these markers for predicting time-to-dementia.

Results: For prediction of dementia in MCI, the AD signature cortical thickness biomarker performed better than hippocampal volume. Although CSF tau measures were better than CSF amyloid-β at predicting dementia within 1 year, the AD signature was better than all CSF measures at prediction over this relatively short-term interval. CSF amyloid-β was superior to tau and AD signature at predicting dementia over 3 years. When CSF amyloid-β was dichotomized using previously published cutoff values and treated as a categorical variable, a multivariate stepwise Cox regression model indicated that both the AD signature MRI marker and the categorical CSF amyloid-β marker were useful in predicting time-to-event diagnosis of AD dementia.

Conclusion: In amnesic MCI, short-term (1 year) prognosis of progression to dementia relates strongly to baseline markers of neurodegeneration, with the AD signature MRI biomarker of cortical thickness performing the best among MRI and CSF markers studied here. Longer-term (3 year) prognosis in these individuals was better predicted by a marker indicative of brain amyloid. Prediction of time-to-event in a survival model was predicted by the combination of these biomarkers. These results provide further support for emerging models of the temporal relationship of pathophysiologic events in AD and demonstrate the utility of these biomarkers at the prodromal stage of the illness.

Keywords: Alzheimer's disease, MRI, biomarkers, mild cognitive impairment, CSF biomarkers

INTRODUCTION

When insidious in onset and gradually progressive, mild cognitive impairment (MCI) is a clinical syndrome commonly arising as a result of neurodegenerative pathology (Petersen et al., 2006). In living persons, evidence of neurodegenerative pathology is provided by a growing array of imaging and fluid biomarkers. If the

goal is to determine whether MCI appears highly likely to be due to underlying Alzheimer pathology, the recently published MCI diagnostic criteria require evidence of (1) cerebral amyloidosis [amyloid positron emission tomography (PET) or cerebrospinal fluid (CSF) amyloid-β] and (2) neurodegeneration [magnetic resonance imaging (MRI)-derived atrophy, fluorodeoxyglucose (FDG)-PET-derived hypometabolism, or CSF tau; Albert et al., 2011]. A number of studies have now shown that, within a group of persons with MCI, the presence and prominence of these biomarkers are predictive of the likelihood of Alzheimer's disease (AD) dementia within a few years (Jack et al., 1999; Hansson et al., 2006; Wang et al., 2006; Vemuri et al., 2009b; Visser et al., 2009; Blennow et al., 2010; De Meyer et al., 2010; Jack et al., 2010; Landau et al., 2010; Buchhave et al., 2012). Despite the importance of observations from these studies, a number of questions remain, particularly when considering how to use biomarkers in the design of clinical trials of putative interventions. Further, as more clinicians are beginning to incorporate these measures into clinical practice, a deeper understanding of the relative implications of these biomarkers is critical.

In persons with MCI, what are the best MRI-derived biomarkers of neurodegeneration with regard to prediction of progression to dementia? One very commonly used measure is hippocampal volume, which has consistently been shown to predict dementia in MCI (Frisoni et al., 2010). We have developed an AD signature cortical thickness marker (Dickerson et al., 2009), and hypothesize that this marker will outperform commonly used MRI-derived biomarkers as an indicator of AD-related neurodegeneration in MCI that is predictive of AD dementia.

Another major question relates to the temporal utility of biomarkers. What are the best markers for short-term vs. longer-term prediction of dementia? Although current clinico-pathologic constructs of AD require evidence of cerebral amyloidosis, data are conflicting as to whether markers of amyloid or neurodegeneration best predict dementia and to our knowledge none have specifically tested hypotheses about the comparative utility of amyloid vs. neurodegenerative markers at different time intervals. We tested two hypothesis here: (1) rapid progression (i.e., over 1 year) from MCI to AD dementia is better predicted by markers of neurodegeneration rather than the presence of amyloid; (2) longer-term progression from MCI to dementia (i.e., 3 years) is best predicted by the presence of abnormal levels of brain amyloid. This prediction follows from the notion that cerebral amyloidosis may be a relatively earlier development in AD pathophysiology compared to evidence of neurodegeneration measured using *in vivo* methods (Jack et al., 2013). Further, neurodegenerative markers appear to be more sensitive to disease state than measures of cerebral amyloid (Jack et al., 2009; Vemuri et al., 2009a). As such, amyloid measures may differentiate individuals who will eventually progress to AD over longer-term follow-up while neurodegenerative markers may indicate an elevated risk for more proximate cognitive decline and dementia.

Finally, the focus of a number of studies of biomarker prediction of AD dementia in amnestic MCI has been on the 50–75% of subjects with evidence of cerebral amyloidosis. What about the other individuals, especially those who may show evidence suggestive of neurodegeneration (Knopman et al., 2012; Petersen et al., 2013)? Are MRI-derived markers useful in predicting dementia in individuals with MCI who do not have evidence of cerebral amyloidosis?

Here we undertook a set of analyses of the Alzheimer's Disease Neuroimaging Initiative (ADNI) dataset to investigate these questions, focusing on the utility of MRI and CSF biomarkers for prognosis in MCI.

MATERIALS AND METHODS

PARTICIPANTS

Data used in the preparation of this article were obtained from the ADNI database[1]. The ADNI was launched in 2003 by the National Institute on Aging (NIA), the National Institute of Biomedical Imaging and Bioengineering (NIBIB), the Food and Drug Administration (FDA), private pharmaceutical companies, and nonprofit organizations, as a $60 million, 5-year public–private partnership. The primary goal of ADNI has been to test whether serial MRI, PET, other biological markers, and clinical and neuropsychological assessment can be combined to measure the progression of MCI and early AD. Determination of sensitive and specific markers of very early AD progression is intended to aid researchers and clinicians to develop new treatments and monitor their effectiveness, as well as lessen the time and cost of clinical trials.

The Principal Investigator of this initiative is Michael W. Weiner, MD, VA Medical Center and University of California – San Francisco. ADNI is the result of efforts of many co-investigators from a broad range of academic institutions and private corporations, and subjects have been recruited from over 50 sites across the U.S. and Canada. The initial goal of ADNI was to recruit 800 subjects but ADNI has been followed by ADNI-GO and ADNI-2. To date these three protocols have recruited over 1500 adults, ages 55–90, to participate in the research, consisting of cognitively normal older individuals, people with early or late MCI, and people with early AD. The follow-up duration of each group is specified in the protocols for ADNI-1, ADNI-2, and ADNI-GO. Subjects originally recruited for ADNI-1 and ADNI-GO had the option to be followed in ADNI-2. For up-to-date information, see www.adni-info.org.

For the current analysis, we selected individuals with a baseline diagnosis of MCI who had baseline MRI and CSF data available, and at least 1 year of clinical follow-up ($n = 154$). Detailed diagnostic, inclusion, and exclusion criteria are described on the ADNI website[2].

STANDARD PROTOCOL APPROVALS, REGISTRATIONS, AND PATIENT CONSENTS

Each participant gave written informed consent in accordance with institutional Human Subjects Research Committee guidelines.

MRI IMAGING AND ANALYSIS

Magnetic resonance imaging scans were collected on a 1.5T scanner using a standardized MPRAGE protocol: sagittal plane, TR/TE/TI, 2400/3/1000 ms, flip angle 8°, 24 cm FOV, 192 × 192

[1] www.adni.loni.ucla.edu

[2] http://www.adni-info.org/

in-plane matrix, 1.2 mm slice thickness (Jack et al., 2008). Fully pre-processed scans were downloaded for analysis.

T1 image volumes were examined quantitatively by a cortical surface-based reconstruction and analysis of cortical thickness, using a hypothesis-driven approach as described in multiple previous publications (Bakkour et al., 2009; Dickerson et al., 2009, 2011; Wolk et al., 2010). Briefly, we utilized nine regions of interest (ROIs, see **Figure 1**) previously determined to be associated with AD, the "cortical signature" of AD (Bakkour et al., 2009; Dickerson et al., 2009).

For the purposes of this study, we employed a primary diagnostic biomarker, the single summary "AD signature measure," the average thickness of all nine ROIs. With the goal of adjusting this measure for normal age-related influences on these brain regions, we also measured a set of "Aging signature" ROIs, as previously published (Bakkour et al., 2013). We calculated an "AD signature index" measure by first performing a linear regression in the amyloid-negative control group with the Aging signature as the independent variable and the AD signature as the dependent variable. We then used this equation to calculate the "AD signature index values for each MCI patient." Thus, an individual with a lower AD signature index value has cortical thickness within the AD signature ROIs that is disproportionately smaller than the thickness of the Aging signature ROIs, likely reflecting more specific AD-related neurodegeneration. Alternatively, an individual with a higher AD signature index value has cortical thickness within the AD signature ROIs that is of similar relative magnitude to Aging signature ROIs, possibly reflecting more diffuse effects.

In addition, for comparison purposes, we analyzed hippocampal volume using the measure provided by the automated segmentation procedure from FreeSurfer, divided by total intracranial volume. Our standard procedure is to visually inspect selected coronal slices of each automated segmentation and identify scans with errors in processing of the structure of interest. We also inspect the distribution of the quantitative volumetric data and review scans at either tail of the distribution and outliers in greater detail. In the present analysis, no scans were identified with important errors of hippocampal segmentation.

BASELINE CEREBROSPINAL FLUID MEASURES

We also examined baseline CSF levels of amyloid-β, total tau (t-tau), and phosphorylated tau (p-tau). For the primary analyses, we used the raw values as continuous measures; however, t-tau and p-tau were log-transformed to better approximate normality in distribution. For analyses in which we classified subjects as having CSF amyloid-β values consistent with those of autopsy-proven AD, we used a cutoff value of levels less than 192 (Shaw et al., 2009). Individuals with levels $\geq$192 were considered to be unlikely to have cerebral amyloidosis.

LONGITUDINAL OUTCOMES

Here we used outcomes at 1 or 3 years. The primary outcome measures used in the present analysis were conversion to a diagnosis of AD dementia at 1 or at 3 years.

STATISTICAL ANALYSIS

Tests of group differences were performed using Chi-square analysis (for frequencies) or Analysis of Variance (for continuous measures) with *post hoc* pairwise comparisons where relevant; $a = 0.05$. Since effect sizes were expected to be subtle and strong *a priori* hypotheses were being tested, no multiple comparisons correction procedures were performed. In addition, the impact of biomarkers on clinical outcome was analyzed using separate logistic regression models for each of the two intervals of follow-up, constructed using the dichotomous conversion to dementia outcome measure as the dependent variable. Cox regression models were constructed to investigate the relationship of baseline biomarkers to the likelihood of progression to AD dementia using a more fine-grained time-to-event outcome rather than the two follow-up intervals employed in the other analyses. A multivariate

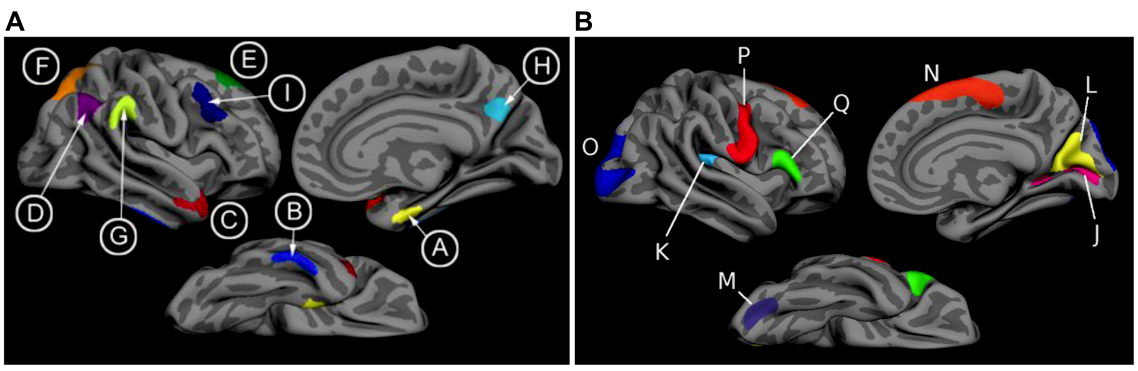

FIGURE 1 | (A) The cortical signature of AD is composed of *a priori* regions of interest in which consistent atrophy has been previously observed in multiple samples of patients with mild AD dementia. **(B)** The cortical signature of normal aging is composed of *a priori* regions of interest in which consistent atrophy has been previously described in healthy cognitively intact older adults compared with younger adults. We calculated the "AD signature index" measure by performing a linear regression with the Aging signature (excluding regions overlapping with AD signature regions; see Figures 1 and 2 of Bakkour et al., 2013) as the independent variable and the AD signature as the dependent variable. The residuals of this regression analysis were then saved as the "AD signature index." Key: A: medial temporal, B: inferior temporal, C: temporal pole, D: Angular, E: superior frontal, F: superior parietal, G: supramarginal, H: precuneus, I: middle frontal, J: calcarine, K: caudal insula, L: cuneus, M: caudal fusiform, N: dorsomedial frontal, O: lateral occipital, P: precentral, Q: inferior frontal.

Cox regression model was then constructed including independent variables that reached a trend-level effect ($p < 0.1$) in the univariate analyses (p-value-to-enter <0.05). Covariates of age, education, and gender were generally not significant in the models and had minimal impact on the findings. Statistical analyses were performed using IBM SPSS 21.0.

RESULTS

Of the 156 MCI participants with baseline MRI and CSF data who were followed for 1 year, 31 (20%) were diagnosed with probable AD dementia. Of the 111 who had 3-year outcome data, 48 (43%) were diagnosed with probable AD dementia. In the subset of MCI participants with baseline CSF evidence of cerebral amyloidosis, 26 of 116 (22%) were diagnosed with probable AD dementia at 1 year and 45 of 83 (54%) at 3 years. In contrast, in the subgroup of MCI participants with normal baseline CSF amyloid-β levels, only 5 of 40 (13%) converted to AD dementia at 1 year and 3 of 27 (11%) at 3 years. See **Table 1** for additional details.

We first sought to determine which of the baseline biomarkers would be useful in prediction of the likelihood of a diagnosis of probable AD dementia in the entire sample of MCI subjects. For the 1-year outcome interval, baseline cortical thickness measured with the AD signature MRI biomarker index was strongly associated with the likelihood of probable AD: a logistic regression model predicting a 1-year AD outcome indicated a nearly threefold increase in the likelihood of AD dementia for each 1 SD thinner cortex [odds ratio (OR) = 2.7, 95% C.I.: [1.7–4.5], $p < 0.0001$). In addition, baseline CSF p-tau levels were predictive of AD dementia, with each 1 SD increase in CSF p-tau levels being associated with a 1.7-fold increase in the likelihood of AD dementia (OR = 1.7, 95% C.I.: [1.09–2.7], $p = 0.02$). None of the other biomarkers demonstrated effects or trend-level effects. In the stepwise multivariate logistic regression model, the AD signature MRI marker entered but CSF p-tau did not, indicating that CSF p-tau did not explain additional variance in outcome beyond that explained by the AD signature MRI marker.

In contrast, 3-year conversion was best predicted by baseline CSF amyloid-β levels, with each 1 SD of reduction indicating a 1.9-fold increase in 3-year likelihood of AD dementia (OR = 1.9, 95% C.I.: [1.2–3.0], $p = 0.003$). A slightly weaker effect was observed for the AD signature index (OR = 1.7, 95% C.I.: [1.12–2.6], $p = 0.01$). Significant effects were also observed for CSF p-tau (OR = 1.8, 95% C.I.: [1.14–2.7], $p = 0.01$) and CSF t-tau (OR = 1.6, 95% C.I.: [1.06–2.5], $p = 0.03$) while hippocampal volume displayed a strong trend (OR = 1.5, 95% C.I.: [1.00–2.29], $p = 0.05$). In the stepwise multivariate model, CSF amyloid-β entered but the other two did not.

Figure 2 depicts the values for the AD signature cortical thickness MRI marker and CSF amyloid-β for each of the three MCI subgroups based on outcome (stable over 3 years, 3-year converters who did not convert by year 1, and 1-year converters). The mean values for CSF amyloid-β are lower in both groups of converters than in stable MCI (1-year: $p < 0.05$; 3-year: $p < 0.01$), but there is no difference based on year of conversion ($p > 0.3$). Alternatively, values for AD signature cortical thickness are lower for both groups of converters than the stable group (1-year: $p < 0.001$; 3-year: $p = 0.05$), but also for the 1-year converters compared to the 3-year converters ($p < 0.05$; all values shown are Z scores derived from the normative values of controls).

We next investigated the utility of biomarkers for prediction of a diagnosis of AD dementia in subgroups of MCI subjects divided on the basis of baseline CSF amyloid-β levels. In the subgroup of MCI subjects with abnormally low baseline CSF amyloid-β levels (consistent with cerebral amyloidosis), 1-year conversion to AD dementia was predicted by the AD signature MRI biomarker (OR = 2.2, 95% C.I.: [1.3–3.8], $p = 0.005$). None of the other biomarkers were predictive in these univariate models. For 3-year prediction, a significant effect for the AD signature MRI biomarker (OR = 1.7, 95% C.I.: [1.1–2.7], $p = 0.03$) and a trend for hippocampal volume (OR = 1.5, 95% C.I.: [0.95–2.5], $p = 0.08$) were observed.

Table 1 | Demographic and baseline biomarker characteristics of sample.

Subject group	1-year outcome ($N = 156$)		3-year outcome ($N = 111$)	
N (%) or M (SD)	MCI ($N = 125$)	AD ($N = 31$)	MCI ($N = 63$)	AD ($N = 48$)
Age (years)	74.9 (7.6)	72.3 (6.90)	74.7 (7.3)	74.3 (7.7)
Gender	84 M: 41 F	17 M: 14 F	47 M: 16 F	30 M: 18 F
Education (years)	15.8 (3.0)	15.1 (3.2)	15.6 (3.0)	15.6 (3.4)
MMSE	27.5 (1.7)	26.7 (1.9)	27.3 (1.8)	26.7 (1.9)
CDR-SB	1.9 (0.8)	2.4 (0.9)*	1.7 (0.6)	2.2 (1.0)*
CSF amyloid-β Z score	−0.73 (1.00)	−0.99 (0.70)	−0.56 (1.12)	−1.15 (0.65)**
CSF Total tau Z score	0.69 (1.07)	1.17 (1.13)	0.74 (1.22)	1.26 (1.13)*
CSF P-tau Z score	0.69 (1.06)	1.20 (0.99)*	0.62 (1.04)	1.12 (0.93)*
AD signature Z score	−0.82 (1.13)	−1.82 (1.27)**	−0.63 (1.12)	−1.26 (1.19)*
Hippo vol Z	−0.94 (1.14)	−1.24 (1.06)	−0.75 (1.05)	−1.15 (1.04)†

*$p < 0.05$, **$p < 0.005$ groups are different from each other.
†$p = 0.05$, groups demonstrate trend-level difference from each other.

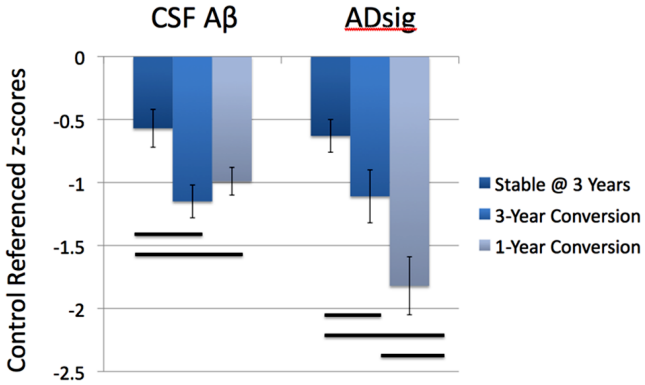

FIGURE 2 | Values for the AD signature cortical thickness and CSF amyloid-β for each of the three MCI subgroups based on outcome (stable over 3 years, 3-year converters, and 1-year converters). The mean values for CSF amyloid-β are lower in both groups of converters than in stable MCI (left), while the values for AD signature index of cortical thickness are lower in the 1-year converters than in the other two groups (right; all values shown are Z scores derived from the normative values of controls and bars represent statistically significant comparisons).

Table 2 | Results of Cox regression analyses of baseline CSF and MRI biomarker measures predicting probable AD diagnosis.

	X^2	HR	95% CI
AD signature	13.7 ($p < 0.001$)**	1.61	1.25–2.08
AD signature dichotomous	12.9 ($p < 0.001$)**	2.28	1.44–3.63
CSF amyloid-β dichotomous	12.2 ($p < 0.001$)**	3.66	1.68–7.99
CSF amyloid-β	7.4 ($p < 0.01$)*	1.42	1.10–1.83
CSF p-tau	9.2 ($p < 0.01$)*	1.47	1.15–1.90
CSF t-tau	5.5 ($p < 0.05$)*	1.33	1.05–1.70
Hippocampal volume	4.8 ($p < 0.05$)*	1.31	1.03–1.67
Combination of CSF dichotomous amyloid-β and AD signature	19.4 ($p < 0.0001$)**	Aβ 3.0 ADsig 1.4	1.38–6.7 1.07–1.77

*$p < 0.05$, **$p < 0.005$.

In the subgroup of MCI subjects with normal CSF amyloid-β levels, indicating the likely absence of cerebral amyloidosis, 1-year conversion to AD dementia was best predicted by the AD signature MRI biomarker (OR = 6.4, 95% C.I.: [1.5–27.5], $p = 0.01$), with hippocampal volume showing utility as well (OR = 3.5, 95% C.I.: [1.2–10.7], $p = 0.03$) but not entering the multivariate model. None of the CSF markers demonstrated predictive value. For 3-year prediction, none of the markers were useful although power was extremely low due to the small number of individuals who were diagnosed with AD dementia.

Finally, we performed a survival analysis to investigate the utility of these biomarkers for predicting the time to a diagnosis of AD dementia. Univariate Cox proportional hazards regression models indicated that each of the biomarkers was a predictor of time to diagnosis of AD dementia over the 3-year follow-up period (**Table 2**). In multivariate analysis, a stepwise forward conditional model demonstrated that the AD signature MRI biomarker was the best and only predictor when each independent variable was entered as a continuous variable. However, when CSF amyloid-β was dichotomized using previously published cutoff values (Shaw et al., 2009) and treated as a categorical variable, the multivariate stepwise Cox regression model indicated that both the AD signature MRI marker and the categorical CSF amyloid-β marker were useful in predicting time-to-event diagnosis of AD dementia. Of all the models, this was the model with the overall strongest statistical results ($X^2 = 19.4$, $p < 0.001$). This result is illustrated in **Figure 3** in which the AD signature was also dichotomized to maximize sensitivity and specificity between amyloid-negative controls and amyloid-positive mild AD patients from the ADNI cohort.

Finally, to begin to assess the specificity of the refined AD signature index measure we analyzed the relationships between CSF biomarkers and the raw AD signature measure (in millimeters) and the adjusted AD signature index measure (adjusted for thickness of the Aging signature regions as described in Section "Materials and Methods." The adjusted AD signature index exhibited substantially stronger correlations (**Table 3**) with all CSF biomarkers relative to the raw AD signature, suggesting that this adjustment for "brain age" improves the specificity of this MRI biomarker for AD-related neurodegeneration.

DISCUSSION

When individuals are diagnosed with MCI, the two most pressing clinical questions relate to etiology and prognosis. We now have a growing armamentarium of biomarkers for AD and other neurodegenerative diseases, and reasonably mature diagnostic criteria for "MCI of the Alzheimer type" (Albert et al., 2011) which hinge on a typical clinical syndrome and the presence of one or more imaging or fluid biomarkers. In this analysis, we used ADNI data to test two major hypotheses in patients with MCI: (1) markers of amyloid and neurodegeneration provide distinct and complementary prognostic information over different time intervals, and that (2) evidence of neurodegeneration in amyloid-negative MCI individuals is useful prognostically. We found compelling support for both hypotheses.

For prediction of AD dementia in MCI, the AD signature cortical thickness biomarker performed better than hippocampal volume. Although CSF tau measures, also putative neurodegenerative biomarkers, were better than CSF amyloid-β at predicting dementia within 1 year, the AD signature was better than all CSF measures at prediction over this relatively short-term interval. CSF amyloid-β was superior to tau and AD signature at predicting dementia over 3 years. In an analysis examining the combined use of CSF and MRI measures, when CSF amyloid-β was dichotomized using previously published cutoff values and treated as a categorical variable, a Cox regression model indicated that both the AD signature MRI marker and the categorical CSF amyloid-β marker were useful in predicting time-to-event diagnosis of AD dementia. These results provide further support for emerging models of the pathophysiology of AD and demonstrate the utility of the combined use of these biomarkers at the prodromal stage of the illness (Jack et al., 2010; Landau et al., 2010; Vemuri et al., 2010).

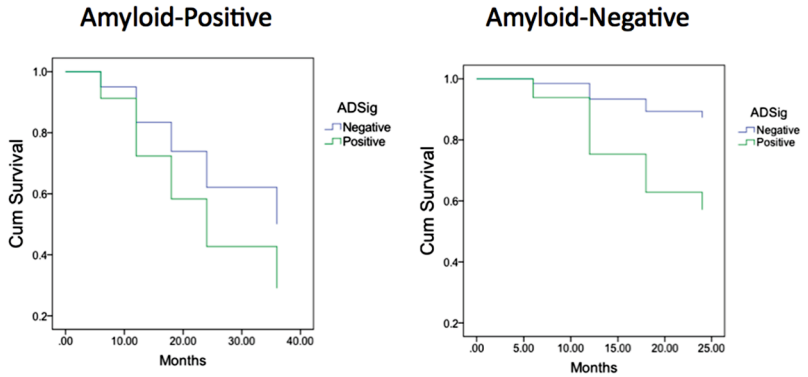

FIGURE 3 | Survival curves in MCI participants who were "amyloid-negative" at baseline (left) vs. those who were "amyloid positive" (right) as a function of baseline AD signature index using dichotomous cutoff.

Table 3 | Relationships of CSF biomarkers to MRI biomarkers.

	Age	CSF t-tau	CSF p-tau	CSF amyloid-β
Aging signature	$r = -0.38$ ($p < 0.001$)	$r = -0.05$ NS	$r = -0.04$ NS	$r = -0.06$ NS
AD signature	$r = -0.30$ ($p < 0.001$)	$r = -0.26$ ($p < 0.01$)	$r = -0.21$ ($p < 0.01$)	$r = -0.09$ NS
Adjusted AD signature	$r = 0.05$ NS	$r = -0.37$ ($p < 0.001$)	$r = -0.35$ ($p < 0.001$)	$r = 0.22$ ($p < 0.01$)
Hippocampal volume	$r = -0.19$ ($p < 0.05$)	$r = -0.04$ NS	$r = -0.03$ NS	$r = 0.05$ NS

A major novel contribution of the present study is the investigation of the prognostic utility of different biomarkers over intervals of varying times after the markers were obtained at baseline. To our knowledge, no prior study has explicitly examined separate follow-up intervals in MCI and measured the differential utility of amyloid vs. structural MRI markers. As we plan clinical trials of pharmacologic and non-pharmacologic interventions in MCI, it is critical not only to consider methods to homogenize the patient population for inclusion (e.g., requiring MCI patients to have cerebral amyloidosis for inclusion); it may also be valuable in some trial designs to use a marker of neurodegeneration to identify patients in whom progression to dementia is likely within a relatively short time interval, such as 1 year. Such a stratified design for inclusion might be valuable in that most such participants would be likely to decline substantially during a reasonable follow-up interval, thereby maximizing power to detect a beneficial effect of the intervention. Of course, it is also possible that in these more "aggressive" cases of prodromal AD a drug might be less efficacious than in more indolent forms of the disease, but that remains an open question.

These considerations are also becoming of greater relevance in clinical practice, particularly in light of recent FDA approval of the amyloid PET ligand florbetapir. Further, with the development of the above-described guidelines for incorporation of biomarkers into the assessment of MCI patients, it is likely that clinicians will be bringing these measures into their clinical practice for prognostication of MCI. The current work emphasizes that these tests may provide somewhat different information, which may have important implications for their value depending on the question that is being addressed. For example, MRI may be more valuable when interested in determining the likelihood of decline in the near future, which could influence life decisions that need to be made within that timeframe whereas the presence of amyloid may more definitively reflect the likelihood of progression, but have less value in predicting the timing.

It seems intuitive, based on current models of biomarkers of AD pathophysiology (Jack et al., 2013), that the presence of cerebral amyloidosis would be valuable for longer-term prognosis while an MRI-derived marker of neurodegeneration would demonstrate utility in shorter-term prognosis. As the individuals with MCI in this study were followed longitudinally, those with baseline cerebral amyloid progressed to dementia at a rate of about 15–20% per year, while only about 10–15% of those without baseline brain amyloid progressed to dementia after 3 years, most doing so within the first year of follow-up. Those who progressed to AD dementia at 3 years had baseline CSF amyloid-β levels that are similarly reduced to those who progressed at 1 year. This is consistent with models that suggest that amyloid deposition is an early feature of the disease that largely plateaus by the symptomatic stage of disease resulting in relatively poor resolution of disease state (i.e., proximity to dementia) at that stage (Villemagne et al., 2013). In contrast, the baseline MRI-derived AD signature measure of cortical thickness was substantially lower in individuals who progressed at 1 year than in those who progressed at 3 years (**Figure 2**). This indicates that once AD-related neurodegenerative cortical atrophy is prominent enough in MCI patients, further cognitive decline and loss of functional independence is imminent. Such a finding demonstrates the greater degree by which markers of neurodegeneration,

particularly structural MRI measures, track disease state during symptomatic stages of disease.

The differences described here in temporal prediction and, ultimately, the complementary nature of biomarkers of cerebral amyloidosis with neurodegeneration are quite consistent with a number of recent studies in the literature exploring this issue. For example, Buchhave et al. (2012) recently described that while the presence of low CSF amyloid-β predicted conversion to AD in MCI patients, CSF p-tau status was associated with the timing of this conversion (abnormal: conversion in 0–5 years; normal: conversion in 5–10 years). Another group, also using the ADNI dataset, compared dichotomous measures of hippocampal atrophy, memory testing, and CSF total tau, p-tau, and amyloid-β in prediction of conversion. They found that median survival was generally shorter for neurodegenerative biomarkers while CSF amyloid-β had the longest median time before conversion (Heister et al., 2011). Further, using a FDG-PET "signature" of AD, similar to the structural one applied here, Landau et al. (2010) found that this measure was also superior to CSF amyloid-β for prediction of conversion in MCI patients with mean follow-up under 2 years. This group also described a tighter link between cognitive decline and cerebral amyloidosis, based on amyloid imaging, in asymptomatic individuals, but stronger association of decline with FDG-PET status in MCI (Landau et al., 2012). Thus, the current findings serve as additional support for the leading model of the proposed biomarker cascade (Jack et al., 2013), which has also found additional verification in longitudinal study of asymptomatic dominantly inherited AD mutation carriers (Bateman et al., 2012).

A variety of MRI measures have been proposed as potential biomarkers of neurodegeneration in early AD, both with regard to the identification of presumed atrophy consistent with AD and with regard to monitoring changes over time that indicate progression of neurodegeneration. Hippocampal volume is the most widely employed and discussed measure of this type, and while clearly informative, it is increasingly appearing to be less sensitive and specific than other measures such as regional cortical thickness. We have previously shown using receiver operating characteristic analyses that the AD signature measure is superior to hippocampal volume in discriminating individuals with prodromal AD who progress to dementia within 3 years from those who do not (Bakkour et al., 2009). Here we used logistic and Cox regression models to demonstrate the superiority of the AD signature over hippocampal volume in predicting progression to dementia in both amyloid-positive and amyloid-negative individuals with MCI. Nonetheless, it is worth noting that while not as strongly predictive of conversion as the AD signature, hippocampal volume still had predictive value in most of these analyses consistent with prior work using this measure (for review, see Frisoni et al., 2010). Further, much of the literature has applied cutoff values or categorical groupings of hippocampal volumes in similar analyses to those presented here, which may provide additional predictive power (Jack et al., 1999, 2010; Landau et al., 2010; Heister et al., 2011). Future work should explore optimized cutoffs for the AD signature and other structural measures, allowing for comparison of these measures in both continuous and dichotomous forms.

It is also important to note that we compared CSF molecular biomarkers on an individual basis, as opposed to the combination of these markers. However, it appears that a combination of these measures may further enhance prediction (Shaw et al., 2009; De Meyer et al., 2010). In particular, ratios of t-tau or p-tau to amyloid-β may improve prediction by incorporating both neurodegenerative and amyloid-based measures, akin to our finding that the combination of the AD signature and CSF amyloid-β produced the strongest model in the Cox regression analysis. Nonetheless, the current analysis was developed to specifically compare across these classes of biomarkers and, as such, we chose to keep the CSF measures uncoupled.

In the present study, we employed a novel approach to the calculation of our AD signature measure. In the past, we have generally not adjusted for age-related cortical atrophy, but in some analyses have simply corrected statistically for a participant's chronological age. We recently reported on the cortical signature of normal aging (the "Aging signature"), describing a set of association and sensorimotor regions that undergo the most prominent loss of thickness in cognitively normal elderly adults compared to young adults (Bakkour et al., 2013). In the analyses here, we used the Aging signature set of regions to adjust for the "cortical age" of the individuals, creating an AD signature index, which represents the residual variance of the AD signature after accounting for variations in the Aging signature regional measurements. This corrects for the fact that some individuals may have thinner cortex in at least some of the regions vulnerable to AD simply as a result of more widespread cortical atrophy associated with normal aging, while those with thinner cortex in AD-vulnerable regions who have preserved thickness in Aging-vulnerable regions are much more likely to be exhibiting atrophy associated specifically with AD pathology. To our knowledge, this type of an adjustment of MRI biomarkers has not been performed previously. We are continuing to explore the strengths and weaknesses of this approach.

Finally, our analysis indicated that the MRI-derived AD signature biomarker was useful for predicting progression to dementia within 1 year in MCI participants with baseline CSF amyloid-β levels not low enough to meet typical cutoffs indicating cerebral amyloidosis. Even though the percentage of individuals who progressed to dementia in this subgroup was low (13%), the MRI marker was still useful for prediction in this short time interval. To interpret this finding, we have considered several possibilities. First, it is possible that these individuals have a non-Alzheimer pathology that is associated with atrophy in some of the same structures affected by AD. Although this consideration certainly seems reasonable when the structural MRI measure is of the hippocampus, since pathologies such as hippocampal sclerosis could be playing a role, it seems harder to reconcile with an MRI biomarker measuring a spatially distributed pattern of atrophy. We are currently examining the use of the AD signature marker in differential diagnosis of other neurodegenerative diseases, including frontotemporal dementias and Lewy body dementia; findings from this work will provide important data on the specificity of this marker in other neurodegenerative diseases. It is also possible that these individuals actually have underlying AD pathology but are "below the threshold" of amyloid pathology to meet current CSF cutoffs. This group could also be akin to previously reported

cognitively normal and MCI individuals with evidence of AD-like neurodegeneration and negative amyloid status, which has been labeled suspected non-Alzheimer pathology (sNAP; Knopman et al., 2012; Petersen et al., 2013; Prestia et al., 2013). While debate continues regarding the underlying pathology in these individuals, Prestia et al. (2013) also similarly reported that such individuals with an MCI phenotype also had a high rate of conversion to clinical dementia. As they note, it is worth at least considering that these patients may require adaptation of the model of biomarker change used here, as has been recently discussed (Jack et al., 2013). It is also worth noting that the individuals in this group in the present analysis who progressed to dementia were diagnosed clinically with probable AD dementia rather than a non-AD dementia.

Limitations of the present study include the relatively short follow-up period and the small number of individuals who were amyloid-negative at baseline with adequate longitudinal follow-up data. Furthermore, a more broadly representative sample of individuals with MCI might be helpful to better determine whether these findings are generalizable to clinical practice. Nevertheless, we believe the results of the present analysis provide valuable insights about the use of biomarkers in an MCI sample likely to be similar to that considered for clinical trials of putative AD interventions.

ACKNOWLEDGMENTS

Data collection and sharing for this project was funded by the Alzheimer's Disease Neuroimaging Initiative (ADNI; National Institutes of Health Grant U01 AG024904). ADNI is funded by the National Institute on Aging, the National Institute of Biomedical Imaging and Bioengineering, and through generous contributions from the following: Alzheimer's Association; Alzheimer's Drug Discovery Foundation; BioClinica, Inc.; Biogen Idec Inc.; Bristol-Myers Squibb Company; Eisai Inc.; Elan Pharmaceuticals, Inc.; Eli Lilly and Company; F. Hoffmann-La Roche Ltd and its affiliated company Genentech, Inc.; GE Healthcare; Innogenetics, N.V.; IXICO Ltd.; Janssen Alzheimer Immunotherapy Research & Development, LLC.; Johnson & Johnson Pharmaceutical Research & Development LLC.; Medpace, Inc.; Merck & Co., Inc.; Meso Scale Diagnostics, LLC.; NeuroRx Research; Novartis Pharmaceuticals Corporation; Pfizer Inc.; Piramal Imaging; Servier; Synarc Inc.; and Takeda Pharmaceutical Company. The Canadian Institutes of Health Research is providing funds to support ADNI clinical sites in Canada. Private sector contributions are facilitated by the Foundation for the National Institutes of Health (www.fnih.org). The grantee organization is the Northern California Institute for Research and Education, and the study is coordinated by the Alzheimer's Disease Cooperative Study at the University of California, San Diego. ADNI data are disseminated by the Laboratory for Neuro Imaging at the University of California, Los Angeles. This research was also supported by NIH grants P30 AG010129 and K01 AG030514. This research was also supported by NIH grants P30 AG010129, K01 AG030514, and the Dana Foundation. This analysis was also supported by grants from the NIA P50-AG005134, P30AG010124, and the Alzheimer's Association. We thank Michael Brickhouse for his assistance in data management and analysis.

REFERENCES

Albert, M. S., DeKosky, S. T., Dickson, D., Dubois, B., Feldman, H. H., Fox, N. C., et al. (2011). The diagnosis of mild cognitive impairment due to Alzheimer's disease: recommendations from the National Institute on Aging-Alzheimer's Association workgroups on diagnostic guidelines for Alzheimer's disease. *Alzheimers Dement.* 7, 270–279. doi: 10.1016/j.jalz.2011.03.008

Bakkour, A., Morris, J. C., and Dickerson, B. C. (2009). The cortical signature of prodromal AD: regional thinning predicts mild AD dementia. *Neurology* 72, 1048–1055. doi: 10.1212/01.wnl.0000340981.97664.2f

Bakkour, A., Morris, J. C., Wolk, D. A., and Dickerson, B. C. (2013). The effects of aging and Alzheimer's disease on cerebral cortical anatomy: specificity and differential relationships with cognition. *Neuroimage* 76, 332–344. doi: 10.1016/j.neuroimage.2013.02.059

Bateman, R. J., Xiong, C., Benzinger, T. L. S., Fagan, A. M., Goate, A., Fox, N. C., et al. (2012). Clinical and biomarker changes in dominantly inherited Alzheimer's disease. *N. Engl. J. Med.* 367, 795–804. doi: 10.1056/NEJMoa1202753

Blennow, K., Hampel, H., Weiner, M., and Zetterberg, H. (2010). Cerebrospinal fluid and plasma biomarkers in Alzheimer disease. *Nat. Rev. Neurol.* 6, 131–144. doi: 10.1038/nrneurol.2010.4

Buchhave, P., Minthon, L., Zetterberg, H., Wallin, A. K., Blennow, K., and Hansson, O. (2012). Cerebrospinal fluid levels of beta-amyloid 1-42, but not of tau, are fully changed already 5 to 10 years before the onset of Alzheimer dementia. *Arch. Gen. Psychiatry* 69, 98–106. doi: 10.1001/archgenpsychiatry.2011.155

De Meyer, G., Shapiro, F., Vanderstichele, H., Vanmechelen, E., Engelborghs, S., De Deyn, P. P., et al. (2010). Diagnosis-independent Alzheimer disease biomarker signature in cognitively normal elderly people. *Arch. Neurol.* 67, 949–956. doi: 10.1001/archneurol.2010.179

Dickerson, B. C., Bakkour, A., Salat, D. H., Feczko, E., Pacheco, J., Greve, D. N., et al. (2009). The cortical signature of Alzheimer's disease: regionally specific cortical thinning relates to symptom severity in very mild to mild AD dementia and is detectable in asymptomatic amyloid-positive individuals. *Cereb. Cortex* 19, 497–510. doi: 10.1093/cercor/bhn113

Dickerson, B. C., Wolk, D. A., and Alzheimer's Disease Neuroimaging Initiative. (2011) Dysexecutive versus amnesic phenotypes of very mild Alzheimer's disease are associated with distinct clinical, genetic and cortical thinning characteristics. *J. Neurol. Neurosurg. Psychiatry* 82, 45–51. doi: 10.1136/jnnp.2009.199505

Frisoni, G. B., Fox, N. C., Jack, C. R. Jr., Scheltens, P., and Thompson, P. M. (2010). The clinical use of structural MRI in Alzheimer disease. *Nat. Rev. Neurol.* 6, 67–77. doi: 10.1038/nrneurol.2009.215

Hansson, O., Zetterberg, H., Buchhave, P., Londos, E., Blennow, K., and Minthon, L. (2006). Association between CSF biomarkers and incipient Alzheimer's disease in patients with mild cognitive impairment: a follow-up study. *Lancet Neurol.* 5, 228–234. doi: 10.1016/S1474-4422(06)70355-6

Heister, D., Brewer, J. B., Magda, S., Blennow, K., and McEvoy, L. K. (2011). Predicting MCI outcome with clinically available MRI and CSF biomarkers. *Neurology* 77, 1619–1628. doi: 10.1212/WNL.0b013e3182343314

Jack, C. R. Jr., Bernstein, M. A., Fox, N. C., Thompson, P., Alexander, G., Harvey, D., et al. (2008). The Alzheimer's Disease Neuroimaging Initiative (ADNI): MRI methods. *J. Magn. Reson. Imaging* 27, 685–691. doi: 10.1002/jmri.21049

Jack, C. R. Jr., Knopman, D. S., Jagust, W. J., Petersen, R. C., Weiner, M. W., Aisen, P. S., et al. (2013). Tracking pathophysiological processes in Alzheimer's disease: an updated hypothetical model of dynamic biomarkers. *Lancet Neurol.* 12, 207–216. doi: 10.1016/S1474-4422(12)70291-0

Jack, C. R. Jr., Lowe, V. J., Weigand, S. D., Wiste, H. J., Senjem, M. L., Knopman, D. S., et al. (2009). Serial PIB and MRI in normal, mild cognitive impairment and Alzheimer's disease: implications for sequence of pathological events in Alzheimer's disease. *Brain* 132, 1355–1365. doi: 10.1093/brain/awp062

Jack, C. R. Jr., Petersen, R. C., Xu, Y. C., O'Brien, P. C., Smith, G. E., Ivnik, R. J., et al. (1999). Prediction of AD with MRI-based hippocampal volume in mild cognitive impairment. *Neurology* 52, 1397–1403. doi: 10.1212/WNL.52.7.1397

Jack, C. R. Jr., Wiste, H. J., Vemuri, P., Weigand, S. D., Senjem, M. L., Zeng, G., et al. (2010). Brain beta-amyloid measures and magnetic resonance imaging atrophy both predict time-to-progression from mild cognitive impairment to Alzheimer's disease. *Brain* 133, 3336–3348. doi: 10.1093/brain/awq277

Knopman, D. S., Jack, C. R. Jr., Wiste, H. J., Weigand, S. D., Vemuri, P., Lowe, V. J., et al. (2012) Brain injury biomarkers are not dependent on beta-amyloid in normal elderly. *Ann. Neurol.* doi: 10.1002/ana.23816 [Epub ahead of print].

Landau, S. M., Harvey, D., Madison, C. M., Reiman, E. M., Foster, N. L., Aisen, P. S., et al. (2010). Comparing predictors of conversion and decline in mild cognitive impairment. *Neurology* 75, 230–238. doi: 10.1212/WNL.0b013e3181e8e8b8

Landau, S. M., Mintun, M. A., Joshi, A. D., Koeppe, R. A., Petersen, R. C., Aisen, P. S., et al. (2012). Amyloid deposition, hypometabolism, and longitudinal cognitive decline. *Ann. Neurol.* 72, 578–586. doi: 10.1002/ana.23650

Petersen, R. C., Aisen, P., Boeve, B. F., Geda, Y. E., Ivnik, R. J., Knopman, D. S., et al. (2013) Criteria for mild cognitive impairment due to Alzheimer's disease in the community. *Ann. Neurol.* doi: 10.1002/ana.23931 [Epub ahead of print].

Petersen, R. C., Parisi, J. E., Dickson, D. W., Johnson, K. A., Knopman, D. S., Boeve, B. F., et al. (2006). Neuropathologic features of amnestic mild cognitive impairment. *Arch. Neurol.* 63, 665–672. doi: 10.1001/archneur.63.5.665

Prestia, A., Caroli, A., van der Flier, W. M., Ossenkoppele, R., Van Berckel, B., Barkhof, F., et al. (2013). Prediction of dementia in MCI patients based on core diagnostic markers for Alzheimer disease. *Neurology* 80, 1048–1056. doi: 10.1212/WNL.0b013e3182872830

Shaw, L. M., Vanderstichele, H., Knapik-Czajka, M., Clark, C. M., Aisen, P. S., Petersen, R. C., et al. (2009). Cerebrospinal fluid biomarker signature in Alzheimer's disease neuroimaging initiative subjects. *Ann. Neurol.* 65, 403–413. doi: 10.1002/ana.21610

Vemuri, P., Wiste, H. J., Weigand, S. D., Knopman, D. S., Trojanowski, J. Q., Shaw, L. M., et al. (2010). Serial MRI and CSF biomarkers in normal aging, MCI, and AD. *Neurology* 75, 143–151. doi: 10.1212/WNL.0b013e3181e7ca82

Vemuri, P., Wiste, H. J., Weigand, S. D., Shaw, L. M., Trojanowski, J. Q., Weiner, M. W., et al. (2009a). MRI and CSF biomarkers in normal, MCI, and AD subjects: diagnostic discrimination and cognitive correlations. *Neurology* 73, 287–293. doi: 10.1212/WNL.0b013e3181af79e5

Vemuri, P., Wiste, H. J., Weigand, S. D., Shaw, L. M., Trojanowski, J. Q., Weiner, M. W., et al. (2009b). MRI and CSF biomarkers in normal, MCI, and AD subjects: predicting future clinical change. *Neurology* 73, 294–301. doi: 10.1212/WNL.0b013e3181af79fb

Villemagne, V. L., Burnham, S., Bourgeat, P., Brown, B., Ellis, K. A., Salvado, O., et al. (2013). Amyloid beta deposition, neurodegeneration, and cognitive decline in sporadic Alzheimer's disease: a prospective cohort study. *Lancet Neurol.* 12, 357–367. doi: 10.1016/S1474-4422(13)70044-9

Visser, P. J., Verhey, F., Knol, D. L., Scheltens, P., Wahlund, L. O., Freund-Levi, Y., et al. (2009). Prevalence and prognostic value of CSF markers of Alzheimer's disease pathology in patients with subjective cognitive impairment or mild cognitive impairment in the DESCRIPA study: a prospective cohort study. *Lancet Neurol.* 8, 619–627. doi: 10.1016/S1474-4422(09)70139-5

Wang, P. N., Lirng, J. F., Lin, K. N., Chang, F. C., and Liu, H. C. (2006). Prediction of Alzheimer's disease in mild cognitive impairment: a prospective study in Taiwan. *Neurobiol. Aging* 27, 1797–1806. doi: 10.1016/j.neurobiolaging.2005.10.002

Wolk, D. A., Dickerson, B. C., and Alzheimer's Disease Neuroimaging Initiative. (2010). Apolipoprotein E (APOE) genotype has dissociable effects on memory and attentional-executive network function in Alzheimer's disease. *Proc. Natl. Acad. Sci. U.S.A.* 107, 10256–10261. doi: 10.1073/pnas.1001412107

Conflict of Interest Statement: The authors declare that the research was conducted in the absence of any commercial or financial relationships that could be construed as a potential conflict of interest.

Received: 31 May 2013; accepted: 08 September 2013; published online: 11 October 2013.

*Citation: Dickerson BC and Wolk DA (2013) Biomarker-based prediction of progression in MCI: comparison of AD signature and hippocampal volume with spinal fluid amyloid-β and tau. Front. Aging Neurosci. **5**:55. doi: 10.3389/fnagi.2013.00055*

This article was submitted to the journal Frontiers in Aging Neuroscience.

frontiers in
AGING NEUROSCIENCE

REVIEW ARTICLE
published: 04 February 2014
doi: 10.3389/fnagi.2014.00012

Network-based biomarkers in Alzheimer's disease: review and future directions

Jaime Gomez-Ramirez [1,2] **** and Jinglong Wu*** [2]

[1] *Autonomous Systems Laboratory, Universidad Politécnica de Madrid, Madrid, Spain*
[2] *Biomedical Engineering Laboratory, Okayama University, Okayama, Japan*

Edited by:
Manuel Menéndez-González, Hospital Álvarez-Buylla, Spain

Reviewed by:
Daniel Ortuño-Sahagun, Centro Universitario de Ciencias Biológicas y Agropecuarias, Mexico
Jose-Luis Gonzalez De Aguilar, University of Strasbourg, France

****Correspondence:***
Jaime Gomez-Ramirez, Autonomous Systems Laboratory, Universidad Politécnica de Madrid, José Gutiérrez Abascal, 2 Madrid 28006, Spain
e-mail: jd.gomez@upm.es

By 2050 it is estimated that the number of worldwide Alzheimer's disease (AD) patients will quadruple from the current number of 36 million people. To date, no single test, prior to postmortem examination, can confirm that a person suffers from AD. Therefore, there is a strong need for accurate and sensitive tools for the early diagnoses of AD. The complex etiology and multiple pathogenesis of AD call for a system-level understanding of the currently available biomarkers and the study of new biomarkers via network-based modeling of heterogeneous data types. In this review, we summarize recent research on the study of AD as a connectivity syndrome. We argue that a network-based approach in biomarker discovery will provide key insights to fully understand the network degeneration hypothesis (disease starts in specific network areas and progressively spreads to connected areas of the initial loci-networks) with a potential impact for early diagnosis and disease-modifying treatments. We introduce a new framework for the quantitative study of biomarkers that can help shorten the transition between academic research and clinical diagnosis in AD.

Keywords: Alzheimer's disease, network degeneration hypothesis, network-based biomarkers, default-mode network DMN, resting-state functional connectivity

INTRODUCTION

A biomarker is a parameter that can be used as an indicator of normal biological processes, pathogenic processes, or pharmacological responses to therapeutic drugs (Biomarkers Definitions Working Group, 2001). In Alzheimer's disease (AD), potential biomarker information comes from multiple sources, including clinical tests for memory impairment, bodily fluid or tissues, neuroimaging, and smell tests among others. AD biomarkers are typically assumed to belong to the following two categories: *biofluid analytes*, e.g., cerebrospinal fluid (CSF), peripheral blood samples such as urine and *imaging measures*, e.g., magnetic resonance imaging (MRI), magnetic resonance spectroscopy (MRS), or positron emission tomography (PET) (Henriksen et al., 2014). At present there are five well-established AD biomarkers: two are CSF analytes that measure abnormal protein aggregates – low level of CSF amyloid-beta and elevated level of both total and phosphorylated CSF tau protein; and three imaging biomarkers – the Pittsburgh compound-B PIB PET tracer for amyloid-beta deposition, for which MRI scans may detect atrophied sensible brain areas; and Fludeoxyglucose FDG PET to quantify abnormal neuronal glucose consumption (Jack, 2012).

The diagnostic criteria for AD has not been modified since its original formulation in 1984 until it was recently updated in 2010 (Dubois et al., 2010). In the original criteria, AD was strictly diagnosed on a clinical basis (McKhann et al., 1984). Other sources of information such as imaging lacked a positive diagnostic role. New diagnostic criteria reckons AD as a complex disorder characterized by a gradual and progressive pathogenesis, with three phases – preclinical or asymptomatic, prodromal or mild cognitive impairment (MCI), and overt dementia (Dubois et al., 2007; Albert et al., 2011; Sperling, 2011). Despite technological and conceptual advances in AD, we are still lacking preventive therapies to delay the onset of AD as well as disease-modifying treatments. Despite the strong need for early diagnose of AD, and the fact that biomarkers have proved useful in correlating with the different stages in which the disease unfolds, CSF and imaging biomarkers still play a surprisingly minor role in clinical diagnosis. They are, however, increasingly prominent in clinical trials and academic research.

There is a growing consensus between clinical researchers that the application of biomarkers should follow a multi-modal and integrative approach. Truly predictive models of disease progression need to take into account the combined effects of biomarkers interactions at the individual subject level. Unfortunately however, few studies have specifically addressed the issue of the integration of different biomarkers for efficient and quantitative diagnostics. Furthermore, it has been particularly difficult to link findings on molecular biomarkers to early stages of the neurodegenerative disease, and no real groundbreaking discovery in imaging-based biomarkers has been produced. Thus, there is a lack of novel therapeutic approaches that efficiently target the underlying mechanisms and disease progression of AD (Corbett and Ballard, 2012). There is clear evidence that AD and other neurodegenerative disorders evolve at the systems level (Eidelberg and Martin, 2013) and that biomarkers – molecular, imaging, or CSF – need to be considered with a holistic point of view. Functional imaging may help us understand disease-related changes in interconnected brain areas. In this regard, functional imaging techniques unburdened of subject compliance such as RS-functional magnetic resonance imaging (fMRI) and TMS/EEG, are being extensively used for biomarkers discovery in neurodegenerative disorders.

In this review, we provide a brief panoramic view on recent research on the discovery of AD biomarkers, putting special emphasis on neuroimaging biomarkers derived from functional connectivity data in resting state, that is, the subject is not performing an explicit task. Network-based biomarkers are introduced, and we provide a new framework for the quantitative study of biomarkers that can help shorten the transition between academic research and clinical diagnosis in AD.

AD BIOMARKERS

Clinical tests for AD diagnosis involve subjective reasoning by experienced practitioners. Episodic memory impairment has little or no relevance in early diagnosis, but it still remains the core diagnostic criterion. Current diagnostic criteria (DSM-IV and NINCDS-ADRDA) have high sensitivity but low specificity (Knopman et al., 2001). The delay from symptoms to diagnosis is 20 months on average in the EU, and 36 months in the UK (Mattila et al., 2012). Furthermore, molecular pathomechanisms of AD become active for several years before symptoms such as cognitive impairment manifests itself.

Blood samples are a non-invasive and cost-effective technique for the identification of plasma biomarkers that has proven useful in distinguishing individuals with AD from cognitively healthy control subjects (Doecke et al., 2012). Plasma biomarkers can be used to extract metabolomics (Trushina et al., 2013) and proteomics biomarker signatures in AD (Hye et al., 2006). Contrary to diagnostic tools like CSF and PET, plasma amyloid-beta measurements are neither invasive nor expensive. Plasma Aβ40 and Aβ42 can be measured in peripheral blood, but they cannot be used in AD identification. Vanderstichele et al. (2000) found no differences in Aβ42 levels between controls and patients with AD. Further work is required before plasma amyloid-beta measurements are unanimously regarded as clinically useful (Mayeux and Schupf, 2011; Toledo et al., 2013).

Using Smell tests to detect hyposmia is another example of inexpensive biomarker in AD (Kjelvik et al., 2007). However, the reduced capability to detect odors shown in AD may be more an effect of the cognitive decline characteristic of the disease than a symptom with predictive value (Serby et al., 1991).

Neuroimaging biomarkers in AD measure brain signals at both mesoscopic (MRI) and macroscopic scales (fMRI, MRS, and PET). Morphometric analysis with MRI data (e.g., atrophy in medial temporal lobes, specifically in the hippocampus and entorhinal cortex) is a well-known marker of disease progression in AD. Hippocampus atrophy correlates with neuronal loss and therefore MRI biomarkers could be used in proof-of-the-concept studies to distinguish between disease-modifying and symptomatic treatment effects (Saumier et al., 2009; Hampel et al., 2011). PET neuroimaging allows us to collect molecular information. PET image analysis can provide evidence of the accumulation of amyloid-beta plaques that is independent from structural brain changes. It also provides evidence of a reduction of glucose metabolism in the parietal and temporal lobe regions that are involved in memory and executive function (Habeck et al., 2012). Both structural MRI and FDG-PET imaging reflect the effects of the disease progress in symptomatic stages, however it is the diagnosis in AD's asymptomatic stages that remains to be solved. Molecular pathomechanisms, such as the accumulation of amyloid plaque, become active several years before cognitive deficit manifest. Furthermore, amyloid-beta is not specific to AD, but may also be found in normal aging.

RESTING-STATE fMRI

Functional magnetic resonance imaging allows us to assess functional connectivity mapping at high temporal resolution by means of correlations in the blood-oxygen-level-dependent (BOLD) signal in spatially distant brain regions. Since the seminal work of Biswal (Biswal et al., 1995), task-free or resting-state fMRI (R-fMRI) has been successfully incorporated into the functional MRI imaging repertoire, and represents a comprehensive alternative to the task-based approach. R-fMRI experiments are considerably less demanding for the subject, which makes this technique especially attractive to brain dementia researchers, as it is relatively free of subject compliance and training demands. R-fMRI measures the spontaneous or intrinsic brain activity in terms of low-frequency (<0.1 Hz) BOLD fluctuations. Fluctuations in the BOLD signal measured in humans in resting state represent the neuronal activity baseline and shape spatially consistent patterns (Fransson, 2005; Raichle and Gusnard, 2005). The systematic study of those patterns using correlation analysis techniques has identified a number of resting-state networks, which are functionally relevant networks found in subjects in the absence of either goal directed-task or external stimuli. Despite the variability in the data acquisition protocols, statistical data analysis, and groups of subjects employed, resting-state networks have been consistently reported in multiple studies. There are at least eight commonly identified resting-state networks: the primary sensorimotor network, the primary visual and extra-striate visual network, bilateral temporal/insular, and anterior cingulate cortex regions, left and right lateralized networks consisting of superior parietal and superior frontal regions, and the default-mode network (DMN) (Van den Heuvel and Hulshoff Pol, 2010).

The DMN is a specific anatomically defined brain system that is preferentially active when individuals are focused on introspective activities such as autobiographical memory retrieval, rather than on the external environment (Buckner et al., 2008). A number of studies indicate that the default network is also relevant for understanding mental disorders including depression (Sheline et al., 2009), autism (Washington et al., 2013), and AD. Studies show a decrease in DMN functional connectivity in normal aging, MCI and AD (Hafkemeijer et al., 2012). Functional connectivity of the DMN may prove to be a sensitive and specific biomarker for mild AD (Greicius et al., 2004; Balthazar et al., 2014).

The visual identification of the overall connectivity patters in R-fMRI has been assessed using either model-based or model-free approaches. In the former, statistical parametric maps of brain activation are built upon voxel-wise analysis location (Wang et al., 2009; Faria et al., 2012). This approach has been successful in the identification of motor networks, but it shows important limitations when the seed voxel cannot be easily identified, for example in brain areas with unclear boundaries such as cognitive networks involved in language or memory. Independent component analysis (ICA) (Comon, 1994; Stone, 2002), on the other hand, is a model-free approach that allows separating resting fluctuations from

other signal variations, resulting in a collection of spatial maps, one for each independent component, that represent functionally relevant networks in the brain. While ICA has an advantage over model-free methods that it is unbiased, that is, it does not need to posit a specific temporal model of correlation between regions of interest (ROI), the functional relevance of the different components is still computed relative to their resemblance to a number of networks based on criteria that are not easily formalized (Friston, 1998). More recently researchers using graph-theory based methods have been able to not only visualize brain networks, but also to quantify their topological properties as well (He et al., 2009; Wang et al., 2010). Graph-theory provides a formal and rigorous framework to quantitatively analyze the connectivity pattern, at either a local or global level, underlying cognitive networks. How these network properties are modified during normal development, aging, or pathological conditions is addressed in the next section.

R-fMRI AND AD

Altered resting-state functional connectivity patterns have been shown in an impressive range of pathologies and conditions – AD, schizophrenia, multiple sclerosis, Parkinson's disease, depression, autism, and attention deficit/hyperactivity disorder – see (Lee et al., 2013) for a review on clinical applications. In the context of AD, both amyloid-beta and tau pathologies affect DMN integrity before the clinical onset of the disease (Li et al., 2013; Wang et al., 2013). DMN regions such as the precuneus and the posterior cingulate are selectively vulnerable to amyloid-beta deposition (Sperling et al., 2010). AD weakens structural and functional connectivity between the cingulate cortex and other regions within the DMN, which is consistent with the reduction in metabolic activity and atrophy observed with FDP-PET and volumetric MRI, respectively within the DMN (Zhu et al., 2013). Patients with severe AD show decreased connectivity between distant brain regions (Liu et al., 2013). Interest in understanding the pathomechanisms of tau-mediated neurodegeneration has been fostered by the failure of amyloid-beta therapies to prevent neurodegeneration by Aβ removal. Tau abnormalities have been found to be more closely related to cognitive dysfunction than Aβ (Yoshiyama et al., 2012). Tau deposition is initially located in the medio-temporal lobe to spread later to lateral temporal and frontal parietal areas. This orderly progression found in hypophosphorylated tau maps the regional specificity in the deployment of symptoms in AD, i.e., episodic memory loss in the MTL is followed by semantic memory loss in lateral temporal cortex to aphasic symptoms in parietal cortex (Pievani et al., 2011).

Functional imaging has been successfully used in population selection in cross-sectional studies to classify between normally aging, MCI, and AD subjects (Rombouts et al., 2005; Damoiseaux, 2012). R-fMRI can be also used to track AD progression in longitudinal studies. For example, in Damoiseaux et al. (2012) it is shown that functional connectivity in default-mode subnetworks decreases in AD patients compared to healthy controls. Resting-state functional connectivity can help detect early manifestations of genetic effects related to AD. For instance, in (Sheline et al., 2010) cognitive normal individuals were categorized into PIB− (no evidence of brain amyloid) and PIB+ (PET evidence of amyloid deposition) and compared with AD patients using resting-state functional connectivity. The study showed that the PIB+ and AD groups share similar modifications in both functional and effective connectivity. Thus, R-fMRI can be used to detect early manifestations of genetic effect, e.g., amyloid deposition in APOE4 carriers, and therefore holds great potential in early diagnosis and disease-modifying strategies. It goes without saying that like any technique, R-fMRI has advantages and disadvantages. fMRI measures the BOLD signal, which is an indirect measure of neural activity and it is susceptible to several imaging artifacts and has, in general, worse temporal resolution than EEG and MEG, and spatial resolution that is not as good as more invasive procedures such as single-unit electrodes. The analysis and interpretation of R-fMRI data is particularly challenging, and further work is still required to address complex issues like network identification, effective connectivity between brain networks, detecting AD risk groups, etc. For a review on the progress and pending problems of statistical approaches to analyzing R-fMRI, see Cole et al. (2010).

NETWORK-BASED BIOMARKERS

Contrary to other conditions such as brain injury whose onset can be tracked both in location and time, late sporadic AD – the most common form of dementia and two orders of magnitude more frequent than inherited AD (Bateman et al., 2012) – has a gradual onset that lacks a specific location or temporal window. Experimental studies based on neuropathology, neuroimaging, and transgenic animal models suggest that neurodegeneration relates to neural network dysfunction. Disease-vulnerable intrinsic functional networks are not diffuse or random (Sanz-Arigita et al., 2010), however, researchers are still uncertain about the specific way in which neurodegeneration spreads beyond the sites of initial impairment. The network degeneration hypothesis (Seeley et al., 2009) – disease starts in small network assemblies, to progressively spread to connected areas of the initial locus – supports the view that neurodegenerative disorders can be study as connectivity disorders. In this light, AD can be understood as a disconnection syndrome in which the structural and functional connectivity of large-scale networks is progressively modified by molecular pathomechanisms that are not fully understood.

A diagnostic biomarker, in order to be considered as such, should reflect a core pathogenic process. The established biomarkers in AD hold this promise as they measure, for example, amyloid-beta and tau deposition levels, which are responsible for the formation of senile plaques and neurofibrillary tangles. However, it is far from clear whether amyloid and tau deposition are etiologically linked to memory deficits or they rather reflect secondary effects of a different pathogenic mechanism (Eidelberg and Martin, 2013). AD is a complex and multifactorial condition and so "secondary processes" such as oxidative stress, immune responses, or inflammation and how they interact with core pathogenic mechanisms need to be properly understood.

The discovery of AD biomarkers must go beyond detecting abnormal protein deposition levels and be able to monitor both disease progression and treatment effects in a coherent and integrative way. To that end, a network-based approach for biomarker discovery is required. Erler and Linding (2010) argue that biomarkers should be deployed as network models themselves. The

rationale behind this idea is that biomarker discovery needs to take into account the network state and the biological context in which the network evolves, rather than focus on individual nodes or events, e.g., phosphorylation. A network-based approach for biomarker discovery is also being fostered in complex diseases such as cancer and diabetes (Ahn et al., 2006).

The multifactorial pathogenesis of complex diseases such as AD is at odds with the current implementation of biomarkers which are single-dimensional. Thus, we propose to redefine biomarker as *a network model that can be used as an indicator of normal (including adaptive) biological processes, pathogenic processes, or pharmacological responses to therapeutic drugs.* Under this definition, biomarkers are multidimensional, as they are embedded into a network model in which network parameters, that represent normal or pathological processes but also adaptive responses, can be characterized. This new definition of biomarker allows us to quantify adaptive processes triggered by early pathogenic events, fostering an integrative and multidimensional approach of use in AD early diagnose. For example, it is unclear if, as the disease progresses, functional connectivity in large neural systems is attenuated, e.g., in the DMN (Wu et al., 2011; Liu et al., 2013; Zhu et al., 2013) or on the contrary, AD may induce an increase in functional connectivity that compensates for the disease related atrophy of affected regions (Sanz-Arigita et al., 2010). An increase in focal frontal connectivity and heightened hippocampal activation during early stages of AD has been reported in Dickerson et al. (2004). Functional disruption has been observed in the prodromal stage or even earlier and therefore a characterization of this imaging phenotype has potential impact in early prevention and disease-modifying therapies. The relationship between brain development, aging and disease and brain connectivity is not univocal, but instead involves a number of complex mechanisms that alter the network topology in multiple ways. The mechanisms that mediate in the increase in functional connectivity observed in prodromal AD are in dispute. There are several potential explanations for this phenomenon. For example, the increase in connectivity in the early phases of AD could reflect compensatory effects to neutralize the disruption in functional integrity, or represent some form of glutamate receptor-mediated excitotoxicity (Wu et al., 1995). An interesting hypothesis borrowed from economic theory is that early network alterations can be interpreted as a discount factor that anticipates the expectation of pending functional network integrity deterioration.

Combining existing biomarkers poses important challenges not only in terms of intelligibility due to the heterogeneous and complex nature of biomarker data, but also in terms of cost of data extraction, e.g., expensive SPECT or MRI can not be used in subjects with metal implants, and genetic mutations account for only a small percentage of AD cases (Bertram and Tanzi, 2004). Truly predictive models of disease progression need to take into account the combined effects of biomarkers interactions at the individual subject level. Few studies however, have specifically addressed the issue of the integration of different biomarkers (Gomar et al., 2011). The long sought goal of early diagnosis of AD necessarily passes by the integration of existing biomarkers and the discovery of new ones. Network-based biomarkers provide a unifying approach for AD biomarker discovery and testing. Graph-based network analysis allows to quantitatively characterize the global organization of the brain and to integrate heterogeneous data in a "neutral" and general mathematical body.

A NETWORK-BASED APPROACH IN AD BIOMARKERS

Biomarkers can be compounds obtained from bodily fluids or tissues, or technically derived correlates of pathophysiological events. While three of the five most important AD biomarkers are imaging-based, functional neuroimaging is absent in current diagnostic criteria.

Markers of alterations in resting-state functional connectivity networks can discriminate between AD patients and healthy elderly people with a satisfactory level of sensitivity and specificity. Functional connectivity analysis of the DMN has great potential as network biomarker able to objectively quantify asymptomatic and prodromal stages of the disease and as secondary endpoint in multicenter clinical trials in AD (Chhatwal et al., 2013). The study of AD biomarkers with R-fMRI imaging, however, has focused on detecting alterations in specific networks such as the DMN and finding abnormal levels of protein deposition, metabolic disruption, and atrophy within the DMN. A system-level understanding of the dependencies that exist among the different biomarkers has not been achieved. The advent of "Big Data" science makes it possible to share large amount of data with unprecedented processing capability. The Alzheimer's disease neuroimaging initiative (ADNI) makes access to clinical imaging and biomarker data freely available to researchers worldwide. The whole genome sequences of the 800 individuals enrolled in the ADNI will be soon available through the Global Alzheimer's Association Interactive Network (GAAIN).

The much-needed insight into the pathomechanisms that mediate in AD will benefit from the construction of probabilistic networks from large databases of AD biomarkers that systematically capture the probabilistic dependencies among biomarkers. Once the network or networks are built, a supervised classification algorithm can be used to classify new subjects within different classes, for example healthy and AD. Thus, in a training set of patients diagnosed as healthy or AD, we first build the generative graphs – M_{H} and M_{AD} – containing biomarker dependencies of healthy and AD subjects, respectively, to later perform a classification inference, that is, estimate the likelihood that M_{H} or M_{AD} has generated new data, i.e., a new subject to be diagnosed.

Let us see this with an example. **Figure 1** shows a classification procedure for AD using a biomarker network-based approach. BM is a list of AD biomarkers considered in this example, BM = (w, o, τ, aβ, hc, fc, tac). For convenience, we assume that BM takes discrete values, that is, $\mathrm{BM}_i = 1$ when biomarker i reaches the threshold of positivity. Thus, w (Word recognition) and o (Orientation) are neuropsychological markers included in the ADAS-Cog (Alzheimer Disease Assessment Scale-Cognitive) (Rosen et al., 1984), τ and Aβ are CSF biomarkers that indicate whether the protein deposition is relevant, hc (hippocampus) is equal to 1 when a significant reduction of the hippocampus volume is found, fc (functional connectivity) indicates whether regions in, for example, the DMN such as the precuneus or the posterior cingulate cortex, has functional connectivity alterations reported in the literature or any other pattern that we want to be tested against other biomarkers. The tactile biomarker (tac) is an inexpensive marker

BM	Word recognition	Orientation	Tau	Amyloid	HC	fMRI	Tactile	Diagnosis
subject_1	w(1)	o(1)	$\tau(1)$	aβ(1)	hc(1)	fmri(1)	tac(1)	AD
subject_2	w(2)	o(2)	$\tau(2)$	aβ(2)	hc(2)	fmri(2)	tac(2)	H
subject_3	w(3)	o(3)	$\tau(3)$	aβ(3)	hc(3)	fmri(3)	tac(3)	AD
	…	…	…			…		
subject_n	w(n)	o(n)	$\tau(n)$	aβ(n)	hc(n)	fmri(n)	hc(n)	AD

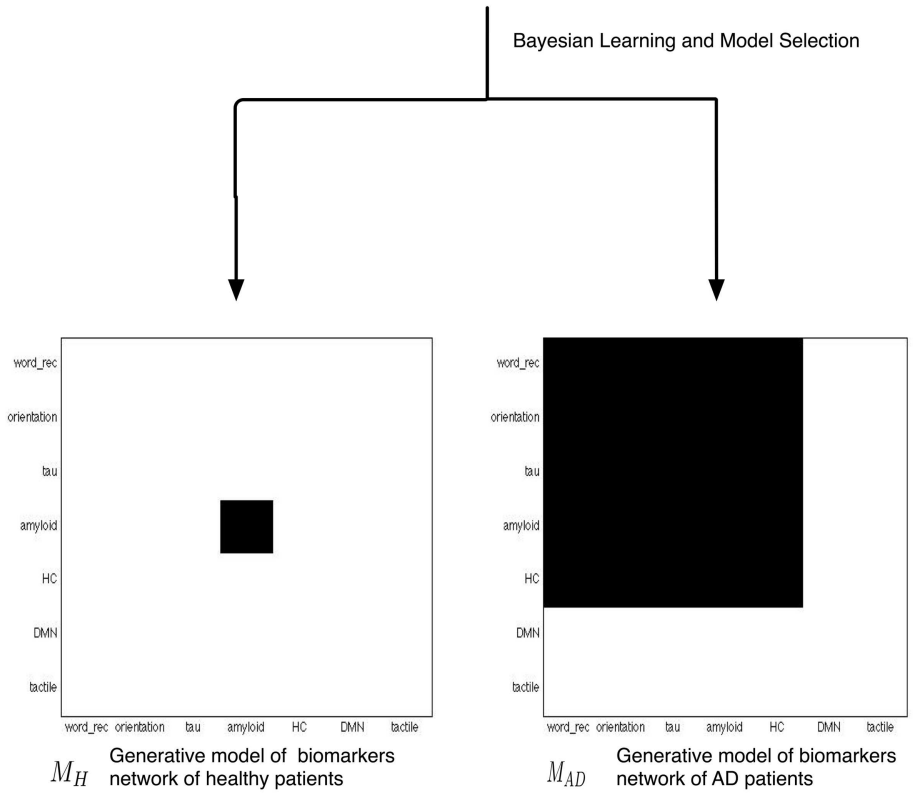

BM_s	Word recognition	Orientation	Tau	Amyloid	HC	fMRI	Tactile
subject_s	w(1)	o(1)	$\tau(1)$	aβ(1)	hc(1)	fmri(1)	tac(1)

$$max_{G=\{M_H, M_{AD}\}} P(BM_s|G)$$

FIGURE 1 | Seven biomarkers of interest are listed in BM. For convenience, we assume that BM is a binary vector, that is, BM(i) = 0,1. For example, if the measurement of the biomarker Word recognition reaches the positive threshold BM(1) = 1, if not, BM(1) = 0. The table in the top of the figure shows the training set S consisting of n samples or subjects with their biomarkers BM, and diagnosed as AD or healthy. The data in the table can be summarized via the construction of generative networks, one for each diagnostic category, in our example H and AD. There is a number of possible network structures that can characterize the training set, so the generative networks M_H and M_{AD} are the result of model selection. The diagnosis of new patients can be thus be addressed via the computation of the probability that the new data, BM_s is generated by the biomarker network that captures the dependencies among biomarkers in healthy subjects or by the biomarker network of healthy subjects.

of cognitive and motor decline of interest in AD found in our laboratory (Yang et al., 2010). This list of biomarkers can be extended with others, e.g., smell, epigenetic, blood, genetic, etc., with the caveat that a large number of parameters need even larger data sets in order to avoid having an overwhelming choice of networks that are potentially good at explaining the data.

The training data set S is ideally composed of a large number of diagnosed subjects with the BM vector of biomarker information for each one. Thus, the training set is given by $S = [(BM_1, y)(BM_2, y),...(BM_n, y)]$, where BM_i is the vector containing the biomarkers measured in patient i, and y represents the diagnostic class in which a subject can be classified, e.g., Healthy or AD. Now, we want to build a probabilistic network that captures dependencies among the biomarkers for each diagnostic class. For example, if the training data set contains biomarker information of n subjects diagnosed as healthy or AD $[y = (y_H, y_{AD})]$, two generative biomarker networks – M_H and M_{AD} – need to be built. This approach is entirely different to conventional AD biomarker

Table 1 | Differences between the standard and the network-based AD biomarker approaches.

	AD biomarker	AD network-based biomarker (NBB)
Dimensionality	1-Dimensional, unsuited for multi-modal integration of heterogeneous data	N-Dissmensional, integrate multi-modal biomarkers in a common framework
Statistical classification	Classifier based on group differences between HC, MCI, AD	Supervised classifier for the assessment of risk disease in relation to large population data. Allows group risk classification based on individual-based risk measure built upon network biomarker parameters
Temporal scale	Temporal window of biomarker efficiency is not considered	Well suited for longitudinal studies by implementing computational models of network disruption effects in temporal windows, e.g., short/long term
Spatial scale	Study of selective vulnerability in region specific neuron classes, i.e., neuronopathy or network component specific, e.g., the precuneus in the DMN	Unbiased, NBB address large-scale distributed networks. Long rage disease spread shaped by network connectivity profiles, i.e., network-opathy (Comon, 1994)
Early diagnosis	Diagnosis of patients with overt dementia	Characterization of asymptomatic and prodromal stages. NBB can be used as surrogate end points and provide *in vivo* intermediate phenotypes of pathology
Preventive therapy	Inefficient for disease-modifying or preventive therapies, e.g., reduction of Aβ production has shown limited therapeutic impact	Potential for early diagnosis and disease-modifying therapies by detecting alterations in functional connectivity
Feature extraction	Absence of standardized quantitative metric for AD imaging biomarkers	Automated extraction of network parameters borrowing tools and methods from network theory

studies, summarized above, that treat biomarkers as quantities that reflect relevant biological processes whose correlations with other biomarkers need to be investigated through heuristics methods (**Table 1**). An interesting improvement in the quantification and integration of AD biomarkers aiming to improve the efficiency and of AD diagnosis can be found in Mattila et al. (2011). A supervised classifier is implemented via a disease state index (DSI) that compares the biomarker measurements of new patients with previously diagnosed patients' biomarkers. Thus, the DSI is an aggregate measure of a number of biomarkers that allows us to classify based on biomarker data.

Our network-based approach in AD biomarkers differs from these approaches in that biomarkers are here characterized as structured objects, i.e., networks, in which the dependencies among the network components, i.e., individual biomarkers, need to be quantified via experimentation or computational simulation of the network dynamics. For a training set of diagnosed biomarker data, the computation of the generative biomarker network for each diagnostic class, e.g., M_{H}, M_{AD} is a network structure discovery problem. The idea is to provide a structural model, i.e., a network of the training data set, i.e., biomarker data. For example, for a training data set of patients diagnosed into the categories healthy and AD, two networks – M_H, M_{AD} – are built. The nodes represent the random variables of the training set (biomarkers) and the edges represent the stochastic dependency between these variables. Dependency structures can be analyzed using Bayesian network models (Buntine, 1996). In the context of AD biomarkers, the network represents the dependency structure of the underlying distribution of any two biomarkers. For example, in **Figure 1**, the generative network M_{H}, which contains a structural representation of the biomarkers dependencies in the subjects diagnosed as healthy, shows no dependency among biomarkers and only one biomarker, amyloid-beta deposition, reaches the threshold of positivity. In the M_{AD} network, the generative matrix of patients diagnosed as AD, we find stochastic dependency between all pairs of biomarkers except in fMRI and tactile.

The identification of the generative models M_{H} and M_{AD} from data is the result of statistical learning followed by model selection. It ought to be noted that when the amount of data – the number of diagnosed individuals – is small compared to the size of the model – the number of biomarkers – there are likely many candidate models that explain the data, and therefore the generative model provided by model selection may not be a good approximation of the underlying process. On the other hand, model selection is more likely to provide a good approximation when a large amount of data is available in models with a relatively small number of parameters. The number of candidate networks is super exponential of the number of model parameters, therefore small size models relative to the large data sample are preferable. For a discussion of the p, n ($p =$ model size, $n =$ data size) problem in statistics, see Gomez-Ramirez and Sanz (2013). The diagnosis of a new subject can be computed via the maximum probability of the biomarker configuration $\mathrm{BM_s}$ conditional to the generative models, M_{H} and M_{AD}, $\max_{\mathrm{G}} = (M_{\mathrm{H}}, M_{\mathrm{AD}})$ $\mathrm{P}(\mathrm{BM_s}|\mathrm{G})$.

The utility of this approach will ultimately rely on its power to generate decision support systems to assist the physician in early diagnosis and symptomatic treatment. This work describes the blueprint for the construction of uncomplicated and cost-effective tools for the identification of disease's signatures, based on a new understanding of biomarkers as multidimensional objects, i.e., networks. Thus, biomarkers can be seen here as the heterogeneous building blocks in network-based models.

Conceptually, the work flow for the implementation of decision models based on the theoretical framework described here can be divided into three phases: (1) data extraction for biomarker selection, (2) network-based model building, and (3) model validation using classification algorithms. The first phase is intrinsically hypothesis driven. Quantities susceptible to work as biomarkers are selected experimentally or via public repositories such as the ADNI initiative. In the second phase, the interdependencies among biomarkers are studied quantitatively. The idea is to understand how the different biomarkers act together within a network model that can be further characterized in terms of network parameters such as clustering or modularity. As a result, generative models of diagnostic categories, e.g., M_{H} and M_{AD} are built. In the last step, new subjects can be diagnosed via the maximum probability of the biomarker configuration for a new subject s ($\mathrm{BM_s}$) conditional to the generative models, $\max_{\mathrm{G}} = (M_{\mathrm{H}}, M_{\mathrm{AD}})\ \mathrm{P}(\mathrm{BM_s}|\mathrm{G})$. Thus, in essence, this approach can be seen as a supervised classifier that allows us to assess the clinical value of the network models built upon heterogeneous and structured biomarker data. It ought to be remarked that the Bayes' theorem allows us to calculate the posterior probability $\mathrm{P}(\mathrm{G}|\mathrm{BM_s})$ or the updating of probabilities from an experiment that results in the biomarker values $\mathrm{BM_s}$. Generally speaking, by increasing the sample size it is possible to reduce the importance of the prior distribution, P(G), which is particularly difficult to specify, and represents the uncertainty about the network structure before the data are examined (Migon and Gamerman, 1999).

CONCLUSION

The network-based biomarker approach described here is in compliance with the new emerging paradigm of network medicine (Barabási et al., 2011). In this respect, network medicine, in order to be successful, must offer healthcare professionals not only a conceptual framework, but also comprehensive methodologies and a practical toolkit able to address the challenges and limitations in AD biomarkers research in new ways. New classification methods, such as support vector machine (SVM), have proven to be effective for the identification of MCIs from normal aging using resting-state functional connectivity data (Wee et al., 2012). Bayesian network analysis of effective connectivity show differences in the DMN between AD and healthy controls and could be used in the future as a biomarker (Wu et al., 2011).

The development of efficient tools for use in clinical diagnosis and monitoring of disease progress require the improved use of already known biomarkers and new methods of biomarkers discovery. There is a strong need for objective- and quantitative-based biomarkers of use in asymptomatic and prodromal stages of AD. The systemic understanding of the interactions between biomarkers can be seen as statistical learning followed by a model selection problem. The inclusion of functional imaging biomarkers in the clinical diagnoses of AD necessarily passes over the standardization of imaging protocols and quantitative metrics. In this respect, the network-based biomarkers approach presented here goes beyond the current emphasis on the study of the relationship between specific networks (e.g., DMN) and molecular biomarkers (e.g., amyloid-beta) to learn dependencies between biomarkers from heterogeneous data implemented as a graph, where the nodes are biomarkers and the edges represent the stochastic dependency among the biomarkers.

There are, however, challenges that are not addressed here. For example, the review has focused on the integration of predetermined biomarkers, but biomarker selection is a standing problem in AD research. Non-linear relationships between biomarker measurements and disease severity, and handling sparse observations constrain biomarker prediction. Alterations in functional connectivity may play a key role in detecting signatures in presymptomatic and prodromal stages. However, functional imaging related biomarkers have so far focused on alterations in intrinsic connectivity networks and the co-occurrence of protein deposition within those networks. Quantified and standardized metrics for AD neuroimaging biomarkers and a system-level understanding of the dependencies among the existing biomarkers are still missing. The network-based approach introduced here aims to bridge this gap by providing a statistical framework able to learn structural representations of biomarkers interactions from biomarker data of previously diagnosed patients. To fully capitalize on the large amount of data that big data science projects are bringing to AD research, a new mathematical framework for finding effective combinations of multi-modal biomarkers is sorely required. Biomarkers deployed as network models rather than as quantities will foster our understanding of disease, paving the way for a predictive, preventive, and personalized medicine.

ACKNOWLEDGMENTS

This work has been funded in part with funds from the Erasmus Mundus Building European Asian Mobility Program of the European Commission (EM-BEAM), Grant Number L03100048.

REFERENCES

Ahn, A. C., Tewari, M., Poon, C.-S., and Phillips, R. S. (2006). The limits of reductionism in medicine: could systems biology offer an alternative? *PLoS Med.* 3:e208. doi:10.1371/journal.pmed.0030208

Albert, M. S., DeKosky, S. T., Dickson, D., Dubois, B., Feldman, H. H., Fox, N. C., et al. (2011). The diagnosis of mild cognitive impairment due to Alzheimer's disease: recommendations from the National Institute on Aging-Alzheimer's Association workgroups on diagnostic guidelines for Alzheimer's disease. *Alzheimers Dement.* 7, 270–279. doi:10.1016/j.jalz.2011.03.008

Balthazar, M. L. F., De Campos, B. M., Franco, A. R., Damasceno, B. P., and Cendes, F. (2014). Whole cortical and default mode network mean functional connectivity as potential biomarkers for mild Alzheimer's disease. *Psychiatry Res.* 221, 37–42. doi:10.1016/j.pscychresns.2013.10.010

Barabási, A.-L., Gulbahce, N., and Loscalzo, J. (2011). Network medicine: a network-based approach to human disease. *Nat. Rev. Genet.* 12, 56–68. doi:10.1038/nrg2918

Bateman, R. J., Xiong, C., Benzinger, T. L. S., Fagan, A. M., Goate, A., Fox, N. C., et al. (2012). Clinical and biomarker changes in dominantly inherited Alzheimer's disease. *N. Engl. J. Med.* 367, 795–804. doi:10.1056/NEJMoa1202753

Bertram, L., and Tanzi, R. E. (2004). The current status of Alzheimer's disease genetics: what do we tell the patients? *Pharmacol. Res.* 50, 385–396. doi:10.1016/j.phrs.2003.11.018

Biomarkers Definitions Working Group. (2001). Biomarkers and surrogate endpoints: preferred definitions and conceptual framework. *Clin. Pharmacol. Ther.* 69, 89–95. doi:10.1067/mcp.2001.113989

Biswal, B., Yetkin, F. Z., Haughton, V. M., and Hyde, J. S. (1995). Functional connectivity in the motor cortex of resting human brain using echo-planar MRI. *Magn. Reson. Med.* 34, 537–541. doi:10.1002/mrm.1910340409

Buckner, R. L., Andrews-Hanna, J. R., and Schacter, D. L. (2008). The brain's default network. *Ann. N. Y. Acad. Sci.* 1124, 1–38. doi:10.1196/annals.1440.011

Buntine, W. L. (1996). A guide to the literature on learning probabilistic networks from data. *IEEE Trans. Knowl. Data Eng.* 8, 195–210. doi:10.1109/69.494161

Chhatwal, J. P., Schultz, A. P., Johnson, K., Benzinger, T. L. S., Jack, C., Ances, B. M., et al. (2013). Impaired default network functional connectivity in autosomal dominant Alzheimer disease. *Neurology* 81, 736–744. doi:10.1212/WNL.0b013e3182a1aafe

Cole, D. M., Smith, S. M., and Beckmann, C. F. (2010). Advances and pitfalls in the analysis and interpretation of resting-state FMRI data. *Front. Syst. Neurosci.* 4. Available at: http://www.ncbi.nlm.nih.gov/pmc/articles/PMC2854531/ doi:10.3389/fnsys.2010.00008

Comon, P. (1994). Independent component analysis, a new concept? *Signal Processing* 36, 287–314. doi:10.1016/0165-1684(94)90029-9

Corbett, A., and Ballard, C. (2012). New and emerging treatments for Alzheimer's disease. *Expert Opin. Emerg. Drugs* 17, 147–156. doi:10.1517/14728214.2012.675327

Damoiseaux, J. S. (2012). Resting-state fMRI as a biomarker for Alzheimer's disease? *Alzheimers Res. Ther.* 4, 8. doi:10.1186/alzrt106

Damoiseaux, J. S., Prater, K. E., Miller, B. L., and Greicius, M. D. (2012). Functional connectivity tracks clinical deterioration in Alzheimer's disease. *Neurobiol. Aging* 33, 828.e19–.e30. doi:10.1016/j.neurobiolaging.2011.06.024

Dickerson, B. C., Salat, D. H., Bates, J. F., Atiya, M., Killiany, R. J., Greve, D. N., et al. (2004). Medial temporal lobe function and structure in mild cognitive impairment. *Ann. Neurol.* 56, 27–35. doi:10.1002/ana.20163

Doecke, J. D., Laws, S. M., Faux, N. G., Wilson, W., Burnham, S. C., Lam, C.-P., et al. (2012). Blood-based protein biomarkers for diagnosis of Alzheimer disease. *Arch. Neurol.* 69, 1318–1325. doi:10.1001/archneurol.2012.1282

Dubois, B., Feldman, H. H., Jacova, C., Cummings, J. L., Dekosky, S. T., Barberger-Gateau, P., et al. (2010). Revising the definition of Alzheimer's disease: a new lexicon. *Lancet Neurol.* 9, 1118–1127. doi:10.1016/S1474-4422(10)70223-4

Dubois, B., Feldman, H. H., Jacova, C., Dekosky, S. T., Barberger-Gateau, P., Cummings, J., et al. (2007). Research criteria for the diagnosis of Alzheimer's disease: revising the NINCDS-ADRDA criteria. *Lancet Neurol.* 6, 734–746. doi:10.1016/S1474-4422(07)70178-3

Eidelberg, D., and Martin, W. (2013). Different β-amyloid binding patterns in Alzheimer and Parkinson diseases: it's the network! *Neurology* 81, 516–517. doi:10.1212/WNL.0b013e31829e703e

Erler, J. T., and Linding, R. (2010). Network-based drugs and biomarkers. *J. Pathol.* 220, 290–296. doi:10.1002/path.2646

Faria, A. V., Joel, S. E., Zhang, Y., Oishi, K., Van Zjil, P. C. M., Miller, M. I., et al. (2012). Atlas-based analysis of resting-state functional connectivity: evaluation for reproducibility and multi-modal anatomy-function correlation studies. *Neuroimage* 61, 613–621. doi:10.1016/j.neuroimage.2012.03.078

Fransson, P. (2005). Spontaneous low-frequency BOLD signal fluctuations: an fMRI investigation of the resting-state default mode of brain function hypothesis. *Hum. Brain Mapp.* 26, 15–29. doi:10.1002/hbm.20113

Friston, K. J. (1998). Modes or models: a critique on independent component analysis for fMRI. *Trends Cogn. Sci. (Regul. Ed.)* 2, 373–375. doi:10.1016/S1364-6613(98)01227-3

Gomar, J. J., Bobes-Bascaran, M. T., Conejero-Goldberg, C., Davies, P., Goldberg, T. E., and Alzheimer's Disease Neuroimaging Initiative. (2011). Utility of combinations of biomarkers, cognitive markers, and risk factors to predict conversion from mild cognitive impairment to Alzheimer disease in patients in the Alzheimer's disease neuroimaging initiative. *Arch. Gen. Psychiatry* 68, 961–969. doi:10.1001/archgenpsychiatry.2011.96

Gomez-Ramirez, J., and Sanz, R. (2013). On the limitations of standard statistical modeling in biological systems: a full Bayesian approach for biology. *Prog. Biophys. Mol. Biol.* 113, 80–91. doi:10.1016/j.pbiomolbio.2013.03.008

Greicius, M. D., Srivastava, G., Reiss, A. L., and Menon, V. (2004). Default-mode network activity distinguishes Alzheimer's disease from healthy aging: evidence from functional MRI. *Proc. Natl. Acad. Sci. U.S.A.* 101, 4637–4642. doi:10.1073/pnas.0308627101

Habeck, C., Risacher, S., Lee, G. J., Glymour, M. M., Mormino, E., Mukherjee, S., et al. (2012). Relationship between baseline brain metabolism measured using [^{18}F]FDG PET and memory and executive function in prodromal and early Alzheimer's disease. *Brain Imaging Behav.* 6, 568–583. doi:10.1007/s11682-012-9208-x

Hafkemeijer, A., Van der Grond, J., and Rombouts, S. A. R. B. (2012). Imaging the default mode network in aging and dementia. *Biochim. Biophys. Acta* 1822, 431–441. doi:10.1016/j.bbadis.2011.07.008

Hampel, H., Wilcock, G., Andrieu, S., Aisen, P., Blennow, K., Broich, K., et al. (2011). Biomarkers for Alzheimer's disease therapeutic trials. *Prog. Neurobiol.* 95, 579–593. doi:10.1016/j.pneurobio.2010.11.005

He, Y., Wang, J., Wang, L., Chen, Z. J., Yan, C., Yang, H., et al. (2009). Uncovering intrinsic modular organization of spontaneous brain activity in humans. *PLoS ONE* 4:e5226. doi:10.1371/journal.pone.0005226

Henriksen, K., O'Bryant, S. E., Hampel, H., Trojanowski, J. Q., Montine, T. J., Jeromin, A., et al. (2014). The future of blood-based biomarkers for Alzheimer's disease. *Alzheimers Dement.* 10, 115–131. doi:10.1016/j.jalz.2013.01.013

Hye, A., Lynham, S., Thambisetty, M., Causevic, M., Campbell, J., Byers, H. L., et al. (2006). Proteome-based plasma biomarkers for Alzheimer's disease. *Brain* 129(Pt 11), 3042–3050. doi:10.1093/brain/awl279

Jack, C. R. (2012). Alzheimer disease: new concepts on its neurobiology and the clinical role imaging will play. *Radiology* 263, 344–361. doi:10.1148/radiol.12110433

Kjelvik, G., Sando, S. B., Aasly, J., Engedal, K. A., and White, L. R. (2007). Use of the Brief Smell Identification Test for olfactory deficit in a Norwegian population with Alzheimer's disease. *Int. J. Geriatr. Psychiatry* 22, 1020–1024. doi:10.1002/gps.1783

Knopman, D. S., DeKosky, S. T., Cummings, J. L., Chui, H., Corey-Bloom, J., Relkin, N., et al. (2001). Practice parameter: diagnosis of dementia (an evidence-based review). Report of the Quality Standards Subcommittee of the American Academy of Neurology. *Neurology* 56, 1143–1153. doi:10.1212/WNL.56.9.1143

Lee, M. H., Smyser, C. D., and Shimony, J. S. (2013). Resting-state fMRI: a review of methods and clinical applications. *AJNR Am. J. Neuroradiol.* 34, 1866–1872. doi:10.3174/ajnr.A3263

Li, X., Li, T.-Q., Andreasen, N., Wiberg, M. K., Westman, E., and Wahlund, L.-O. (2013). Ratio of Aβ42/P-tau181p in CSF is associated with aberrant default mode network in AD. *Sci. Rep.* 3, 1339. doi:10.1038/srep01339

Liu, Y., Yu, C., Zhang, X., Liu, J., Duan, Y., Alexander-Bloch, A. F., et al. (2013). Impaired long distance functional connectivity and weighted network architecture in Alzheimer's disease. *Cereb. Cortex* doi:10.1093/cercor/bhs410

Mattila, J., Koikkalainen, J., Virkki, A., Simonsen, A., Van Gils, M., Waldemar, G., et al. (2011). A disease state fingerprint for evaluation of Alzheimer's disease. *J. Alzheimers Dis.* 27, 163–176. doi:10.3233/JAD-2011-110365

Mattila, J., Soininen, H., Koikkalainen, J., Rueckert, D., Wolz, R., Waldemar, G., et al. (2012). Optimizing the diagnosis of early Alzheimer's disease in mild cognitive impairment subjects. *J. Alzheimers Dis.* 32, 969–979. doi:10.3233/JAD-2012-120934

Mayeux, R., and Schupf, N. (2011). Blood-based biomarkers for Alzheimer's disease: plasma Aβ40 and Aβ42, and genetic variants. *Neurobiol. Aging* 32(Suppl. 1), S10–S19. doi:10.1016/j.neurobiolaging.2011.09.004

McKhann, G., Drachman, D., Folstein, M., Katzman, R., Price, D., and Stadlan, E. M. (1984). Clinical diagnosis of Alzheimer's disease report of the NINCDS-ADRDA Work Group under the auspices of Department of Health and Human Services Task Force on Alzheimer's Disease. *Neurology* 34, 939–939. doi:10.1212/WNL.34.7.939

Migon, H.-S., and Gamerman, D. (1999). *Statistical Inference: An Integrated Approach.* London: CRC press.

Pievani, M., De Haan, W., Wu, T., Seeley, W. W., and Frisoni, G. B. (2011). Functional network disruption in the degenerative dementias. *Lancet Neurol.* 10, 829–843. doi:10.1016/S1474-4422(11)70158-2

Raichle, M. E., and Gusnard, D. A. (2005). Intrinsic brain activity sets the stage for expression of motivated behavior. *J. Comp. Neurol.* 493, 167–176. doi:10.1002/cne.20752

Rombouts, S. A. R. B., Barkhof, F., Goekoop, R., Stam, C. J., and Scheltens, P. (2005). Altered resting state networks in mild cognitive impairment and mild Alzheimer's disease: an fMRI study. *Hum. Brain Mapp.* 26, 231–239. doi:10.1002/hbm.20160

Rosen, W. G., Mohs, R. C., and Davis, K. L. (1984). A new rating scale for Alzheimer's disease. *Am. J. Psychiatry* 141, 1356–1364.

Sanz-Arigita, E. J., Schoonheim, M. M., Damoiseaux, J. S., Rombouts, S. A. R. B., Maris, E., Barkhof, F., et al. (2010). Loss of "small-world" networks in Alzheimer's disease: graph analysis of FMRI resting-state functional connectivity. *PLoS ONE* 5:e13788. doi:10.1371/journal.pone.0013788

Saumier, D., Aisen, P. S., Gauthier, S., Vellas, B., Ferris, S. H., Duong, A., et al. (2009). Lessons learned in the use of volumetric MRI in therapeutic trials in Alzheimer's disease: the ALZHEMED (Tramiprosate) experience. *J. Nutr. Health Aging* 13, 370–372. doi:10.1007/s12603-009-0047-4

Seeley, W. W., Crawford, R. K., Zhou, J., Miller, B. L., and Greicius, M. D. (2009). Neurodegenerative diseases target large-scale human brain networks. *Neuron* 62, 42–52. doi:10.1016/j.neuron.2009.03.024

Serby, M., Larson, P., and Kalkstein, D. (1991). The nature and course of olfactory deficits in Alzheimer's disease. *Am. J. Psychiatry* 148, 357–360.

Sheline, Y. I., Barch, D. M., Price, J. L., Rundle, M. M., Vaishnavi, S. N., Snyder, A. Z., et al. (2009). The default mode network and self-referential processes in depression. *Proc. Natl. Acad. Sci. U.S.A.* 106, 1942–1947. doi:10.1073/pnas.0812686106

Sheline, Y. I., Raichle, M. E., Snyder, A. Z., Morris, J. C., Head, D., Wang, S., et al. (2010). Amyloid plaques disrupt resting state default mode network connectivity in cognitively normal elderly. *Biol. Psychiatry* 67, 584–587. doi:10.1016/j.biopsych.2009.08.024

Sperling, R. (2011). Potential of functional MRI as a biomarker in early Alzheimer's disease. *Neurobiol. Aging* 32(Suppl. 1), S37–S43. doi:10.1016/j.neurobiolaging.2011.09.009

Sperling, R. A., Dickerson, B. C., Pihlajamaki, M., Vannini, P., LaViolette, P. S., Vitolo, O. V., et al. (2010). Functional alterations in memory networks in early Alzheimer's disease. *Neuromolecular Med.* 12, 27–43. doi:10.1007/s12017-009-8109-7

Stone, J. V. (2002). Independent component analysis: an introduction. *Trends Cogn. Sci. (Regul. Ed.)* 6, 59–64. doi:10.1016/S1364-6613(00)01813-1

Toledo, J. B., Shaw, L. M., and Trojanowski, J. Q. (2013). Plasma amyloid beta measurements – a desired but elusive Alzheimer's disease biomarker. *Alzheimers Res. Ther.* 5, 8. doi:10.1186/alzrt162

Trushina, E., Dutta, T., Persson, X.-M. T., Mielke, M. M., and Petersen, R. C. (2013). Identification of altered metabolic pathways in plasma and CSF in mild cognitive impairment and Alzheimer's disease using metabolomics. *PLoS ONE* 8:e63644. doi:10.1371/journal.pone.0063644

Van den Heuvel, M. P., and Hulshoff Pol, H. E. (2010). Exploring the brain network: a review on resting-state fMRI functional connectivity. *Eur. Neuropsychopharmacol.* 20, 519–534. doi:10.1016/j.euroneuro.2010.03.008

Vanderstichele, H., Van Kerschaver, E., Hesse, C., Davidsson, P., Buyse, M. A., Andreasen, N., et al. (2000). Standardization of measurement of beta-amyloid(1-42) in cerebrospinal fluid and plasma. *Amyloid* 7, 245–258. doi:10.3109/13506120009146438

Wang, J., Wang, L., Zang, Y., Yang, H., Tang, H., Gong, Q., et al. (2009). Parcellation-dependent small-world brain functional networks: a resting-state fMRI study. *Hum. Brain Mapp.* 30, 1511–1523. doi:10.1002/hbm.20623

Wang, J., Zuo, X., and He, Y. (2010). Graph-based network analysis of resting-state functional MRI. *Front. Syst. Neurosci.* 4. Available at: http://www.ncbi.nlm.nih.gov/pmc/articles/PMC2893007/ doi:10.3389/fnsys.2010.00016

Wang, L., Brier, M. R., Snyder, A. Z., Thomas, J. B., Fagan, A. M., Xiong, C., et al. (2013). Cerebrospinal fluid Aβ42, phosphorylated Tau181, and resting-state functional connectivity. *JAMA Neurol.* 70, 1242–1248. doi:10.1001/jamaneurol.2013.3253

Washington, S. D., Gordon, E. M., Brar, J., Warburton, S., Sawyer, A. T., Wolfe, A., et al. (2013). Dysmaturation of the default mode network in autism. *Hum. Brain Mapp.* doi:10.1002/hbm.22252

Wee, C.-Y., Yap, P.-T., Denny, K., Browndyke, J. N., Potter, G. G., Welsh-Bohmer, K. A., et al. (2012). Resting-state multi-spectrum functional connectivity networks for identification of MCI patients. *PLoS ONE* 7:e37828. doi:10.1371/journal.pone.0037828

Wu, J., Anwyl, R., and Rowan, M. J. (1995). Beta-Amyloid selectively augments NMDA receptor-mediated synaptic transmission in rat hippocampus. *Neuroreport* 6, 2409–2413. doi:10.1097/00001756-199511270-00031

Wu, X., Li, R., Fleisher, A. S., Reiman, E. M., Guan, X., Zhang, Y., et al. (2011). Altered default mode network connectivity in Alzheimer's disease – a resting functional MRI and Bayesian network study. *Hum. Brain Mapp.* 32, 1868–1881. doi:10.1002/hbm.21153

Yang, J., Ogasa, T., Ohta, Y., Abe, K., and Wu, J. (2010). Decline of human tactile angle discrimination in patients with mild cognitive impairment and Alzheimer's disease. *J. Alzheimers Dis.* 22, 225–234. doi:10.3233/JAD-2010-100723

Yoshiyama, Y., Lee, V. M. Y., and Trojanowski, J. Q. (2012). Therapeutic strategies for tau mediated neurodegeneration. *J. Neurol. Neurosurg. Psychiatry* 84, 784–795. doi:10.1136/jnnp-2012-303144

Zhu, D. C., Majumdar, S., Korolev, I. O., Berger, K. L., and Bozoki, A. C. (2013). Alzheimer's disease and amnestic mild cognitive impairment weaken connections within the default-mode network: a multi-modal imaging study. *J. Alzheimers Dis.* 34, 969–984. doi:10.3233/JAD-121879

Conflict of Interest Statement: The authors declare that the research was conducted in the absence of any commercial or financial relationships that could be construed as a potential conflict of interest.

Received: 15 November 2013; accepted: 19 January 2014; published online: 04 February 2014.

*Citation: Gomez-Ramirez J and Wu J (2014) Network-based biomarkers in Alzheimer's disease: review and future directions. Front. Aging Neurosci. **6**:12. doi: 10.3389/fnagi.2014.00012*

This article was submitted to the journal Frontiers in Aging Neuroscience.

frontiers in
AGING NEUROSCIENCE

ORIGINAL RESEARCH ARTICLE
published: 01 April 2014
doi: 10.3389/fnagi.2014.00056

Diagnoses behind patients with hard-to-classify tremor and normal DaT-SPECT: a clinical follow up study

Manuel Menéndez-González[1,2,3]*, Francisco Tavares[4], Nahla Zeidan[5], José M. Salas-Pacheco[6] and Oscar Arias-Carrión[7]*

[1] *Neurology Unit, Hospital Álvarez-Buylla, Mieres, Spain*
[2] *Morphology and Cellular Biology Department, Universidad de Oviedo, Oviedo, Spain*
[3] *Instituto de Neurociencias, Universidad de Oviedo, Oviedo, Spain*
[4] *Family Medicine, Hospital Álvarez-Buylla, Mieres, Spain*
[5] *Nuclear Medicine, Hospital Universitario Central de Asturias, Oviedo, Spain*
[6] *Instituto de Investigación Científica, Universidad Juárez del Estado de Durango, Durango, Mexico*
[7] *Transcranial Magnetic Stimulation Unit, Sleep and Movement Disorders Clinic, Hospital General Dr. Manuel Gea González, Mexico City, Mexico*

Edited by:
Rodrigo Orlando Kuljiš, Zdrav Mozak Limitada, Chile

Reviewed by:
Junming Wang, University of Mississippi Medical Center, USA
Aruna Sharma, Uppsala University Hospital, Sweden

****Correspondence:***
Manuel Menéndez-González, Neurology Unit, Hospital Álvarez-Buylla, Murias s/n, 33616, Mieres, Spain
e-mail: manuelmenendezgonzalez@gmail.com;
Oscar Arias-Carrión, TMS Lab, Hospital General Dr. Manuel Gea González, Calzada de Tlalpan 4800, Mexico City 14080, Mexico
e-mail: arias@ifc.unam.mx

The [^{123}I]ioflupane—a dopamine transporter radioligand—SPECT (DaT-SPECT) has proven to be useful in the differential diagnosis of tremor. Here, we investigate the diagnoses behind patients with hard-to-classify tremor and normal DaT-SPECT. Therefore, 30 patients with tremor and normal DaT-SPECT were followed up for 2 years. In 18 cases we were able to make a diagnosis. The residual 12 patients underwent a second DaT-SPECT, were then followed for additional 12 months and thereafter the diagnosis was reconsidered again. The final diagnoses included cases of essential tremor, dystonic tremor, multisystem atrophy, vascular parkinsonism, progressive supranuclear palsy, corticobasal degeneration, fragile X–associated tremor ataxia syndrome, psychogenic parkinsonism, iatrogenic parkinsonism and Parkinson's disease. However, for 6 patients the diagnosis remained uncertain. Larger series are needed to better establish the relative frequency of the different conditions behind these cases.

Keywords: DaTSPECT, tremor, Parkinson disease, Movement Disorders, SWEDD

INTRODUCTION

Tremor is an involuntary, rhythmic, oscillatory movement of a body part. It is the most common movement disorder encountered in clinical practice. There is no diagnostic standard to distinguish among common types of tremor, which can make the evaluation challenging. History and physical examination can provide a great deal of certainty in diagnosis. However, some cases showing more than one type of tremor or associating other signs and symptoms are specially difficult. Establishing the underlying cause is important because prognosis and specific treatment plans vary considerably.

PD is a common neurodegenerative disorder characterized by progressive degeneration of dopaminergic neurons in the substantia nigra, with loss of their nerve terminals in the basal ganglia structures, especially in the striatum. The dopaminergic system is the most studied neurochemical system in patients with PD because damage to nigrostriatal neurons is the most important component in the pathophysiology of PD. Clinically it is characterized by the so called "parkinsonian syndrome," consisting of extrapiramidal signs, including bradykinesia and at least one of the following: muscular rigidity, 4–6 Hz rest tremor and postural instability not caused by primary visual, vestibular, cerebellar, or proprioceptive dysfunction. More than 70 percent of patients with Parkinson disease have tremor as the presenting feature. The classic parkinsonian tremor begins as a low-frequency, pill-rolling motion of the fingers, progressing to forearm pronation/supination and elbow flexion/extension. It is typically asymmetric, occurs at rest, and becomes less prominent with voluntary movement. Although rest tremor is one of the diagnostic criteria for Parkinson disease, most patients exhibit a combination of action and rest tremors (Rodriguez-Oroz et al., 2009). The term "parkinsonisms" refers to a group of neurological disorders characterized by a parkinsonian syndrome. In many cases, the differential diagnosis between Parkinson disease and other neurodegenerative parkinsonisms, or other conditions such as essential tremor, psycogenic, or drug-induced parkinsonism is sometimes difficult. This requires an experienced clinician and time to establish the pattern of progression and response to treatment.

Currently, the diagnosis of tremor remains primarily clinical, but complementary tests may be useful to support the diagnostic process for particularly difficult cases, specially in those where tremor associates with parkinsonian syndrome. Structural imaging, such as computed tomography or magnetic resonance imaging (MRI), is of limited value for differentiating parkinsonian syndromes since structural changes are often only evident by the time the disease is far advanced. CT and MRI neuroimaging do play an important role in the diagnosis of patients with vascular parkinsonism. Radiotracer neuroimaging techniques allow to study the integrity of the dopaminergic nigrostriatal system

and are therefore a valuable tool to diagnose neurodegenerative parkinsonisms (Lorenzo Bosquet et al., 2004; Tolosa et al., 2007). Positron emission tomography techniques demonstrate the disruption of selective patterns of regional cerebral metabolism and neurotransmitter systems associated with subcortical degenerations, such as Parkinson's disease, striatonigral degeneration, progressive supranuclear palsy, and corticobasal degeneration (Antonini and Isaias, 2009; Huang et al., 2013). In addition, it allows to determine, where underlying Parkinson's disease may be suspected and whether nigral dysfunction is present in patients with isolated tremor or drug-associated rigidity. However, PET scan is an expensive technique that is not available in most clinical centers. A DaT-SPECT (Dopamine Transporter -DaT- single-photon emission computed tomography), is a less expensive and more widely available technique compared to PET and has already been incorporated into clinical practice. The active ingredient of [123I]FP-CIT SPECT is a cocaine analog, 123I-labeled N-u-fluoropropyl 2b-carbomethoxy-3b-(4-iodophenyl) nortropane ([123I]ioflupane). It binds with high affinity to striatal presynaptic DAT in animals and in humans and helps visualize these neurons with SPECT brain imaging. [123I]FP-CIT SPECT has the advantage of faster kinetics, which allows imaging 3–6 h after injection. DAT is located on the plasma membrane of nerve terminals in a small number of neurons in the brain, especially in the striatum and nucleus accumbens, and in the globus pallidus, cingulate cortex, olfactory tubercle, amygdala, and midbrain. DAT regulates the dopamine concentration in the synaptic cleft through reuptake of dopamine into presynaptic neurons and thus plays a central role in the buffering of the released dopamine (Surasi et al., 2013).

The Food and Drug Administration (FDA) has recently approved the use of DaT-SPECT "to assist in the evaluation of adult patients with suspected parkinsonian syndromes" (**Figure 1**). Paradoxically, however, adequate neuropathologic validation of Parkinson's disease diagnosis based on DaT-SPECT findings is still lacking and the value of DaT-SPECT for clinical decision-making remains unclear. Generally, the clinical based diagnostic accuracy of Parkinson's disease is mathematically identical to the diagnostic accuracy of DaT-SPECT imaging (6). In terms of differential diagnoses, DaT-SPECT imaging cannot distinguish reliably between Parkinson's disease and other degenerative parkinsonisms, such as multiple system atrophy or progressive supranuclear palsy, whenever evaluated on a case-by-case basis. This important point is specifically recognized in the FDA briefing document (De La Fuente-Fernandez, 2012). Finally, the alternative diagnoses to Parkinson's disease when a patient with hard-to-classify tremor shows a normal (negative) study are not well known yet. Herein, we report a series of patients with different types of tremor or tremor plus parkinsonism, where the clinician decided to perform a DaT-SPECT due to diagnostic difficulties and the DaT-SPECT resulted normal. These patients were followed up for 2 years at least, with the aim of revealing the final diagnoses of these patients.

METHODS

Standard protocol approvals, registrations, and patient consents. The study was approved by the Hospital Álvarez-Buylla and informed consent was given by all family members.

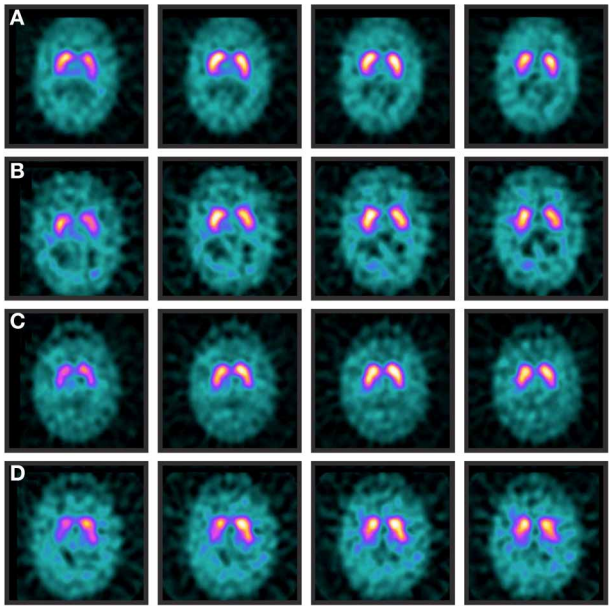

FIGURE 1 | Normal and abnormal DAT-SPECTs. Normal DaT-SPECTs of a patient with essential tremor at baseline **(A)** and 42 months later **(B)**. Normal DaT-SPECT of a patient with Parkinson's disease at baseline **(C)**. However, 84 months later **(D)** the scan was abnormal due to a decrease in postsynaptic uptake on the right striatum.

SUBJECTS

We screened patients with tremor, who had performed a DaT-SPECT and resulted normal. The period of time for screening patients was 5 years. Patients with dementia were ruled out, though patients with mild cognitive impairment were allowed for inclusion (Huang et al., 2013).

FOLLOW UP

Patients included were assessed every 6 months for 2 years at least. Neurological examination was performed to all patients in all visits. Other studies, including a second DaT-SPECT, were done in some cases according to the neurologist criteria. At the end of the follow up period we reconsidered diagnoses based on findings in history, examination, response to treatment and complementary studies. Cases in which we were unable to reach a final diagnosis remained labeled as "uncertain diagnosis."

IMAGING ACQUISITION

Following thyroid iodine uptake blocking with 500 mg of potassium perchlorate, patients underwent intravenous administration of a single dose (148 MBq)in of DaTSCAN (GE Healthcare). SPECT imaging was carried out 3–6 h later with a dual-headed gammacamera (Philips Healthcare) using LEHR collimators. Data were acquired in a 128 × 128 matrix; zoom 2.19; 180° per head; 20 s per view; 128 views; 158 keV; 15% window; filtered back projection and 2-D Butterworth prefilter; power factor 8; cut off 0.6.

DATA ANALYSIS

DaTa analysis was acquired visually and semi-quantitatively with Xeleris 2.0 software (GE Healthcare). In order to analyze the

dopaminergic deficit, two different methods were performed: visual interpretation and semi- quantification with classical manual ROIs (Region of Interest) method. For visual interpretation, a nuclear medicine physician examined the hardcopy images and classified the SPECT images into two different patterns: normal, showing a symmetrical uptake bilaterally in putamen and caudate nuclei; and abnormal, with different levels of uptake reduction in one or both caudate and/or putamina. The semi- quantitative evaluation method allows to calculate binding ratios by comparing activity in striatum with activity in an area of low DaT concentration (usually the occipital area). Three consecutive slices with the highest striatal image count were selected and summed up to a single slice. The ratio of specific to non-specific binding was calculated by standardized two dimensional ROIs, derived from an anatomical brain atlas, which were placed bilaterally over the striatum with subregions for caudate and putamen. A ROI over the occipital cortex was used as reference region to assess non-specific binding. Specific FP-CIT tracer uptake was calculated for caudate and putamen using the formula: [Striatal binding ratio = mean counts of striatal ROI-mean counts of occipital ROI/ mean counts of occipital ROI].

RESULTS

SAMPLE DESCRIPTION

We screened 34 patients with tremor who had underwent a DaTSPECT due to diagnostic difficulties and the result of DaTSPECT was negative (normal). Four of the patients screened were ruled out for suffering from dementia. The demographic and main clinical features of the patients included are summarized in **Table 1**.

DIAGNOSES AND FOLLOW-UP

After a follow up period (24 months) the diagnoses of all cases were reconsidered and recorded (**Figure 2**). The main clinical features allowing us to reach the diagnoses are included under **Table 2**. Diagnoses included cases of essential tremor (6 cases), dystonic tremor (2 cases), multisystem atrophy (2 cases), vascular parkinsonism (2 cases), Parkinson's disease (1 case), progressive supranuclear palsy (1 case), corticobasal degeneration (1 case), Fragile X–associated tremor ataxia syndrome (1 case), psychogenic parkinsonism (1 case), and iatrogenic parkinsonism (1 case) (see **Table 3**). In twelve cases we were unable to reach a diagnosis. These patients were labeled as "uncertain diagnosis." They underwent a second DaT-SPECT and were followed for 12 months more, with the following results: in 4 patients the second DaT-SPECT resulted abnormal and they were finally diagnosed with Parkinson's disease (see Discussion for details); in 8 patients the second DaT-SPECT resulted normal again—of those 2 were finally diagnosed with dystonic tremor, whereas 6 remained undiagnosed and labeled as "uncertain diagnosis."

Thus, the final diagnoses included cases of essential tremor (6 cases), Parkinson's disease (5 cases), dystonic tremor (4 cases), multisystem atrophy (2 cases), vascular parkinsonism (2 cases), progressive supranuclear palsy (1 case), corticobasal degeneration (1 case), Fragile X–associated tremor ataxia syndrome (1 case), psychogenic parkinsonism (1 case), and iatrogenic parkinsonism (1 case) (**Table 3** and **Figure 3**).

Table 1 | Demographics and clinical features of the patients included in the study.

Mean age	67 years (57–79)
Gender distribution	17 males 13 females
Mean age at onset	61 years (52–74)
Evolution time at inclusion	35 months (8–58)
Mean MMSE	26 (20–30)
Mean UPDRS	24 (12–36)
Mean L-DOPA dose	564 mg (0–1200)

DISCUSSION

The acronym SWEDDs (scans without evidence of dopaminergic deficits) (Schneider et al., 2007), relatively recent in usage, arose from the clinical trial literature for Parkinson's disease, in which patients were imaged with ^{18}F-dopa PET or DaT-SPECT in order to monitor disease progression, revealing that a substantial proportion of clinically diagnosed cases of Parkinson's disease had normal SCANS (4–15%) and were therefore designated as SWEDDs (Schneider et al., 2007; Bajaj et al., 2012). Thus, the term SWEDDs can be leveled at any patient diagnosed at first with Parkinson's disease but subsequent functional imaging assessments do not confirm the presynaptic, dopaminergic deficiency origin.

From the semiological point of view, SWEDDs phenotypes vary in much the same way as Parkinson's disease phenotypes do. There are two broad Parkinson's disease phenotypes, akinetic-rigid (also known as postural instability gait disorder variant -PIGD) and tremor dominant (also known as tremulous Parkinson's disease). In the same way, SWEDDs patients can be subdivided into tremor dominant and non-tremor dominant (or tremor absent) subtypes. With this and the knowledge of the clinical picture of other parkinsonisms in mind, the clinician in front of a patient with SWEDDs can usually reach a diagnosis, in many cases after a follow up period (De La Fuente-Fernandez, 2012). In the following, we discuss in detail the different diagnoses we found and describe the main clues to consider each one.

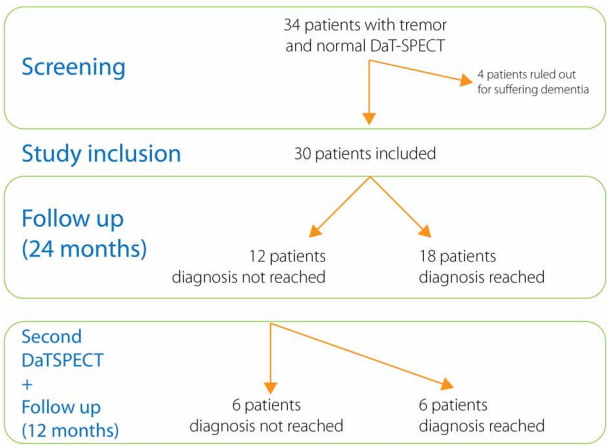

FIGURE 2 | Study design.

Table 2 | Main clinical features of every subject included in the study listed by final diagnoses.

Final diagnos	Tremor	Rigidity	Brady kinesia	Postural stability	Gait	Others	ResponL-dopa
ET1	Sym, P,A,V,C	+	−	+	+	MCI	NT
ET2	Sym, P,A,V,C	−	−	+	+		NT
ET3	Asym, P,A	−	−	+	+		−
ET4	Sym, P,A,V,C	+	−	+	+	MCI	NT
ET5	Sym, P,A	−	−	+	+		−
ET6	Sym, P,A,C	−	−	+	+		NT
PD1	Asym, P, R	+, F	+	+	−		++
PD2	Asym, R	+, F	+	+	+	MCI	++
PD3	Asym, R	+, F	+	−	+		++
PD4	Asym, P, R	+, F	+	−	+	MCI	++
PD5	Asym, R	+	+	−	+		++
DT1	Asym, R	−	−	+	+	Dystonia	−
DT2	Asym, R, J	+	−	−	−	Dystonia	−
DT3	Asym, R	−	−	+	+	Dystonia	−
DT4	Asym, R	−	−	+	+	Dystonia	−
MSA1	Sym, P, J	+	+	−	−	UMS AD AC	+
MSA2	Asym, P, A. R, J	+, F	+	−	−	MCI UMS Stridor	+
VP1	Sym, P,A	+	+	+	+	UMS	+
VP2	Sym, P,A	+	−	+	+	UMS	−
PSP1	Sym, P	+, F	+	−	−	SGP AS	−
CBD1	Asym, P, R	+	+	−	−	MCI MC Apraxia	−
FXTAS	Sym, P,A,R,V,C	+	−	−	−	Ataxia	−
Psycho1	Sym, P,A, R	−	−	−	−	Incons Distrac	NT
Iatro1	Sym, P,A, R	+	+	+	+	Dyskinesia	+
?1	Asym, P, R	+	−	+	+	MCI	−
?2	Asym, P, R	−	+	−	−	MCI UMS	−
?3	Asym, P, R	−	+	+	+	MCI MC Apraxia	−
?4	Asym, P, R	+, F	−	−	−	Dystonia	−
?5	Sym, P,A,R,V,C	−	−	−	−	MCI Ataxia	+
?6	Asym, P, R	−	−	+	+	MCI Apraxia	−

Acronims and clues by columns: Final diagnoses: ET, Essential Tremor; PD, Parkinson's disease; DT, Dystonic tremor; MSA, Multiple system Atrophy; VP, Vascular parkinsonism; PSP, Progressive supranuclear palsy; CBD, Corticobasal degeneration; FXTAS, Fragile X–associated tremor ataxia syndrome; Psychog, Psychogenic parkinsonism; Iatro, Iatrogenic parkinsonism; ?, unclear diagnosis. Tremor: − = Absent Sym, Symmetrical in limbs; Asym, Asymmetrical in limbs; R, Rest tremor; P, Postural tremor; A, Action tremor; J, Jerky tremor; V, Vocal tremor; C, Cephalic tremor. Rigidity: + = present, − = absent, F, Froment sign positive; Bradykinesia: + = present, − = absent, Postural stability: + = normal, − = abnormal, Gait: + = normal, − = abnormal. Others: UMS, upper motor neuron signs; MCI, Mild cognitive imparirment; AD, Autonomic dysfunction; AC, Antecollis; SGP, Supranuclear gaze palsy; AS, Applause sign; MC, Myoclonus; Incons, inconsistent exploratory signs; Distract, Distractability. Response to L-Dopa: ++ = very good, + = good, − = poor or negative, NT, not tested.

Although abnormal in most patients with Parkinson's disease, a normal DaT-SPECT is not capable to totally exclude the disease (Vlaar et al., 2007, 2008; Serrano Vicente et al., 2009). A meta-analysis was conducted by Vlaar and colleagues to review the diagnostic accuracy of SPECT to differentiate between early phase of PD and normalcy. All the 6 cross-sectional studies (using presynaptic tracers) with patients with known PD in an early stage (Hoehn and Yahr score of 2 or lesser) had a specificity of 100% and the sensitivity varied from 8% to 100% (Vlaar et al., 2007, 2008). A possible explanation for the low sensitivity found in some studies is that DaT-SPECT can be normal in the very initial stages of the disease. Indeed we diagnosed 1 case with Parkinson's disease in spite of having a normal DaT-SPECT. At least two studies found that in cases that undergo a second DaT-SPECT the accordance of the result with the final clinical diagnosis was higher in the second DaT-SPECT than in the first one (Vlaar et al., 2007, 2008; Serrano Vicente et al., 2009), thus suggesting that the result of the first DaT-SPECT of patients with Parkinson's disease can be negative if performed too early and become positive later on. In our study 4 out of 12, in which a second DaT-SPECT was performed, resulted abnormal. All these patients responded well to L-DOPA or agonists and had a typical parkinsonian syndrome, therefore they were diagnosed with Parkinson's disease eventually. Another explanation for the relatively high number of false-negative Parkinson's disease patients is the quantitative analysis of the SPECT scans. When recalculating the accuracy of DaT-SPECTs to differentiate patients with idiopathic Parkinson's disease from those with essential tremor using visual qualitative judgment instead of quantitative analysis studies report the sensitivity increased from

80% to 94%, negative predictive value from 48 to 71%, specificity and positive predictive value stayed unchanged (Vlaar et al., 2008; Marshall et al., 2009). However, the rule is that the vast majority of patients with Parkinson's disease have an abnormal DaT-SPECT and a normal DaT-SPECT should always make us reconsider the diagnosis of Parkinsons, even in early stages.

Table 3 | Cases diagnosed after the first and second DaT-SPECTs and follow-up periods.

Diagnoses	DaT-SPECT (prefollow-up)			Total (final diagnoses)
	After first follow-up period ($n = 30$)	After second follow-up period (12/30)		
	Normal	Normal	Abnormal	
Essential tremor	6	–	–	6
Parkinson's disease	1	–	4	5
Dystonic tremor	2	2	–	4
Multisystem atrophy	2	–	–	2
Vascular parkinsonism	2	–	–	2
Progressive Supranuclear Palsy	1	–	–	1
Corticobasal Degeneration	1	–	–	1
Fragile X–associated tremor ataxia syndrome	1	–	–	1
Psychogenic parkinsonism	1	–	–	1
Iatrogenic parkinsonism	1	–	–	1
Uncertain	12	6	–	6

Essential tremor may be confused with parkinsonism for several reasons. Firstly, although essential tremor is characterized by a tremor that is exacerbated by posture-holding and action, these patients may also have a tremor at rest (Cohen et al., 2003; Rajput et al., 2004), whereas parkinsonian patients may also have a postural tremor. Secondly, even though the other cardinal features may be discriminating, some essential tremor patients do have mild rigidity (Rajput et al., 2004), whereas some patients with early Parkinson's disease may present with an isolated rest or postural tremor without any other features of parkinsonism. Some patients with a late onset, markedly asymmetrical postural tremor that was diagnosed initially as essential tremor but who went on after many years to develop typical Parkinson's disease (Chaudhuri et al., 2005). When in doubt, follow up and response to treatments are crucial as those with PD will eventually progress to develop clear parkinsonian features and respond to dopaminergic therapies. Multiple studies report that DaT-SPECT can distinguish parkinsonian syndrome from essential tremor (Asenbaum et al., 1998; Tolosa et al., 2007; Antonini and Isaias, 2009; Surasi et al., 2013). In fact, essential tremor was usually chosen as the comparator disorder for many studies since it was thought to have normal striatal DaT. However, DaT-SPECT in essential tremor is not always normal, or at least not as normal as in controls; further suggesting a potential link of some essential tremor cases with Parkinson's disease (Isaias et al., 2008; Antonini and Isaias, 2009; Gerasimou et al., 2012; Labiano-Fontcuberta and Benito-Leon, 2012). We found essential tremor to be the most common cause of tremor with normal DaT-SPECT (6/30 cases).

Primary adult-onset dystonia can present with an asymmetric resting arm tremor, with impaired arm swing and sometimes also facial hypomimia or a jaw tremor, but without evidence of true akinesia (Schneider et al., 2007). Tremor is a relatively common feature occurring in about 17% of patients with primary late-onset dystonia (Defazio et al., 2013). The association between tremor and dystonia spread suggests that this form of tremor may be a dystonic manifestation. Tremor may be classified either as dystonic tremor or tremor associated with dystonia (TAWD) according to the Movement Disorder Society

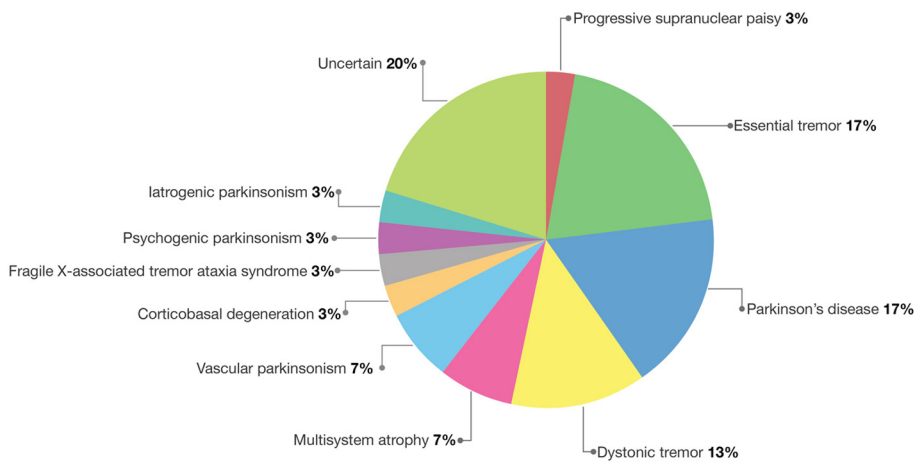

FIGURE 3 | Pie graph showing the distribution of final diagnoses and relative frequencies.

Consensus Statement (Deuschl et al., 1998). Similarities in phenotypic features of dystonic tremor and TAWD predominate over differences, suggesting that the two forms of tremor may be manifestations of the same disease (Defazio et al., 2013; Tinazzi et al., 2013). Differences in gender, body distribution and temporal thresholds of tremor between patients with dystonia and tremor and those of patients with essential tremor also indicate that tremor in dystonia and essential tremor are different entities (Defazio et al., 2013; Tinazzi et al., 2013). Patients with primary adult-onset dystonia show normal DaT-SPECT studies (Schneider et al., 2007). Neurophysiological studies also show that the pattern of plasticity of sensorimotor circuits in patients with tremor dominant SWEDDs resembles the pattern seen in dystonia patients and differs from the pattern found in patients with Parkinson's disease (Schwingenschuh et al., 2010), thus suggesting that many patients with tremulous SWEDDs may have in fact dystonia (Bajaj et al., 2010). In our series 4/30 patients were diagnosed with dystonic tremor. All these patients had a tremoric parkinsonian syndrome with a clear dystonic component in their tremor. Some dystonic signs may also be present in Parkinson's disease, though these are usually mild. In addition, patients with dystonic tremor do not respond to L-DOPA or dopaminergic agonists (Bajaj et al., 2010).

As indicated by its name, progressive supranuclear palsy (PSP) is characterized by a supranuclear gaze palsy with hypometric or slow saccades, particularly on downgaze (Stamelou et al., 2010). However, in the early stages, these abnormalities are often absent and occasionally they do not develop at all (Nath et al., 2003; Williams et al., 2005). DaT-SPECT studies are usually abnormal as in Parkinson's disease. In our series only 1 case was diagnosed with PSP. This case progressed rapidly to the development of the typical picture of PSP with cognitive dysfunction and poor response to L-DOPA.

Fragile X–associated tremor ataxia syndrome (FXTAS) defined by fragile X mental retardation 1 (FMR1) premutation, cerebellar ataxia, intentional tremor, middle cerebellar peduncle hyperintensities in MRI and peripheral neuropathy (Jacquemont et al., 2003; Apartis et al., 2012). About a half of patients with FTAX have abnormal DaT-SPECT (Apartis et al., 2012). One case in our series was diagnosed with FXTAS during follow up based on the genetic study (90–100 CGG Repeats in Gen FMR1). This case was a woman who had been followed in our center for years due to a tremoric parkinsonian syndrome. She was put on several antitremoric treatments, but her tremor only responded to Primidone.

Most cases of symptomatic parkinsonism are vascular parkinsonism. Basal ganglia infarct is a relatively uncommon cause of parkinsonism, but diffuse cerebrovascular disease is much more frequent (Sibon and Tison, 2004; Thanvi et al., 2005). Qualitatively DaT-SPECT images are normal in about a third of patients with vascular parkinsonism. The use of different visual score patterns showed higher ability to differentiate vascular parkinsonism from Parkinson's disease. Semi-quantitative analysis showed significantly higher uptake in the striatum, caudate and putamen in vascular parkinsonism. Among patients with vascular parkinsonism, falls were the only clinical feature that demonstrated a correlation with the SPECT visual pattern (Benitez-Rivero et al., 2013). In spite of the fact that most cases of symptomatic parkinsonism are vascular parkinsonism we only had 2 cases in our series. This is probably due to the fact that in our center all patients with parkinsonian syndrome undergo neuroimaging and those with high vascular load are not asked to perform a DaT-SPECT, for this reason they were not included in this study. However, two patients with vascular risk factors, low vascular load and a normal DaT-SPECT at screening were finally diagnosed with vascular parkinsonism due to fast progression to the typical vascular parkinsonian syndrome and increase in the vascular load in new neuroimaging studies. This suggests that early parkinsonian syndrome may be due to vascular lesions in spite of low vascular load in initial neuroimaging studies, and both clinical and neuroimaging follow up are needed when vascular risk factors are present.

Many drugs can cause parkinsonism, most commonly antipsychotics and antiemetics; and more rarely others such as methyldopa, calcium antagonists, and sodium valproate among many others. Therefore, before making the diagnosis of Parkinson's disease, it is important to check the patient's medication (both current and previous). If the patient is on a relevant drug, it should be stopped if possible, and the patient followed up. Drug induced parkinsonism can take several months to resolve after the drug is discontinued. And even if the symptoms do improve, follow up has shown that a few of these patients will later develop Parkinson's disease, suggesting that the drug had unmasked subclinical Parkinson's disease (Chabolla et al., 1998; Lopez-Sendon et al., 2013). If the drug cannot be stopped, it can be very difficult to distinguish drug induced parkinsonism from idiopathic PD. In this situation, functional imaging with a dopamine transporter ligand may be useful, because patients with pure drug induced parkinsonism have normal scans (Booij et al., 2001; Marshall et al., 2009; Tinazzi et al., 2012). However, contrary to what one would expect, several studies have encountered abnormal DaT-SPECT findings in a surprisingly high number of patients clinically diagnosed as having drug-induced parkinsonism (Sibon and Tison, 2004; Thanvi et al., 2005; Lorberboym et al., 2006). Drug-induced downregulation of DaT expression is certainly a possibility. D_2-receptor blockade may coexist with a dopamine nigrostriatal terminal defect, as assessed by DaT-SPECT abnormalities, in a relevant proportion of patients with drug induced parkinsonism (Schneider et al., 2007). In other words, DaT-SPECT imaging does not predict whether a given neuroleptic-treated patient will develop parkinsonism or not.

Functional or "psychogenic" parkinsonism is well recognized but relatively rare. If there is doubt about this diagnosis, careful follow up and functional imaging may resolve the uncertainty as studies are usually normal. However, contrary to what one would expect, several authors reported abnormal DaT-SPECT findings in a surprisingly high number of patients clinically diagnosed as having psychogenic (Lang et al., 1995; Hallett, 2011; Lang and Voon, 2011). It remains unknown whether these imaging changes are functional or structural in nature. In our study only 1 patient was diagnosed with psychogenic parkinsonian syndrome.

Multiple system atrophy (MSA), also known as striatonigral degeneration or one variant as Shy-Drager syndrome is characterized by a variable combination of parkinsonism, cerebellar ataxia and/or autonomic dysfunction (Ubhi et al., 2011; Ahmed et al., 2012). In our study 2 patients were diagnosed with MSA. They progressed quickly although responded well to L-DOPA initially.

Corticobasal degeneration is characterized by a combination of atypical parkinsonism and higher cortical dysfunction, even when one of these often dominates the clinical picture. Decreased presynaptic dopamine transporter binding have been found in most CBD patients (Hossain et al., 2003; Klaffke et al., 2006). Other study in a large CBS population found DaT-SPECT to be normal in about 10% of cases despite prominent bilateral extrapyramidal signs. In these cases, clinical and neuropsychological features were not distinct from those with evidence of SNc neuronal loss. The lack of any correlation between presynaptic nigrostriatal dysfunction and disease duration might suggest an unpredictable and possibly delayed SNc degeneration in CBD and further supports the hypothesis of a variable contribution of supranigral pathology to its motor phenotype (Cilia et al., 2011). In our series only 1 patient was diagnosed with corticobasal degeneration. She progressed toward dementia and severe dyspraxia quickly.

Repeating DaT-SPECT studies over time can reduce the diagnostic uncertainty that is present even after a prolonged period of observation (Vlaar et al., 2007; Antonini and Isaias, 2009). Of the 12 cases in which we repeated a second SPECT, the result changed to abnormal in 4. These patients were diagnosed with Parkinson's disease. However, after a second DaT-SPECT some patients still remain undiagnosed and other studies (such as PET studies) or even longer times of follow up are needed to move these patients in the diagnostic classification from "SWEDDs" to true nosological entities. As we have seen here, it seems clear that some patients with SWEDDs (those with predominant tremor subtype) have in fact dystonia, whereas others have other entities which are also well-known but may need some reassessment and follow-up to reach the diagnosis. In addition, it is conceivable that a number of patients might suffer from a disorder that has not yet been described.

Some patients with clinically uncertain parkinsonian syndrome exhibit outstanding frontal dysfunction. It is well known that cognitive impairment in early Parkinson's disease and other synucleinpathies (Parkinson-plus syndromes) are accompanied by reductions in activity in frontostriatal neural circuitry (Zgaljardic et al., 2003, 2004). These patients usually have an abnormal DaT-SPECT as the damage in frontostriatal neural circuitry occurs from down (basal ganglia) to up (frontal cortex) (Zgaljardic and Feigin, 2004). We speculate that some of the patients with clinically uncertain parkinsonian syndrome and normal DaT-SPECT studies may have a frontal neurodegenerative process involving fronto-subcortical circuits from top to bottom, that remains to be described. We have the hypothesis that some kind of neurodegenerative disorder affecting motor frontosubcortical circuits primary may exist, where parkinsonism is remarkable and frequently the first manifestation besides a disejecutive syndrome, although these patients do not usually meet the full criteria of frontotemporal lobe dementia. Functional neuroimaging and eventually neuropathological studies should be done in a cohort of these patients to confirm this extreme.

In conclusion, DaT-SPECT can be useful in the process of diagnosing tremor but it should not be relied on as a substitute for a careful, experienced clinical assessment and follow up. It is important to be well aware of the clinical clues to differentiate between these disorders. There is a list of alternative diagnoses to consider when a patient with tremor presents with normal DaT-SPECT, including disorders where it is expected to be normal, such essential tremor, dystonic tremor, vascular parkinsonism, drug induced parkinsonism among others, although the diagnosis of presynaptic parkinsonisms, including Parkinson's disease, is possible too. Repeating DaT-SPECTs over time may be useful in some circumstances since it can reduce the remaining diagnostic uncertainty that is present even after a prolonged period of observation. Especially, clinicians should consider repeating the DaT-SPECT when the clinical picture is consistent with typical early Parkinson's disease. However, after a second DaT-SPECT some patients still remain undiagnosed and other studies or even longer times of follow up are needed to move the diagnose of these patients from "SWEDDs" to true nosological entities.

AUTHOR CONTRIBUTIONS

Manuel Menéndez-González, Francisco Tavares, Nahla Zeidan, José M. Salas-Pacheco, and Oscar Arias-Carrión designed, analyzed and performed research. All authors contributed to and have approved the final manuscript.

REFERENCES

Ahmed, Z., Asi, Y. T., Sailer, A., Lees, A. J., Houlden, H., Revesz, T., et al. (2012). The neuropathology, pathophysiology and genetics of multiple system atrophy. *Neuropathol. Appl. Neurobiol.* 38, 4–24. doi: 10.1111/j.1365-2990.2011.01234.x

Antonini, A., and Isaias, I. U. (2009). Imaging evidence supports a link between essential tremor and Parkinson's disease. *Nucl. Med. Commun.* 30, 93–94. doi: 10.1097/MNM.0b013e328313e580

Apartis, E., Blancher, A., Meissner, W. G., Guyant-Marechal, L., Maltete, D., De Broucker, T., et al. (2012). FXTAS: new insights and the need for revised diagnostic criteria. *Neurology* 79, 1898–1907. doi: 10.1212/WNL.0b013e318271f7ff

Asenbaum, S., Pirker, W., Angelberger, P., Bencsits, G., Pruckmayer, M., and Brucke, T. (1998). [123I]beta-CIT and SPECT in essential tremor and Parkinson's disease. *J. Neural Transm.* 105, 1213–1228.

Bajaj, N. P., Gontu, V., Birchall, J., Patterson, J., Grosset, D. G., and Lees, A. J. (2010). Accuracy of clinical diagnosis in tremulous parkinsonian patients: a blinded video study. *J. Neurol. Neurosurg. Psychiatry* 81, 1223–1228. doi: 10.1136/jnnp.2009.193391

Bajaj, N. P., Wang, L., Gontu, V., Grosset, D. G., and Bain, P. G. (2012). Accuracy of subjective and objective handwriting assessment for differentiating Parkinson's disease from tremulous subjects without evidence of dopaminergic deficits (SWEDDs): an FP-CIT-validated study. *J. Neurol.* 259, 2335–2340. doi: 10.1007/s00415-012-6495-5

Benitez-Rivero, S., Marin-Oyaga, V. A., Garcia-Solis, D., Huertas-Fernandez, I., Garcia-Gomez, F. J., Jesus, S., et al. (2013). Clinical features and 123I-FP-CIT SPECT imaging in vascular parkinsonism and Parkinson's disease. *J. Neurol. Neurosurg. Psychiatry* 84, 122–129. doi: 10.1136/jnnp-2012-302618

Booij, J., Speelman, J. D., Horstink, M. W., and Wolters, E. C. (2001). The clinical benefit of imaging striatal dopamine transporters with [123I]FP-CIT

SPET in differentiating patients with presynaptic parkinsonism from those with other forms of parkinsonism. *Eur. J. Nucl. Med.* 28, 266–272. doi: 10.1007/s002590000460

Chabolla, D. R., Maraganore, D. M., Ahlskog, J. E., O'Brien, P. C., and Rocca, W. A. (1998). Drug-induced parkinsonism as a risk factor for Parkinson's disease: a historical cohort study in Olmsted County, Minnesota. *Mayo Clin. Proc.* 73, 724–727. doi: 10.4065/73.8.724

Chaudhuri, K. R., Buxton-Thomas, M., Dhawan, V., Peng, R., Meilak, C., and Brooks, D. J. (2005). Long duration asymmetrical postural tremor is likely to predict development of Parkinson's disease and not essential tremor: clinical follow up study of 13 cases. *J. Neurol. Neurosurg. Psychiatry* 76, 115–117. doi: 10.1136/jnnp.2004.046292

Cilia, R., Rossi, C., Frosini, D., Volterrani, D., Siri, C., Pagni, C., et al. (2011). Dopamine transporter SPECT imaging in corticobasal syndrome. *PLoS ONE* 6:e18301. doi: 10.1371/journal.pone.0018301

Cohen, O., Pullman, S., Jurewicz, E., Watner, D., and Louis, E. D. (2003). Rest tremor in patients with essential tremor: prevalence, clinical correlates, and electrophysiologic characteristics. *Arch. Neurol.* 60, 405–410. doi: 10.1001/archneur.60.3.405

Defazio, G., Gigante, A. F., Abbruzzese, G., Bentivoglio, A. R., Colosimo, C., Esposito, M., et al. (2013). Tremor in primary adult-onset dystonia: prevalence and associated clinical features. *J. Neurol. Neurosurg. Psychiatry* 84, 404–408. doi: 10.1136/jnnp-2012-303782

De La Fuente-Fernandez, R. (2012). Role of DaTSCAN and clinical diagnosis in Parkinson disease. *Neurology* 78, 696–701. doi: 10.1212/WNL.0b013e318248e520

Deuschl, G., Bain, P., and Brin, M. (1998). Consensus statement of the movement disorder society on tremor. Ad *hoc* Scientific Committee. *Mov. Disord.* 13(Suppl. 3), 2–23. doi: 10.1002/mds.870131303

Gerasimou, G., Costa, D. C., Papanastasiou, E., Bostanjiopoulou, S., Arnaoutoglou, M., Moralidis, E., et al. (2012). SPECT study with I-123-Ioflupane (DaTSCAN) in patients with essential tremor. Is there any correlation with Parkinson's disease? *Ann. Nucl. Med.* 26, 337–344. doi: 10.1007/s12149-012-0577-4

Hallett, M. (2011). Psychogenic parkinsonism. *J. Neurol. Sci.* 310, 163–165. doi: 10.1016/j.jns.2011.03.019

Hossain, A. K., Murata, Y., Zhang, L., Taura, S., Saitoh, Y., Mizusawa, H., et al. (2003). Brain perfusion SPECT in patients with corticobasal degeneration: analysis using statistical parametric mapping. *Mov. Disord.* 18, 697–703. doi: 10.1002/mds.10415

Huang, C., Ravdin, L. D., Nirenberg, M. J., Piboolnurak, P., Severt, L., Maniscalco, J. S., et al. (2013). Neuroimaging markers of motor and nonmotor features of Parkinson's disease: an 18f fluorodeoxyglucose positron emission computed tomography study. *Dement. Geriatr. Cogn. Disord.* 35, 183–196. doi: 10.1159/000345987

Isaias, I. U., Canesi, M., Benti, R., Gerundini, P., Cilia, R., Pezzoli, G., et al. (2008). Striatal dopamine transporter abnormalities in patients with essential tremor. *Nucl. Med. Commun.* 29, 349–353. doi: 10.1097/MNM.0b013e3282f4d307

Jacquemont, S., Hagerman, R. J., Leehey, M., Grigsby, J., Zhang, L., Brunberg, J. A., et al. (2003). Fragile X premutation tremor/ataxia syndrome: molecular, clinical, and neuroimaging correlates. *Am. J. Hum. Genet.* 72, 869–878. doi: 10.1086/374321

Klaffke, S., Kuhn, A. A., Plotkin, M., Amthauer, H., Harnack, D., Felix, R., et al. (2006). Dopamine transporters, D2 receptors, and glucose metabolism in corticobasal degeneration. *Mov. Disord.* 21, 1724–1727. doi: 10.1002/mds.21004

Labiano-Fontcuberta, A., and Benito-Leon, J. (2012). [Essential tremor and Parkinson's disease: are they associated?]. *Rev. Neurol.* 55, 479–489.

Lang, A. E., Koller, W. C., and Fahn, S. (1995). Psychogenic parkinsonism. *Arch. Neurol.* 52, 802–810. doi: 10.1001/archneur.1995.00540320078015

Lang, A. E., and Voon, V. (2011). Psychogenic movement disorders: past developments, current status, and future directions. *Mov. Disord.* 26, 1175–1186. doi: 10.1002/mds.23571

Lopez-Sendon, J., Mena, M. A., and de Yébenes, J. G. (2013). Drug-induced parkinsonism. *Expert Opin. Drug Saf.* 12, 487–496. doi: 10.1517/14740338.2013.787065

Lorberboym, M., Treves, T. A., Melamed, E., Lampl, Y., Hellmann, M., and Djaldetti, R. (2006). [123I]-FP/CIT SPECT imaging for distinguishing drug-induced parkinsonism from Parkinson's disease. *Mov. Disord.* 21, 510–514. doi: 10.1002/mds.20748

Lorenzo Bosquet, C., Miquel Rodriguez, F., Roca Bielsa, I., Mila, M., Aguade Bruix, S., and Castell Conesa, J. (2004). [Differential diagnosis of parkinsonism using dopamine transporters brain SPECT]. *Med. Clin. (Barc.)* 122, 325–328. doi: 10.1016/S0025-7753(04)74224-4

Marshall, V. L., Reininger, C. B., Marquardt, M., Patterson, J., Hadley, D. M., Oertel, W. H., et al. (2009). Parkinson's disease is overdiagnosed clinically at baseline in diagnostically uncertain cases: a 3-year European multicenter study with repeat [123I]FP-CIT SPECT. *Mov. Disord.* 24, 500–508. doi: 10.1002/mds.22108

Nath, U., Ben-Shlomo, Y., Thomson, R. G., Lees, A. J., and Burn, D. J. (2003). Clinical features and natural history of progressive supranuclear palsy: a clinical cohort study. *Neurology* 60, 910–916. doi: 10.1212/01.WNL.0000052991.70149.68

Rajput, A., Robinson, C. A., and Rajput, A. H. (2004). Essential tremor course and disability: a clinicopathologic study of 20 cases. *Neurology* 62, 932–936. doi: 10.1212/01.WNL.0000115145.18830.1A

Rodriguez-Oroz, M. C., Jahanshahi, M., Krack, P., Litvan, I., Macias, R., Bezard, E., et al. (2009). Initial clinical manifestations of Parkinson's disease: features and pathophysiological mechanisms. *Lancet Neurol.* 8, 1128–1139. doi: 10.1016/S1474-4422(09)70293-5

Schneider, S. A., Edwards, M. J., Mir, P., Cordivari, C., Hooker, J., Dickson, J., et al. (2007). Patients with adult-onset dystonic tremor resembling parkinsonian tremor have scans without evidence of dopaminergic deficit (SWEDDs). *Mov. Disord.* 22, 2210–2215. doi: 10.1002/mds.21685

Schwingenschuh, P., Ruge, D., Edwards, M. J., Terranova, C., Katschnig, P., Carrillo, F., et al. (2010). Distinguishing SWEDDs patients with asymmetric resting tremor from Parkinson's disease: a clinical and electrophysiological study. *Mov. Disord.* 25, 560–569. doi: 10.1002/mds.23019

Serrano Vicente, J., Garcia Bernardo, L., Duran Barquero, C., Constantino Silva, A., Infante De La Torre, J. R., Dominguez Grande, M. L., et al. (2009). [Negative predictive value of (123)I Ioflupane SPECT in movement disorders]. *Rev. Esp. Med. Nucl.* 28, 2–5. doi: 10.1016/S0212-6982(09)70207-1

Sibon, I., and Tison, F. (2004). Vascular parkinsonism. *Curr. Opin. Neurol.* 17, 49–54. doi: 10.1097/00019052-200402000-00009

Stamelou, M., De Silva, R., Arias-Carrion, O., Boura, E., Hollerhage, M., Oertel, W. H., et al. (2010). Rational therapeutic approaches to progressive supranuclear palsy. *Brain* 133, 1578–1590. doi: 10.1093/brain/awq115

Surasi, D. S., Peller, P. J., Szabo, Z., Mercier, G., and Subramaniam, R. M. (2013). Dopamine Transporter SPECT Imaging in Parkinson Disease and Dementia. *PET Clin.* 8, 459–467. doi: 10.1016/j.cpet.2013.08.006

Thanvi, B., Lo, N., and Robinson, T. (2005). Vascular parkinsonism–an important cause of parkinsonism in older people. *Age Ageing* 34, 114–119. doi: 10.1093/ageing/afi025

Tinazzi, M., Cipriani, A., Matinella, A., Cannas, A., Solla, P., Nicoletti, A., et al. (2012). [(1)(2)(3)I]FP-CIT single photon emission computed tomography findings in drug-induced Parkinsonism. *Schizophr. Res.* 139, 40–45. doi: 10.1016/j.schres.2012.06.003

Tinazzi, M., Fasano, A., Di Matteo, A., Conte, A., Bove, F., Bovi, T., et al. (2013). Temporal discrimination in patients with dystonia and tremor and patients with essential tremor. *Neurology* 80, 76–84. doi: 10.1212/WNL.0b013e31827b1a54

Tolosa, E., Borght, T. V., Moreno, E., and Da, TSCAN Clinically Uncertain Parkinsonian Syndromes Study Group. (2007). Accuracy of DaTSCAN (123I-Ioflupane) SPECT in diagnosis of patients with clinically uncertain parkinsonism: 2-year follow-up of an open-label study. *Mov. Disord.* 22, 2346–2351. doi: 10.1002/mds.21710

Ubhi, K., Low, P., and Masliah, E. (2011). Multiple system atrophy: a clinical and neuropathological perspective. *Trends Neurosci.* 34, 581–590. doi: 10.1016/j.tins.2011.08.003

Vlaar, A. M., De Nijs, T., Kessels, A. G., Vreeling, F. W., Winogrodzka, A., Mess, W. H., et al. (2008). Diagnostic value of 123I-ioflupane and 123I-iodobenzamide SPECT scans in 248 patients with parkinsonian syndromes. *Eur. Neurol.* 59, 258–266. doi: 10.1159/000115640

Vlaar, A. M., Van Kroonenburgh, M. J., Kessels, A. G., and Weber, W. E. (2007). Meta-analysis of the literature on diagnostic accuracy of SPECT in parkinsonian syndromes. *BMC Neurol.* 7:27. doi: 10.1186/1471-2377-7-27

Williams, D. R., De Silva, R., Paviour, D. C., Pittman, A., Watt, H. C., Kilford, L., et al. (2005). Characteristics of two distinct clinical phenotypes in pathologically proven progressive supranuclear palsy: Richardson's syndrome and PSP-parkinsonism. *Brain* 128, 1247–1258. doi: 10.1093/brain/awh488

Zgaljardic, D. J., Borod, J. C., Foldi, N. S., and Mattis, P. (2003). A review of the cognitive and behavioral sequelae of Parkinson's

disease: relationship to frontostriatal circuitry. *Cogn. Behav. Neurol.* 16, 193–210.

Zgaljardic, D. J., and Feigin, A. (2004). Neuroimaging of Parkinson's disease and atypical parkinsonism. *Curr. Neurol. Neurosci. Rep.* 4, 284–289. doi: 10.1007/s11910-004-0053-1

Zgaljardic, D. J., Foldi, N. S., and Borod, J. C. (2004). Cognitive and behavioral dysfunction in Parkinson's disease: neurochemical and clinicopathological contributions. *J. Neural Transm.* 111, 1287–1301. doi: 10.1007/s00702-004-0178-z

Conflict of Interest Statement: The authors declare that the research was conducted in the absence of any commercial or financial relationships that could be construed as a potential conflict of interest.

Received: 28 January 2014; accepted: 10 March 2014; published online: 01 April 2014.
Citation: Menéndez-González M, Tavares F, Zeidan N, Salas-Pacheco JM and Arias-Carrión O (2014) Diagnoses behind patients with hard-to-classify tremor and normal DaT-SPECT: a clinical follow up study. Front. Aging Neurosci. ***6****:56. doi: 10.3389/fnagi.2014.00056*
This article was submitted to the journal Frontiers in Aging Neuroscience.

frontiers in
AGING NEUROSCIENCE

ORIGINAL RESEARCH ARTICLE
published: 31 March 2014
doi: 10.3389/fnagi.2014.00053

Differential role of CSF alpha-synuclein species, tau, and Aβ42 in Parkinson's Disease

Lucilla Parnetti[1]*, Lucia Farotti[1], Paolo Eusebi[1,2], Davide Chiasserini[3], Claudia De Carlo[1], David Giannandrea[1], Nicola Salvadori[1], Viviana Lisetti[1], Nicola Tambasco[1], Aroldo Rossi[1], Nour K. Majbour[4], Omar El-Agnaf[4,5] and Paolo Calabresi[1,6]

[1] *Clinica Neurologica, Università degli Studi di Perugia, Perugia, Italy*
[2] *Dipartimento di Epidemiologia, Regione Umbria, Perugia, Italy*
[3] *Dipartimento di Scienze Farmaceutiche, Sezione di Biochimica, Università degli Studi di Perugia, Perugia, Italy*
[4] *Department of Biochemistry, Faculty of Medicine and Health Sciences, United Arab Emirates University, Al Ain, United Arab Emirates*
[5] *Faculty of Medicine, King Abdulaziz University, Jeddah, Saudi Arabia*
[6] *IRCCS Fondazione S. Lucia, Roma, Italy*

Edited by:
Manuel Menéndez-González, Hospital Álvarez-Buylla, Spain

Reviewed by:
Jose-Luis Gonzalez De Aguilar, University of Strasbourg, France
Pooja Rao, European Neuroscience Institute, Germany
Victoria M. Leavitt, Manhattan Memory Center, USA

****Correspondence:***
Lucilla Parnetti, Clinica Neurologica, Università di Perugia, Sant'Andrea delle Fratte, 06132 Perugia, Italy
e-mail: parnetti@unipg.it

There is a great interest in developing cerebrospinal fluid (CSF) biomarkers for diagnosis and prognosis of Parkinson's disease (PD). CSF alpha synuclein (α-syn) species, namely total and oligomeric α-syn (t-α-syn and o-α-syn), have shown to be of help for PD diagnosis. Preliminary evidences show that the combination of CSF t-α-syn and classical Alzheimer's disease (AD) biomarkers—β-amyloid 1–42 ($A\beta_{42}$), total tau (t-tau), phosphorylated tau (p-tau)—differentiate PD patients from controls, and that reduced levels of $A\beta_{42}$ represent a predictive factor for development of cognitive deterioration in PD. In this prospective study carried out in 44 PD patients and 25 neurological controls we wanted to verify whether the combination of CSF α-synuclein species—t-α-syn and o-α-syn—and classical AD biomarkers may help in differentiating PD from neurological controls, and if these biomarkers may predict cognitive decline. The median of follow-up duration was 3 years (range: 2–6 years). Mini Mental State Examination (MMSE) and Montreal Cognitive Assessment (MoCA) were used for monitoring cognitive changes along time, being administered once a year. Oligo/total α-syn ratio (o/t-α-syn ratio) confirmed its diagnostic value, significantly contributing to the discrimination of PD from neurological controls. A greater diagnostic accuracy was reached when combining o/t-α-syn and $A\beta_{42}$/tau ratios (Sens = 0.70, Spec = 0.84, AUC = 0.82; PPV = 0.89, NPV = 0.62, LR+ = 4.40, DOR = 12.52). Low CSF $A\beta_{42}$ level was associated with a higher rate of MMSE and MoCA decline, confirming its role as independent predictive factor for cognitive decline in PD. None of the other biomarkers assessed (t-tau, p-tau, t-α-syn and o-α-syn) showed to have prognostic value. We conclude that combination of CSF o/t-α-syn and $A\beta_{42}$/tau ratios improve the diagnostic accuracy of PD. PD patients showing low CSF $A\beta_{42}$ levels at baseline are more prone to develop cognitive decline.

Keywords: cerebrospinal fluid biomarkers, alpha synuclein, total tau, phosphorylated tau, $A\beta_{42}$, Parkinson's disease, cognitive decline

INTRODUCTION

Parkinson's disease (PD) is a common neurodegenerative disorder evolving, in a substantial proportion of patients, to dementia. Although it is defined as a typical movement disorder and its diagnosis is mainly based on motor-related clinical criteria, other functional domains are also involved. Accordingly, post-mortem findings of alpha-synuclein (α-syn) pathology—the histopathologic hallmark of PD—show that the involvement of the dorsal motor nucleus of the vagal nerve and the olfactory bulb takes place much earlier before midbrain involvement (Braak et al., 2003).

PD is a complex neurodegenerative disorder in which many different pathophysiological processes take place, such as protein aggregation, oxidative damage and lysosomal dysfunction (Parnetti et al., 2013). Concomitant pathologies (i.e., Alzheimer and Lewy bodies pathologies) resulting from the mutual interaction between $A\beta_{42}$, tau and α-syn during the course of the disease have major role in the neuropathological processes underlying dementia in PD (Tsigelny et al., 2008; Ciaccioli et al., 2013). In PD the spread of fibrillar α-syn pathology from the brainstem to limbic and neocortical structures, and the cortical deposition of β-amyloid plaques, represent major events (Compta et al., 2011; Irwin et al., 2012). Co-occurrence of tau and α-syn pathology has been found in neurons of brains affected by tauopathies and synucleinopathies, including PD (Vekrellis et al., 2011). Also, α-syn causes aggregation and polymerization of tau, which then induces the formation of intracellular amyloid-tau inclusions (Waxman and Giasson, 2011).

Since molecular changes in the brain are reflected in cerebrospinal fluid (CSF) composition, the CSF represents an ideal

source for biomarkers of different pathophysiological processes characterizing the early phases of the disease, when the clinical diagnosis is more challenging. For example, $A\beta_{42}$, total tau (t-tau) and phosphorylated tau (p-tau) are state markers of Alzheimer's disease (AD), as they reliably reflect AD pathology also in pre-dementia phases. This knowledge has been translated into operational diagnostic criteria (Dubois et al., 2010). Analogously, there is great interest for improving early diagnosis in PD, hopefully in the pre-motor phases, as well as for detecting PD patients at risk of dementia.

Currently, detection of reliable CSF biomarkers for PD is under intensive investigation. Several recent studies have explored the potential use of CSF total α-syn (t-α-syn) as a putative PD biomarker. A clear trend of lower CSF t-α-syn levels in PD and other synucleinopathies has been consistently reported (Tokuda et al., 2006; Noguchi-Shinohara et al., 2009; Spies et al., 2009; Hong et al., 2010; Mollenhauer et al., 2011; Parnetti et al., 2011; Aerts et al., 2012; Tateno et al., 2012), although with a large overlap between the PD and control groups (Noguchi-Shinohara et al., 2009; Spies et al., 2011). Therefore, the measurement of CSF t-α-syn doesn't seem to have enough specificity to correctly discriminate patients with synucleinopathies from normal individuals or other neurodegenerative diseases. The measurement in CSF of other α-syn species, namely soluble oligomers (o-α-syn) has improved the discrimination between PD and other diseases. O-α-syn levels are elevated in brain homogenates in PD and dementia with Lewy bodies compared with normal brains (Paleologou et al., 2009) suggesting a role for o-α-syn in PD pathogenesis. CSF o-α-syn levels and o/t-α-syn ratio have been consistently found to be significantly higher in PD patients as compared to other neurological disorders, with good sensitivity and specificity, as confirmed in independent reports (Tokuda et al., 2010; Park et al., 2011; Sierks et al., 2011; Parnetti et al., 2014). The high risk of cognitive impairment in PD also calls for biomarkers able to predict dementia onset. Many studies have focused on classical AD CSF biomarkers (Parnetti et al., 2008; Compta et al., 2009; Alves et al., 2010; Montine et al., 2010; Siderowf et al., 2010; Leverenz et al., 2011) and most of them have identified the reduction of CSF $A\beta_{42}$ levels as a prognostic factor for cognitive impairment in PD. Data on the possible relationship between α-syn species and the risk of dementia in PD are still scanty.

In this study we evaluated both the diagnostic accuracy and the capability in predicting cognitive decline of CSF AD biomarkers ($A\beta_{42}$, t-tau, p-tau and $A\beta_{42}$/t-tau ratio) and α-syn species (t-α-syn, o-α-syn and o/t-α-syn ratio) in PD patients and neurological controls with a median follow up duration of 3 years.

MATERIALS AND METHODS

PATIENTS

The subjects included in this study (44 PD, 25 neurological controls) were consecutively recruited between 2007 and 2011 and followed-up. They underwent a baseline clinical examination by experienced neurologists, detailed neuropsychological testing, blood chemistry, neuroimaging (computed tomography and/or magnetic resonance imaging), and lumbar puncture. CSF was collected according to the hospital standard protocol and with the local ethical committee approval, after informed written consent was given by the patient. All PD patients fulfilled the United Kingdom Parkinson's Disease Society Brain Bank clinical diagnostic criteria. All of them were treated with L-DOPA and the great majority (39 out of 44) were also taking DA-agonists. PD patients had good control of motor symptoms (mean UPRDS-III 25.39 ± 12.97), and were functionally independent or minimally dependent (Hoehn and Yahr, 1–2.5). Disease duration was calculated from the onset of the first motor symptoms to the time of lumbar puncture. As a control group, 25 cognitively normal age-matched subjects who underwent lumbar puncture as a part of diagnostic work up for other neurological conditions (OND) were recruited to our study. The OND group included: primary headache ($n = 15$), postural instability ($n = 3$), seizures ($n = 2$) and polyneuropathy ($n = 5$). Follow-up visits included clinical examination and neuropsychological testing carried out yearly by means of MMSE (Folstein et al., 1975), a popular screening tool mostly measuring cortical functions with special attention to memory, and MoCA (Gill et al., 2008), another screening tool assessing executive functions.

CSF SAMPLING

Lumbar puncture was performed between 8:00 and 10:00 A.M., after an overnight fast. CSF (10 mL) was collected in sterile polypropylene tubes, centrifuged for 10 min at 2000× g, and 0.5-mL aliquots were immediately frozen at −80°C. None of the samples was contaminated by blood during the procedure (samples showing an erythrocyte count $>500/mm^3$ were not included in the study). CSF $A\beta_{42}$, t-tau and p-tau were measured with ELISA assays (Innotest βAmyloid 1–42, hTAU-Ag, p-TAU 181 Ag; Innogenetics NV, Gent, Belgium, now Fujirebio). For CSF α-syn, 0.5 mL samples were thawed on ice and then divided into aliquots of 110 μL in siliconized tubes containing a cocktail of protease inhibitors, including AEBSF, aprotinin, E-64, EDTA, and leupeptin (Calbiochem-Novabiochem Corporation, San Diego, CA), and 0.05% Tween 20, and the samples were then stored at −80°C until used in the immunoassay for α-syn. While CSF t-α-syn is expressed as ng/mL, CSF o/t-α-syn ratio is expressed in CPS (counts per second). All the samples were obtained at the Section of Neurology, Perugia General Hospital, according to the protocol approved by the Regional Ethical Committee (Prot. N. 19369/AV), after informed written consent was obtained.

IMMUNOASSAY FOR α-SYNUCLEIN IN CSF

Total and oligomeric CSF α-syn were measured as previously reported (Tokuda et al., 2006). Briefly, for CSF t-α-syn anti-human α-syn monoclonal antibody (clone Syn211) (Santa Cruz Biotechnology, USA) was used for capturing while the anti-human α-syn polyclonal antibody FL-140 (Santa Cruz Biotechnology, USA) was used for antigen detection. The standard curve for the ELISA assay was constructed using recombinant human α-syn solution at different concentrations diluted in blocking buffer. For α-syn oligomers, the antibody clone Syn211 was used for capturing, while biotinylated Syn211 (Santa Cruz Biotechnology, USA) was used for antigen detection. The plate was incubated with 50 μL/well of ExtrAvidin-Peroxidase

(Sigma-Aldrich, UK) and with the enhanced chemiluminescent substrate. For both immunoassays, the samples were screened in blind fashion and were randomly tested. A series of internal controls were run to check for run-to-run variations.

DATA ANALYSIS

Statistical analyses were performed using R software v. 2.15 (R Core Team, 2013). Continuous variables were described by median and ranges since data distributions were skewed. Correlations were calculated using Spearman's Rho (r). Kruskal-Wallis test was initially used for comparisons between the two diagnostic groups ($p < 0.05$). The accuracy of the diagnostic value of the biomarkers was assessed by area under the curve (AUC) of the receiver operating characteristic (ROC) curve (Robin et al., 2011; Eusebi, 2013). Cut-off values were calculated using sensitivity and specificity values that maximized Youden's index (sensitivity + specificity − 1). For evaluating the role of multiple biomarkers a multivariable logistic regression approach was used. With the aim to find the best predictors of PD to be included in the final model, we considered all the CSF enzyme activities which had already shown significant differences between OND and PD groups after the univariate analysis.

Multivariate linear regression analysis was used for analyzing the biomarker role in predicting cognitive decline. Change in MMSE and MoCA score were considered as dependent variables. Multiple imputations for missing values were performed in multivariable analyses (Rubin, 1987). Missing data were filled in five times to generate five complete data sets. The completed datasets were analyzed by using the mixed-effects model and the results were combined for the inference.

RESULTS

DESCRIPTIVE ANALYSIS

Demographic data, clinical features, and biomarkers values are listed in **Table 1**. As expected, no significant difference between PD and OND groups was found with respect to age, gender, and follow-up duration. Both MMSE and MoCA scores were significantly lower at baseline ($p = 0.009$ and $p = 0.025$, respectively) and after follow-up ($p = 0.004$ and $p < 0.001$, respectively). Follow-up observations refer to the last visit carried out.

CSF BIOMARKERS IN DIAGNOSTIC GROUPS

Values of CSF biomarkers showed substantial overlap between the two groups (**Table 2** and **Figure 1**). Although the differences did not reach the statistical significance, in PD group median $A\beta_{42}$ levels were higher as opposite to lower median t-tau levels. As a consequence, $A\beta_{42}$/t-tau ratio was significantly increased in the PD group with respect to OND subjects ($p < 0.01$, **Table 2**). Analogously to previous observation (Balducci et al., 2007), a significant decrease of t-α-syn ($p = 0.015$) and an increase of o-α-syn levels ($p = 0.041$) were found in PD group (**Table 2**). Interestingly the o/t-α-syn ratio greatly improved the discrimination between PD and OND groups ($p < 0.001$, **Table 2**). ROC analysis showed a sensitivity of 0.82 and a specificity of 0.56 for $A\beta_{42}$/t-tau ratio. T-α-syn had a sensitivity of 0.59 and a specificity of 0.80. O-α-syn disclosed a sensitivity of 0.89 and a specificity of 0.48. O/t-α-syn ratio reached the best diagnostic performance having a sensitivity of 0.82 and a specificity of 0.64.

In **Table 3** the correlation analysis for all the CSF biomarkers considered is reported. Interestingly, in the PD group, an inverse association between t-α-syn and t-tau was found. Such a negative correlation was also observed in the OND group, where it did not reach the statistical significance. As expected, in the OND group a significant positive association between t-α-syn and $A\beta_{42}$/tau ratio was observed.

Table 4 reports the correlation analysis between CSF biomarkers and clinical parameters in OND and PD groups. In PD t-tau was positively correlated with the H&Y stage, as opposite to the $A\beta_{42}$/t-tau ratio, which was inversely related to H&Y. Cognitive changes along time were measured as points lost in MMSE and MoCA scores between baseline and follow-up visits. In PD $A\beta_{42}$ was negatively correlated with decline in MMSE and MoCA scores. $A\beta_{42}$/t-tau ratio was negatively correlated with decrease in MMSE score. In OND group no significant correlation was found between CSF parameters and decrease in MMSE and MoCA scores.

MULTIPLE BIOMARKERS EVALUATION IN DIAGNOSTIC GROUPS

In order to assess the diagnostic performance of multiple biomarkers combination a logistic regression approach was used. **Table 5** shows a summary of the best model according to several measures of test effectiveness, including sensitivity and specificity, positive and negative predictive values, positive/negative likelihood ratio, AUC and diagnostic odds ratio (DOR). The model included $A\beta_{42}$/t-tau and o/t-α-syn ratios, which together reached a specificity of 84% and a sensitivity of 70%.

Figure 2 shows how the model separates PD patients from OND, allowing for a good discrimination of PD and how the model predictions reach a superior diagnostic performance with respect to the o/t-α-syn or $A\beta_{42}$/t-tau ratios, separately.

CSF BIOMARKERS FOR PREDICTING COGNITIVE DECLINE IN PD

As reported in the previous section, $A\beta_{42}$ and the $A\beta_{42}$/t-tau ratio were the only parameters showing a correlation with MMSE and MoCA scores. To investigate the relationship between the decrease of these two neuropsychological measurements with $A\beta_{42}$ and $A\beta_{42}$/t-tau ratio, a multivariate linear regression model was applied, adjusting for the baseline values and follow-up duration (**Table 6**). MMSE score decrease confirmed to be significantly associated with low CSF $A\beta_{42}$ levels at baseline; the same trend was also observed for MoCA scores; $A\beta_{42}$/t-tau ratio was not significantly associated with cognitive decline.

DISCUSSION

As in other neurodegenerative disorders, PD is characterized by a large time gap between the beginning of neurodegenerative processes and the onset of clinical neurological manifestations. The disease's natural history includes a first asymptomatic stage, followed by a long pre-motor phase; finally, when the classical motor symptoms appear, the majority of nigral dopaminergic neurons are already affected by degeneration. The classical diagnostic criteria for PD mostly rely on motor symptoms, making the formulation of an early diagnosis very challenging. Another challenge

Table 1 | Demographic data and clinical features for OND and PD.

	OND	PD	*p*-value
N	25	44	–
Age	58 (R 31–78; IQR 47–73)	66 (R 41–79; IQR 57.8–72)	0.117
Sex (*M*)	9 (36.0%)	27 (61.4%)	0.076
PD duration (years)	–	3 (R 1–9; IQR 1–5.25)	–
Hoehn and Yahr score	–	2 (R 1–4; IQR 1.5–2.5)	–
MMSE score at baseline	29 (R 27–30; IQR 28–30)	27 (R 20–30; IQR 25.8–30)	0.009
MMSE score at follow-up	28 (R 26–30; IQR 27–30)	26.5 (R 17–30; IQR 23.8–29)	0.004
MoCA score at baseline	28 (R 27–30; IQR 25.5–28.5)	25.5 (R 17–30; IQR 22.8–28)	0.025
MoCA score at follow-up	26 (R 20–29; IQR 24–27)	22 (R 10–28; IQR 18.75–25)	<0.001
Follow-up duration (years)	4 (R 2–7; IQR 3–5)	2 (R 1–7; IQR 2–6)	0.197

P-values, count, and percentages for sex and medians, ranges (R), interquartile ranges (IQR) for the other variables.

Table 2 | CSF biomarkers in PD and OND.

	OND	PD	*p*-value	AUC	Sens	Spec	cut-off
$A\beta_{42}$	530 (431–752)	693 (493–852)	0.057	0.64 (0.51–0.78)	0.59	0.72	636.00
t-tau	194 (117–257)	146 (109–204)	0.085	0.63 (0.48–0.77)	0.64	0.68	159.00
p-tau	19 (11–24)	19.5 (9.75–30.25)	0.793	0.52 (0.38–0.66)	0.36	0.80	25.50
$A\beta_{42}$/t-tau ratio	2.85 (1.88–4.88)	4.70 (3.47–6.38)	0.004	0.71 (0.59–0.84)	0.82	0.56	3.15
t-α-syn	36.5 (25.8–49.6)	22.15 (11.86–38.64)	0.015	0.68 (0.55–0.81)	0.59	0.80	24.45
o-α-syn	3139 (1500–6140)	4838 (3049–8141)	0.041	0.72 (0.59–0.84)	0.89	0.48	2565.50
o/t-α-syn ratio	0.021 (0.014–0.043)	0.061 (0.034–0.175)	<0.001	0.78 (0.67–0.89)	0.82	0.64	0.03

Median values with interquartile ranges (IQR); ROC analysis summary with AUC (95% CI), sensitivity and specificity.

for the research focused on this disorder is the understanding of the mechanisms underlying the development of dementia taking place in a subgroup of parkinsonian patients. It would be very important to have the possibility to individuate those patients at risk to develop this devastating complication to initiate possible protective pharmacological and non-pharmacological interventions. Thus, the availability of objective measures such as reliable "biomarkers," indicators of biological/pathogenetic processes, will be of great importance both for diagnostic accuracy and prognostic evaluation.

In this context, CSF analysis might be of great importance since CSF dynamically reflects the pathophysiological processes taking place in the brain. At present, CSF biomarkers are a routine analysis for early diagnosis of AD. Accordingly, increasing interest is focused on CSF biomarkers in PD, with major expectations on α-syn species and other misfolding proteins, namely β-amyloid and tau. With respect to diagnostic performance, data available so far indicate that there is not a unique ideal CSF biomarker, rather the combination of molecules related to different pathophysiological pathways involved in PD may represents a good strategy for obtaining a more accurate diagnosis (Parnetti et al., 2014). Concerning the prediction of cognitive decline in PD, the most consistent role as predictive factor is played by low CSF $A\beta_{42}$ levels (Parnetti et al., 2008; Alves et al., 2010; Siderowf et al., 2010; Leverenz et al., 2011) although also tau species have been postulated to represent prognostic factors (Zhang et al., 2013). Interestingly, a recent investigation (Kang et al., 2013) carried out in drug-naïve patients with early PD, showed slightly lower CSF levels of both t-tau and t-α-syn in PD compared to healthy controls. This finding offered the Authors the opportunity to speculate that the interaction between tau proteins and α-syn may limit the release of tau proteins into CSF.

In this investigation we assessed both the diagnostic accuracy and the performance in predicting cognitive decline of the combination of CSF AD biomarkers ($A\beta_{42}$, t-tau, p-tau, and $A\beta_{42}$/t-tau ratio) and α-syn species (t-α-syn, o-α-syn, and o/t-α-syn ratio) in a cohort of PD patients and neurological controls followed up for 2–6 years (median follow-up duration: 3 years).

With respect to the diagnostic performance of the biomarkers considered, none of them demonstrated acceptable values in terms of sensitivity and specificity when taken separately. $A\beta_{42}$/t-tau and o/t-α-syn ratios showed good sensitivity (0.82) but low specificity (0.56 and 0.64, respectively). While the usefulness of o/t-α-syn ratio in discriminating PD and controls has already been reported in recent investigations (Tokuda et al., 2010; Park et al., 2011; Sierks et al., 2011; Parnetti et al., 2014), the $A\beta_{42}$/t-tau ratio deserves some comments. Interestingly, in the PD group, we found slightly higher values of $A\beta_{42}$ together with lower values of t-tau as compared to OND group. As a consequence, the mean value of $A\beta_{42}$/t-tau ratio was significantly higher in PD patients with respect to the OND group. This may be due to the fact that our control group was not including healthy subjects, being composed by patients with other neurological diseases. Interestingly, reduced CSF $A\beta_{42}$ levels at baseline represented a

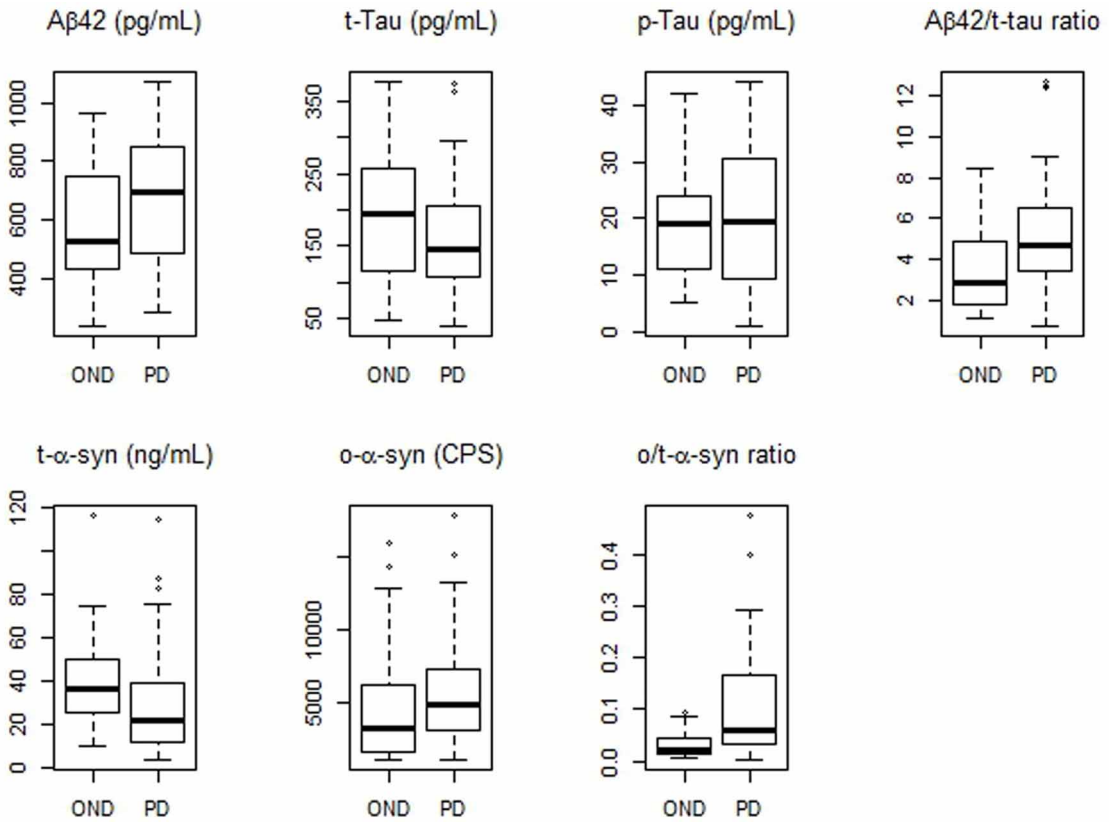

FIGURE 1 | Boxplots of CSF biomarkers values observed in PD and OND cohorts. The horizontal bold lines indicate the medians; the lower part of boxes indicates the first quartile and the upper part the third quartile; the dashed vertical lines indicate the range of values.

Table 3 | Spearman's rank correlation matrix for CSF biomarkers in PD and OND groups.

		$A\beta_{42}$	t-tau	p-tau	$A\beta_{42}$/tau ratio	t-asyn	o-asyn	o/t-asyn ratio
PD	$A\beta_{42}$	1.00						
	t-tau	0.07	1.00					
	p-tau	0.25	**0.71*****	1.00				
	$A\beta_{42}$/t-tau ratio	–	–	**−0.44****	1.00			
	t-α-syn	−0.25	**−0.33***	−0.25	0.13	1.00		
	o-α-syn	−0.12	−0.15	−0.14	0.07	0.06	1.00	
	o/t-α-syn ratio	0.15	0.11	−0.01	−0.02	–	–	1.00
OND	$A\beta_{42}$	1.00						
	t-tau	0.28	1.00					
	p-tau	0.11	**0.56****	1.00				
	$A\beta_{42}$/t-tau ratio	–	–	**−0.41***	1.00			
	t-α-syn	0.24	−0.25	−0.24	**0.43***	1.00		
	o-α-syn	0.01	−0.14	−0.08	0.04	0.21	1.00	
	o/t-α-syn ratio	−0.34	−0.03	−0.04	−0.32	–	–	1.00

*$p < 0.05$, **$p < 0.01$, ***$p < 0.001$.

predictive factor for cognitive decline only in the PD group. In fact, only in PD patients lower CSF $A\beta_{42}$ levels were correlated to a more marked decrease in MMSE and MoCA scores at follow-up. The finding of reduced CSF $A\beta_{42}$ levels in PD patients is quite controversial, being reported in some (Sjögren et al., 2002; Zhang et al., 2008; Alves et al., 2010) but not in other papers (Pøikrylová Vranová, 2010; Siderowf et al., 2010; Leverenz et al., 2011).

Table 4 | Spearman's rank correlations between CSF biomarkers, age, disease duration, and clinical scores in PD group.

		Age	Disease duration	Hoehn and Yahr scale	MMSE score decrease	MoCA score decrease
PD	$A\beta_{42}$	−0.28	−0.13	−0.19	**−0.52*****	**−0.45****
	t-tau	**0.31***	0.04	**0.39****	0.18	0.08
	p-tau	0.24	0.10	0.09	−0.10	−0.16
	$A\beta_{42}$/t-tau ratio	**−0.42****	−0.11	**−0.50*****	**−0.37***	−0.26
	t-α-syn	0.00	0.30	0.10	0.06	−0.03
	o-α-syn	−0.26	−0.17	−0.14	−0.07	−0.07
	o/t-α-syn ratio	−0.18	−0.27	−0.12	−0.02	0.05
OND	$A\beta_{42}$	−0.37			−0.01	−0.38
	t-tau	0.18			0.17	0.09
	p-tau	0.18			−0.26	0.26
	$A\beta_{42}$/t-tau ratio	**−0.43***			−0.12	−0.24
	t-α-syn	**−0.41***			−0.37	−0.07
	o-α-syn	−0.02			−0.20	−0.41
	o/t-α-syn ratio	0.33			0.02	−0.24

*$p < 0.05$, **$p < 0.01$, ***$p < 0.001$.

Table 5 | Logistic regression analysis of multiple CSF biomarkers between PD and OND.

	Estimate	*SE*	*p*-value	Accuracy measures	
Intercept	−2.540	0.882	–	Sens = 0.70	LR+ = 4.40
$A\beta_{42}$/t-tau ratio	0.405	0.162	0.012	Spec = 0.84	LR− = 0.35
o/t-αsyn ratio	28.514	11.124	0.010	PPV = 0.89	DOR = 12.52
				NPV = 0.62	AUC = 0.82 (95%CI = 0.73–0.92)

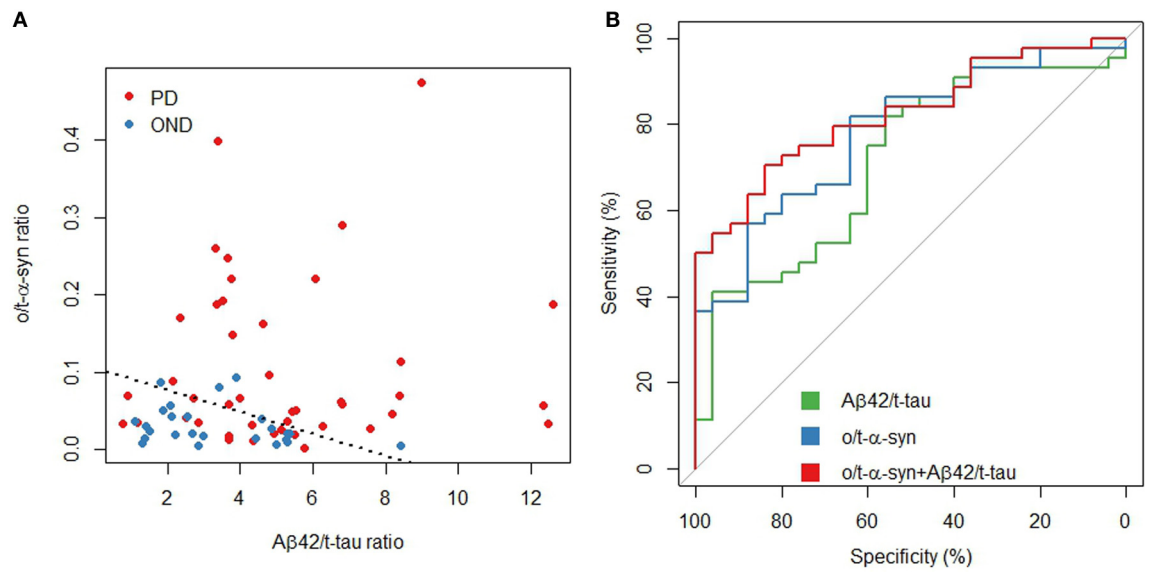

FIGURE 2 | $A\beta_{42}$/t-tau and o/t-α-syn ratios in PD and OND. **(A)** Scatterplot: the dashed line represents a partition of the o/t-α-syn and $A\beta_{42}$/t-tau space such that below the line the model predicts OND, above the line the model predicts PD **(B)** ROC curves of $A\beta_{42}$/t-tau and o/t-α syn ratios and the fitted values of the multivariable logistic regression model.

Table 6 | Linear regression analyses of cognitive decline in PD cohort.

		Estimate	*SE*	*p*-value
MMSE score decrease	Intercept	3.60	–	–
	$1/A\beta_{42}$	1139.92	329.08	0.012
	MMSE score at baseline	−0.17	0.08	0.038
	Follow-up duration (years)	0.18	0.08	0.029
MoCA score decrease	Intercept	2.75	–	–
	$1/A\beta_{42}$	1395.25	482.93	0.007
	MoCA score at baseline	−0.08	0.09	0.387
	Follow-up duration (years)	0.22	0.11	0.048

A clear positive association was also observed between t-tau and t-α-syn in PD group. These findings are consistent with the observation of Kang and coworkers, describing the occurrence of lower CSF levels of t-tau and t-α-syn in PD patients. A reasonable explanation may be the mutual interaction of the two molecules, leading to a reduced release of tau in CSF. The discriminative power between PD and OND significantly improved when considering both o/t-α-syn ratio and $A\beta_{42}$/t-tau ratio, as shown by the logistic regression analysis, and further illustrated in **Figure 2**. This confirms that the combination of several biomarkers is more helpful than single biomarkers for adding diagnostic accuracy of PD.

About the predictive value of CSF biomarkers for cognitive decline in PD, our study confirmed the specific role of low CSF levels of $A\beta_{42}$ in this pathological condition; no other biomarker was significantly associated to this outcome measure. For assessing cognitive function along time, we used both MMSE and MoCA (Gill et al., 2008). Both neuropsychological instruments showed to be related to CSF $A\beta_{42}$ levels, i.e., lower the CSF $A\beta_{42}$ levels, greater the decrease in MMSE and MoCA scores. The same holds true for $A\beta_{42}$/t-tau ratio with respect to MMSE. Multivariate analysis (adjusting for follow-up time and baseline measurements) confirmed that low CSF $A\beta_{42}$ levels are independent predictor of cognitive decline in PD, either measured by MMSE or MOCA.

In conclusion, this study further contributes to the evidence of the usefulness of CSF biomarkers for PD diagnosis and prognosis. Major points are the need to combine several CSF biomarkers for improving the diagnostic accuracy, and the confirmed role of low CSF $A\beta_{42}$ levels as independent predictor of cognitive decline in PD. Longitudinal studies measuring biomarkers and clinical parameters over several years represent a major contribution in this field. Analogously to the longitudinal AD Neuroimaging Initiative (ADNI, http://adni-info.org/) in AD, the Parkinson's Progression Markers Initiative (PPMI, http://ppmi-ifo.org/) will give important knowledge in the field of PD, thanks to the measurement of several CSF, blood, and imaging biomarkers in early *de novo* PD followed up for several years.

ACKNOWLEDGMENTS

We would like to thank Mr. Cristiano Spaccatini for his technical assistance. Prof. Lucilla Parnetti and Prof. Omar El-Agnaf received grants from Michael J. Fox Foundation for Parkinson's disease.

REFERENCES

Aerts, M. B., Esselink, R. A., Abdo, W. F., Bloem, B. R., and Verbeek, M. M. (2012). CSF α-synuclein does not differentiate between parkinsonian disorders. *Neurobiol. Aging* 33, 430.e1–430.e3. doi: 10.1016/j.neurobiolaging.2010.12.001

Alves, G., Brønnick, K., Aarsland, D., Blennow, K., Zetterberg, H., Ballard, C., et al. (2010). CSF amyloid-beta and tau proteins, and cognitive performance, in early and untreated Parkinson's disease: the Norwegian ParkWest study. *J. Neurol. Neurosurg. Psychiatry* 81, 1080–1086.doi: 10.1136/jnnp.2009.199950

Balducci, C., Pierguidi, L., Persichetti, E., Parnetti, L., Sbaragli, M., Tassi, C., et al. (2007). Lysosomal hydrolases in cerebrospinal fluid from subjects with Parkinson's disease. *Mov. Disord.* 22, 1481–1484. doi: 10.1002/mds.21399

Braak, H., Del Tredici, K., Rüb, U., de Vos, R. A., Jansen Steur, E. N., and Braak, E. (2003). Staging of brain pathology related to sporadic Parkinson's disease. *Neurobiol. Aging* 24, 197–211. doi: 10.1016/S0197-4580(02)00065-9

Ciaccioli, G., Martins, A., Rodrigues, C., Vieira, H., and Calado, P. (2013). A powerful yeast model to investigate the synergistic interaction of α-synuclein and tau in neurodegeneration. *PLoS ONE* 8:e55848. doi: 10.1371/journal.pone.0055848

Compta, Y., Parkkinen, L., O'Sullivan, S. S., Vandrovcova, J., Holton, J. L., Collins, C., et al. (2011). Lewy- and Alzheimer-type pathologies in Parkinson's disease dementia: which is more important? *Brain* 134(Pt 5), 1493–1505. doi: 10.1093/brain/awr031

Compta, Y., Martí, M. J., Ibarretxe-Bilbao, N., Junqué, C., Valldeoriola, F., Muñoz, E., et al. (2009). Cerebrospinal tau, phospho-tau, and beta-amyloid and neuropsychological functions in Parkinson's disease. *Mov. Disord.* 24, 2203–2210. doi: 10.1002/mds.22594

Dubois, B., Feldman, H. H., Jacova, C., Cummings, J. L., Dekosky, S. T., Barberger-Gateau, P., et al. (2010). Revising the definition of Alzheimer's disease: a new lexicon. *Lancet Neurol.* 9, 1118–1127. doi: 10.1016/S1474-442270223-442270224

Eusebi, P. (2013). Diagnostic accuracy measures. *Cerebrovasc. Dis.* 36, 267–272. doi: 10.1159/000353863

Folstein, M. F., Folstein, S. E., and McHugh, P. R. (1975). Mini-mental state. A practical method for grading the cognitive state of patients for the clinician. *J. Psychiatr. Res.* 12, 189–198. doi: 10.1016/0022-3956(75)90026-6

Gill, D. J., Freshman, A., Blender, J. A., and Ravina, B. (2008). The montreal cognitive assessment as a screening tool for cognitive impairment in Parkinson's disease. *Mov. Disord.* 23, 1043–1046. doi: 10.1002/mds.22017

Hong, Z., Shi, M., Chung, K. A., Quinn, J. F., Peskind, E. R., Galasko, D., et al. (2010). DJ-1 and alpha-synuclein in human cerebrospinal fluid as biomarkers of Parkinson's disease. *Brain* 133(Pt 3), 713–726. doi: 10.1093/brain/awq008

Irwin, D. J., White, M. T., Toledo, J. B., Xie, S. X., Robinson, J. L., Van Deerlin, V., et al. (2012). Neuropathologic substrates of Parkinson disease dementia. *Ann. Neurol.* 72, 587–598. doi: 10.1002/ana.23659

Kang, J. H., Irwin, D. J., Chen-Plotkin, A. S., Siderowf, A., Caspell, C., Coffey, C. S., et al. (2013). Association of cerebrospinal fluid β-Amyloid 1-42, T-tau, P-tau181, and α-synuclein levels with clinical features of drug-naive patients with early Parkinson disease. *JAMA Neurol.* 70, 1277–1287. doi: 10.1001/jamaneurol.2013.3861

Leverenz, J. B., Watson, G. S., Shofer, J., Zabetian, C. P., Zhang, J., and Montine, T. J. (2011). Cerebrospinal fluid biomarkers and cognitive performance in non-demented patients with Parkinson's disease. *Parkinsonism Relat. Disord.* 17, 61–64. doi: 10.1016/j.parkreldis.2010.10.003

Mollenhauer, B., Locascio, J. J., Schulz-Schaeffer, W., Sixel-Döring, F., Trenkwalder, C., and Schlossmacher, M. G. (2011). α-Synuclein and tau concentrations in cerebrospinal fluid of patients presenting with parkinsonism: a cohort study. *Lancet Neurol.* 10, 230–240. doi: 10.1016/S1474-442270014-X

Montine, T. J., Shi, M., Quinn, J. F., Peskind, E. R., Craft, S., Ginghina, C., et al. (2010). CSF Aβ(42) and tau in Parkinson's disease with cognitive impairment. *Mov. Disord.* 25, 2682–2685. doi: 10.1002/mds.23287

Noguchi-Shinohara, M., Tokuda, T., Yoshita, M., Kasai, T., Ono, K., Nakagawa, M., et al. (2009). CSF alpha-synuclein levels in dementia with Lewy bodies and Alzheimer's disease. *Brain Res.* 1251, 1–6. doi: 10.1016/j.brainres.2008.11.055

Paleologou, K. E., Kragh, C. L., Mann, D. M., Salem, S. A., Al-Shami, R., Allsop, D., et al. (2009). Detection of elevated levels of soluble alpha-synuclein oligomers in post-mortem brain extracts from patients with dementia with Lewy bodies. *Brain* 132(Pt 4)1093–1101. doi: 10.1093/brain/awn349

Park, M. J., Cheon, S. M., Bae, H. R., Kim, S. H., and Kim, J. W. (2011). Elevated levels of α-synuclein oligomer in the cerebrospinal fluid of drug-naïve patients with Parkinson's disease. *J. Clin. Neurol.* 7, 215–222. doi: 10.3988/jcn.2011.7.4.215

Parnetti, L., Castrioto, A., Chiasserini, D., Persichetti, E., Tambasco, N., El-Agnaf, O., et al. (2013). Cerebrospinal fluid biomarkers in Parkinson disease. *Nat. Rev. Neurol.* 9, 131–140. doi: 10.1038/nrneurol.2013.10

Parnetti, L., Chiasserini, D., Persichetti, E., Eusebi, P., Varghese, S., Qureshi, M. M., et al. (2014). Cerebrospinal fluid lysosomal enzymes and α-synuclein in Parkinson's disease. *Mov. Disord.* doi: 10.1002/mds.25772. [Epub ahead of print].

Parnetti, L., Chiasserini, D., Bellomo, G., Giannandrea, D., De Carlo, C., Qureshi, M. M., et al. (2011). Cerebrospinal fluid Tau/α-synuclein ratio in Parkinson's disease and degenerative dementias. *Mov. Disord.* 26, 1428–1435. doi: 10.1002/mds.23670

Parnetti, L., Tiraboschi, P., Lanari, A., Peducci, M., Padiglioni, C., D'Amore, C., et al. (2008). Cerebrospinal fluid biomarkers in Parkinson's disease with dementia and dementia with Lewy bodies. *Biol. Psychiatry* 64, 850–855. doi: 10.1016/j.biopsych.2008.02.016

Pøikrylová Vranová, H., Mareš, J., Nevrlý, M., Stejskal, D., Zapletalová, J., Hluštík, P., et al. (2010). CSF markers of neurodegeneration in Parkinson's disease. *J. Neural. Transm.* 117, 1177–1181. doi: 10.1007/s00702-010-0462-z

R Core Team. (2013). *R: A. Language and Environment for Statistical Computing*. Vienna: R Foundation for Statistical Computing. Available online at: http://www.R-project.org/

Robin, X., Turck, N., Hainard, A., Tiberti, N., Lisacek, F., Sanchez, J. C., et al. (2011). pROC: an open-source package for R and S+ to analyze and compare ROC curves. *BMC Bioinformatics* 12:77. doi: 10.1186/1471-2105-12-77

Rubin, D. B. (1987). *Multiple Imputation for Nonresponse in Surveys*. New York, NY; Chichester: Wiley. doi: 10.1002/9780470316696

Siderowf, A., Xie, S. X., Hurtig, H., Weintraub, D., Duda, J., Chen-Plotkin, A., et al. (2010). CSF amyloid {beta} 1-42 predicts cognitive decline in Parkinson disease. *Neurology* 75, 1055–1061. doi: 10.1212/WNL.0b013e3181f39a78

Sierks, M. R., Chatterjee, G., McGraw, C., Kasturirangan, S., Schulz, P., and Prasad, S. (2011). CSF levels of oligomeric alpha-synuclein and beta-amyloid as biomarkers for neurodegenerative disease. *Integr. Biol. (Camb.)* 3, 1188–1196. doi: 10.1039/c1ib00018g

Sjögren, M., Davidsson, P., Wallin, A., Granérus, A. K., Grundström, E., Askmark, H., et al. (2002). Decreased CSF-beta-amyloid 42 in Alzheimer's disease and amyotrophic lateral sclerosis may reflect mismetabolism of beta-amyloid induced by disparate mechanisms. *Dement. Geriatr. Cogn. Disord.* 13, 112–118. doi: 10.1159/000048642

Spies, P. E., Slats, D., Rikkert, M. G., Tseng, J., Claassen, J. A., and Verbeek, M. M. (2011). CSF α-synuclein concentrations do not fluctuate over hours and are not correlated to amyloid β in humans. *Neurosci. Lett.* 504, 336–338. doi: 10.1016/j.neulet.2011.09.063

Spies, P. E., Melis, R. J., Sjögren, M. J., Rikkert, M. G., and Verbeek, M. M. (2009). Cerebrospinal fluid alpha-synuclein does not discriminate between dementia disorders. *J. Alzheimers Dis.* 16, 363–369. doi: 10.3233/JAD-2009-0955

Tateno, F., Sakakibara, R., Kawai, T., Kishi, M., and Murano, T. (2012). Alpha-synuclein in the cerebrospinal fluid differentiates synucleinopathies (Parkinson Disease, dementia with Lewy bodies, multiple system atrophy) from Alzheimer disease. *Alzheimer Dis. Assoc. Disord.* 26, 213–216. doi: 10.1097/WAD.0b013e31823899cc

Tokuda, T., Qureshi, M. M., Ardah, M. T., Varghese, S., Shehab, S. A., Kasai, T., et al. (2010). Detection of elevated levels of α-synuclein oligomers in CSF from patients with Parkinson disease. *Neurology* 75, 1766–1772. doi: 10.1212/WNL.0b013e3181fd613b

Tokuda, T., Salem, S. A., Allsop, D., Mizuno, T., Nakagawa, M., Qureshi, M. M., et al. (2006). Decreased alpha-synuclein in cerebrospinal fluid of aged individuals and subjects with Parkinson's disease. *Biochem. Biophys. Res. Commun.* 349, 162–166. doi: 10.1016/j.bbrc.2006.08.024

Tsigelny, I. F., Crews, L., Desplats, P., Shaked, G. M., Sharikov, Y., Mizuno, H., et al. (2008). Mechanisms of hybrid oligomer formation in the pathogenesis of combined Alzheimer's and Parkinson's diseases. *PLoS ONE* 3:e3135. doi: 10.1371/journal.pone.0003135

Vekrellis, K., Xilouri, M., Emmanouilidou, E., Rideout, H. J., and Stefanis, L. (2011). Pathological roles of α-synuclein in neurological disorders. *Lancet Neurol.* 10, 1015–1025. doi: 10.1016/S1474-442270213-442270217

Waxman, E. A., and Giasson, B. I. (2011). Induction of intracellular tau aggregation is promoted by α-synuclein seeds and provides novel insights into the hyperphosphorylation of tau. *J. Neurosci.* 31, 7604–7618. doi: 10.1523/JNEUROSCI.0297-0211.2011

Zhang, J., Mattison, H. A., Liu, C., Ginghina, C., Auinger, P., McDermott, M. P., et al. (2013). Longitudinal assessment of tau and amyloid beta in cerebrospinal fluid of Parkinson disease. *Acta Neuropathol.* 126, 671–682. doi: 10.1007/s00401-013-1121-x

Zhang, J., Sokal, I., Peskind, E. R., Quinn, J. F., Jankovic, J., Kenney, C., et al. (2008). CSF multianalyte profile distinguishes Alzheimer and Parkinson diseases. *Am. J. Clin. Pathol.* 129, 526–529. doi: 10.1309/W01Y0B808EMEH12L

Conflict of Interest Statement: The authors declare that the research was conducted in the absence of any commercial or financial relationships that could be construed as a potential conflict of interest.

Received: 15 January 2014; accepted: 05 March 2014; published online: 31 March 2014.
*Citation: Parnetti L, Farotti L, Eusebi P, Chiasserini D, De Carlo C, Giannandrea D, Salvadori N, Lisetti V, Tambasco N, Rossi A, Majbour NK, El-Agnaf O, and Calabresi P (2014) Differential role of CSF alpha-synuclein species, tau, and Aβ42 in Parkinson's Disease. Front. Aging Neurosci. **6**:53. doi: 10.3389/fnagi.2014.00053*
This article was submitted to the journal Frontiers in Aging Neuroscience.

frontiers in
AGING NEUROSCIENCE

OPINION ARTICLE
published: 18 March 2014
doi: 10.3389/fnagi.2014.00045

The many questions on the use of biomarkers for neurodegenerative diseases in clinical practice

Manuel Menéndez-González [1,2,3]*

[1] Neurología, Hospital Álvarez-Buylla, Mieres, Spain
[2] Morfología y Biología Celular, Universidad de Oviedo, Oviedo, Spain
[3] Instituto de Neurociencias, Oviedo, Spain
*Correspondence: manuelmenendezgonzalez@gmail.com

Edited by:
Oscar López, University of Pittsburgh School of Medicine, USA

Keywords: biomarker, dementia, clinical practice, mild cognitive impairment, treatment outcome

There are two basic questions always raised when biomarkers are proposed to be used for diagnosing neurodegenerative diseases (ND) in clinical practice (Wilner, 2010). The first question is, do biomarkers enhance the diagnostic accuracy? Clinical-based diagnosis accuracy of ND varies depending on the disease, stage and the criteria used, but in general terms it is about 75–90% accuracy. Today, there is consensus that several biomarkers, combined with the traditional clinical process, may allow a more accurate diagnosis in many ND (Galluzzi et al., 2013). This fact is particularly important in early stages, when the diagnosis is specially challenging. For most patients with mild deficits concerned about the development of ND, a careful history, and a physical, neurological and neuropsychological evaluation with a close follow-up (a "wait and see" approach) used to be the standard practice. Today we can offer a more proactive approach for discerning whether there is an underlying neurodegenerative process behind these mild deficits (Heister et al., 2011). The National Institute on Aging-Alzheimer's Association criteria for AD or MCI recommend the use of amyloid ligands with caution, and only in exceptional circumstances they should be used in clinical practice (Albert et al., 2011; Sperling et al., 2011). The use of different biomarkers for differential diagnosis should not be discouraged. On the other hand, use of biomarkers as predictive instruments should be discouraged.

The second question is, does the additional diagnostic accuracy provided by biomarkers really matter? In clinical practice, a test that confirmed or ruled out a ND would remove uncertainty. This would also disregard or reinforce the need to consider other diseases that may present symptoms similar to those of ND. In some of these diseases, prompt diagnosis can lead to earlier effective treatment, such as shunting for normal pressure hydrocephalus, supplementation with thyroid hormones in hypothyroidism or antidepressive medications for depression.

The best argument for using biomarkers in clinical practice would be the possibility of treating patients with a disease-modifying therapy that prevents or delays the progression of the disease. In other words, putting patients on drugs with neuroprotective effect. However, no drug have proven prevention of any ND yet.The current therapies only provide symptomatic improvement at best so there is an urgent need to discover neuroprotective treatments. But how can we conduct clinical trials for testing such drugs when diagnosing ND at its very early stages is so difficult? Again, the support of biomarkers should be mandatory for enrolling patients in research studies.

Then, if there is not a disease-modifying therapy yet, what is the importance of an early diagnosis in routine clinical practice today? There are several reasons to make an early diagnosis even when we cannot modify the course of the disease. For instance, once people become demented, they can no longer plan for their future or dictate their end-of-life care. An early diagnosis of Alzheimer's disease gives a person the opportunity to decide on important questions before he or she gets demented (Martínez-Rivera et al., 2008). It also has important consequences for the patient's family. However, an early diagnosis of a ND may also have negative psychological consequences in an otherwise well-functioning person who must now consider an inexorable decline towards a state of illness and dependency. Consequently, the pros and cons of early diagnosis must be carefully weighed up in each individual prior to perform a confirmatory test.

And even if we have decided to use biomarkers for supporting the diagnosis of a ND, there are many questions to face. It is important to emphasize that standardization of these biomarkers is currently limited, and results often vary from laboratory to laboratory. Ultimately, it will be necessary to interpret biomarker data in the context of well-established normative values. Moreover, procedures for acquisition and analysis of samples need to be established to implement these biomarker criteria on a broad scale. Although we consider biomarkers as "negative" or "positive" for purposes of classification, it is recognized that varying severities of an abnormality may confer different likelihoods or prognoses, which is difficult to quantify accurately for broad application. Currently it is difficult to understand the relative importance of different biomarkers when used together, and to interpret results when biomarker data conflict with one another.

Equally important, there is a dearth of truly predictive studies at the individual subject level or in unselected populations. The use of biomarkers in the clinical practice will require the ability to assign a likelihood of progression in an individual person over a specific time interval through the use of a single or multiple biomarkers. Another major limitation is knowledge about the timing of decline

because the ability to detect change is dependent on the period of observation or prediction. A complete understanding of the role of biomarkers in prediction of decline will require both short and long-term periods of observation.

Finally, little is known about outcome when biomarkers provide conflicting results. When a panel of biomarkers is used, it is possible that for some individuals, one biomarker will be positive, one will be negative, and one equivocal. The long-term significance of such findings may also vary with the length of follow-up.

Therefore, questions such as "what biomarker is better for making the early diagnosis of each ND?," or "which one is better for the follow up," "which one for making the differential diagnosis with other disease?", "how to interpret the results of these tests in coordination with clinical or genetic findings" and "how to combine the results from different biomarkers?" have important repercussion on the management of patients suspected of suffering from ND and still remain unresponsed. The answers to these questions are not always easy and rely on upcoming science.

We need more data and more networking to find appropriate conclusions. Collaboration between basic, translational and clinic researchers is paramount for giving answers relevant to everyday clinical practice. In this regard, the topic research issue accompanying this editorial letter gathers together a bunch of review and original articles exploring the use of biomarkers for ND from different perspectives.

REFERENCES

Albert, M. S., DeKosky, S. T., Dickson, D., Dubois, B., Feldman, H. H., Fox, N. C., et al. (2011). The diagnosis of mild cognitive impairment due to Alzheimer's disease: recommendations from the National Institute on Aging-Alzheimer's Association workgroups on diagnostic guidelines for Alzheimer's disease. *Alzheimers Dement*. 7, 270–279. doi: 10.1016/j.jalz.2011.03.008

Galluzzi, S., Geroldi, C., Amicucci, G., Bocchio-Chiavetto, L., Bonetti, M., Bonvicini, C., et al. (2013). Translational outpatient memory clinic working group. Supporting evidence for using biomarkers in the diagnosis of MCI due to AD. *J. Neurol.* 260, 640–650. doi: 10.1007/s00415-012-6694-0

Heister, D., Brewer, J. B., Magda, S., Blennow, K., and McEvoy, L. K. (2011). Alzheimer's disease neuroimaging initiative. Predicting MCI outcome with clinically available MRI and CSF biomarkers. *Neurology* 77, 1619–1628. doi: 10.1212/WNL.0b013e3182343314

Martínez-Rivera, M., Menénedez-González, M., and Pérez-Piñera, P. (2008). Biomarcadores para la Enfermedad de Alzheimer y otras demencias degenerativas. *Archivos de Medicina* 4:3.

Sperling, R. A., Aisen, P. S., Beckett, L. A., Bennett, D. A., Craft, S., Fagan, A. M., et al. (2011). Toward defining the preclinical stages of Alzheimer's disease: recommendations from the National Institute on Aging-Alzheimer's Association workgroups on diagnostic guidelines for Alzheimer's disease. *Alzheimers Dement*. 7, 280–292. doi: 10.1016/j.jalz.2011.03.003

Wilner, A. N. (2010). Alzheimer's CSF test: useful or useless? *Medscape*.

Received: 10 December 2013; accepted: 01 March 2014; published online: 18 March 2014.

*Citation: Menéndez-González M (2014) The many questions on the use of biomarkers for neurodegenerative diseases in clinical practice. Front. Aging Neurosci. **6**:45. doi: 10.3389/fnagi.2014.00045*

This article was submitted to the journal Frontiers in Aging Neuroscience.

frontiers in
AGING NEUROSCIENCE

OPINION ARTICLE
published: 09 April 2014
doi: 10.3389/fnagi.2014.00065

Routine lumbar puncture for the early diagnosis of Alzheimer's disease. Is it safe?

Manuel Menéndez-González [1,2]*

[1] *Sección de Neurología, Hospital Álvarez-Buylla, Mieres, Spain*
[2] *Morfología y Biología Celular, Universidad de Oviedo, Oviedo, Spain*
**Correspondence: manuelmenendezgonzalez@gmail.com*

Edited and reviewed by:
Oscar López, University of Pittsburgh School of Medicine, USA

Keywords: lumbar puncture, CSF, safety, feasibility studies, Alzheimer, dementia, mild cognitive impairment

Diagnosing Alzheimer's disease (AD) early is itself a controversial topic—not to be addressed here—, as many believe that adequate therapeutics are not available for modifying the course of the disease. Although this may be the case today, it is perhaps due to the fact that existing therapies do not have positive results as the disease process is too far advanced. Distinguishing the cases who will progress to AD among individuals with mild cognitive impairment (MCI), would allow early administration of these currently and future available treatments. Together, this can prolong a meaningful life and also reduce the burden on caregivers as well as the cost of care, now that both the prevalence and cost of AD are rising at a rapid rate.

However, diagnosing AD at its early stage still remains a challenge, even in specialized AD centers. Numerous studies suggest that CSF biomarkers have a high potential as diagnostic tools: the measurement of the 2 key AD proteins, Amyloid-beta and Tau, is very helpful for detecting neuropathologic changes related to AD early. CSF levels of Amyloid-beta, but not of Tau, are fully changed already 5–10 years before the onset of clinical AD (Buchhave et al., 2012). CSF TAU changes some time later, when the brain atrophy starts, being a good marker of injury. Thus, in subjects with MCI and evidence of amyloid pathology, CSF Tau can predict further cognitive decline (van Rossum et al., 2012).

According to sensitivity, specificity, and predictive values of CSF biomarkers, one may think neurologists should be sharpening their lumbar puncture needles in order to improve their diagnostic accuracy in cases of MCI. Nevertheless, there is a wide range of attitudes and beliefs about the convenience and feasibility of lumbar punctures (LP; commonly referred to as spinal taps), and its practical value in the management of patients today. LP may be regarded as invasive or complicated and time consuming. In addition patients may have fear to undergo LP. One of the most controversial issues when discussing CSF biomarkers for early AD diagnosis has to do with the collection procedure itself. A debate exists on whether or not this technique can and should be used regularly, or if it is still too risky for routine practice. Clinically, LP are performed routinely in clinics for various laboratory analyses to diagnose diseases such as meningitis, encephalitis or inflammatory diseases like Multiple Sclerosis as well as to inject spinal anaesthetics or chemotherapy drugs. However, many still feel that the benefits of its use for testing AD biomarkers do not outweigh the risks.

As a result, the use of LP for testing CSF biomarkers in the diagnosis of AD is surprisingly culturally dependent and subject to changes in fashion today. From clinicians who support its use in daily clinical practice (Ariza-Zafra and Torrente-Orihuela, 2005; Lanari and Parnetti, 2009; Galluzzi et al., 2013) and countries where lumbar punture is almost a routine (Scandinavian countries, The Netherlands.) to other territories (Northamerica) where it is regarded as a very serious issue and used for research purposes under strict protocols only (Wilner, 2010; Cummings, 2011).

Some studies have already assessed the risks of LP; and the procedure seems to be both "safe and acceptable" to do. In a multi-site US study, 342 people underwent 428 LP. Side effects such as pain, anxiety and the well-known post-lumbar puncture headaches (PLPHAS) were quantified and compared to controls. Overall, pain and anxiety levels were low as rated on a visual analog scale but generally were rated higher in the younger normal subjects as compared to the older participants. This theme remains true amongst studies looking at PLPHA frequency and severity, where those who are younger are at higher risk, especially females (Evans et al., 2000). In terms of PLPHAs, they were unrelated to factors such as the position during the procedure (seated vs. lying) and the frequency of these headaches was lowest in the MCI/AD (over age 60) group than any other subject group. This is a promising conclusion as far as AD is concerned, as all of the participants are older and many have MCI or AD. Other study designed to assess LP procedures specifically in patients with AD also demonstrated that LP performed with a 24 g Sprotte atraumatic needle (blunt, "bullet" tip) is a well-tolerated procedure, with good acceptability (Peskind et al., 2009).

As many other medical techniques, the more often a procedure is done, the safer it becomes. In order to obtain more in depth knowledge on the factors affecting the complications of LP for testing biomarkers in patients with cognitive impairment, the Alzheimer's Association is supporting a multi-center feasibility study. This study will allow to establish the incidence of post-LP headache and other complications in cases with cognitive disturbances and to know the factors related to the occurrence of post-LP headache, including type of center/experience of physician, patient characteristics (e.g., diagnosis, cognitive function), patient attitude/knowledge on LP and the LP procedure itself.

Once it seems that complications related to LP for testing biomarkers in patients with cognitive decline are limited and controllable, next step should be to achieve consensus in order to state which patients should be offered a CSF analysis and how to interprect results in terms of clinical management. There is also a need to homogenize the different analysis techniques, protocols, and establishing universal cut-off levels for the biomarkers. Fortunately several international projects are ongoing in these regards. Hopefully we are envisioning the possibility of using LP for an earlier diagnosis in most AD patients.

REFERENCES

Ariza-Zafra, G., and Torrente-Orihuela, C. (2005). Llegará a ser la punción lumbar una prueba de rutina para el diagnóstico de la enfermedad de Alzheimer? *Archivos de Medicina* 1, 10.

Buchhave, P., Minthon, L., Zetterberg, H., Wallin, A. K., Blennow, K., and Hansson, O. (2012). Cerebrospinal fluid levels of β-amyloid 1-42, but not of tau, are fully changed already 5 to 10 years before the onset of Alzheimer dementia. *Arch. Gen. Psychiatry* 69, 98–106. doi: 10.1001/archgenpsychiatry.2011.155

Cummings, J. L. (2011). Biomarkers in Alzheimer's disease drug development. *Alzheimers Dement.* 7, e13–e44. doi: 10.1016/j.jalz.2010.06.004

Evans, R. W., Armon, C., Frohman, E. M., and Goodin, D. S. (2000). Assessment: prevention of post-lumbar puncture headaches: report of the therapeutics and technology assessment subcommittee of the American academy of neurology. *Neurology* 55, 909–914. doi: 10.1212/WNL.55.7.909

Galluzzi, S., Geroldi, C., Amicucci, G., Bocchio-Chiavetto, L., Bonetti, M., Bonvicini, C., et al. (2013). Translational outpatient memory clinic working group. Supporting evidence for using biomarkers in the diagnosis of MCI due to AD. *J. Neurol.* 260, 640–650. doi: 10.1007/s00415-012-6694-0

Lanari, A., and Parnetti, L. (2009). Cerebrospinal fluid biomarkers and prediction of conversion in patients with mild cognitive impairment: 4-year follow-up in a routine clinical setting. *ScientificWorldJournal* 9, 961–966. doi: 10.1100/tsw.2009.106

Peskind, E., Nordberg, A., Darreh-Shori, T., and Soininen, H. (2009). Safety of lumbar puncture procedures in patients with Alzheimer's disease. *Curr. Alzheimer Res.* 6, 290–292. doi: 10.2174/156720509788486509

van Rossum, I. A., Vos, S. J., Burns, L., Knol, D. L., Scheltens, P., Soininen, H., et al. (2012). Injury markers predict time to dementia in subjects with MCI and amyloid pathology. *Neurology* 79, 1809–1816. doi: 10.1212/WNL.0b013e3182704056

Wilner, A. N. (2010). *Alzheimer's CSF Test: Useful or Useless?* New York, NY: Medscape.

Conflict of Interest Statement: The author declares that the research was conducted in the absence of any commercial or financial relationships that could be construed as a potential conflict of interest.

Received: 10 December 2013; accepted: 24 March 2014; published online: 09 April 2014.

Citation: Menéndez-González M (2014) Routine lumbar puncture for the early diagnosis of Alzheimer's disease. Is it safe? Front. Aging Neurosci. ***6****:65. doi: 10.3389/fnagi.2014.00065*

This article was submitted to the journal Frontiers in Aging Neuroscience.

frontiers in
AGING NEUROSCIENCE

BOOK REVIEW
published: 08 November 2013
doi: 10.3389/fnagi.2013.00054

An atlas on biomarkers for Alzheimer's disease

Marta Martínez-Rivera*

Hospital Álvarez-Buylla, Mieres, Spain
**Correspondence: maildemarta@gmail.com*

Edited by:
Manuel Menéndez-González, Hospital Álvarez-Buylla, Spain

Reviewed by:
Oscar Arias-Carrion, Hospital General Dr. Manuel Gea González, Mexico

Keywords: Alzheimer, biomarker, dementia, mild cognitive impairment, atlas, differential diagnosis, book review, treatment

A book review on
Atlas on Biomarkers for Alzheimer's disease

Edited by Menéndez González, M., M-Y Books, 2011, ISBN: 978-1-44772-356-1

The search of methods to ease the diagnosis of Alzheimer's disease (AD) as early as possible is in the center of attention. Such methods (biomarkers) are a range of blood or CSF tests on one hand, and several types of neuroimaging scans on the other. Biomarkers are going to be included not only in the neuroscience research area but also in the diagnosis process with a practical application in the next years. The potential for these biomarkers to serve diagnostic purposes of AD has been highlighted in the proposed diagnostic criteria for preclinical AD from an NIH/NIA working group (Sperling et al., 2011). In these criteria, biomarkers are defined in terms of whether they reflect Aβ deposition, tau deposition, or signs of neuronal injury. Markers of Aβ deposition include both positron-emission tomography (PET) evidence of Aβ deposition and cerebrospinal fluid (CSF) measures of lower Aβ42 levels, using a variety of specific ligands. Markers of tau accumulation include CSF measures of increased total tau or phosphorylated-tau (p-tau). Together with low CSF Aβ42, elevated CSF tau provides a high likelihood of progression to AD in patients with MCI (mild cognitive impairment). A third group of biomarkers reflect biochemical changes related to processes such as cell death, synaptic damage, oxidative stress, or inflammation that may be part of the cascade of events that mediate damage, or the response to damage, in AD. This is a field, as many others in science, that suffers a quick evolution every year; and the moment of apply biomarkers in clinical practice is coming. It is necessary to make the clinical community aware of these scientific advances in a clear and concise manner, as well as counting with references that can guide our clinical practice with a consensus point of view.

Many of the images coming both from laboratory and neuroimaging studies are very illustrative. These images, accompanied by a short description, can perfectly explain the main results and usefulness of each biomarker. And this is just what the Atlas created by Dr Manuel Menéndez does (Menéndez González, 2011). The objective of this book is to summarize the most important studies made in this field. Few publications have systematically compiled results on this topic and none as an atlas. The book starts clarifying concepts as "biomarker", "mild cognitive impairment" and other preclinical conditions, and then focus on classification and description of all biomarkers for AD. A collection of imagines selected from outstanding research studies are provided for both laboratory and neuroimaging biomarkers. Finally the author finishes with a chapter on the rational use of biomarkers for AD in the clinical setting.

Readers will be interested in this publication because it allows reviewing the current status of research at the time that visualizing outstanding results easily. The possibility of coming across an optimal and well done review of biomarkers for AD is crucial not only for expertees, but also for the large public seeking to make a first approach to the world of biomarkers for AD. Such an easy to use manual, with the purpose to make the broad and often confusing biomarkers discussion surrounding AD accessible to a wider audience, notably in the clinic, is invaluable. The contents seem adequate, and Dr. Menéndez has a well-established track record in this field that ensures the quality of the final product, and therefore I am certain the scientific contents are solid. Overall it is a solid and timely proposal, at a competitive price range, which I am sure will make an impact where it matters the most, in the clinic with patients.

REFERENCES

Menéndez González, M. (Ed.). (2011). Atlas on Biomarkers for Alzheimer's disease. M-Y Books. ISBN: 978-1-44772-356-1

Sperling, R. A., Aisen, P. S., Beckett, L. A., Bennett, D. A., Craft, S., Fagan, A. M., et al. (2011). Toward defining the preclinical stages of Alzheimer's disease: recommendations from the National Institute on Aging-Alzheimer's Association workgroups on diagnostic guidelines for Alzheimer's disease. *Alzheimers Dement.* 7, 280–292. doi: 10.1016/j.jalz.2011.03.003

Received: 12 May 2013; accepted: 04 September 2013; published online: 08 November 2013.
*Citation: Martínez-Rivera M (2013) An atlas on biomarkers for Alzheimer's disease. Front. Aging Neurosci. **5**:54. doi: 10.3389/fnagi.2013.00054*
This article was submitted to the journal Frontiers in Aging Neuroscience.